

Toshiaki Murai *Editor*

# Chemistry of Thioamides

 Springer

# Chemistry of Thioamides

Toshiaki Murai  
Editor

# Chemistry of Thioamides

 Springer

*Editor*  
Toshiaki Murai  
Gifu University  
Gifu, Japan

ISBN 978-981-13-7827-0                      ISBN 978-981-13-7828-7 (eBook)  
<https://doi.org/10.1007/978-981-13-7828-7>

© Springer Nature Singapore Pte Ltd. 2019

This work is subject to copyright. All rights are reserved by the Publisher, whether the whole or part of the material is concerned, specifically the rights of translation, reprinting, reuse of illustrations, recitation, broadcasting, reproduction on microfilms or in any other physical way, and transmission or information storage and retrieval, electronic adaptation, computer software, or by similar or dissimilar methodology now known or hereafter developed.

The use of general descriptive names, registered names, trademarks, service marks, etc. in this publication does not imply, even in the absence of a specific statement, that such names are exempt from the relevant protective laws and regulations and therefore free for general use.

The publisher, the authors and the editors are safe to assume that the advice and information in this book are believed to be true and accurate at the date of publication. Neither the publisher nor the authors or the editors give a warranty, expressed or implied, with respect to the material contained herein or for any errors or omissions that may have been made. The publisher remains neutral with regard to jurisdictional claims in published maps and institutional affiliations.

This Springer imprint is published by the registered company Springer Nature Singapore Pte Ltd. The registered company address is: 152 Beach Road, #21-01/04 Gateway East, Singapore 189721, Singapore

# Preface

I have been involved in the development of synthetic methods and new reactions using thioamides for about 20 years. On the basis of the teaching that it is not necessary to stay in a busy place from the beginning when we start new research in the fields of synthetic chemistry, at first I hesitated to start that chemistry. Until then, I had studied compounds involving selenium and tellurium atoms, which are heavier elements of the sulfur atom in the Periodic Table. A limited number of researchers were engaged in selenium and tellurium chemistry, and there was a high possibility that the originality of our own research was guaranteed. In those studies, one of graduate students in the laboratory discovered that new active chemical species were generated from selenoamides, which was a selenium analogue of amides, and the carbon–carbon bond-forming reaction using those was achieved. I thought we could provide new synthetic chemistry with those reactions. However, handling of organoselenium compounds are generally non-trivial. So I decided to start research based on thioamides, whose rich chemistry has already been reported even at that time. Therefore, we had to be very careful to see if similar reactions were already reported or not. Fortunately, even in those situations, we encountered several novel synthetic reactions.

A few years ago, Springer Japan invited me to publish books on chemistry. As a result of searching literature and on-line search, I noticed that there were no books that overlook the chemistry of thioamides even if the abundant achievement with thioamides is known over half a century. Fortunately, my proposal with the chapters shown in the table of Contents was approved.

I then asked an expert to write each chapter, and all the distinguished scientists accepted my invitation. Since then, as I received the manuscript from them, I strongly felt the responsibility to complete this book as soon as possible. At the same time, I am full of gratitude for all the scientists, who wrote each chapter using

valuable time with expertise and enthusiasm. All the chapters provide abundant information and cover broad aspects of thioamides. Alternatively, you may be able to grasp the clues of new research by looking over a certain part.

Gifu, Japan  
March 2019

Toshiaki Murai

# Contents

<b>1 Thioamides: Overview</b> .....	1
Toshiaki Murai	
<b>2 Theoretical Aspects of Thioamides</b> .....	7
José V. Cuevas, José García-Calvo, Víctor García-Calvo, Gabriel García-Herbosa and Tomás Torroba	
<b>3 Synthesis of Thioamides</b> .....	45
Toshiaki Murai	
<b>4 Reaction of Thioamides</b> .....	75
Toshiaki Murai	
<b>5 Asymmetric Synthesis Using Thioamides</b> .....	103
Naoya Kumagai and Masakatsu Shibasaki	
<b>6 Synthesis of Heterocycles from Thioamides</b> .....	127
Hong Yan and Hai-Chao Xu	
<b>7 Thioamide-Based Transition Metal Complexes</b> .....	157
Ken Okamoto, Junpei Kuwabara and Takaki Kanbara	
<b>8 Thioamide-Containing Peptides and Proteins</b> .....	193
Taylor M. Barrett, Kristen E. Fiore, Chunxiao Liu and E. James Petersson	

# Chapter 1

## Thioamides: Overview



Toshiaki Murai

**Abstract** A range of sulfur isologues of carbonyl compounds are introduced. Among them, focus has been laid on the sulfur isologue of amides, i.e., thioamides. Research fields on thioamides have been spread from elucidation of the fundamental properties to biological applications. Historical background of thioamides is shortly introduced. Recent results on these studies such as conformation, hydrogen-bonding interaction, self-disproportionation of enantiomers, and biological aspects are then briefly introduced to enter each chapter of this book, where the details are shown.

**Keywords** Thioamides · Conformation · Hydrogen-bonding · Self-disproportionation · Metal complexes · Biological activity

The replacement of the oxygen atom in amides with the sulfur atom gives rise to the formation of thioamides. Amides have been recognized as the least reactive carboxylic acid derivatives. In that sense, similar tendency may be seen when you compare the reactivity of thioaldehydes **1** (thials), thioketones **2** (thiones) [1], and thioic acid *O*-esters **3** (Fig. 1.1). The isolation of thioaldehydes **1** and thioketones **2** is nontrivial unless bulky substituents are introduced around thiocarbonyl groups [2]. In contrast, sulfur isologues of amides such as thioformamide **4** (methanethioamide), thioacetamide **5** (ethanethioamide), and benzothioamide **6** (benzenecarbothioamide) have appeared in the literature in the late nineteenth centuries [3–6], and their synthesis and properties have been continuously studied, although these primary thioamides can decompose via the elimination of hydrogen sulfide to give mixtures including nitriles.

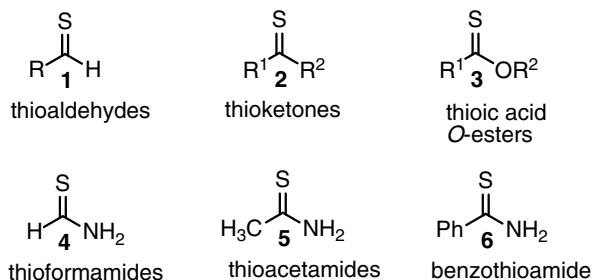
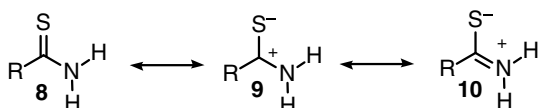
Studies in the early twentieth century may have laid on a viewpoint of how the properties of the compounds change when one of the elements in molecules belonging to the second row of the periodic table is replaced by the element in the third and subsequent periods. Hereafter, the thioamide moiety (C=S–N) was found to show unique properties, and compounds having this unit were found in nature, so that

---

T. Murai (✉)

Department of Chemistry and Biomolecular Science, Faculty of Engineering, Gifu University,  
Yanagido, Gifu 501-1193, Japan  
e-mail: [mtoshi@gifu-u.ac.jp](mailto:mtoshi@gifu-u.ac.jp)



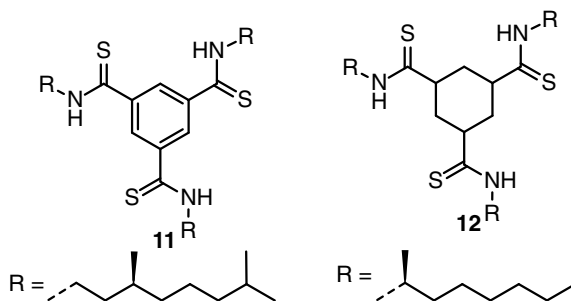
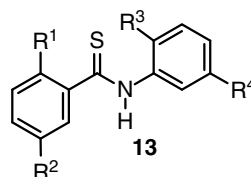
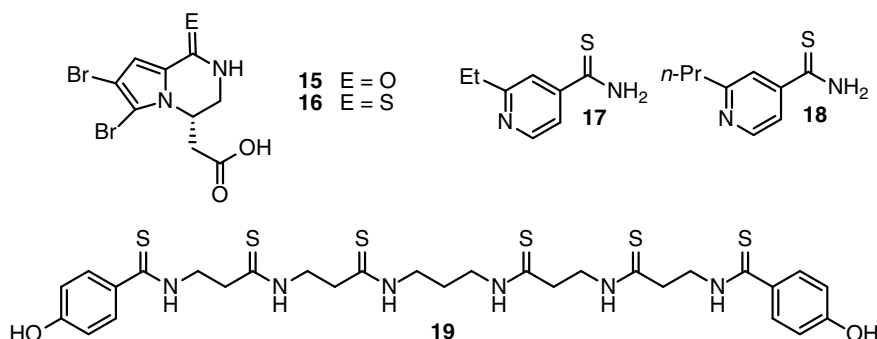
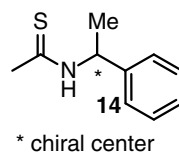
**Fig. 1.1** Some of thiocarbonyl compounds**Fig. 1.2** Resonance structures of thioamides

research fields have extensively expanded from fundamental chemistry to biochemistry and material chemistry.

Similarly to amides, resonance structures of thioamides **8** can be depicted as **9** and **10** (Fig. 1.2). However, the contribution of the resonance structure **9** is markedly smaller than that in the corresponding amides mainly because of the similarity of the electronegativity of carbon and sulfur atoms [7]. As a result, thioamides are less polar than the corresponding amides, and the purification of thioamides is easier than the amides having identical carbon skeletons. In contrast to amides, the charge transfer from the nitrogen atom to the C=S bonds is greater, and the rotational barrier of C=N bond is larger [8].

Hydrogen-bonding including S–H bonds and conformations around C=S–NH bonds are of interest in the fields of pure chemistry as well as thiopeptide chemistry. Generally, the C=S–NH bonds are weaker acceptor of the hydrogen bonds, and the NH proton is more acidic and can work as a hydrogen bond donor [9, 10]. To gain insights of the hydrogen-bonded systems, thioamides such as **11** and **12** (Fig. 1.3) are prepared, and their structures and hydrogen-bonding interaction, and  $\pi$ - $\pi$  stacking are elucidated. The relationship of the substituents on the aromatic rings and conformation around C=S–NH bonds is extensively studied with *N*-aryl arylthioamides **13** (Fig. 1.4) [11]. *Z*-Conformation is usually preferable, and the detail of the isomerization is revealed by variable-temperature NMR and NOESY experiments and DFT calculations.

Self-disproportionation of enantiomers (SDE) is observed during the purification of the optically active compounds with some enantiomeric excess (ee) [12]. The ee of the purified products is not identical in some fractions collected during the achiral chromatographic separation. The phenomena are related to the strength of the hydrogen-bonding interactions. To show this phenomenon of thioamides, optically active thioamide **14** is prepared (Fig. 1.5). Its SDE is observed, although SDE is substantially lower than that of the corresponding amide. The softness of the sulfur atom enables thioamides to behave as ligands mainly to soft metals.

**Fig. 1.3** benzene-1,3,5-tricarbothioamides**Fig. 1.4** *N*-Aryl arylthioamides**Fig. 1.5** Chiral *N*-1-phenylethyl thioacetamide**Fig. 1.6** Some of biologically relevant thioamides

The replacement of the oxygen atom to the sulfur atom also affects the physiological activity of the molecules. In some cases, the activity may decrease, but some of the results have shown that the replacement enhanced the activity [13]. For example, the oxygen atom of longamide B (**15**) is replaced with a sulfur atom to form thioamide **16** (Fig. 1.6) [14]. The compound **16** shows higher inhibitory activity than **15** as an indoleamine 2,3-dioxygenase 1 inhibitor.

One of the examples of the application of thioamides as an antibiotic is the use of thioamides **17** and **18**, which have been called as ethionamide and prothionamide, for the treatment of tuberculosis [15–19]. The studies on its effect, possibility as a drug for other diseases, side effect, and resistant bacteria have been continued [20]. The thioamide **19**, which has been called as a closthioamide, is isolated from the cellulose-degrading bacterium *Clostridium cellulolyticum* [21]. Its biological activity and biosynthetic pathway have been elucidated with the aim to apply for drugs [22, 23].

In addition to a brief summary of chemistry of thioamides described above, the fields related to thioamides such as the development of new synthetic methods and reactions, evaluation of their properties, and applications of thioamides are dramatically growing. Therefore, although this book cannot cover all of them, on the basis of the recent results mainly revealed by 2018, this book deals with theoretical aspects of thioamides (Chap. 2), synthesis of thioamides (Chap. 3), reaction of thioamides (Chap. 4), asymmetric synthesis using thioamides (Chap. 5), synthesis of heterocycles from thioamides (Chap. 6), thioamides-based transition metal complexes (Chap. 7), and thioamide-containing peptides and proteins (Chap. 8). Each chapter is written by experts in their respective fields. Some of the topics may partially duplicate in different chapters, but this indicates the importance of those topics in the corresponding chapters.

## References

1. T. Murai, *Topics. Curr. Chem.* **376**, 1 (2018)
2. R. Okazaki, *Heteroat. Chem.* **25**, 293 (2014)
3. E.A. Werner, *J. Chem. Soc. Trans.* **57**, 283 (1890)
4. R. Willstätter, T. Wirth, *Ber. Deutch. Chem. Gesell.* **42**, 1908 (1909)
5. K. Hubacher, *Justus Liebigs Annal. Chem.* **259**, 228 (1890)
6. O. Wallach *Justus Liebigs Annal. Chem.* **259**, 300 (1890)
7. K.B. Wiberg, D.J. Rush, *J. Am. Chem. Soc.* **123**, 2038 (2001)
8. H.-J. Lee, Y.-S. Choi, K.-B. Lee, J. Park, C.-J. Yoon, *J. Phys. Chem.* **106**, 7010 (2002)
9. R.W. Newberry, B. VanVeller, R.T. Raines, *Chem. Commn.* **51**, 9624 (2015)
10. C. Kulkarni, E.W. Meijer, A.R.A. Palmans, *Acc. Chem. Res.* **50**, 1928 (2017)
11. J. Kozic, Z. Novak, V. Rimal, V. Profant, J. Kunes, J. Vinsova, *Tetrahedron.* **72**, 2072 (2016)
12. J. Drabowicz, A. Jasiak, A. Wzorek, A. Sato, V.A. Soloshonok, *Arkivoc*, part ii, 557 (2017)
13. H. Verma, B. Khatri, S. Chakraborti, J. Chatterjee, *Chem. Sci.* **9**, 2443 (2018)
14. Z. Shiokawa, E. Kashiwabara, D. Yoshidome, K. Fukase, S. Inuki, Y. Fujimoto, *Chem. Med. Chem* **11**, 2682 (2016)
15. S. Thee, A.J. Garcia-Prats, P.R. Donald, A.C. Hesselring, H.S. Schaaf, *Tuberculosis.* **97**, 126 (2016)
16. S. Chetty, M. Ramesh, A. Singh-Pillay, M.E.S. Soliman, *Bioorg. Med. Chem. Lett.* **27**, 370 (2017)
17. J. Laborde, C. Deraeve, V. Bernardes-Genisson, *Chem. Med. Chem* **12**, 1657 (2017)
18. P. Miotto, B. Tessema, E. Tagliani, L. Chindelevitch, A.M. Starks, C. Emerson, D. Hanna, P.S. Kim, R. Liwski, M. Zignol, C. Gilpin, S. Niemann, C.M. Denking, J. Fleming, R.M. Warren, D. Crook, J. Posey, S. Gagneux, S. Hoffner, C. Rodrigues, I. Comas, D.M. Engelthaler, M. Murray, D. Alland, L. Rigouts, C. Lange, K. Dheda, R. Hasan, U.D.K. Ranganathan, R.

- McNerney, M. Ezewudo, D.M. Cirillo, M. Schito, C.U. Köser, T.C. Rodwell, *Eur. Respir J.* **50**, 1701354 (2017)
19. A. Khusroa, C. Aartia, A. Barbabosa-Pliegob, A.Z.M. Salemb, *Microbial Pathogenesis*, vol. 114 (2018), p 80. (f) A. Chollet, L. Maveyraud, C. Lherbet, V. Bernardes-Génisson, *Eur. J. Med. Chem.* **146**, 318 (2018)
  20. M. Gashaw, in *Anaerobes in Biotechnology*, (2016), p. 433
  21. S. Behnken, C. Hertweck, *Appl. Microbiol. Biotechnol.* **96**, 61 (2012)
  22. F. Kloss, A.I. Chiriatic, C. Hertweck, *Chem. Eur. J.* **20**, 15451 (2014)
  23. K.L. Dunbar, H. Büttner, E.M. Molloy, M. Dell, J. Kumpfmüller, C. Hertweck, *Angew. Chem. Int. Ed.* **57**, 14080 (2018)

# Chapter 2

## Theoretical Aspects of Thioamides



José V. Cuevas, José García-Calvo, Víctor García-Calvo,  
Gabriel García-Herbosa and Tomás Torroba

**Abstract** Quantum chemical calculations can afford valuable information to understand the chemical processes and the structural features of chemical species. This tool has become very informative, and several aspects can be discussed on the thioamides under a theoretical point of view such as the effects of structure in their planarity and some cases with derivations of that planarity, C–N bond rotation in comparison to the related amides and selenoamides and implications in the transition state, and the influence of the solvent or the influence of remote substituents. This review will deal as well with isomerization processes such as tautomerization or rotation of *N*-bonded methyl groups. Some aspects of reactivity of thioamides such as the bond-dissociation enthalpy (BDE) or their behavior as radical scavengers are discussed as well. Some comments on the theoretical aspects of thiopeptides are briefly analyzed.

**Keywords** Thioamides · Quantum chemistry · DFT · HF

### 2.1 Basic Structural Features of Thioamides

#### 2.1.1 Planarity of Thioamides

The planarity of thioamides has been a deeply explored subject not only from a theoretical point of view but also from the multiple implications it might have in life science or materials. In this review, we will cover the thioamides under a theoretical point of view focused on the effects of structure in their planarity and the consequences on their behavior. Judge et al. studied the structure of thioformamide at the HF/3-21G\* level finding that the lower energy state is strictly planar (structures **1** in Fig. 2.1) [1]. High-level theoretical calculations performed by Kowal confirm the pla-

---

J. V. Cuevas (✉) · J. García-Calvo · V. García-Calvo · G. García-Herbosa · T. Torroba (✉)  
Department of Chemistry, University of Burgos, 09001 Burgos, Spain  
e-mail: [jvcv@ubu.es](mailto:jvcv@ubu.es)

T. Torroba  
e-mail: [ttorroba@ubu.es](mailto:ttorroba@ubu.es)

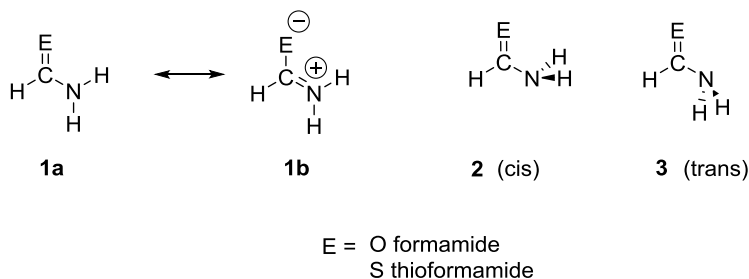


**Fig. 2.1** Resonance forms of the amides and thioamides (**1a** and **1b**) and transition states (**2** and **3**) in the rotation around the C–N bond

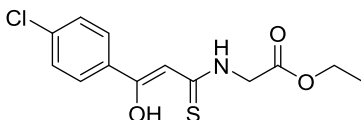


**Fig. 2.2** Structure of ethyl 2-[(Z)3-(4-chlorophenyl)-3-hydroxy-2-propene-1-thione]amino}acetate

nar geometry of the thioformamide  $\text{H}_2\text{NC(S)H}$  [2]. In the same work, it is described that correlation-corrected vibrational self-consistent field (CC-VSCF) affords a good description of the vibrational features of the thioamide group.

Hambley et al. [3] have shown how the optimized structure (BLYP/6-311++G\*\*) of thioacetamide is in good agreement with its crystal structure. The thioacetamide shows a planar structure in which there is conjugation in the S–C bond but little hyper-conjugation in the C–N bond. These results indicate that the canonical form (**1a**) shown in Fig. 2.1 predominates in the solid state.

More complicated thioamides such as ethyl 2-[(Z)3-(4-chlorophenyl)-3-hydroxy-2-propene-1-thione]amino}acetate (Fig. 2.2) studied at the levels of theory HF/6-31G(d) and B3LYP/6-31G(d) display a planar geometry on the thioamide unit in good agreement with the crystallographic characterization [4].

### 2.1.2 Derivations from Planarity

Despite the trend of thioamides to adopt a planar geometry, the electronic nature on the substituents of the thiocarbonyl group can determine the planarity of the thioamide, as shown by Hori et al. [5]. They found that in a series of *para*-substituted or unsubstituted thioaroyl-7-azabicyclo[2.2.1]heptanes, the planarity of the thioamide can be tuned by altering the electronic nature of the substituent.

For example, the H-substituted compound was substantially both nitrogen pyramidal and twisted (**3a**,  $\alpha = 167.3^\circ$  and  $|\tau| = 11.0^\circ$ ), while in the *p*-nitro-substituted compound, planarity was substantially restored (**3h**,  $\alpha = 175.2^\circ$  and  $|\tau| = 0.1^\circ$ ). The

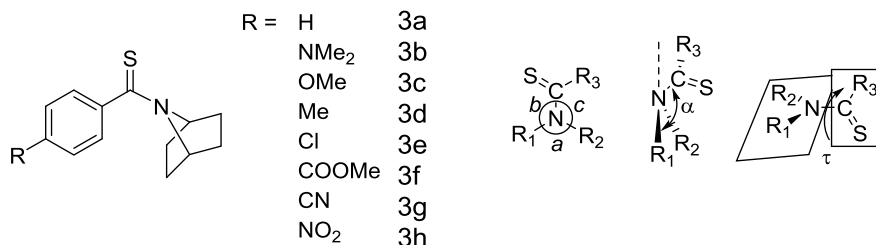


**Fig. 2.3** Thioamides studied by Hori et al. and definition of angle parameters. Adapted with permission from [5]. Copyright 2008 American Chemical Society (further permissions related to the material excerpted should be directed to the ACS)

planarity of thioamide nitrogen can be represented in terms of three angle parameters,  $\theta$ ,  $\alpha$ , and  $\tau$ , the definitions of which are shown in Fig. 2.3:  $\theta$  is the sum of the three valence angles around the nitrogen atom ( $\theta = a + b + c$ ); the hinge angle  $\alpha$  is the angle between the N–C(S) bond and the plane defined by the nitrogen atom, R<sub>1</sub>, and R<sub>2</sub>; and the twist angle  $|\tau|$  is the absolute value of the mean of two torsion angles,  $\omega_1(\text{R}_3\text{CNR}_2)$  and  $\omega_2(\text{SCNR}_1)$  ( $|\tau| = 1/2|\omega_1 + \omega_2|$ ) [6]. Values of  $\theta$ ,  $\alpha$ , and  $\tau$  of the ideal planar thioamide are 360°, 180°, and 0°, respectively. The former two values will decrease, and the third value will increase as the thioamide functionality deviates from planarity to a greater extent.

In the solid state, an electronic effect of the aromatic substituent (R) on thioamide planarity was clear in the case of the bicyclic thioamides (not observed on analogous amides), and the degree of planarity represented in terms of R is in the order **3h** > **3e** > **3a** > **3d** > **3b**. The thioamide **3h** (R = NO<sub>2</sub>) takes a nearly planar structure, whereas **3b** (R = NMe<sub>2</sub>) takes a significantly nitrogen-pyramidalized structure (Fig. 2 on the reference [5]). This trend is consistent with the idea that an electron-withdrawing group tends to restore nitrogen planarity, except for **3f** (R = COOMe) on which packing effects induce a distortion. To estimate the N–C(S) double-bond character of these thioamides in solution, rotational barriers with respect to the thioamide bond were evaluated by variable-temperature <sup>1</sup>H NMR spectroscopy. It is observed that the substituent on the benzene ring showed a significant electronic effect on the rotational barrier of the thioamides (a wide discussion on rotational barriers in thioamides will be found below in the Sect. 2.3). A more electron-withdrawing group tends to increase the rotational barriers of these thioamides.

These experimental facts were modeled with DFT calculations at the B3LYP/6-311+G(d,p)//B3LYP/6-31G(d) level of theory. For the punctual calculations, solvent effects were taken into account using the PCM model and a relative permittivity  $\epsilon = 35.6$  to simulate nitrobenzene. There is a tendency that the degrees of nitrogen pyramidalization of the calculated structures are consistently larger than those of the solid-state structures. Also, the calculated rotational barriers of these thioamides showed that the rotational barriers of the bicyclic thioamides are consistently smaller than those of the monocyclic thioamides displaying a good linear relationship with the Hammett parameter  $\sigma_p^+$  values of the substituents [7].

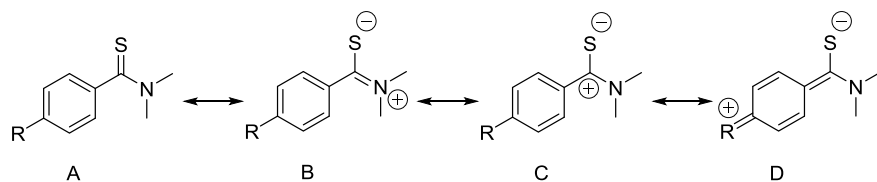


**Fig. 2.4** Resonance forms including the effect of the substituents on the *para*-substituted thioaroyl group. Reprinted with permission from [5]. Copyright 2008 American Chemical Society (further permissions related to the material excerpted should be directed to the ACS)

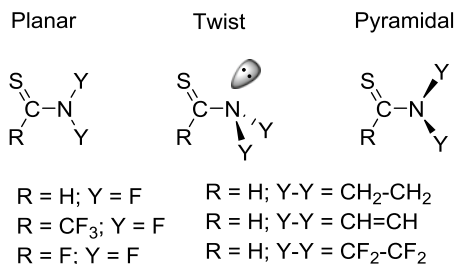


**Fig. 2.5** Thioamides studied by Kesharwani et al. in [8]

To explain these observations, it is needed a scheme of resonance including a new structure (Fig. 2.4).

The results obtained by Hori et al. are consistent with the idea that the relative contributions from resonance B versus resonance D (Fig. 2.4) control the planarity of the nitrogen. Only resonance B requires the nitrogen to be planar (pyramidalization and twisting will destabilize the C=N bond). Strongly electron-withdrawing substituents (R) at the *para* position destabilize resonance D (increasing A and B), thereby increasing planarity.

In the same work, the authors have found that tying the nitrogen into a bicyclic structure pyramidalizes nitrogen and decreases the contribution from resonance B (increasing A and D) in comparison with thioamides with the nitrogen atom belonging to a pyrrolidine monocyclic structure.

Kesharwani et al. [8] have studied the theoretical possibility to stabilize the non-planar forms of thioamides when compared with their planar structures (Fig. 2.5).

In the models studied, twist and pyramidal forms are more stable than planar form. The destabilization caused in the planar form of *N,N*-difluorothioformamide is due to the repulsion between the lone pairs of the C=S sulfur atom and the *N*-substituted fluorine atom [8]. Negative hyperconjugative type interactions, in addition to the electrostatic effect, are proposed to be responsible to the stabilization of the twisted conformation because second-order perturbative (NBO [9, 10]) analysis suggests that the negative hyperconjugative type interactions ( $n_N \rightarrow \sigma^*_{C-F}$ ) in the twisted form with substituents R = F, Y = F (Fig. 2.5) is stronger by 3.2 kcal/mol than that with substituents R = H and Y = F ( $n_N \rightarrow \sigma^*_{C-H}$ ) at B3LYP/aug-cc-pVDZ level



[11]. Nevertheless, the fact that in some cases the twisted form has not been found indicates that electrostatic repulsions override these interactions.

Thioamides with three-membered azirine and aziridine rings have been studied as well in the same work [8], finding that only the azirine rings stabilized the twisted form with substituents  $R = H$  and  $Y = CH=CH$  when compared with the prototype planar structure. The aziridine derivatives do not show twisted form, and in all cases, the pyramidal form is the most stable structure. The hybrid approach using a combination of explicit solvent molecules and continuum model shows that the twisted form of thioamide derivatives would be much more favored due to the hydrogen bonding interaction with solvent molecules.

## 2.2 Tautomerization

One of the simplest analyses that can be proposed for thioamides is the tautomeric equilibrium shown in Fig. 2.6.

Quantum chemical calculations have been carried out to evaluate the relative energies of both tautomers by Leszczynski et al. [12]. Hartree–Fock and post-Hartree–Fock calculations show that the thioamide form is about 10 kcal/mol more stable than the acidic form (thiol form, the structure on the right side in Fig. 2.6).

Zhang et al. have studied this kind of intramolecular proton transfer in the 6-thioguanine (a drug with cytotoxic and immunosuppressive properties) and the influence of alkali metals cations in the equilibrium at the level of theory B3LYP/6-31+G(d) [13] (Fig. 2.7).

**Fig. 2.6** Tautomeric equilibrium in thioamides

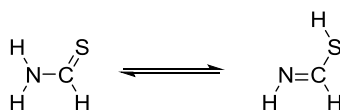
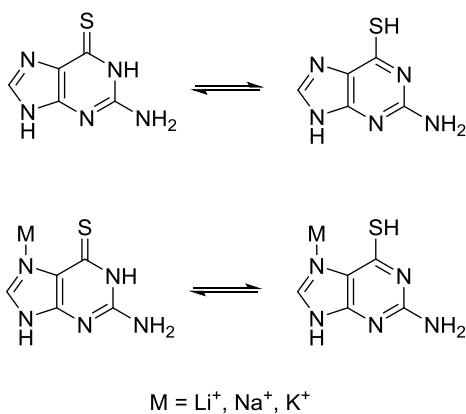


**Fig. 2.7** Tautomeric forms of 6-thioguanine in the absence of the alkali metal (above) and in the presence of the metal (below)



Although the 6-thioguanine is capable of existing in fourteen tautomeric forms, the work of Zhang et al. focuses on the intramolecular proton transfer shown in Fig. 2.7. Despite the amide form is more stable in the simplest thioamide studied by Leszczynski et al. [12], in the more complex system of 6-thioguanine at the level of theory B3LYP/6-31+G(d), it is found to be more stable the thiol form by 1.9 kcal/mol. When the alkali cations are present, the amide form is more stable by 17.0, 15.4, and 11.7 kcal/mol for  $\text{Li}^+$ ,  $\text{Na}^+$  and  $\text{K}^+$  respectively. The comparison of the calculated barriers indicates that the presence of the cations increases the activation barrier for the proton transfer. And considering only the systems with alkali metals present, the greater the radius of the alkali metal cations, the easier the intramolecular proton transfer in 6-thioguanine.

## 2.3 Rotations Around the C–N Amide Bond

### 2.3.1 Simple Examples

The dynamic modification that has been most studied both experimentally and theoretically is the **rotation around the C–N amide bond**. Several of these studies have been performed in comparison with the analogous amides and selenoamides.

At first sight, as the difference in electronegativity between C and S is small [14], the C=S bond should not be strongly polarized as it is in the C=O of formamide, indicating that the resonance form **1b** (Fig. 2.1) should have more importance in amides than in thioamides. The C–N bond should display a higher character of double bond in formamide than in thioformamide and a higher rotational barrier for formamide should be expected. Nevertheless, the energy value for rotational barrier in thioformamide is larger than for formamide [15, 16].

Ferretti et al. have studied the deformation of the fragment  $\text{R}(\text{X}=\text{C})\text{--NR}_2$  present in amides, thioamides, amidines, enamines, and anilines by a combination of the analysis of crystal structures and ab initio calculations HF/4-31G [16]. The authors find that the thioamides have a higher rotational barrier than amides.

Wiberg and Rablen had studied the rotational barrier at MP2/6-31+G\* and G2 levels of theory to rationalize the higher rotational barrier of thioamide (see values in Table 2.1) [15]. The change in the charge density on the rotating the amino group in formamide and thioformamide has been examined finding that there is a bigger net charge change in the sulfur atom of the thioformamide (a net change of 0.116e) than in the oxygen atom of the formamide (0.057e). The bigger change on the values of charge found on rotating about the C–N bond indicates that thioformamide is closer to the representation of the resonance picture **1a** and **1b** shown in Fig. 2.1 than the formamide.

The authors of this work propose that there is a considerable transfer of  $\pi$  charge to the sulfur in the planar form. To justify the important charge transfer from N to S in thioamides (and not very important from N to O in amides), it is possible to propose

**Table 2.1** Energy of rotational barriers of formamide and thioformamide

Rotational barriers (kcal/mol) <sup>a</sup>		
Compound	MP2/6-31+G*	G2
Formamide	17.2	16.0
Thioformamide	18.8	18.0
Formic acid	12.9	11.5
Thioformic acid	12.9	12.3

Adapted with permission from reference [15]. Copyright 1995 American Chemical Society (further permissions related to the material excerpted should be directed to the ACS)

<sup>a</sup>The values include the change in zero-point energy

two important factors. Initially, the sulfur atom in the C=S bond has a relatively small charge, whereas the oxygen of the C=O group has a relatively large negative charge, and consequently, the energetic cost of further polarization is quite large. A second factor is the size of the sulfur atom. The larger size of the sulfur makes it able to accommodate additional charge transfer. Therefore, it is important to keep in mind that charge transfer is a factor that contributes to the barrier. This higher barrier is in accord with a higher wave number of the NH<sub>2</sub> out-of-plane wagging mode in gaseous thioformamide than in formamide. Calculation of the NH<sub>2</sub> wagging mode potential in formamide and thioformamide on the G2 level revealed that the potential is steeper in the case of thioformamide, leading to the conclusion that the thioformamide molecule is less floppy than its oxygen analog.

Ou et al. [17] performed NBO calculations [9, 10] at the levels of theory HF/6-31G\*\*, MP2/6-31\*\*, and MP4/6-31\*\* founding that the rotational barrier height of thioformamide relative to formamide is due to the more important contribution from the zwitterionic structure **1b** (Fig. 2.1) in the former, in a similar description than the description of Wiberg and Rablen [15]. The zwitterionic structure strengthens the C–N bond with the double-bond character and thus inhibits the C–N rotation.

Laidig and Cameron proposed that the higher barrier observed in the rotation of thioformamide when compared to the formamide is difficult to explain with a simple resonance model [18]. These authors rationalize that the higher electronegativity of O attracts charge to itself, shortening the C–N bond length and increasing the bond order (hindering rotation). In thioformamides, the O atom is replaced by a less electronegative S atom. Although the S atom is more polarizable than O and could better stabilize a negative charge, it is not sufficient electronegative to pull charge from the N atom, making difficult to understand the higher rotational barrier found in thioformamide. In this different approach, the authors consider that in the C–N rotation process, there is a pyramidalization of the nitrogen atom and the dominant change is the interaction between the C and N atoms, with much smaller changes in the interaction between C and S, or C and O in formamide. For these authors, there is no significant delocalization of electronic charge between the N and S atoms in planar thioformamide or between N and O in formamide.

The planar conformation (structures **1a** and **1b** in Fig. 2.1) is the lowest energy structure (as described previously [1, 2]), with the *cis* and *trans* structures (**2** and **3** in Fig. 2.1) transitions states 19.9 and 21.6 kcal mol<sup>-1</sup> less stable. The energetic changes are consistent with bond lengthening processes in which the loss in attraction between the bonded fragments outstrips any decrease in repulsion as the atoms move away from one another. The largest geometric change in bond length upon rotation on the amide bond is the lengthening of the C–N bond, while the other bond lengths show very small changes and the energetics are dominated by the lengthening of the C–N bond. As the NH<sub>2</sub> fragment rotates away from planarity, the nitrogen pyramidalizes and charge is transferred from N to its bonded neighbors, C and H. The interaction between C and S (or C and O in formamide) is relatively unchanged, with only a small transfer of charge from S to C and small change in bond length. The energetics is dominated by the lengthening of the C–N bond and the resulting loss in intra and inter-atomic stabilization of N. The driving force for the planarization of N is the stabilization of N through its increased electronegativity (more *s* character in *sp*<sup>2</sup> hybridization than in *sp*<sup>3</sup>) and subsequent withdrawal of charge from its bonded neighbors. Under the point of view of Laidig and Cameron, thioformamide can be considered as a “thioformyl-amine.” The thioformyl group behaves merely as a substituent on an amine, and the barriers to rotations are special cases of a barrier to inversion of the corresponding amines. As the planar *sp*<sup>2</sup> N pyramidalizes, its hybridization shifts toward *sp*<sup>3</sup>, the result of which is that N becomes effectively less electronegative and submits electronic charge to its bonded neighbors. Considering the difference between amides and thioamides, the softer thioformyl group donates more charge to the NH<sub>2</sub> group than does the more polarized formyl group in the planar conformation. Thus, rotating about the C–N bond, which leads to the rehybridization of the N and its pyramidalization, is more costly for the N atom and the NH<sub>2</sub> group in thioformamide.

Laidig and Cameron find in their work that the structure **2** of Fig. 2.1 is more accessible than the structure **3**. Interestingly, Lim and Francl [19] using the level of theory HF/3-31G found that the structure **3** was lower in energy than the structure **2** for thioformamide and thioacetamide.

The point of view of Laidig and Cameron has been used by Choe et al. [20] to explain the higher C–N bond rotational barrier of thioacetamide in comparison with acetamide at the MP2/6-31G\*\* and B3LYP/6-31G\*\* levels of theory. They carried out a NBO population analysis finding that the lone pair electrons on the nitrogen of acetamide have more *s* character than that of thioacetamide in transition state (*sp*<sup>2.40</sup> vs. *sp*<sup>2.28</sup>, respectively). The relatively large *s* character of lone pair electrons of acetamide nitrogen in its transition state reduced the orbital energy, leading to the lower rotational barrier.

Lauvergnat and Hiberty have checked the validity of the resonance representation by means of an ab initio valence bond study [21]. The authors of this work studied the problem by a method that allows to directly measure the stabilization brought by the delocalization of the nitrogen lone pair in planar (thio)amide, by comparing the energy of the fully delocalized ground state to that of an adiabatic state in which the lone pair is constrained to remain strictly localized on the nitrogen atom. Doing

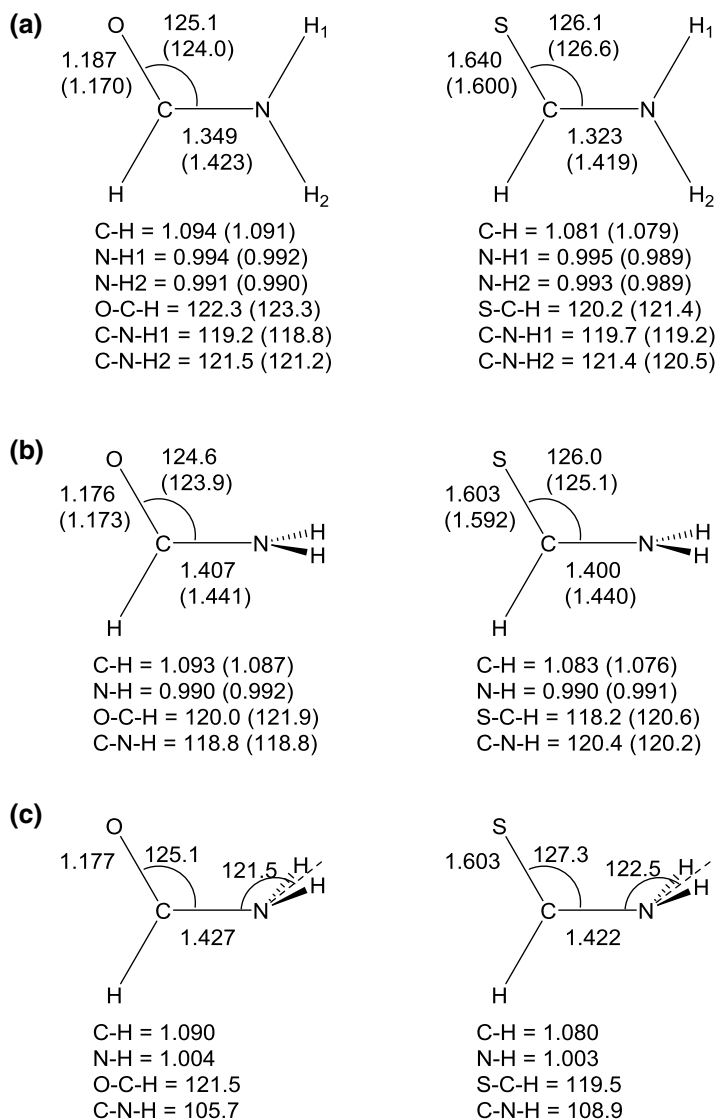


**Fig. 2.8** Geometries of the delocalized states and, in parentheses, of the localized states of formamide and thioformamide: **a** planar conformers; **b**  $sp^2$ - $90^\circ$ -rotated conformers, and **c**  $sp^3$ - $90^\circ$ -rotated conformers. Reprinted with permission from reference [21]. Copyright 1997 American Chemical Society (further permissions related to the material excerpted should be directed to the ACS)

this for both the planar and the twisted forms allows the contribution of resonance to the rotational barrier and, more generally, to the properties associated to the special stability of the planar form to be estimated (Fig. 2.8).

In their study, the authors have compared structures with planar (thio)formamide,  $90^\circ$  rotated (thio)formamide keeping  $sp^2$  hybridization on N (referred as  $sp^2$ - $90^\circ$ , see Fig. 2.8) and  $90^\circ$  rotated (thio)formamide changing to  $sp^3$  hybridization on N atom (referred as  $sp^3$ - $90^\circ$ , see Fig. 2.8). The first point the authors highlight is the shorter C–N distance in the conformer  $sp^2$ - $90^\circ$  than in the  $sp^3$ - $90^\circ$ , indicating that the C–N lengthening upon rotation is not entirely due to the loss of conjugation but partly arises from a change of hybridization at the nitrogen atom, as  $sp^3$  hybrids are generally known to form longer bonds than  $sp^2$ . The authors found, as well, little differences between the C–O, C–S, and C–N bond lengths of the planar conformers in their lone pair localized diabatic states (i.e., with the nitrogen lone pair localized on the nitrogen atom) and those of the pyramidal–twisted conformers in their ground states ( $sp^3$ - $90^\circ$ ), supporting the idea that the rotation around the C–N bond is mainly a matter of localization–delocalization. The analysis of the structural values showed a significant C=S shortening accompanying loss of conjugation in thioformamide (0.040 Å) suggesting the two-structure resonance model picture as an adequate representation for thioformamide (Fig. 2.1). In addition, the comparison of structures with and without delocalization suggests that the C–N linkage has more double-bond character in thioformamide than in formamide, accounting for a higher rotational barrier.

The analysis of the energies of these structures allowed to have directly measured the stabilization that delocalization of the lone pairs of the nitrogen atom brings to planar conformations and  $90^\circ$ -rotated conformations, and the contribution of this resonance stabilization to the rotational barrier around the C–N bond, finding that conjugation of the  $\pi$  electrons is an important feature of the electronic structure of (thio)amides with the lone pair of the nitrogen atom significantly delocalized over the (thio)carbonyl group. The authors estimate a more important conjugation in thioamides than in amides. Nevertheless, the resonance stabilization to the C–N rotational barrier is not the only one factor accounting for this energy, suggesting tentatively the preference of the lone pair of the nitrogen atom for a direction perpendicular to the molecular plane, following the minimum of electron density at the carbon atom as an additional factor to this rotational barrier. Finally, despite this additional factor affecting the C–N rotational barrier, the authors indicate that the larger barrier of thioamides is due to a greater importance of conjugation effects relative to amides.

A new study with valence bond resonance model for derivatives of formamide  $H CX(NH_2)$ , where  $X=O, NH, CH_2, S,$  and  $Se$ , using the block-localized wave method (BLW) [22–24] was carried out by Mo et al. [25] (Fig. 2.9).

The rotational barriers of  $H CX(NH_2)$  are decomposed into various energy components, including resonance conjugation energy,  $\sigma$ -framework steric effects, hyperconjugation energy, and pyramidization energy, using a BLW function method with the 6-31G(d) basis set. The ground-state electronic delocalization, represented by resonance structure **III** of Fig. 2.9, makes the largest contribution to the torsional barrier about the C–N bond, though the gain in hyperconjugation stabilization of a structure with the  $NH_2$  fragment rotated  $90^\circ$  reduces the overall delocalization effects. Steric effects due to conformational change in the  $\sigma$ -framework and amino

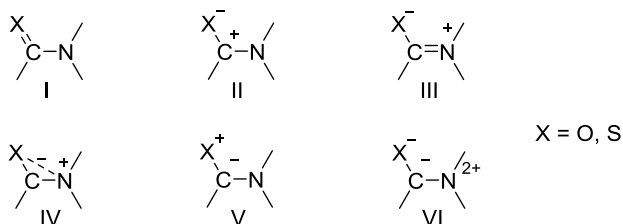


**Fig. 2.9** Six resonance structures resulting from four  $\pi$  electrons and three  $\pi$ -type atomic orbitals according to valence bond theory in amides and thioamides. Adapted with permission from reference [25]. Copyright 2003 American Chemical Society (further permissions related to the material excerpted should be directed to the ACS)

group pyramidization are also important in determining the barrier height of these compounds. The difference in torsional barrier in the chalcogen series,  $\text{HCXNH}_2$  ( $X = \text{O}, \text{S},$  and  $\text{Se}$ ), primarily results from the difference in electronic delocalization of the ground-state structure, which is significantly greater for  $X = \text{S}$  and  $\text{Se}$  ( $-35.7$  and  $-37.6$  kcal/mol, respectively) than  $X = \text{O}$  ( $-25.5$  kcal/mol).

An additional work validating the resonance representation of the formamide and its chalcogen replacement analogs (thioformamide among them) was presented by Glendening and Hrabal [26]. These authors study the influence of resonance on the structure and rotational barrier of formamide and its S, Se, and Te replacements analogs using the natural bond orbital methods, NPA [27] and NRT [28–30]. This study suggested that the weight of the dipolar form **1b** (Fig. 2.1) increases from formamide to telluroformamide in good agreement with the increase of the C–N rotational barrier.

The authors find the same structural features described previously upon rotation around the C–N bond (more significant changes for the C–N bond than for the C–S). The elongation of the C–N bond is due to two contributions: One of them is the rehybridization of the nitrogen atom (about one-third), and the other contribution is delocalizing effect (about two-thirds, treated by resonance theory). The analysis of the influence of rotation on the natural charges of NPA shows stronger charge transfer for the heavier chalcogens from the nitrogen atom to the chalcogen atom, and rotation from non-planar to planar geometry is principally accompanied by charge transfer from N to the chalcogen. It can be surprising that the less electronegative elements can accommodate more formal negative charge (increasing the contribution of the form **1b** Fig. 2.1); nevertheless, the larger polarizability of the heavier elements explains this fact [15, 18] and it is in good agreement with increased rotational barriers and decreased C–N bond lengths (i.e., more participation of the form **1b** of Fig. 2.1) for the heavier chalcogen derivatives. Nevertheless, a similar analysis of the variation of charges upon rotation using AIM theory [31] gives a different charge transfer that do not matches with the conventional resonance theory (in AIM theory, the authors find that rotation from non-planar to planar geometry is principally accompanied by charge transfer from C to the S and N atoms in an almost identical amount—Fig. 3 in the article [26]). The authors conclude that atomic charges cannot be uniquely

defined, so neither NPA nor AIM should be considered to give the “correct” charges and they focus the solution of the problem through natural resonance theory (NRT). This theory explains the planar structure as hybrid of resonance with two principal structures (**1a** and **1b** in Fig. 2.1). The structure **1b** has a higher relative weight in thioformamide than in formamide. As a result, C–N double-bond character is higher in thioformamide than in formamide, accounting for a higher C–N rotational barrier.

The amide and thioamide have been used to present a two-state model based on the BLW method on which no empirical parameter is required (BLW-DFT) [32]. The results of the structural changes indicate higher resonance energies in thioformamide than in formamide. These calculations provide contributions to the resonance structures shown in Fig. 2.1, giving values of 72 and 28% for structures **1a** and **1b**, respectively, in amide and values of 58 and 42% in thioformamide, in accordance with its high resonance energy as compared to formamide.

Prasad et al. [33] have performed a comparative study of the C–N bond rotational barriers of amide, thioamide, and selenoamide at the HF/6-31G\* and MP2/6-31G\* levels of theory. The analysis of the variation of the C–N bond length shows that this value decreases in the order amide > thioamide > selenoamide, indicating that the C–N bond order is increasing when moving from O to Se. The difference of the values of this length in planar and rotated structure (structure **2** of Fig. 2.1) increases from O to Se, indicating that the thioamide has a C=N double-bond character that is intermediate to amide and selenoamide. The calculated rotational barriers show the same trend, being the barrier of the thioamide an intermediate value between the amide and selenoamide barriers. The variation of NPA charges, evolving from the structure **2** of Fig. 2.1 to the planar structure, shows the increase in the charge of X and the decrease in the charges of NH<sub>2</sub>. The charge flow from the NH<sub>2</sub> group to X increases in the order amide < thioamide < selenoamide. These results support the delocalization of the nitrogen lone pair onto the  $\pi$  framework as suggested by the resonance model, especially for thioamide and selenoamide. However, the electronegativity does not seem to be the driving force of the electronic delocalization.

The NBO theory [9, 10] has been used by Kim et al. [34] to explain the nature of rotational barriers of the C–N bond in amides, thioamides, ureas, and thioureas, on the basis of barrier-forming N(lp)/C–O( $\pi$ )\* interaction and the anti-barrier-forming N(lp)/C–O( $\sigma$ )\* interactions. Kim et al. found that the N(lp)/C–S( $\pi$ )\* interaction in thioamide is stronger than the N(lp)/C–O( $\pi$ )\* interaction in amide.

Using as well NBO theory [9, 10], Bharatam et al. [35] have performed a comparative study of the rotation around the C–N bond in amides, thioamides, and selenoamides (X=C(H)–NH<sub>2</sub> where X = O, S, or Se) (Table 2.2). The C–N rotational barriers obtained at the G2 level are in the order 15.97 < 18.02 < 19.72 kcal/mol, respectively. The calculated C–N rotational barriers in these systems account for two factors: (1) the energy rise due to breaking the partial  $p\pi$ – $p\pi$  bond between carbon and nitrogen and (2) the energy gain due to the  $n_N \rightarrow \sigma^*_{C-X}$  negative hyperconjugation in the rotational transition state. NBO calculations show that the  $n_N \rightarrow \pi^*_{C-Se}$  delocalization is very strong with a second-order interaction energy  $\sim 120.4$  kcal/mol (the second-order delocalization energies,  $E^{(2)} = qF_{ij}^2/\Delta E_{ij}$ , are quantitative and representative of the extend of lone pair delocalization, where  $E_{ij} = E_i - E_j$  is energy



difference between the interaction of molecular orbitals  $i$  and  $j$ ,  $F_{ij}$  is the Fock matrix element for the interaction between  $i$  and  $j$ , and  $q$  is the donor orbital occupancy). This strong delocalization is due to the small energy difference  $\Delta E$  (0.45 au) and strong  $F_{ij}$  (0.208) between the interacting orbitals. The partial  $p\pi-p\pi$  C–N bond strength increases in the order formamide < thioformamide < selenoformamide because the N-lone pair delocalization in these systems follows the same order (Table 2.2). This is evidenced by the decrease in electron density on the nitrogen lone pair in formamide (1.802), thioformamide (1.740), and selenoformamide (1.723) and the increase in the second-order energy  $E^{(2)}$  due to bond delocalization in formamide (89.05 kcal/mol), thioformamide (111.2 kcal/mol), and selenoformamide (120.4 kcal/mol).

Careful analysis of NBO data indicates that the increase in the delocalization as going down the period is mainly attributable to the decrease in the energy difference between the energies of the N-lone pair and the  $\pi^*$  orbital of C–X bond: 0.59 (formamide), 0.47 (thioformamide), and 0.45 kcal/mol (selenoformamide). On the other hand, the electronegativity of X strongly influences the  $n_N \rightarrow \sigma^*_{C-X}$  negative hyperconjugative interaction. Hence, in the transition state **2** of Fig. 2.1 for formamide (entry f-2 on Table 2.2) this interaction is much stronger than in analogous transition state for thioformamide. The increase in the  $p\pi-p\pi$  delocalization (in formamide < thioformamide < selenoformamide) and decrease in the anomeric  $\pi$  interaction (in the transition states **2** of formamide > thioformamide > selenoformamide) complement each other in increasing the C–N rotational barrier in thioformamide relative to formamide. In selenoformamide, the  $\Delta E$  between the N-lone pair and  $\pi^*$  of C–Se is small, and hence, the N-lone pair delocalization is strong, relative to thioformamide and formamide. Moreover, as the observed delocalization order does not follow the increasing electronegativity order, it can be concluded that the electronegativity of X does not play an important role in the delocalization in these systems and the NBO analyses indicates that it is the  $\pi^*$  orbital who plays an important role in increasing the electron delocalization. The  $\pi^*$  interaction in the C=X bond in X=CRNH<sub>2</sub> mainly depends on the p orbital coefficients on X and C and the distance between the atoms. With the increase in the  $n$  value, the 2p–np antibonding overlap decreases ( $n$  is 2, 3, and 4 for O, S, and Se, respectively) in addition, the C=X bond length increases with the size of X, decreasing the  $\pi^*$  strength, which leads to a decrease of the energy of the  $\pi^*$  orbital and a decrease in the energy difference ( $\Delta E$ ) between the N-lone pair and the  $\pi^*$  C–X orbital. As  $\Delta E$  decreases, charge transfer from the lone pair to the  $\pi^*$  orbital increases, and hence, the charge transfer to X increases as reported [15, 21, 36].

The same arguments based on conjugative  $n_N \rightarrow \pi^*_{C-S}$  delocalization interactions have been used by Zukerman-Schpector et al. to explain the significant double character of the C–N bond in the energy minimum structures of *N,N'*-bis(pyridin-*n*-ylmethyl)ethanedithiodiamides ( $n = 2, 3,$  and  $4$ ) [37].

In an extension of the work of Bharatam et al. [35], the different variation of the C–N and C–X (X = O, S, Se) bonds upon rotation has been reported by Kaur et al. [11] by studying a collection of amides, thioamides, and selenoamides, H<sub>2</sub>NC(=X)Y, where X = Se, S, O and Y = H, F, Cl, Br, NO<sub>2</sub>, CN, NH<sub>2</sub>, CF<sub>3</sub>, CH<sub>3</sub>, SH, at the MP2/6-31+G\* level of theory, in a comparative study. In this study, the authors ana-

**Table 2.2** NBO analysis of formamide (f), thioformamide (tf), and selenoformamide (sf) at the MP2(full)/6-31+G\* level

Compound	Interaction	Second-order interaction			Occupancy		Charges				
		$E^{(2)a}$	$E_i - E_j^b$	$F_{ij}^b$	$\rho_n(N)$	$\rho_{\pi^*C-O}$	X	C	H	NH <sub>2</sub>	
f-1	$n_{N3}-\pi^*O1-C2$	89.05	0.59	0.205	1.802	0.192	-0.724	0.661	0.147	-0.083	
f-2	$n_{N3}-\sigma^*O1-C2$	14.45	1.41	0.128	1.970	0.030	-0.633	0.658	0.158	-0.183	
f-3	$n_{N3}-\sigma^*O1-C2$	7.36	1.41	0.091	1.969	0.031	-0.599	0.943	0.137	-0.180	
tf-1	$n_{N3}-\pi^*S1-C2$	111.20	0.47	0.205	1.740	0.252	-0.204	-0.002	0.223	-0.007	
tf-2	$n_{N3}-\sigma^*S1-C2$	12.14	1.07	0.102	1.968	0.034	-0.018	-0.057	0.227	-0.152	
tf-3	$n_{N3}-\sigma^*S1-C2$	2.24	1.07	0.053	1.973	0.035	0.037	0.089	0.208	-0.157	
sf-1	$n_{N3}-\pi^*Se1-C2$	120.40	0.45	0.208	1.723	0.269	-0.161	-0.059	0.228	-0.008	
sf-2	$n_{N3}-\sigma^*Se1-C2$	12.87	0.94	0.098	1.965	0.036	0.049	-0.127	0.230	-0.153	
sf-3	$n_{N3}-\sigma^*Se1-C2$	3.20	0.94	0.049	1.971	0.037	0.109	-0.163	0.213	-0.159	

Adapted from reference [35]. Copyright 2003 American Chemical Society (further permissions related to the material excerpted should be directed to the ACS)

<sup>a</sup>In kcal/mol

<sup>b</sup>In au

The indexes 1, 2, and 3 refer to planar, *cis*, and *trans* structures, respectively, in Fig. 2.1

lyzed the influence of the groups Y directly bonded to the carbon atom on the rotation around the C–N bond. In all cases, the C–N bond distance elongates and C–X bond distance (X = O, S, Se) contracts in the transition state. The variation in C–X bond distance is smaller than that in C–N bond distance, in good agreement with reported previous works [18, 21]. The planar geometry is found in the ground state of most compounds, while a pyramidal character in N atom is found in the transition states (geometries **2** and **3** of Fig. 2.1). The study of variation of charges done at MP2/6-31+G\* level, using MP2 densities by NBO method, focusing on the compounds with Y = H shows a parallel behavior on the nitrogen atom between thioamides and selenoamides. In both cases, the nitrogen atom carries negative charge (0.82 and 0.83 units for selenoamide and thioamide, respectively). The charge density on nitrogen increases by 0.15 units in both the rotational transition states (structures **2** and **3** in Fig. 2.1), which is clearly reflective of delocalization of electrons from nitrogen in the ground state that is disrupted in the transition states. In the ground state, the charge of sulfur and selenium is slightly negative (–0.09 and –0.05 units, respectively) and decreases by 0.18/0.22 and 0.21/0.25 units, respectively, in TS represented by structures **2/3**, while the carbonyl atom undergoes a very small change in the charge during the rotation. For comparison, formamide shows a more negative charge on oxygen (–0.72 units) than that on selenium or sulfur in seleno- and thioformamide, respectively, but the variation of this charge with C–N bond rotation is smaller than the analogous in thioamides and selenoamides (0.09/0.12 units in structures **2/3**). This higher charge is attributed to the higher electronegativity of oxygen, and therefore, positive charge on carbon is also increased. Interestingly, the nitrogen is more negatively charged than the same atom in thio- and selenoformamide (–0.82 units for selenoformamide, –0.83 units for thioformamide, and –0.95 units for formamide). The variation in charge on nitrogen in formamide from ground state to structures **2** and **3** is only 0.06 and 0.04 units, respectively. These values are clearly lower than the charge variations observed for thio- and selenoamides (0.14 units for both structures in thioformamide and 0.15 units for both structures in selenoformamide), and the different substituents do not change the tendency. It can be clearly seen that charge transfer from nitrogen to chalcogen in transition states is larger in heavier chalcogens than lighter ones, because of the larger polarizability of the heavier chalcogens, that allow them to accept more charge density. These results are in good agreement with the earlier report of Wiberg and Rablen [15] and confirmed by Kaur et al. [11]. The second-order delocalization energy value  $E^{(2)}$  for  $n_N \rightarrow \pi^*_{S-C}$  delocalization in thioformamides is slightly lower to that in selenoformamides (for Y = H, these values are 111.5 kcal/mol in the thioformamide and 120.4 kcal/mol in the selenoformamide, and similar trend is observed for the rest of the examples studied) which explains the higher rotational barrier in the selenoformamides relative to that in thioformamides. As said above, the higher delocalization in selenoformamide is the result of smaller energy difference between the donor and acceptor orbitals, which in turn indicates better charge acceptor capability of selenium. The  $E^{(2)}$  value for  $n_N \rightarrow \pi^*_{O-C}$  is further reduced in amides in comparison to substituted thio- and selenoamides. The effect of substituents on  $n_N \rightarrow \pi^*_{O-C}$  is stronger than in thio- and selenoamides, playing a relatively more important role in stabilization of the transition states in

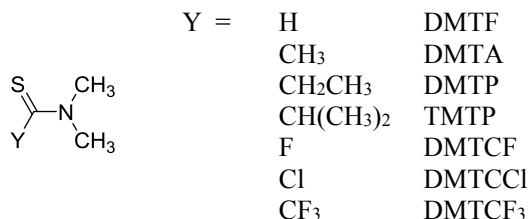


**Fig. 2.10** Thioamides studied on reference [38]. Adapted with permission from reference [38]. Copyright 1997 American Chemical Society (further permissions related to the material excerpted should be directed to the ACS)

amides than in thio- and selenoamides. It is the  $n_N \rightarrow \pi^*_{X-C}$  interaction that stabilizes the ground state and contributes mainly to the rotational barrier. The  $n_N \rightarrow \sigma^*_{C-Y}$  interactions are decisive of the substituent effect in thio- and selenoamides. These interactions tend to stabilize the transition states, thereby decreasing the rotational barrier. The C–N rotational barriers for all the substituted thio- and selenoamides studied decrease relative to their respective thio- and selenoformamides due to a stabilization of transition states and that decrease is more significant in halo substituted selenoamides. The NBO analysis explains the decrease in rotational barrier as resulting from stabilization of transition states (increase in  $n_N \rightarrow \sigma^*_{C-Y}$  and  $n_N \rightarrow \pi^*_{X-C}$  interactions). The presence of methyl substituents decreases the C–N rotational barrier in oxo-, thio-, and selenoamides which can be understood as the result of stabilization of the transition state. The decrease is more pronounced in the rotational barrier through a transition state represented by structure 2.

An experimental and theoretical study performed on the *N,N*-dimethylthioamides shown in Fig. 2.10 has been developed by Neugebauer Crawford et al. [38].

The authors of this work calculated through temperature-dependent gas-phase <sup>1</sup>H NMR spectra the free activation energies,  $\Delta G^\ddagger_{298}$ , of the C–N rotation in the thioamides. Experimentally, a higher  $\Delta G^\ddagger_{298}$  value for DMTA (18.0 kcal/mol) than for DMTCF<sub>3</sub> (17.2 kcal/mol) was found, and this fact is explained on the basis of a higher steric effect of the CF<sub>3</sub> group when compared to CH<sub>3</sub>. To further explore the changes in atomic charge and polarity of the thiocarbonyl bond when electron-withdrawing substituents are present, the authors performed ab initio calculations at the 6-31+G\* level on thioformamide, thiocarbonyl fluoride, and thiocarbonyl chloride (and the related amides). They found small changes on the polarity of the C=S bond, maintaining a positive charge on the thiocarbonyl carbon atom, and they explain that the ab initio results are consistent with a small effect of electron-withdrawing substituents on thioamides, being the rotational barrier in *N,N*-dimethylthioamides extremely sensitive to the steric features of the thiocarbonyl substituent.

Vassilev and Dimitrov have performed a similar study on thioamides X–C(S)N(CH<sub>3</sub>)<sub>2</sub> (X = H, F, Cl, CH<sub>3</sub> and CF<sub>3</sub>) checking the influence of the X substituent in the C–N bond rotational barriers at the MP2(fc)/6-31+G\*\*/6-31G\*

and MP2(fc)/6-311++G\*\*//6-311++G\*\* levels of theory and compared with literature NMR gas-phase data [39]. The most significant structural changes found in the process of rotation are that the nitrogen is pyramidalized, the C–N bond lengthens by 0.07–0.10 Å, and the C=S bond shortens by 0.05 Å. Similar calculations performed on related amides showed a shortening of the C=O bond length of about 0.01–0.02 Å, indicating that the thiocarbonyl group is relatively more affected by the rotation in comparison to carbonyl group in the oxoamides.

The experimental rotational barriers of the studied compounds in the gas phase follow the trend: H > F > CH<sub>3</sub> > CF<sub>3</sub> > Cl, and correlate mainly with the substituent size and not with the substituent electronegativity. The calculations carried out indicate that the repulsion between X and the *anti* CH<sub>3</sub> group (*anti* refers to the relative position with respect to the sulfur atom) is mainly responsible for the differences in the rotational barriers in thioamides.

### 2.3.2 Solvent Effects

The nature of the solvent is an additional influence to the rotational barrier since the charge-separated structure of the rotational ground state is stabilized by polar solvents. It is expected that the barrier heights will be increased with more polar solvents.

Wiberg and Rush have studied solvent effects on the C–N rotational barriers of *N,N*-dimethylthioformamide (DMFT) and *N,N*-dimethylthioacetamide (DMTA) both theoretically (*ab initio*) and experimentally (NMR) [36]. The authors find a good correlation between the experimental and theoretical data obtained at the level G2(MP2) in gas phase. The solvent effects are satisfactorily modeled via the SCI-PCM reaction field model [40] at the HF/6-31+G\* level of theory for many aprotic, nonaromatic solvents that do not engage in specific interactions with the solute molecules. The C–N bond rotation may occur via both TS1 and TS2, and the final calculated barrier heights include the contribution from the two paths. The experimental values for DMTA are uniform, about 0.4 kcal/mol higher than those of the calculated barriers. In the case of DMFT, the experimentally observed values are close to the calculated barriers. In both cases, the agreement between the calculated and observed rotational barriers is satisfactory. The conclusion that the authors reach is that the solvent effects on the rotational barriers are considerably larger for DMTA than for DMA, and this results from the larger ground-state dipole moments for the thioamides than for amides. This fact correlates well with a larger dipole moment of the thioamide and its larger change in dipole moment on going to the transition state as compared with DMA [15, 17]. The dipole moments for the transition state are similar for the two systems.

Kaur et al. have studied solvent effects using self-consistent reaction field calculations at B3LYP/6-31+G\* level on the value of the C–N bond rotation of C-substituted amides, thioamides, and selenoamides [11]. They found that the differences in dipole moments of ground states and transition states both in gas phase and

solvation increase from amide to thioamide and from thioamide to selenoamide. The dipole moment of substituted amides and their thio- and seleno-analogs undergoes variations, which are the result of variations in electronegativity, polarizability, and relative orientations of different atoms in a given conformation. The smaller difference in dipole moments of ground states and transition states of amides leads one to expect smaller solvent effect on the rotational barriers. The effect of solvents is more prominent in selenoformamide, thioformamide, and formamide than in respective substituted amides. The rotational barriers increase with increase in polarity of solvent, thereby suggesting the role of electrostatic interactions in solution phase.

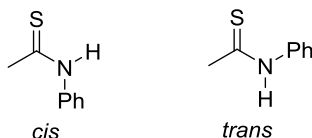
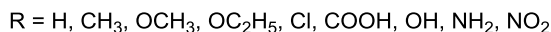
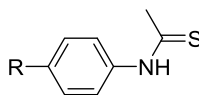
Combined *ab initio* quantum mechanical, molecular mechanical (QM/MM), and molecular mechanical Monte Carlo simulations, followed by BLW-based two-state model analyses, has been performed to study the behavior of thioformamide and formamide in aqueous solution [32]. In this work, it is found that on average, about three or five water molecules are found to form hydrogen bonds with the carbonyl oxygen or sulfur in the first hydration shell, while two water molecules are found to solvate the amino group in solutes. In the analysis of the solvent–solute interaction energies, it is found that the thioformamide interacts more strongly with water molecules than formamide. There are interesting structural changes of solutes from gas phase to solution such as the shortening of the C–N bond in both cases and lengthening of the C=E (E = O, S) bonds. This strongly implies the enhancement of resonance and the increasing role of the structure **1b** of Fig. 2.1 in good agreement with the chemical intuition that the ionic structure will be favored in polar solutions.

### 2.3.3 Influence of Remote Substituents

Galabov et al. [41] have used density functional theory at the B3LYP/6-31G(d,p) level to determine the geometries, vibrational frequencies, and rotational barriers in a series of nine *p*-substituted thioacetanilides (Fig. 2.11). Now, for the planar geometry, it is possible to distinguish two isomers because the amide nitrogen atom has two different substituents (the examples commented above have two hydrogen atoms or two methyl substituents).

Among the structural parameters of the optimized structures, the authors focus on the amide C–N bond length,  $r_{\text{C-N}}$ , because this parameter can be considered as a quantity characterizing the strength of the bond and could, therefore, be related to the barrier of rotation. On a previous work, the same group has studied the rotation of *para*-substituted acetanilides [42], and by comparison of the bond length  $r_{\text{C-N}}$  in both families of compounds, a shorter distance is found in thioacetamides, which suggests a stronger bond that would involve higher barriers of rotation. The *trans* thioacetanilides have a planar structure of the main skeleton of the molecule, with the thioamide group lying in the plane of the aromatic ring (deviations from planarity are  $<3^\circ$ ). The *cis* form is non-planar, and the authors find values for the dihedral angle between the –CS–NH– group and the aromatic ring in the range of  $33^\circ$ – $57^\circ$ . Similar structural features are also found in the substituted acetanilides. The

**Fig. 2.11** *N*-substituted thioacetanilides



calculations performed for Galabov et al. show a very small difference between the energies of the *cis* and *trans* forms in the range of 0.03–0.63 kcal/mol, indicating that both rotameric forms should be populated at room temperature as it is found experimentally [43–46]. In the theoretical calculations, two transition states are found for the conversion between the two rotameric forms, reflecting two possible orientations of the nitrogen lone pair, with respect to the C=S bond. Nevertheless, the authors consider only the smallest barrier because the conformational change is more likely to occur via the lower-energy transition state. The comparison of the rotational barriers calculated for thioacetanilides with the respective acetanilides showed higher values for thioacetanilides, and the influence of the remote substituents in the aromatic ring over the rotational barriers is almost twice as high in the thioanilides (Table 2.3). The authors explain these differences based on the electronic structure of the compounds at equilibrium and also on its dynamics with the internal rotation around the C–N bond (see below). Steric hindrance effects that result from the size of the S atom in the thioacetanilide series can be ruled out because of the almost perfectly planar structure for the *trans* conformers. For the *cis* conformers, the equilibrium structure is non-planar, evidently because of the steric interaction between the methyl group and the *ortho* H atom.

The analysis of the values of Table 2.3 reveals that the presence of electron-donating substituents (OCH<sub>3</sub>, NH<sub>2</sub>) increases the differences in barrier heights, while the presence of strong electron-withdrawing substituents (COOH, NO<sub>2</sub>) diminishes this difference, being practically equal in the case of NO<sub>2</sub>. These findings can be explained in terms of resonance interactions in the systems. The electron-donating substituents make more accessible the structure **1b** of Fig. 2.1 resulting in an increased barrier of rotation. Inversely, the electron-withdrawing substituents hamper the electronic delocalization of the lone pair of the nitrogen atom resulting in a lower rotational barrier.

There are correlations between the theoretically evaluated barriers of rotation in the studied thioacetanilides and intrinsic structural and electronic parameters of the thioamide group. For example, there is a good linear relationship between the C–N bond length (related to the strength of the bond) and the energy barriers  $\Delta E$ . Never-

**Table 2.3** B3LYP/6-31G(d,p) calculated rotational barriers in *para*-substituted thioacetanilides and acetanilides

<i>para</i> Substituent	$\Delta E = E_{\text{TS2}} - E_{\text{trans}}^{\text{a}}$ (kcal/mol)	
	Thioacetanilides	Acetanilides
H	19.29	18.25
CH <sub>3</sub>	19.70	18.42
OCH <sub>3</sub>	20.66	18.85
OC <sub>2</sub> H <sub>5</sub>	20.67	19.06
Cl	19.08	18.26
COOH	17.74	17.31
OH	20.30	18.85
NH <sub>2</sub>	21.05	19.17
NO <sub>2</sub>	17.06	17.08
SO <sub>2</sub> NH <sub>2</sub>		17.49

Adapted with permission from reference [41]. Copyright 2003 American Chemical Society (further permissions related to the material excerpted should be directed to the ACS)

<sup>a</sup>The rotational barriers are calculated as the differences between the energy of the TS2 transition state ( $E_{\text{TS2}}$ ) and the energy of the *trans* conformer ( $E_{\text{trans}}$ )

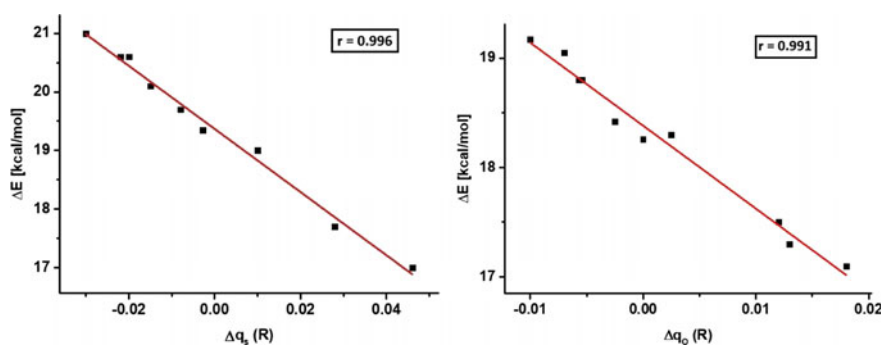


**Fig. 2.12** Dependence of rotational barriers ( $\Delta E$ ) on shifts of NBO charges at the S and O atoms ( $\Delta q_S$  and  $\Delta q_O$ ) induced by aromatic substituents in thioacetanilides (left) and acetanilides (right). Adapted with permission from reference [41]. Copyright 2003 American Chemical Society (further permissions related to the material excerpted should be directed to the ACS)

theless, the range of variation of  $r_{\text{C-N}}$  is very close in both anilides and thioanilides (0.013 Å) indicating that this length variation does not provide a sufficiently sensitive basis for rationalizing the differences in rotational barriers that are induced by the substituents. The variation of barrier heights can also be linked to the charge rearrangements in the  $-\text{CX}-\text{NH}-$  ( $X = \text{S}, \text{O}$ ) moiety. Linear correlation dependences between rotational barriers,  $\Delta E$ , and the NBO charge shifts at the S and O atoms induced by the aromatic substituent are found (charge shifts are referred to the equilibrium structure of the *trans* conformers, Fig. 2.12).



In these correlations, it is found that the same substituents induce much greater charge shifts in the thioacetanilide series than in the respective acetanilides and also it is found that greater electronic interactions in the thioamides lead to a stronger C–N bond and a higher rotational barrier. The electronic effect of *para*-aromatic substituents is exerted primarily through resonance. Finally, the analysis of the charge shifts upon rotation from the ground state to the transition state indicates that a much greater portion of negative charge is withdrawn from the S atom in thioacetanilides upon rotation, compared with the respective charge shifts at the carbonyl O atom in acetanilides. Analysis of the NBO charge fluctuations reveals that most of the charge transfer is located between the carbonyl S (or O) and the N atoms. The shifts of carbon charges are small in both series. The results are in accordance with the classical picture of amide resonance in which the conjugative effects are strong in the *trans* planar structures while being essentially eliminated in the transition states. The relationships between  $\Delta E$  and shifts of the NBO charges show that the linear correlation is consistent with the interpretation of rotational barriers in terms of amide resonance. The disruption of resonance interactions upon rotation is accompanied by greater charge shifts within the amide grouping in the thioacetanilides. The results indicate that these interactions are significantly greater in the thioamides. Similar conclusions are reached by analyzing the atomic charges at equilibrium.

Interestingly, the influence of the substituent depends on the position of the aromatic group bonded to the thioamide. When the aromatic group is bonded to the thioamide nitrogen, electron-donating substituents on the ring increase the barrier of rotation and electron-withdrawing substituents decrease the rotational barrier (as described by Galabov et al. [41], see above). But when the aromatic group is bonded to the thiocarbonyl carbon of the thioamide (Fig. 2.3), the more electron-withdrawing groups on the ring tend to increase the thioamide rotational barriers [5].

A recent work of Śmiszek-Lindert et al. [47] reports the comparative study of *m*-acetotoluidide and *m*-thioacetotoluidide. The authors study the models at the B3LYP/6-311++G(d,p) and B3LYP/6-311++G(3df,2pd), and they find a good correlation between the experimental and the optimized structures, as well as good agreements in vibrational calculations and experimental FT-IR and FT-Raman spectra. Nevertheless, in this work a very small value for the barrier of rotation around the C–N bond of the thioamide is reported (1.49 kcal/mol) when compared with the value reported by Galabov et al. for the very related compound with the methyl group located in *para* position (19.70 kcal/mol, Table 2.3). Although the bases used are different, the reported difference in energy is huge to be justified by the change of basis. In addition, the value of the energy of the rotation for the *m*-acetotoluidide (3.9 kcal/mol) is bigger than the value of the related thioamide, which is in contrast with the examples found, and still it is a small value when compared with the one calculated by Galabov (18.42 kcal/mol, Table 2.3) for the similar *p*-acetotoluidide.

### 2.3.4 Photoisomerization

Helbing et al. have studied both experimentally and theoretically the photoisomerization of the *trans* form of *N*-methylthioacetamide (Fig. 2.13) [48]. Ab initio CASPT2//CASSCF photochemical reaction path calculations indicate that, in vacuo, the *trans*  $\rightarrow$  *cis* isomerization event takes place on the  $S_1$  and/or  $T_1$  triplet potential energy surfaces and is controlled by very small energy barriers, in agreement with the experimentally observed picosecond time scale.

The *trans* stereoisomer is more stable by 1.9 kcal/mol. Two fully asymmetric  $S_0$  transition states describe the *trans*  $\rightarrow$  *cis* thermal isomerization reaction. They are located 24.9 and 20.7 kcal mol<sup>-1</sup> above *trans*-NMTAA, respectively. Ab initio CASPT2//CASSCF reaction path computations for  $\pi$ - $\pi^*$  excitation of *trans*-NMTAA yield consistent mechanistic information on the *trans*  $\rightarrow$  *cis* isomerization of NMTAA. The initial  $S_2$  population evolves on  $S_2$  mainly via a C-S bond expansion (and out-of-plane deformation) leading to efficient  $S_2 \rightarrow S_1$  decay in the region of the  $S_2/S_1$  conical intersection. Relaxation on  $S_1$  delivers the system to a very flat region of the potential energy surface, characterized by multiple conformers and multiple  $S_1/S_0$  conical intersections located a few kcal/mol above them. Decay to the ground state may then occur directly via the  $S_1/S_0$  conical intersections or indirectly. Approximately half of the excited molecules seem to follow the direct relaxation pathway and return to the electronic ground state with a time constant of less than 7 ps. The second half of the excited molecules become temporarily trapped in an electronically excited state and reach the electronic ground state with a much longer time constant of  $\sim$ 250 ps. This population trapping can be the result of either competition between vibrational energy relaxation on  $S_1$  and  $S_1 \rightarrow S_0$  electronic decay or competition between fast  $S_1 \rightarrow S_0$  decay and a somehow slower relaxation process via the triplet states. On both the fast and the slow time scale, *cis*-NMTAA is formed

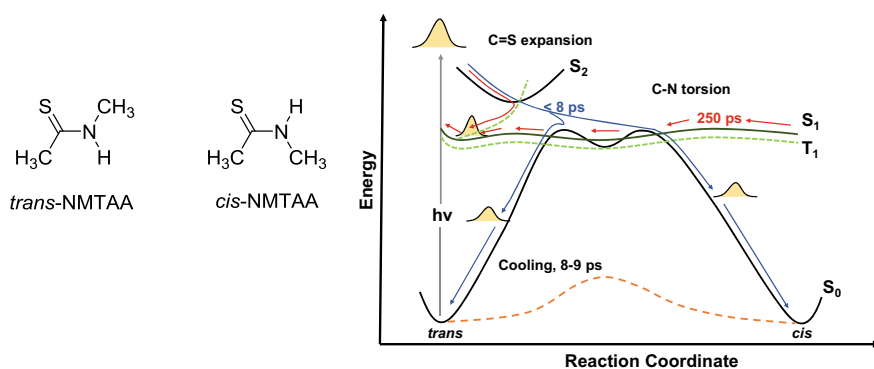


**Fig. 2.13** Isomers of the *N*-methylthioacetamide and schematic representation of the photoisomerization reaction of *trans*-NMTAA. Adapted with permission from reference [48]. Copyright 2004 American Chemical Society (further permissions related to the material excerpted should be directed to the ACS)

with a quantum efficiency of 30–40%. Olivucci et al. establish that the final ground-state conformation of NMTAA is predetermined by the molecular geometries of the  $S_1/S_0$  conical intersections and  $T_1/S_0$  intersystem crossings and is therefore independent of the followed route, provided nearly full sampling of the torsional coordinate in  $S_1$  and/or  $T_1$  is possible prior to decay.

### 2.3.5 C–N Bond Rotation in Complex Systems

The rotational studies around C–N bonds on thioamides are not studied only on simple systems. Kleinpeter et al. [49] have studied both experimentally and theoretically amino-substituted thio(seleno)acrylamides. The possible isomers of the skeleton studied are depicted in Fig. 2.14.

The compounds exist as preferred  $E(s-cis)$  isomers, and the additional isomers observed when  $N(\text{Me})\text{Ph}$  substituents are present were assigned using the GIAO ab initio-calculated ring current effect of  $N$ -phenyl.

Experimental rotational barriers have been calculated using NMR techniques, but the theoretical calculations (at different levels of theory including ab initio and DFT) have been used to confirm the experimental observations. As discussed in other works, the values of the barriers of rotation found in amino-substituted thioacrylamides are smaller than in seleno analogs due to the higher polarizability of the bigger selenium atom.

By means of the NBO analysis, the occupation numbers of the lone electron pairs of  $N-1/N-3$ , of the bonding/antibonding  $\pi/\pi^*$  orbitals of the central  $C_1=C_2$  partial double bond and of the antibonding  $\pi^*$  orbitals of the  $C=S$  bonds were calculated and

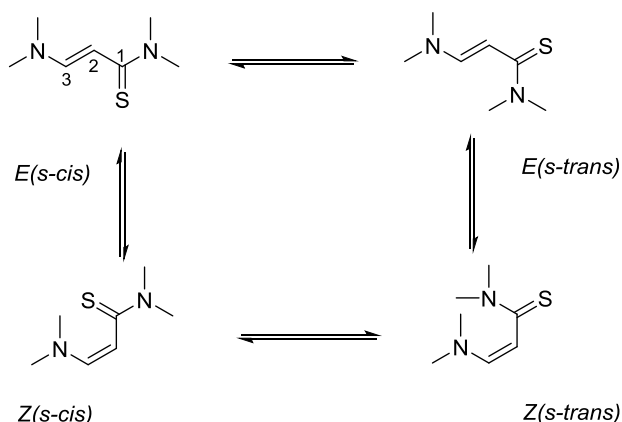
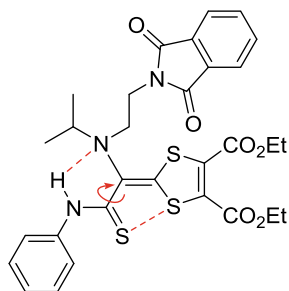


**Fig. 2.14** Rotational isomers of thioacrylamides. Adapted with permission from reference [49]. Copyright 2005 American Chemical Society (further permissions related to the material excerpted should be directed to the ACS)

**Fig. 2.15** Rotational bond and S–S hypervalent bonding interaction. Adapted with permission from reference [50]. Copyright 2015 American Chemical Society (further permissions related to the material excerpted should be directed to the ACS)



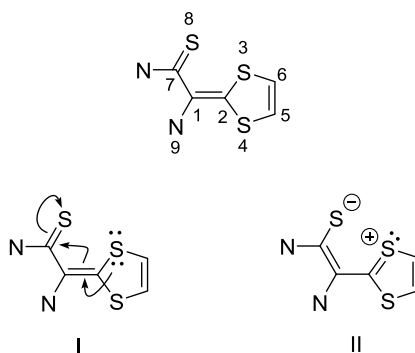
shown to quantitatively describe thioamide/vinylogous thioamide resonance. Thus, similar  $\Delta G^\ddagger_c$  values for C<sub>1</sub>–N and C<sub>3</sub>–N restricted rotations do not indicate the same amount of the two resonance interactions as thioamide resonance proved to be much stronger. However, the difference to the vinylogous resonance is balanced by additional N-1 lone pair/ $\pi^*(C_1,C_2/N_2)$  orbital interactions.

Fuertes et al. described a dynamic behavior in solution of (1,3-Dithiol-2-ylidene)ethanethioamides [50]. These compounds were studied by a combination of dynamic NMR, single-crystal X-ray diffraction, and DFT modeling of the dynamic behavior observed in solution. The bigger size of the substituents of the thioamide is the reason of the appearance of additional factors to understand the energetics of the C–N bond rotation. The steric hindering of the crowded substitution at the central amine group was found to be the reason for the presence of permanent atropisomers (Fig. 2.15).

The absolute minimum found in the optimization of the model used for the theoretical study (Fig. 2.15) displays a planar geometry on the thioamide environment in good agreement with smaller thioamides described above. This absolute minimum displays a distance of 1.999 Å between the hydrogen atom of the thioamide group and the amine nitrogen atom which is in the range of the hydrogen bond interactions, and it can be classified as a moderate–weak hydrogen bond [51]. Although several bond rotations can be proposed to explain the dynamic behavior observed in solution, the rotation that shows a better agreement with the experimental values is the rotation about the C–N bond of the thioformamide. For the compound used as a model, an experimental value of 14.85 kcal/mol was determined in comparison with 13.92 kcal/mol calculated in gas phase at the theory level B3LYP/6-31G(d). The consideration of the solvation effects with a PCM model at the level of theory B3LYP/6-311G(2d,p)//B3LYP/6-31G(d) afforded a free energy value of 12.20 kcal/mol.

A closer inspection of the electronic structure by using the NBO population approach analysis was performed for the evaluation of the electronic delocalization. These calculations clearly indicated the presence of two lone pair orbitals formally attached at the thiocarboxylic sulfur atom and to the dithiafulvene sulfur atoms. The nature of one of these orbitals on each sulfur atom is a pure *p*-type [ $lp_p(S)$ ], having the orbitals of the sulfur atoms of the dithiafulvene a low electron occupancy of

**Fig. 2.16** Labeling of the atoms used for the NBO analysis. Adapted with permission from reference [50]. Copyright 2015 American Chemical Society (further permissions related to the material excerpted should be directed to the ACS)



1.65 and 1.68 e, indicating the electron-donating capacity for this orbital. Delocalizing interactions evaluated by a second-order perturbation approach revealed that the lone pair orbital located at the dithiafulvene sulfur atoms contributed to a resonance interaction with double bond C(1)=C(2) (see Fig. 2.16 for numbering)  $lp_p(S) \rightarrow \pi^*_{C-C}$ .

The computed  $E^{(2)}$  interaction value was 26.1 and 23.3 kcal/mol for sulfur atoms S(3) and S(4), respectively. Interestingly, in the analysis of more delocalizing interactions, it was possible to find a second delocalization of the pair of electrons located at the bonding orbital  $\pi_{C-C}$  involving atoms C(1) and C(2) with the double bond C(7)=S(8),  $\pi_{C-C} \rightarrow \pi^*_{C-S}$ . In this second delocalization, the computed  $E^{(2)}$  interaction value was 19.0 kcal/mol. The combination of these two delocalization events was in good agreement with the resonance structures I and II shown in Fig. 2.16, and both structures accounted for the planar geometry found in this structure. In addition, the atomic charges obtained by using the natural population analysis (NPA) approach revealed a positive charge +0.34 located at the sulfur atom S(3) and a negative charge -0.15 located at the thioamide sulfur atom S(8), in good agreement with the resonance structure II of Fig. 2.16. These opposite charges reinforced the hypervalent interaction through electrostatic attraction.

A conformational study was performed for proline (Pro) derivatives shown in Fig. 2.17 to examine the effects of oxygen-to-sulfur and oxygen-to-selenium isosteric substitutions on conformational preferences and prolyl *cis-trans* isomerizations of Pro-containing peptides in water [52]. In this review, we are only going to comment on the results of the effects of oxygen-to-sulfur substitutions.

The isosteric replacement of a peptide bond by a thiopeptide bond at the preceding residue of the Pro residue in the first model in Fig. 2.17 (i.e., the *N* terminus), resulted in changes in the preferences of the backbone conformation and puckering of the proline residue in Ac-Pro-NHMe (X = O). In particular, the up-puckered

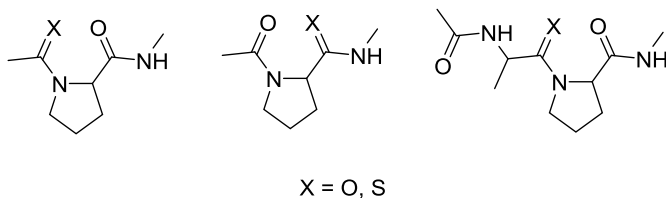


**Fig. 2.17** Chemical structures of modeled compounds in reference [52]. Adapted with permission from reference [52]. Copyright 2017 Royal Society of Chemistry (further permissions related to the material excerpted should be directed to the RSC)

polyproline II ( $P_{II}$ ) structure was energetically, enthalpically, and entropically preferred for Ac-Pro-NHMe, whereas the down-puckered  $P_{II}$  structure was energetically and enthalpically preferred for S substituted Pro-dipeptides. In the second model of Fig. 2.17, the substitution of oxygen by sulfur at the C terminus of the Pro residue, the thiopeptide resulted in puckering of the proline residue in Ac-Pro-NHMe. In the third model of Fig. 2.17, Ac-Ala-Pro-NHMe, open conformers with the *trans* prolyl peptide bond were preferred, and the substitution of oxygen by sulfur leads to an up-puckered  $3_{10}$ -helical structure for the Pro residue.

The rotational barriers to the prolyl *cis-trans* isomerization of Ac-Pro-NHMe and Ac-Ala-Pro-NHMe increased with isosteric replacements at the *N* terminus in the order  $O < S$ . However, the isosteric replacement at the *C* terminus did not alter the rotational barriers to the prolyl *cis-trans* isomerization of Ac-Pro-NHMe.

## 2.4 Rotational Barriers of N-Substituents

Rotation around other bonds different to the C-N amide bond has been modeled. Wiberg and Rush have studied the methyl rotational barriers in amides and thioamides focusing on the C-N bonds of *N*-methyl and *N,N*-dimethyl [53]. As shown in Fig. 2.18, several conformers can be proposed for *N*-methylthioformamide, and *N,N*-dimethylthioformamide (analogous forms can be proposed for *N*-methylthioacetamide and *N,N*-dimethylthioacetamide, but considering the rotation of the acetyl methyl group as well). According to the relative orientation of the *N*-methyl group and the sulfur atom in *N*-methylthioformamide, *E*- and *Z*-forms can be proposed. Additionally, for each of these orientations the relative rotamers of the methyl group have to be taking into account, and a second symbol refers to a methyl hydrogen being either *syn* (*s*) or *anti* (*a*) with respect to the thio-carbonyl group. In the *E*-form of the *N*-methylthioformamide, the methyl rotational barrier is somewhat reduced as compared to *N*-methylformamide (0.47 kcal/mol

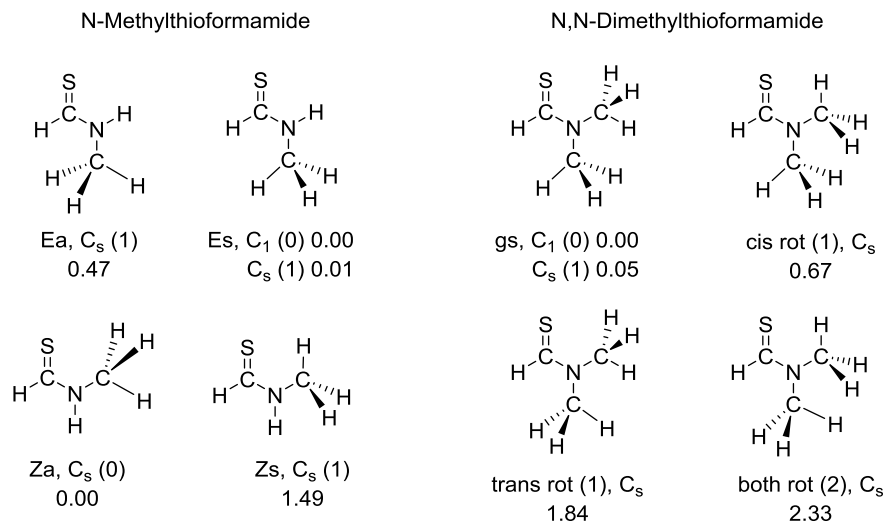


**Fig. 2.18** Rotamers of *N*-methylthioformamide and *N,N*-dimethylthioformamide. Adapted with permission from reference [53]. Copyright 2002 American Chemical Society (further permissions related to the material excerpted should be directed to the ACS)

for *N*-methylthioformamide and 0.88 kcal/mol for *N*-methylformamide). Following the comparison between *N*-methylthioformamide and *N*-methylformamide, it is interesting to highlight the increase in the barrier for the *Z*-form, which is over 1 kcal/mol greater than that for the corresponding formamide (1.49 kcal/mol for *N*-methylthioformamide and 0.33 kcal/mol for *N*-methylformamide). The steric hindrance of the bigger sulfur in comparison to the size of the oxygen can be the reason of a bigger repulsive interaction between the sulfur and an eclipsed hydrogen of the methyl group of the *Z*-form. These higher repulsive interactions in the thioamides are reflected in the C–N–C bond angles. For the *N*-methylformamide, the values of these angles are 120.7° in the isomer *Za* and 123.0° in the isomer *Zs*, while for the *N*-methylthioformamide the values of the same angles are 122.4° in the isomer *Za* and 125.0° in the isomer *Zs*. The same factor is responsible for the differences found on the geometry of the lowest energy conformers of the *N,N*-dimethylthioformamide and its analogous amide. In the amide, the *Z*-methyl group is rotated so that a methyl hydrogen is eclipsed with the carbonyl oxygen. In the *N,N*-dimethylthioformamide, the *cis*-Me–C–N–H torsional interaction is greater than the O···H non-bonded interaction, but the *Z*-methyl group is rotated so that it is not eclipsed with the sulfur, which may be related to the larger size of the sulfur, making the S···H non-bonded interaction the dominant term. Similar facts have been described for thioacetamides. The *E*-forms of *N*-methylthioacetamide show similar relative energies as for *N*-methylacetamide indicating that the replacement of oxygen by sulfur has little effect on the barrier. The reason of this little effect is the long distance between the *N*-methyl group and the sulfur. However, there are marked changes in the relative energies of the *Z*-forms. In

Z-forms, the proximity between the O/S atom and the *N*-methyl group is bigger than in *E*-forms and the rotamers of *N*-methylthioacetamide having a methyl hydrogen eclipsed with the sulfur display an increase in energy of about 1.5 kcal/mol with respect to the alternate forms. The *N,N*-dimethylthioacetamide has a ground-state rotamer with a rotated *Z*-methyl avoiding proximity between the sulfur atom and the hydrogen atoms (in the analogous *N,N*-dimethylacetamide, the same *Z*-methyl locates a hydrogen atom eclipsed with the oxygen atom).

## 2.5 Conjugation with Different Substituents

Velkov et al. [54] have studied the interaction of the carbonyl and thiocarbonyl group of the amide and thioamide of *o*-coumaric acid using HF and DFT theoretical methods (Fig. 2.19).

Several structural parameters show that there is conjugation between the *o*-coumaric acid and the amide or thioamide. One of them is the length of the C–N bond, which is found to be longer in the *o*-coumaric derivatives than amide and thioamide. The conjugation degree in the thioamide is considerably higher than that in the amide. For example, the calculated bond length for the double C=C bond connecting the aryl group with the carboxylic (or thiocarboxylic) group is shorter for the thioamide. Data based on NBO analysis point toward the same direction (see Table 2.4). The lone pair delocalization of the nitrogen atom (estimated through second-order energies on NBO analysis) is more effective in the thioamide than in the amide. The direction of this delocalization is toward the C=O and the C=S double bonds, respectively. The interaction energy between the electron pair of the C=C bond (connecting the aryl group with the amide/thioamide fragment) and unoccupied neighboring orbitals shows a favored direction of conjugation which is toward the amide/thioamide group.

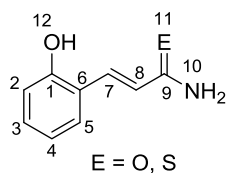


**Fig. 2.19** Amide and thioamide of *o*-coumaric acid. Adapted from reference [54]. Copyright 2006 Wiley Periodicals, Inc. (further permissions related to the material excerpted should be directed to Wiley Periodicals, Inc.)



**Table 2.4** Some second-order energies (in kcal/mol) obtained by the B3LYP and HF methods and basis 6-31+G(d)

Compound	Method	Second-order energies		
		$n_{N10} \rightarrow to$	$\pi_{C7=C8} \rightarrow to$	$n_{O12} \rightarrow to$
Amide	UB3LYP	$\pi^*_{C9=E}$ (55.47)	$\pi^*_{C9=E}$ (19.41) $\pi^*_{C5=C6}$ (10.04)	$\pi^*_{C1=C2}$ (28.38)
	UHF	$\pi^*_{C9=E}$ (39.00)	$\pi^*_{C9=E}$ (13.02) $\pi^*_{C5=C6}$ (4.79)	$\pi^*_{C1=C2}$ (22.80)
Thioamide	UB3LYP	$\pi^*_{C9=E}$ (68.84)	$\pi^*_{C9=E}$ (23.72) $\pi^*_{C5=C6}$ (10.41)	$\pi^*_{C1=C2}$ (34.81)
	UHF	$\pi^*_{C9=E}$ (58.81)	$\pi^*_{C9=E}$ (18.26) $\pi^*_{C5=C6}$ (5.29)	$\pi^*_{C1=C2}$ (23.30)
Amide radical	UB3LYP	$\pi^*_{C9=E}$ (28.88)	$\pi^*_{C9=E}$ (10.91)	$n^*_{C1}$ (69.17) $\pi^*_{C1=C6}$ (10.43) $\pi^*_{C1=C2}$ (9.34)
	UHF	$\pi^*_{C9}$ (54.56)	$n^*_{C9}$ (69.17)	$\pi^*_{C1=C2}$ (59.83) $\pi^*_{C1=C6}$ (11.41)
Thioamide radical	UB3LYP	$\pi^*_{C9=E}$ (36.35)	$\pi^*_{C9=E}$ (14.47)	$n^*_{C1}$ (72.03) $\pi^*_{C1=C6}$ (9.50) $\pi^*_{C1=C2}$ (8.43)
	UHF	$\pi^*_{C8=C9}$ (54.70)	$\pi^*_{C8=N10}$ (2.36) $\pi^*_{C8=C9}$ (2.12)	$\pi^*_{C1=C6}$ (13.95) $\pi^*_{C1=C2}$ (12.86) $r^*_{C1}$ (10.42)

Adapted with permission from reference [54]. Copyright 2006 Wiley Periodicals, Inc. (further permissions related to the material excerpted should be directed to Wiley Periodicals, Inc.)

Symbols  $\pi$ ,  $n$  (lone pair), and  $r$  (Rydberg orbitals), and  $\pi^*$ ,  $n^*$  and  $r^*$ , are used for notation of the filled and vacant NBOs of the formal Lewis structures

## 2.6 Thiopeptides

Thioamide substitution into peptide structures has been explored by several groups. Artis and Lipton have studied the potential energy surface of four model dipeptides containing thioamide bond (Fig. 2.20) [55]. The study has been developed at the HF/6-31G\* level of theory, and then, they have used selected regions as starting points for full geometry optimization at the HF/6-31G\* and MP2/6-31G\* levels. Both levels of theory afford similar results with small changes in relative energies that were small when compared to the consequences of sulfur substitution.

The authors find that the conformations of the C-terminal thioamides were generally close to those of the corresponding peptides, and the N-terminal thioamides displayed markedly different conformational behavior. The changes in the conformational profile of thioamide-containing peptides appear to result from a combination of the decreased hydrogen bonding-accepting ability and increased size of sulfur versus oxygen and lengthening of the C=S bond in the thioamide as compared to

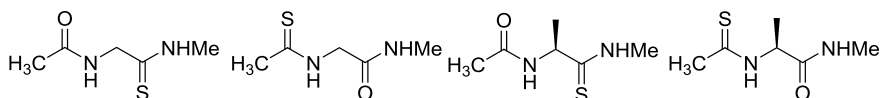


**Fig. 2.20** Model dipeptides studied by Artis and Lipton. Adapted with permission from reference [55]. Copyright 1998 American Chemical Society (further permissions related to the material excerpted should be directed to the ACS)

the C=O bond in an amide. The predominant effect of the substitution of sulfur is on the residue following the thioamide bond in the sequence (i.e., to the C-terminal side) and serves to strongly bias this residue toward a conformation in the region of negative  $\phi$  and positive  $\psi$ .

Tran et al. [56] have studied the conformational analysis of thiopeptides. The authors of this work found that the hydrogen bond lengths calculated at the HF/6-31G\* level of theory are much longer than the corresponding hydrogen bond lengths for normal peptides when the bulkier sulfur atom acts as hydrogen bond acceptor in the  $C_5$  conformation or in the  $C_7^{ax}$  and  $C_7^{eq}$  conformations in a vacuum environment. For this reason, the  $\phi$ ,  $\psi$  dihedral angles of the  $C_5$ ,  $C_7^{ax}$  and  $C_7^{eq}$  conformations of thiopeptides change to accommodate the longer hydrogen bonds. The authors also predict that upon thio substitution at the amino terminal, the  $C_7$  conformations will be disfavored relative to the  $C_5$  conformations. However, upon thio substitution at the carboxyl terminal, the  $C_7$  conformations are favored relative to the  $C_5$  conformation. The authors hypothesize that the change of the type of hydrogen bonding can be the reason for this switch in conformational preference. The ( $\phi$ ,  $\psi$ ) conformational energy maps for the glycine, alanine, and thio-substituted dipeptides calculated using several relative permittivities to simulate the conformations in solution indicated that thio substitution does restrict the conformations available to amino acids residues in peptides. The areas on the ( $\phi$ ,  $\psi$ ) energy maps for the thiopeptides, which will be accessed spontaneously under standard temperature and pressure conditions, are considerably smaller than the corresponding areas for normal peptides. Thio substitution at the amino terminal and at the carboxyl terminal introduces an unfavorable interaction that restricts some conformations. This restriction of conformations does not mean that the thiopeptides show only one conformation, and some of them can prefer one or two conformations, as it has been demonstrated by Tran et al. at the CFF91 force field level of theory [57, 58].

Molecular dynamic simulations have been performed by Tran et al. [59] to study the effects of thio substitutions on the conformation on dipeptides finding that thio substitution favors conformations were  $\phi < 0$  because of the deeper  $\beta$  and right-handed  $\alpha$ -helix. The same group has developed molecular dynamics simulations to study the effects of thio substitutions on the conformation on of  $\alpha$ -helices,  $3_{10}$ -helix, and their relative stability on longer polypeptides [60]. The dynamic simulations show that the most prominent structural change to the  $\alpha$ -helices and  $3_{10}$ -helices conformations introduced by the thio substitution is the increased hydrogen bond distance from 2.1 to 2.7 Å. Consequently, there is a modification in the value of the

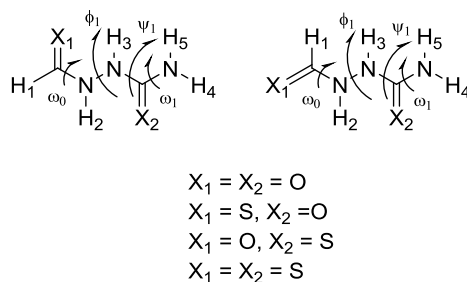


**Fig. 2.21** Chemical structures of For–AzaGly–NH<sub>2</sub>, For–[ΨCSNH]–AzaGly–NH<sub>2</sub>, For–AzaGly–[ΨCSNH]–NH<sub>2</sub>, and For–[ΨCSNH]–AzaGly–[ΨCSNH]–NH<sub>2</sub>. Adapted from reference [61]. Copyright 2003 Wiley Periodicals, Inc. (further permissions related to the material excerpted should be directed to Wiley Periodicals, Inc.)

$\phi$  and  $\psi$  dihedral angles to accommodate for the longer C=S...H–N hydrogen bond. The conformation  $3_{10}$ -helix is more likely in thiopeptides than in normal peptides. The  $3_{10}$ -helix conformation is favored because the hydrogen bond conformation can adopt more conformations (it is more flexible) relative to the  $\alpha$ -helix and there is an increase of entropy. This differential flexibility is more apparent upon thio substitution.

Lee et al. [61] have examined the effect of thioamide substitution into azapeptide For–AzaGly–NH<sub>2</sub> (Fig. 2.21).

Through the analysis of the potential energy surface, the authors find the minimum energy conformations that were optimized. The minima prefer the secondary structures in proteins such as the  $\beta$ -strand, polyproline II,  $\beta$ I(II), or  $\beta$ VI-turn scaffolds. The analysis of the bond order for the N–N ( $\phi_1$ ) and N–C ( $\psi_1$ ) bonds demonstrates that these bonds have close to single-bond character. The barriers of the N–C ( $\psi_1$ ) bond are <10 kcal/mol, suggesting that the  $\psi_1$  bond is partially restricted at the  $0 \pm 30^\circ$  or  $180 \pm 30^\circ$ . The rotational barriers of the N–N ( $\phi_1$ ) bond are estimated in the range from about 4 to 24 kcal/mol, depending on the orientation of the formyl group and the  $\psi_1$  angle of 0 or  $180^\circ$  at the B3LYP/6-31G\*//HF/6-31G\* level. Noteworthy, the rotation about the N–N ( $\phi_1$ ) bond as the  $\omega_0$  and  $\psi_1$  angles are  $\approx 180^\circ$ , for the studied structures, shows a single barrier, whose value is about 24 kcal/mol at the B3LYP/6-31G\*//HF/6-31G\* level. This implies that conformers of minimum energy, corresponding to the  $\beta$ -strand structure, are restricted in these regions.

A theoretical study of the electronic structure of thio-substituted dipeptides and tripeptides has been performed by Joy et al. [62] at the DFT and TD-DFT levels of theory. The substitution of oxygen by sulfur has influence in geometrical parameters including bond lengths and bond angles, and this influence is higher when the substitution occurs at N terminus. For example, the *N*-terminal substitutions increase the C–S bond distances. Two types of transitions are found in these peptides,  $n-\pi^*$  and  $\pi-\pi^*$ . In general, the former transition is from the lone pair on sulfur atom to the empty carbonyl group  $\pi^*$  at the other end. The latter is from  $\pi$  electron cloud at the *N*-terminal to the  $\pi^*$  orbital at the *C*-end. The presence of *N*-terminal substitutions

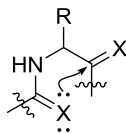


**Fig. 2.22** Interaction displaying the  $n \rightarrow \pi^*$  electronic delocalization. Adapted with permission from reference [67]. Copyright 2009 American Chemical Society (further permissions related to the material excerpted should be directed to the ACS)

is found to give orbitals localized at *N*-terminal, whereas substitutions at other positions are found to have delocalized orbitals shifting the wavelength to a lower region (blue shift).

DFT theoretical studies performed by Raines et al. on peptides and thiopeptides show an attractive  $n \rightarrow \pi^*$  interaction between adjacent backbone carbonyl groups (Fig. 2.22). This interaction stems from the delocalization of the electron pair ( $n$ ) of a donor group (O, S) into the antibonding orbital ( $\pi^*$ ) of a neighbor (thio)carbonyl group. The substitution of an amide donor with a thioamide could increase ligand affinity as a result of enhanced  $n \rightarrow \pi^*$  electronic delocalization due to increased overlap and reduced energy difference between the donor and acceptor orbitals [63–67].

## 2.7 N–H Bond Dissociation Enthalpy (BDE)

Kaur et al. have used theoretical methods to study the dissociation enthalpies of amines and amides [68]. Here, we are going to focus on the results in thioamides and the comparison with amides. The N–H BDE decreases in compounds  $\text{H}_2\text{NC}(=\text{X})\text{Y}$  in the order of X as  $\text{O} > \text{S} > \text{Se}$  for  $\text{Y} = \text{H}, \text{F}, \text{Cl}, \text{CH}_3, \text{NH}_2, \text{NO}_2, \text{CN}, \text{OH}$ . For the simplest models ( $\text{Y} = \text{H}$ ), the lower N–H BDE in case of  $\text{HC}(=\text{S})\text{NH}_2$  and  $\text{HC}(=\text{Se})\text{NH}_2$  is the result of shift of radical center to S or Se, respectively, along with  $\text{C}=\text{N}$   $\pi$ -bond formation, as it is suggested by the occupancies of  $\alpha$  and  $\beta$  molecular orbitals in the Restricted Open calculations. The substituents can alter the stability of molecule and the stability of radical, thereby resulting in the variation in N–H BDE of the molecule relative to that of the reference molecule. Considering substituents at the (thio)carbonyl carbon, in thioamides both electron-donating and electron-withdrawing substituents decrease the N–H BDE relative to  $\text{HC}(=\text{S})\text{NH}_2$ , while in amides  $\sigma$  withdrawing substituents like F and  $\pi$  acceptor groups like  $\text{NO}_2$  and CN at the carbonyl carbon increase the N–H BDE while the electron donor groups like  $\text{CH}_3, \text{NH}_2, \text{Cl},$  and OH decrease the N–H BDE relative to  $\text{HC}(=\text{O})\text{NH}_2$  (Table 2.5).

The effect of different substituents at the nitrogen atom in amides  $\text{HC}(=\text{X})\text{NH}\text{Y}$  [ $\text{X} = \text{O}, \text{S}, \text{Se}$ ;  $\text{Y} = \text{H}, \text{F}, \text{Cl}, \text{CH}_3, \text{NH}_2, \text{NO}_2, \text{CN}, \text{OH}$ ] has been analyzed as well. The geometry optimization leads to two minima (*syn* and *anti* conformers) on the potential energy surface, the *syn* being more stable in most cases (some

**Table 2.5** N–H bond dissociation enthalpies (in kcal/mol) for  $\beta$ -substituted amides  $\text{H}_2\text{NC}(=\text{X})\text{Y}$  at ROB3LYP/6-31+G\*/B3LYP/6-31+G(d,p) [L1], ROB3LYP/6-311++G(d,p)/B3LYP/6-31+G\* [L2], and MP2/6-311++G(d,p)/MP2/6-31+G\* [L4] theoretical level

Substituent	L1			L2			L4		
	X=O	X=S	X=Se	X=O	X=S	X=Se	X=O	X=S	X=Se
H	111.85	99.30	91.48	114.50	101.56	91.67	113.82	92.67	85.50
F	109.28	95.50	88.22	114.94	97.45	88.04	113.10	92.71	91.33
Cl	110.57	93.42	86.90	112.87	95.32	86.06	111.71	90.70	81.07
CH <sub>3</sub>	108.76	95.97	90.06	111.50	98.37	86.99	110.54	90.01	82.05
NH <sub>2</sub>	104.49	93.41	88.82	107.21	95.76	89.55	107.35	92.92	85.04
NO <sub>2</sub>	116.35	94.42	86.75	118.75	96.76	87.40	114.09	–	–
CN	113.34	–	90.80	116.35	98.63	90.73	114.51	111.96	110.81
OH	109.46	107.20	106.94	113.42	113.36	111.78	112.08	111.22	110.58

Adapted from reference [68]. Copyright 2008 Wiley Periodicals, Inc. (further permissions related to the material excerpted should be directed to Wiley Periodicals, Inc.)

For Y=H; X=O N–H BDE is 111.95, 115.88 at G3MP2 and CBS-QB3 level, respectively

Y=H; X=S N–H BDE is 98.49, 99.60 at G3MP2 and CBS-QB3 level, respectively

Y=H; X=Se N–H BDE is 91.55 at G3MP2 level

**Table 2.6** N–H bond dissociation enthalpies (in kcal/mol) for *N*-substituted amides  $\text{YHNC}(=\text{X})\text{H}$  at ROB3LYP/6-31+G\*/B3LYP/6-31+G(d,p) [L1], ROB3LYP/6-311++G(d,p)/B3LYP/6-31+G\* [L2], and MP2/6-311++G(d,p)/MP2/6-31+G\* [L4] theoretical level

Substituent	L1			L2			L4		
	X=O	X=S	X=Se	X=O	X=S	X=Se	X=O	X=S	X=Se
H	111.85	99.30	91.48	114.50	101.56	91.67	113.82	92.67	85.50
F	118.73	79.49	77.05	121.46	82.68	76.14	97.11	80.51	70.82
Cl	94.93	90.49	79.58	98.04	93.21	86.13	100.72	83.45	75.96
CH <sub>3</sub>	105.14	96.44	90.27	108.10	99.15	92.69	119.84	102.55	83.58
NH <sub>2</sub>	80.74	74.34	71.77	81.35	76.72	73.78	83.03	86.23	80.07
NO <sub>2</sub>	107.31	84.17	77.97	109.76	87.01	79.74	110.59	83.27	75.40
CN	113.69	87.66	81.50	116.36	90.08	83.44	112.27	86.71	81.09
OH	82.82	79.49	90.12	86.33	82.98	92.69	88.41	84.44	82.65

Adapted from reference [68]. Copyright 2008 Wiley Periodicals, Inc. (further permissions related to the material excerpted should be directed to Wiley Periodicals, Inc.)

exceptions are *N*-amino and *N*-methyl thioformamides). Considering the most stable conformation out of the two, the N–H BDEs are observed to be lower than the values for  $\text{H}_2\text{NC}(=\text{X})\text{Y}$  molecules, but the same trend is conserved with a more pronounced effect than when the substituent is bonded to the carbonyl carbon (Table 2.6).

## 2.8 Others

Thioamides involved in different chemical processes have been studied using quantum chemical calculations.

4-Thioamidopyridine (4-thiocarbamoylpyridine) is the parent compound of ethionamide (2-ethyl-4-thiamidopyridine, 2-ethylthioisonicotinamide). It is a drug for the treatment of multidrug-resistant tuberculosis. Wysokiński et al. have performed a theoretical study of this compound [69] by full geometry optimization at the B3LYP/6-311G(d,p) level of theory for an isolated molecule and a pair of molecules linked by hydrogen bond (Fig. 2.23). The authors find a good agreement between the experimental structure and the optimized geometry.

The formation of the intermolecular hydrogen bond  $N-H\cdots N_{py}$  induces changes in the bond lengths of the  $NH_2-C=S$  group with a shortening of the  $C-N$  bond and an elongation of the  $C=S$  bond. The vibrational analysis has been very helpful to assign all the signal of the vibrational spectroscopies that otherwise would be very difficult to do. For example, the vibrational analysis shows that the  $\nu(C=S)$  stretching vibration contributes mainly to the medium–strong bands at  $926$  and  $725\text{ cm}^{-1}$  in infrared, and  $947$  and  $728\text{ cm}^{-1}$  in the FT-Raman spectrum.

Palmer and Sherwood have performed theoretical studies HF with and without Moller–Plesset correlation effects to discuss the Nuclear Quadrupole Coupling Constants from microwave spectroscopy and quadrupole resonance [70]. The authors describe that the larger dipole moments from thioamides than the corresponding amides are a function of enhanced resonance in the former. The principal mechanism seems to be the push/pull  $\sigma/\pi$  effects of the N atom with respect to the CO and CS groups, with S being a better  $\sigma$ -donor than O; however, the effect is still present with formamidine where electronegativity effects are important, so the overall effect is the  $2,1,1-\pi$  electron contribution to the allylic system from N, C, O(S). The natural orbitals localize readily to localized orbitals, and these account for the gross magnitudes of the electronic terms in the electric field gradient. However, in the summation with the nuclear terms, the more distant centers still have some defining impact. Hence, the general trends for  $^{14}\text{N}$  Nuclear Quadrupole Coupling Constants to be higher in amides than thioamides do emerge from the localized orbital analysis.

Velkov et al. have used quantum chemical calculations to study the radical scavenging activity of *o*-coumaric acid thioamide in comparison with the related amide (Fig. 2.24) [71].

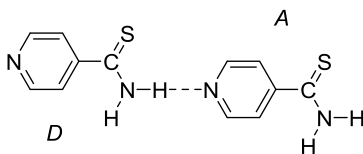


**Fig. 2.23** Hydrogen-bonded pair of *A-D* molecules of 4-thiocarbamoylpyridine. *A* denotes proton acceptor, and *D* is a proton donor subunit

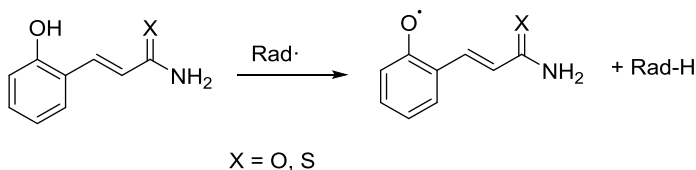


**Fig. 2.24** Radical scavenging reaction and structures of *o*-coumaric acid amide and thioamide (and corresponding radicals). Adapted with permission from reference [71]. Copyright 2007 Elsevier B.V. (further permissions related to the material excerpted should be directed to Elsevier B.V.)

Although the reactivity focus on the relative transformation of a substituted phenol to a substituted phenoxyl radical, the different behavior of the sulfur and the oxygen makes a difference. The HOMO energies also indicate that the thioamide should be a better scavenger than the amide, since ionization should be easier for the thioamide than for the amide. The spin density distribution in the amide and thioamide radicals is in agreement with the conclusions for higher stability of the latter; for example, the spin density at the phenoxyl oxygen in the thioamide radical is smaller by 0.03 than the one at the corresponding atom in the amide radical.

Finally, thioamides have been used as fluorescent probes by Petersson et al. through a mechanism of quenching that can be either Förster resonance energy transfer (FRET) or photoinduced electron transfer (PET) [72–74]. Nevertheless, to be best of our knowledge there is only one report by using theoretical modeling to study the behavior of thioamides as probes. In that work, the thioamide (thiourea) sensor has been theoretically modeled [75] using DFT calculations to describe the structure of the complex formed between the probe and  $\text{Zn}^{2+}$ . The scarce use of theoretical models to understand the behavior of the thioamides as sensors is an attractive field to be developed.

## 2.9 Conclusions

The structural features of thioamides can be rationalized on the basis of quantum chemical calculations. The planar conformation found is in good agreement with the experimental determinations. Derivations from planarity can be explained as well under a theoretical point of view by finding the explanation on the nature of the different substituents. The rotation about the C–N bond has been studied under different theoretical approaches and basically all of them agree that the higher charge transfer from the nitrogen to the chalcogen atom, when this atom is heavier, is the reason of the higher contribution of the structure **1b** (Fig. 2.1). Although this fact is counterintuitive in terms of electronegativity concepts, the increasing polarizability of the elements going down on the chalcogen group is the reason of this higher charge transfer when heavier elements are involved.

The calculated C–N rotational barriers in these systems account for two factors: (1) the energy rise due to breaking the partial  $p\pi-p\pi$  bond between carbon and nitrogen and (2) the energy gain due to the  $n_N \rightarrow \sigma^*_{C-X}$  negative hyperconjugation in the rotational transition state. The increase in the delocalization  $n_N \rightarrow \pi^*_{C-X}$  as going down the period in the group 16 is mainly attributable to the decrease in the energy difference between the energies of the N-lone pair and the  $\pi^*$  orbital of C–X bond and that stabilizes the planar conformation. On the other hand, the electronegativity of X strongly influences the  $n_N \rightarrow \sigma^*_{C-X}$  negative hyperconjugative interaction and stabilizes the transition state. These two interactions complement each other in increasing the C–N rotational barrier in thioformamide relative to formamide. The effect of the substituents bonded to the carbon atom of the thiocarbonyl atom is mainly steric effects.

The solvent effects calculated reveal that the rotational barrier increases with increase in polarity of the solvent, and this fact suggests electrostatic interactions in solution that are in good agreement with an important participation of the structure of resonance **1b** of Fig. 2.1. Remote substituents have their influence on the C–N bond rotational barrier, and interestingly, this influence depends on the position of bonding of the substituent. When the aromatic group is bonded to the thioamide nitrogen, electron-donating substituents increase the barrier of rotation and electron-withdrawing substituents decrease that barrier. But when the aromatic group is bonded to the thiocarbonyl carbon of the thioamide, the more electron-withdrawing groups tend to increase the thioamide rotational barriers.

Other features of the thioamides have been studied under a theoretical approach. The higher size of the sulfur atom with respect to the oxygen is important in the rotation of *N*-bonded methyl groups in (thio)formamides and (thio)acetamides. In thioamides, both electron-donating and electron-withdrawing substituents at the thiocarbonyl carbon decrease the N–H BDE relative to  $HC(=S)NH_2$ , while in amides,  $\sigma$  withdrawing and  $\pi$  acceptor substituents at the carbonyl carbon increase the N–H BDE and electron donor groups decrease the N–H BDE relative to  $HC(=O)NH_2$ . Finally, theoretical calculations have been used to help to understand the behavior of some thioamide compounds in establishing hydrogen bonding, scavenging of radicals or to discuss the Nuclear Quadrupole Coupling Constants.

**Acknowledgements** We gratefully acknowledge financial support from the Ministerio de Economía y Competitividad, Spain, and Fondo Europeo de Desarrollo Regional (FEDER) (Project CTQ2015-71353-R) and Junta de Castilla y León, Consejería de Educación y Cultura y Fondo Social Europeo (Project BU263P18).

## References

1. R.H. Judge, D.C. Moule, J.D. Goddard, *Can. J. Chem.* **65**, 2100 (1987)
2. A.T. Kowal, *J. Chem. Phys.* **124**, 14304 (2006)
3. T.W. Hambley, D.E. Hibbs, P. Turner, S.T. Howard, M.B. Hursthouse, *J. Chem. Soc. Perkin Trans. 2*, 235 (2002)



4. S. Prasanth, M. Varughese, N. Joseph, P. Mathew, T.K. Manojkumar, C. Sudarsanakumar, J. Mol. Struct. **1081**, 366 (2015)
5. T. Hori, Y. Otani, M. Kawahata, K. Yamaguchi, T. Ohwada, J. Org. Chem. **73**, 9102 (2008)
6. F.K. Winkler, J.D. Dunitz, J. Mol. Biol. **59**, 169 (1971)
7. C. Hansch, A. Leo, R.W. Taft, Chem. Rev. **91**, 165 (1991)
8. M.K. Kesharwani, B. Ganguly, J. Comput. Chem. **32**, 2170 (2011)
9. A.E. Reed, F. Weinhold, J. Chem. Phys. **78**, 4066 (1983)
10. J.P. Foster, F. Weinhold, J. Am. Chem. Soc. **102**, 7211 (1980)
11. D. Kaur, P. Sharma, P.V. Bharatam, N. Dogra, J. Mol. Struct. THEOCHEM **759**, 41 (2006)
12. J. Leszczynski, J.S. Kwiatkowski, D. Leszczynska, J. Am. Chem. Soc. **114**, 10089 (1992)
13. J.-Q. Zhang, C.-M. Shi, W. Wan, T.-Z. Ji, N. Yi, Comput. Theor. Chem. **1002**, 37 (2012)
14. I.D. Brown, K.R. Poeppelmeier (eds.), *Bond Valences* (Springer, Berlin, 2014)
15. K.B. Wiberg, P.R. Rablen, J. Am. Chem. Soc. **117**, 2201 (1995)
16. V. Ferretti, V. Bertolasi, P. Gilli, G. Gilli, J. Phys. Chem. **97**, 13568 (1993)
17. M.-C. Ou, M.-S. Tsai, S.-Y. Chu, J. Mol. Struct. **310**, 247 (1994)
18. K.E. Laidig, L.M. Cameron, J. Am. Chem. Soc. **118**, 1737 (1996)
19. K.T. Lim, M.M. Francl, J. Phys. Chem. **91**, 2716 (1987)
20. Y.K. Choe, G.I. Song, Y.S. Choi, C.J. Yoon, Bull. Korean Chem. Soc. **18**, 1094 (1997)
21. D. Lauvergnat, P.C. Hiberty, J. Am. Chem. Soc. **119**, 9478 (1997)
22. Y. Mo, J. Gao, S.D. Peyerimhoff, J. Chem. Phys. **112**, 5530 (2000)
23. Y. Mo, S.D. Peyerimhoff, J. Chem. Phys. **109**, 1687 (1998)
24. Y. Mo, Y. Zhang, J. Gao, J. Am. Chem. Soc. **121**, 5737 (1999)
25. Y. Mo, P.V.R. Schleyer, W. Wu, M. Lin, Q. Zhang, J. Gao, J. Phys. Chem. A **107**, 10011 (2003)
26. E.D. Glendening, J.A. Hrabal, J. Am. Chem. Soc. **119**, 12940 (1997)
27. A.E. Reed, R.B. Weinstock, F. Weinhold, J. Chem. Phys. **83**, 735 (1985)
28. E.D. Glendening, F. Weinhold, J. Comput. Chem. **19**, 593 (1998)
29. E.D. Glendening, F. Weinhold, J. Comput. Chem. **19**, 610 (1998)
30. E.D. Glendening, J.K. Badenhop, F. Weinhold, J. Comput. Chem. **19**, 628 (1998)
31. R.F.W. Bader, *Atoms in Molecules: A Quantum Theory* (1994)
32. Y. Mo, J. Chem. Phys. **126**, 224104 (2007)
33. B.V. Prasad, P. Uppal, P.S. Bassi, Chem. Phys. Lett. **276**, 31 (1997)
34. W. Kim, H.-J. Lee, Y. Sang, J.-H. Sang Choi, C.-J. Yoon, J. Chem. Soc. Faraday Trans. **94**, 2663 (1998)
35. P.V. Bharatam, R. Moudgil, D. Kaur, J. Phys. Chem. A **107**, 1627 (2003)
36. K.B. Wiberg, D.J. Rush, J. Am. Chem. Soc. **123**, 2038 (2001)
37. J. Zukerman-Schpector, L.S. Madureira, P. Poplaukhin, H.D. Arman, T. Miller, E.R.T. Tiekink, Zeitschrift Für Krist. - Cryst. Mater. **230**, 531 (2015)
38. S.M. Neugebauer Crawford, A.N. Taha, N.S. True, C.B. LeMaster, J. Phys. Chem. A **101**, 4699 (1997)
39. N.G. Vassilev, V.S. Dimitrov, J. Mol. Struct. **654**, 27 (2003)
40. J.B. Foresman, T.A. Keith, K.B. Wiberg, J. Snoonian, M.J. Frisch, J. Phys. Chem. **100**, 16098 (1996)
41. B. Galabov, S. Ilieva, B. Hadjieva, E. Dinchova, J. Phys. Chem. A **107**, 5854 (2003)
42. S. Ilieva, B. Hadjieva, B. Galabov, J. Org. Chem. **67**, 6210 (2002)
43. K. Waisser, M. Polásek, I. Nemeč, O. Exner, J. Phys. Org. Chem. **13**, 127 (2000)
44. W. Walter, in edited by J. Zabicky (Interscience, London, 1970)
45. W. Walter, Zeitschrift Für Chemie **10**, 371 (2010)
46. I.D. Rae, Can. J. Chem. **45**, 1 (1967)
47. W.E. Śmiszek-Lindert, E. Chelmecka, S. Góralczyk, M. Kaczmarek, J. Mol. Struct. **1128**, 619 (2017)
48. J. Helbing, H. Bregy, J. Bredenbeck, R. Pfister, P. Hamm, R. Huber, J. Wachtveitl, L. De Vico, M. Olivucci, J. Am. Chem. Soc. **126**, 8823 (2004)
49. E. Kleinpeter, A. Schulenburg, I. Zug, H. Hartmann, J. Org. Chem. **70**, 6592 (2005)

50. P. Fuertes, M. García-Valverde, R. Pascual, T. Rodríguez, J. Rojo, J. García-Calvo, P. Calvo, J.V. Cuevas, G. García-Herbosa, T. Torroba, *J. Org. Chem.* **80**, 30 (2015)
51. T. Steiner, *Angew. Chemie Int. Ed.* **41**, 48 (2002)
52. H.S. Park, Y.K. Kang, *New J. Chem.* **41**, 6593 (2017)
53. K.B. Wiberg, D.J. Rush, *J. Org. Chem.* **67**, 826 (2002)
54. Z. Velkov, Y. Velkov, E. Balabanova, A. Tadjer, *Int. J. Quantum Chem.* **107**, 1765 (2007)
55. D.R. Artis, M.A. Lipton, *J. Am. Chem. Soc.* **120**, 12200 (1998)
56. T.T. Tran, H. Treutlein, A.W. Burgess, *J. Comput. Chem.* **22**, 1026 (2001)
57. T.T. Tran, A.W. Burgess, H. Treutlein, J. Perich, *J. Pept. Res.* **58**, 67 (2001)
58. T.T. Tran, *Protein Eng. Des. Sel.* **19**, 401 (2006)
59. T.T. Tran, A.W. Burgess, H. Treutlein, J. Zeng, *J. Mol. Graph. Model.* **20**, 245 (2001)
60. T.T. Tran, J. Zeng, H. Treutlein, A.W. Burgess, *J. Am. Chem. Soc.* **124**, 5222 (2002)
61. H.-J. Lee, J.H. Kim, H.J. Jung, K.-Y. Kim, E.-J. Kim, Y.-S. Choi, C.-J. Yoon, *J. Comput. Chem.* **25**, 169 (2004)
62. S. Joy, V.V. Sureshbabu, G. Periyasamy, *Theor. Chem. Acc.* **136**, 123 (2017)
63. R.W. Newberry, B. VanVeller, R.T. Raines, *Chem. Commun.* **51**, 9624 (2015)
64. A. Choudhary, R.W. Newberry, R.T. Raines, *Org. Lett.* **16**, 3421 (2014)
65. R.W. Newberry, B. VanVeller, I.A. Guzei, R.T. Raines, *J. Am. Chem. Soc.* **135**, 7843 (2013)
66. A. Choudhary, R.T. Raines, *ChemBioChem* **12**, 1801 (2011)
67. A. Choudhary, D. Gandla, G.R. Krow, R.T. Raines, *J. Am. Chem. Soc.* **131**, 7244 (2009)
68. D. Kaur, R.P. Kaur, R. Kohli, *Int. J. Quantum Chem.* **109**, 559 (2009)
69. R. Wysokiński, D. Michalska, D.C. Bieńko, S. Ilakiamani, N. Sundaraganesan, K. Ramalingam, *J. Mol. Struct.* **791**, 70 (2006)
70. M.H. Palmer, P. Sherwood, *ZEITSCHRIFT FÜR Naturforsch. Sect. A-A J. Phys. Sci.* **51**, 460 (1996)
71. Z. Velkov, E. Balabanova, A. Tadjer, *J. Mol. Struct. THEOCHEM* **821**, 133 (2007)
72. Y. Huang, J.J. Ferrie, X. Chen, Y. Zhang, D.M. Szantai-Kis, D.M. Chenoweth, E.J. Petersson, *Chem. Commun.* **52**, 7798 (2016)
73. J.M. Goldberg, X. Chen, N. Meinhardt, D.C. Greenbaum, E.J. Petersson, *J. Am. Chem. Soc.* **136**, 2086 (2014)
74. E.J. Petersson, J.M. Goldberg, R.F. Wissner, *Phys. Chem. Chem. Phys.* **16**, 6827 (2014)
75. M.-M. Li, F.-W. Wang, X.-Y. Wang, T.-T. Zhang, Y. Xu, Y. Xiao, J.-Y. Miao, B.-X. Zhao, *Anal. Chim. Acta* **826**, 77 (2014)

# Chapter 3

## Synthesis of Thioamides



Toshiaki Murai

**Abstract** Improved versions of traditionally employed synthetic reactions and newly developed synthetic reactions for thioamides and thiolactams reported within five years are introduced in this chapter. As starting materials, carbonyl compounds such as aldehydes, ketones, acids, amides, and esters are used in combination with elemental sulfur or other sulfur sources, and amines. Alkynes, benzylic halides, amines, and nitriles also provide the carbon atom of the C=S group. To achieve the direct replacement of the oxygen atom of ordinary amides with the sulfur atom, thionating reagents involving the P=S bonds are developed. Alternatively, reactive sulfur species are generated in situ.

**Keywords** Willgerodt–Kindler reaction · Thionation · Isothiocyanates · Thioacetic acids · Thiocarbamoyl chlorides

### 3.1 Introduction

A range of synthetic methods [1, 2] for thioamides and thiolactams have been developed since early times. They can be classified on the basis of the sulfur sources. The powder of sulfur is directly introduced to organic molecules to form carbon–sulfur double bonds. Alternatively, compounds bearing P=S bonds, thiols, disulfides, and compounds bearing C=S bonds such as isothiocyanates, thioacetic acids, thiocarbamoyl chlorides are also used. In this chapter, recent examples of synthetic reactions of thioamides are described and classified by sulfur sources.

---

T. Murai (✉)

Department of Chemistry and Biomolecular Science, Faculty of Engineering, Gifu University,  
Yanagido, Gifu 501-1193, Japan  
e-mail: [mtoshi@gifu-u.ac.jp](mailto:mtoshi@gifu-u.ac.jp)

© Springer Nature Singapore Pte Ltd. 2019  
T. Murai (ed.), *Chemistry of Thioamides*,  
[https://doi.org/10.1007/978-981-13-7828-7\\_3](https://doi.org/10.1007/978-981-13-7828-7_3)

## 3.2 The Direct Incorporation of Elemental Sulfur

Ketones react with amines and elemental sulfur at high temperature to give thioamides. The protocol of this reaction, which has been called Willgerodt–Kindler reaction, was first reported by Willgerodt in 1887 [3]. Later on, tremendous amounts of improved methods and variants are developed [4].

### 3.2.1 Combination of Ketones, Amines, and Elemental Sulfur

The reaction of ketones, amines, and elemental sulfur leading to the formation of thioamides usually requires high temperatures. To reduce the temperature, ultrasound irradiation is used for the reaction of aryl methyl ketones **1** with cyclic amines (Fig. 3.1) [5]. With this method, the reaction time is also reduced. The reaction under reflux of solvents is carried out for 20 h, whereas the reaction under irradiation conditions needs less than 25 min to give thioamides **2**. As amines, cyclic amines such as morpholine, pyrrolidine, and piperidine are used.

To facilitate the reaction, a range of catalysts such as sulfated polyborate,  $\text{HBF}_4\text{-SiO}_2$ , sulfated tungstate,  $[\text{bmim}]\text{BF}_4$ , and p-toluenesulfonic acid are employed. Among them, the reaction with sulfated polyborate is complete within 30 min at 100 °C (Fig. 3.2) [6]. No solvent is necessary, and stoichiometric amounts of each reagent are enough to achieve high yield reactions.

Alternatively, deep eutectic solvents, which are formed from a combination of Lewis and Brønsted acids and bases, are used for the reaction (Fig. 3.3) [7]. The combination of glycerol and  $\text{K}_2\text{CO}_3$  in a ratio of 10–1 works very well. Various

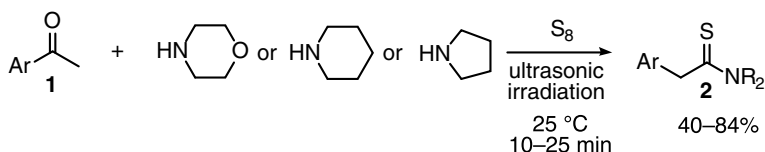


**Fig. 3.1** Reaction of aryl methyl ketones with cyclic amines and elemental sulfur under ultrasound irradiation

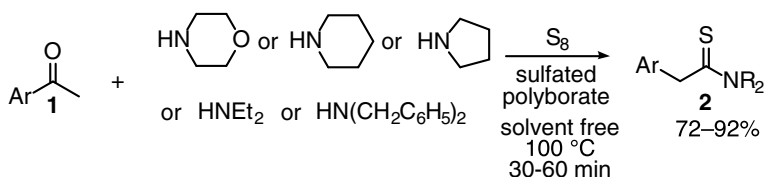


**Fig. 3.2** Reaction of aryl methyl ketones with cyclic amines and elemental sulfur in the presence of sulfated polyborate

**Fig. 3.3** Reaction of aryl methyl ketones with cyclic amines and elemental sulfur in the presence of glycerol:  $K_2CO_3$

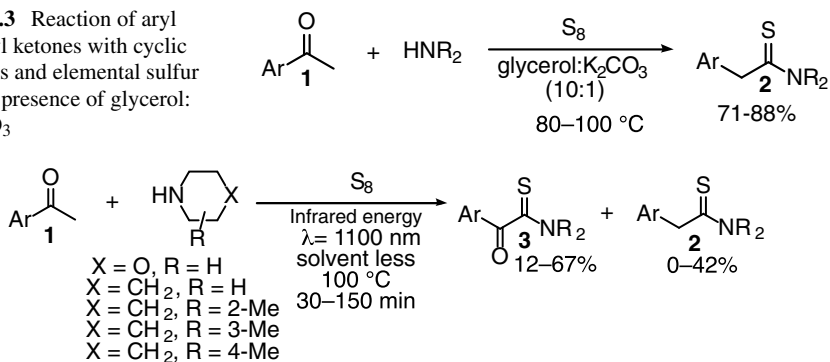


**Fig. 3.4** Reaction of aryl methyl ketones with cyclic amines and elemental sulfur under the irradiation of infrared energy

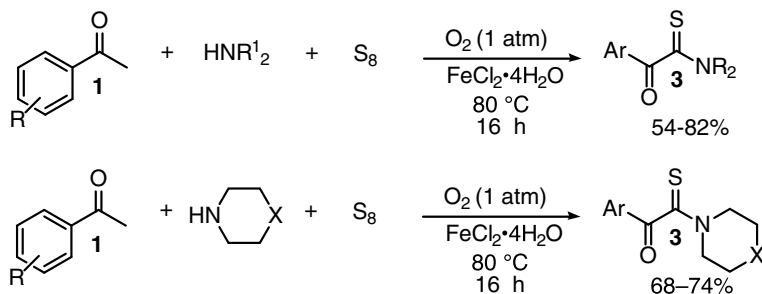


**Fig. 3.5** Reaction of aryl methyl ketones with cyclic amines and elemental sulfur in the presence of catalytic amounts of  $FeCl_2 \cdot 4H_2O$

amines and aryl methyl ketones **1** are used, and electron-withdrawing groups in the aromatic ring of the ketones enhance the yields of the resulting thioamides.

The reaction of aryl methyl ketones **1**, cyclic amines, and elemental sulfur under the irradiation of infrared energy gives  $\alpha$ -keto thioamides **3** along with the formation of thioamides **2** (Fig. 3.4) [8]. The ratio of **2** and **3** is dependent on the substituents on the aromatic ring of aryl methyl ketones. The use of 2-methylpiperidine gives the product **3** in a reduced yield. For the synthesis of  $\alpha$ -keto thioamides **3**, ferrous chloride ( $FeCl_2$ ) is used as a catalyst under oxygen atmosphere (Fig. 3.5) [9]. The reaction temperature at  $80^\circ\text{C}$  is the best temperature. Higher and lower temperatures give the corresponding  $\alpha$ -keto thioamides **3** in reduced yields. Nevertheless, the reaction of diethylamine is carried out at  $60^\circ\text{C}$  to give the products in reasonable yields.

Several reaction pathways have been proposed for the reaction of aryl methyl ketones, amines, and elemental sulfur (Fig. 3.6). It generally involves the generation of enamines **4**. The amino group in **4** has to shift from the carbon atom having an aromatic group to the carbon atom of the methyl group in the original aryl methyl ketones. One possibility is that enamines **4** react with elemental sulfur to generate

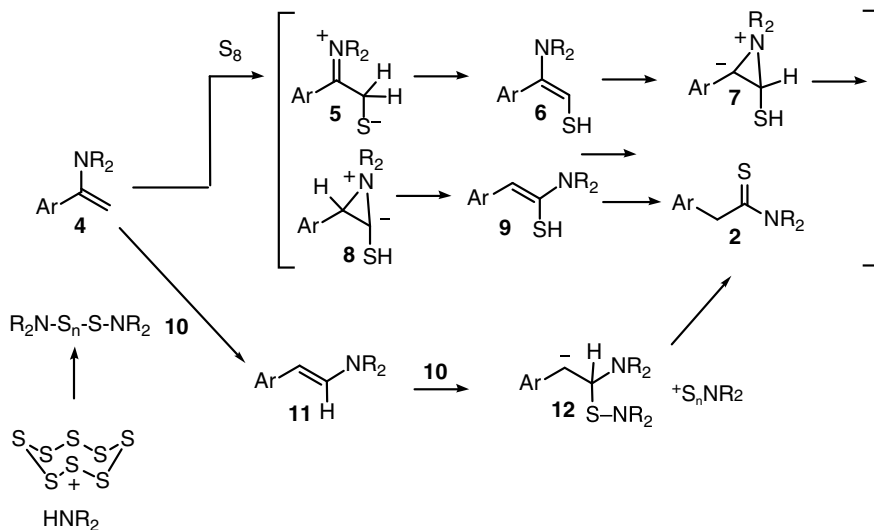
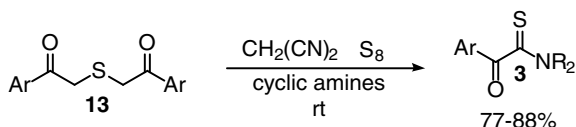


**Fig. 3.6** Plausible reaction pathway of the reaction of aryl methyl ketones with amines and elemental sulfur

**Fig. 3.7** Reaction of diphenacyl sulfides with dicyanomethane, cyclic amines, and elemental sulfur



the intermediate **5**. The proton transfer takes place in **5** to give enethiols **6**, followed by the formation of aziridinium intermediates **7** and the further proton transfer to give rise to the formation of isomerized enethiols **9** via **8**. Alternatively, disulfene diamides **10** may be formed between amines and elemental sulfur. The diamides **10** may facilitate the isomerization of enamines **4** to generate isomerized enamines **11**, which then react with **10** to lead to the formation of thioamides **2** via **12**.

As in the plausible reaction pathway wherein enamines can react with elemental sulfur, elemental sulfur can react with carbanions. Diphenacyl sulfides **13** react with dicyanomethane, cyclic amines such as morpholine, pyrrolidine, and piperidine, and elemental sulfur to give  $\alpha$ -keto thioamides **3** (Fig. 3.7) [10].

### 3.2.2 Combination of Aldehydes, Amines, and Elemental Sulfur

The reaction of aromatic aldehydes, amines, and elemental sulfur gives aromatic thioamides. The yields of the products are highly dependent on the substituents in

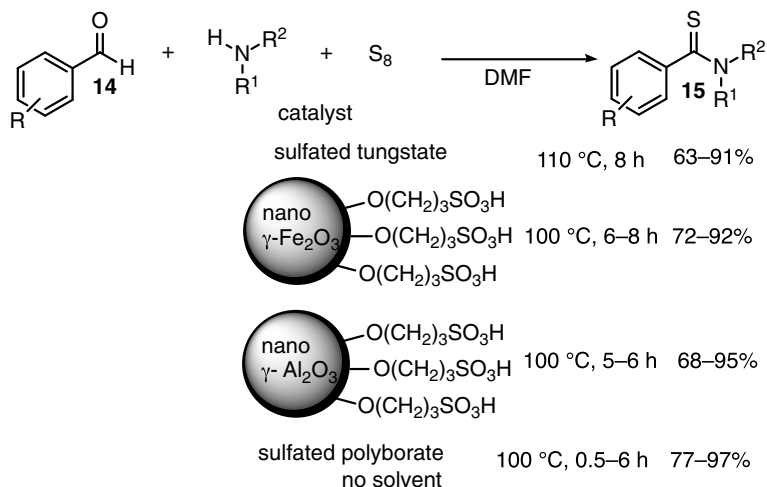


**Fig. 3.8** Reaction of aromatic aldehydes with amines and elemental sulfur in the presence of catalysts

the aldehydes and amines. The purity of DMF, which has been usually used as a solvent, is also highly influential to the efficiency of the reaction. It is desirable to use freshly distilled DMF. As one of the examples, benzaldehyde reacts with aniline and elemental sulfur at 110 °C in DMF for 8 h to give the corresponding *N*-phenyl benzthioamide only in 15% yield [11]. The use of  $Na_2S$  as a catalyst improves the yield of the product [12, 13]. To further enhance the yields of the product [11], Brønsted acids such as acetic acid and *p*-toluenesulfonic acid are tested to give the product in better yields. Furthermore, sulfated tungstate [14] facilitates the reaction to lead to the thioamide in 90% yields [11]. A range of aromatic aldehydes having electron-withdrawing and electron-donating functional groups are used. As amines, ammonia, aromatic amines, and acyclic and cyclic amines are used. Sulfonic acids having nano- $\gamma$ - $Fe_2O_3$  [15] or nano- $\gamma$ - $Al_2O_3$  [16] catalyze the reactions (Fig. 3.8). Sulfated polyborate [17] also catalyzes the reaction [18]. In this case, no solvent is used, and the reaction is complete within shorter reaction times, although aromatic amines such as aniline are not effective.

Microwave irradiation to the DMF solution of aromatic aldehydes, morpholine or *N*-benzylpiperazine, and elemental sulfur gives the corresponding thioamides in better yields than the conventional heating [19].

Water is also employed as a solvent for the reaction of aromatic aldehydes **14** or arylglyoxals **16**, amines, and elemental sulfur (Fig. 3.9). In the reaction of **14**, potassium carbonate is used, and the reaction requires 24 h [20]. In contrast, the reaction of **16** is complete within 1 h [21]. As amines, only cyclic amines are effective, while the reaction of acyclic amines gives unidentified mixtures. In this case, iminium salts **17** may be formed from **16** and amines (Fig. 3.10). The amines may also react with elemental sulfur to generate ammonium sulfur **18**. The addition of **18** to the

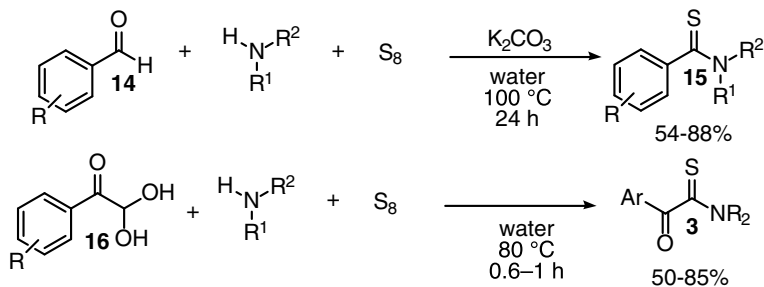


**Fig. 3.9** Reaction of aromatic aldehydes or arylglyoxals with amines and elemental sulfur in water

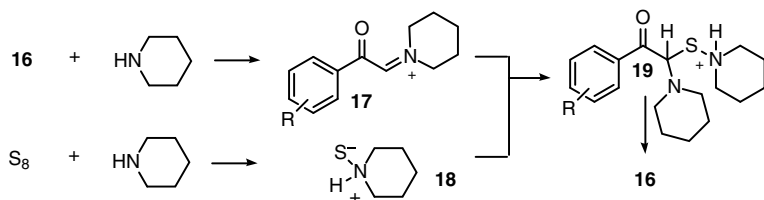


**Fig. 3.10** Plausible reaction pathway for the reaction of arylglyoxals with amines and elemental sulfur in water

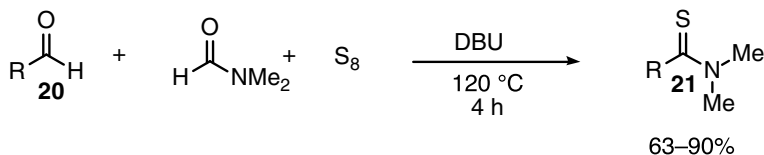


**Fig. 3.11** Reaction of aldehydes with DMF and elemental sulfur

salts **17** may lead to the intermediates **19**, followed by the elimination of ammonium salts to give the corresponding products **3**. Solvent-free reactions from **16** to **3** are also achieved [21].

The ability of acetonitrile as a solvent for the reaction of **14**, amines, and elemental sulfur is tested under ordinary conditions and under electrochemical conditions [22]. The reaction is carried out at 60 °C, and the corresponding thioamides **15** are obtained in comparable yields to other methods.

For the preparation of *N,N*-dimethyl thioamides, aldehydes are treated with DMF and elemental sulfur in the presence of DBU (Fig. 3.11) [23]. The reaction of aromatic aldehydes gives the aromatic thioamides in high yields. Aliphatic aldehydes also participate in the reaction, but the corresponding thioamides are formed in slightly lower yields.



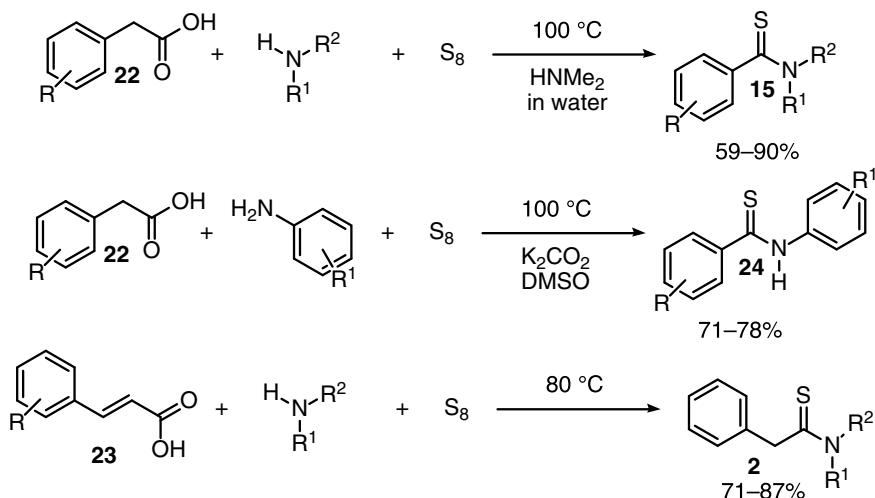


**Fig. 3.12** Reaction of  $\alpha$ -arylacetic acids or  $\alpha,\beta$ -unsaturated carboxylic acids with amines and elemental sulfur

### 3.2.3 Combination of Carboxylic Acids, Amines, and Elemental Sulfur

Instead of aldehydes and ketones,  $\alpha$ -arylacetic acids **22** or  $\alpha,\beta$ -unsaturated carboxylic acids **23** are used as a starting material for the reaction with secondary or primary or aromatic amines and elemental sulfur (Fig. 3.12) [24]. The reaction is carried out at  $80$ – $100^\circ\text{C}$ . In the reaction of **22** and aliphatic amines, 40% aqueous solution of dimethylamine is added. For the reaction with aromatic amines, potassium carbonate is employed with DMSO as a solvent. Noteworthy is that a variety of amines participate in the reactions leading to a wide range of substituents on the nitrogen atom in **2**, **15**, and **24**. Mechanistic studies have been carried out, and the details are shown in the supporting information of the original paper. It involves decarboxylation and the formation of iminium salts as an intermediate. In addition to amines,  $N,N$ -dialkyl formamides **25** are available as a source of amino groups, although **25** are used as a solvent (Fig. 3.13) [25]. The reaction of commercially available  $N,N$ -dimethyl formamide (DMF), which is more readily handled than dimethylamine, gives  $N,N$ -dimethyl thioamides as a product.

### 3.2.4 Combination of Amines and Elemental Sulfur

The reaction of carbonyl compounds and amines giving thioamides is believed to involve imines or iminium salts as an intermediate. Alternative methods for the

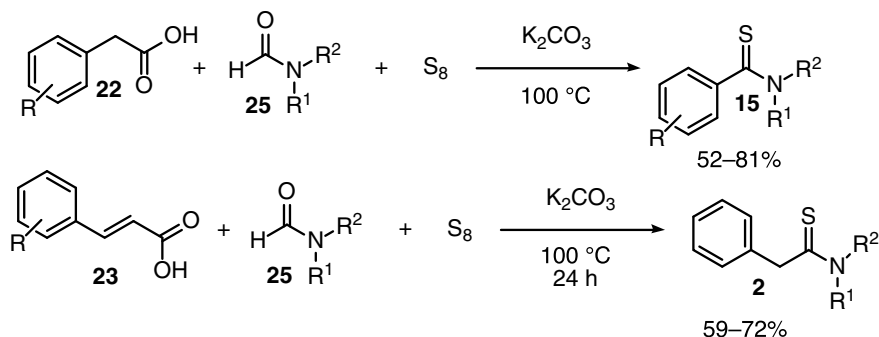


**Fig. 3.13** Reaction of  $\alpha$ -arylacetic acids or  $\alpha,\beta$ -unsaturated carboxylic acids with  $N,N$ -dialkyl formamides and elemental sulfur

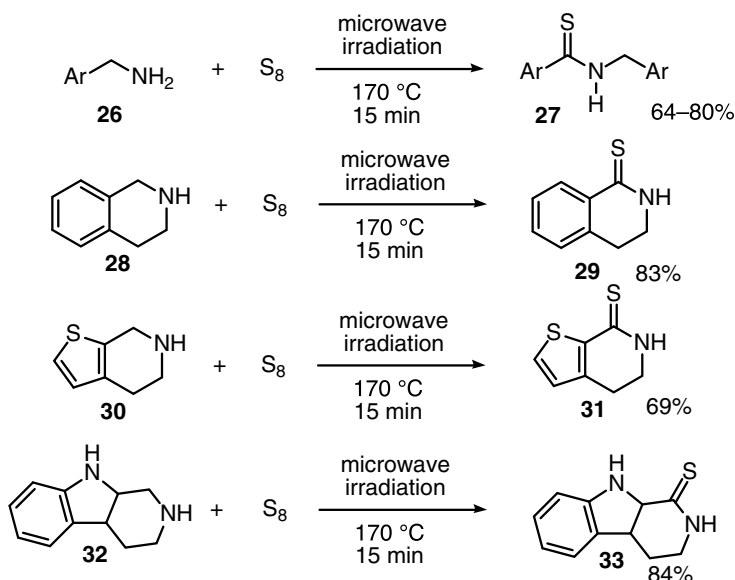


**Fig. 3.14** Reaction of amines and elemental sulfur under microwave irradiation

generation of imines are the oxidation of primary and secondary amines. The mixture of arylmethanamines and elemental sulfur is treated under the microwave irradiation conditions (Fig. 3.14) [26]. As a result,  $N$ -arylmethyl aromatic thioamides **27** are obtained as products. The cyclic amines such as **28**, **30**, and **32** are also used as a starting material to give cyclic thioamides **29**, **31**, and **33**. The use of lesser amounts of iron-based imidazolium salts and sodium phosphoric acid lowers the reaction temperature to  $100\text{ }^\circ\text{C}$ , although the reactions are carried out for 60 min [27].

(Dimethylaminomethyl)ferrocene and (dimethylaminomethyl)ruthenocene **34** are used as an amine in combination with other primary or secondary or aromatic

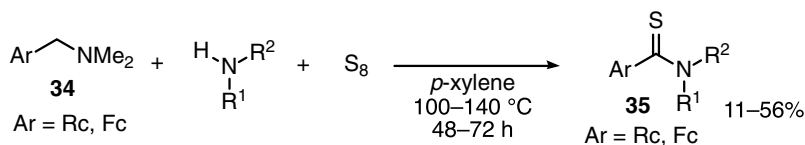


**Fig. 3.15** Reaction of (dimethylaminomethyl)ferrocene or (dimethylaminomethyl)ruthenocene with amines and elemental sulfur

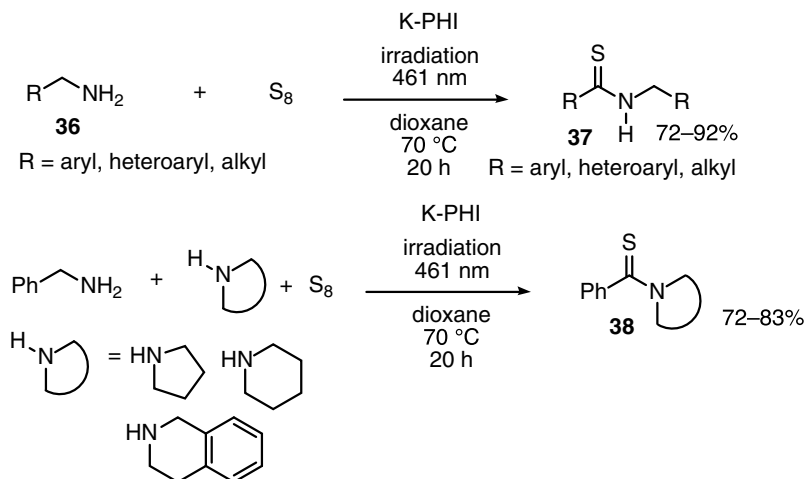


**Fig. 3.16** Reaction of amines and elemental sulfur in the presence of K-PHI under the irradiation of visible light

amines (Fig. 3.15) [28]. The reactions require higher temperatures (100–140 °C) and longer reaction times (48–72 h). Nevertheless, primary amines bearing hydroxyl, carbomethoxy, or carboxyl groups are available, and these functional groups remain in the products **35**.

Potassium poly(heptazine imide) (K-PHI), which is a carbon nitride-based photocatalyst, catalyzes the reaction of two different amines and elemental sulfur to afford thioamides (Fig. 3.16) [29]. The reaction is carried out under the irradiation of visible light (461 nm) at 70 °C with dioxane as a solvent. Arylmethylamines, heteroarylmethylamines, as well as simple primary amines such as propylamine and pentylamine **36** are used to give the corresponding thioamides **37** with high efficiency, although the reaction of primary amine is performed at 30 °C for 100 h in *tert*-BuOH. In the combination of benzylamine and cyclic amines, the phenyl group in benzylamine is selectively introduced to the thiocarbonyl carbon atom in **38**.

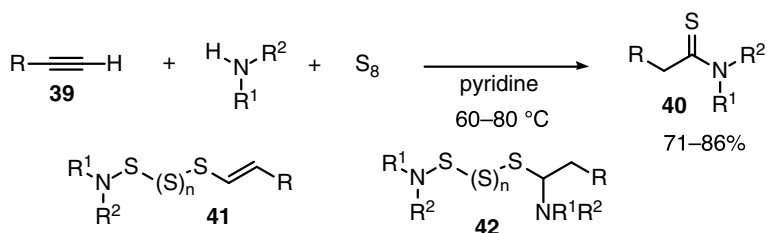


**Fig. 3.17** Reaction of terminal alkynes, aliphatic amines, and elemental sulfur

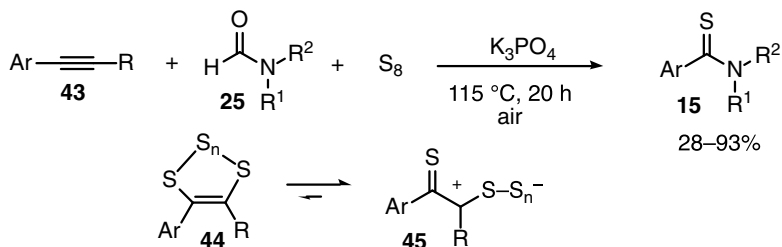


**Fig. 3.18** Reaction of alkynes, formamides, and elemental sulfur

### 3.2.5 Combination of Alkynes, Amines, and Elemental Sulfur

A range of terminal alkynes **39** react with a wide variety of aliphatic amines and elemental sulfur in pyridine at 60–100 °C to give thioamides **40** (Fig. 3.17) [30]. In the reaction of silylacetylene, the silyl group eliminates to give thioacetamide as a product. Phenyl methyl alkyne as internal alkynes is also tested as a starting material to give the thioamide, in which the primary alkyl group is introduced to the thiocarbonyl carbon atom. In this case, isomerization of the internal alkynes to terminal alkynes may be involved. Attempt to react with aniline is not successful. As a plausible reaction pathway, the generation of vinyl sulfides **41** and the addition of amines to **41** giving **42** are postulated. The use of aliphatic diamines and aromatic diynes affords polythioamides [31].

Cleavage of the carbon–carbon triple bonds in aromatic alkynes **43** followed by the introduction of the sulfur atom and amino groups is achieved by using formamides **25** and elemental sulfur (Fig. 3.18) [31]. Aromatic terminal and internal alkynes are used, and in the latter case, aryl groups are introduced to the resulting thioamides. Initial step of the reaction is postulated to be cycloaddition reaction between alkynes and  $S_8$  to generate multi-sulfur 1,2-dithiolene intermediates **44**, which is in equilibrium with **45**. However, further studies would be necessary since the step of the elimination of R group in **43** is still ambiguous.

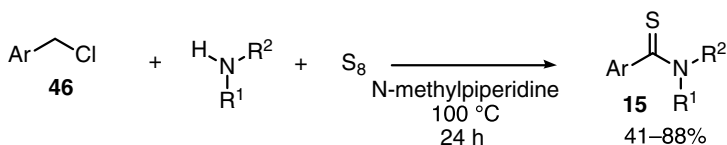


**Fig. 3.19** Reaction of benzylic chlorides with amines and elemental sulfur

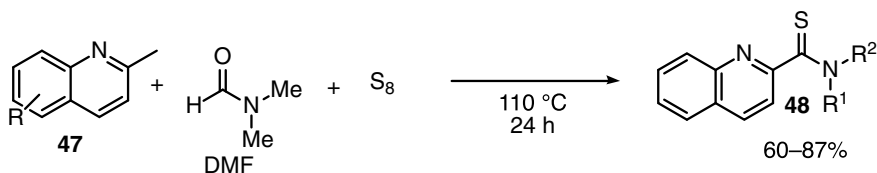


**Fig. 3.20** Reaction of methyl heteroarenes, DMF, and elemental sulfur

### 3.2.6 *Combination of Benzylic Halides, Amines, and Elemental Sulfur*

Similarly to benzylic amines, benzylic groups in benzylic chlorides **46** are converted to the carbon skeletons of thioamides **15** (Fig. 3.19) [32]. The original benzylic carbon atoms correspond to the thiocarbonyl carbon atom. As primary amines, cyclohexylamine and propylamine, and as cyclic amines, morpholine and piperidine are used. Aniline derivatives having halogens and a methoxy group and 2-aminopyridine give the corresponding thioamides **15** in good to high yields.

### 3.2.7 *Combination of Methyl Heteroarenes, N,N-Dimethyl Formamide, and Elemental Sulfur*

The methyl group in 2-methylquinoline **47** is acidic and reacts with DMF and elemental sulfur at 110 °C to give *N,N*-dimethyl heteroaromatic thioamides **48** as a product (Fig. 3.20) [33]. In addition to 2-methylquinoline, 2-methyl-, 2,6-dimethyl-, and 2,5-dimethylpyridine, 2-methylbenzthiazole, 2-methylbenzimidazole, 2-methylquinoxaline, and 2,3-dimethylquinoxaline participate in the reaction to give the corresponding thioamides **48** in moderate to good yields. Instead of DMF, diethylamine and pyrrolidine also afford the thioamides, albeit in low yields. The generation of arylmethyl radicals from methyl arenes and *t*-butyl hydroperoxide and NBS and their addition to elemental sulfur and amines are also reported to give aromatic thioamides [34].

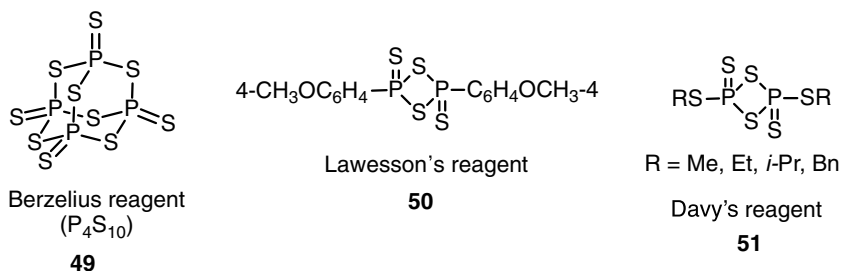


Fig. 3.21 Some of the thionating agents having P=S bonds

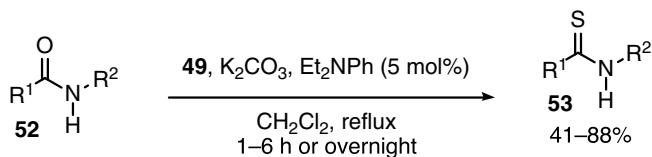
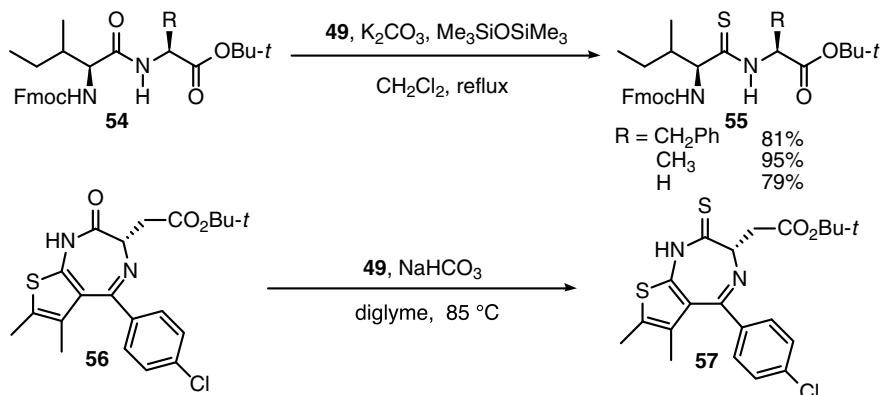
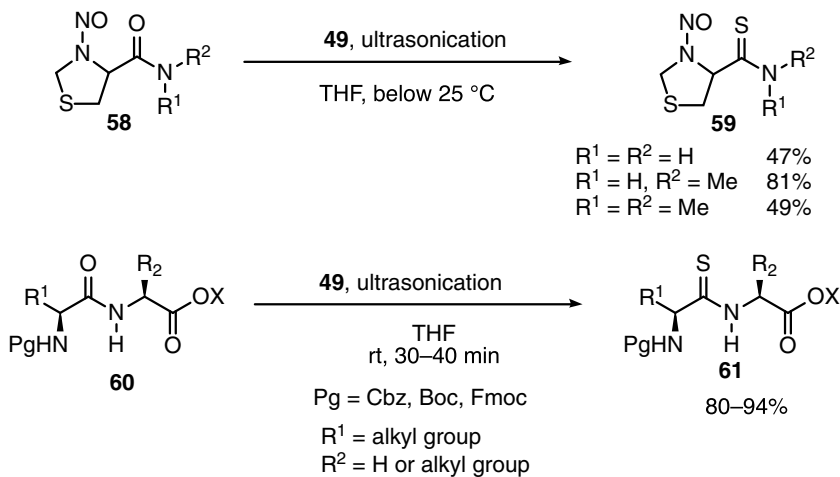
### 3.3 Thionation of Amides

Thionation of amides and carboxylic acids is a promising method for preparing thioamides. In particular, if thionating agents exhibit functional compatibility and selectively convert the oxygen atom in the amide moieties to the sulfur atom, they can be applied to one step of the syntheses of complex natural products and biologically relevant molecules.

#### 3.3.1 Thionating Agents having P=S Bonds

One of the frequently used thionating agents possesses P=S bonds [35], and some of them such as  $P_4S_{10}$  (also shown as  $P_2S_5$  called Berzelius reagent) **49** [36], Lawesson's reagent **50**, and Davy's reagent **51**, are shown in Fig. 3.21. Some of the synthetic examples using **49** and **50** are shown below.

Berzelius reagent **49** readily converts amides to thioamides [36]. Various solvents such as THF, diethyl ether, dioxane, dichloromethane, acetonitrile, and pyridine are used with or without bases. As an improved method, potassium carbonate and a catalytic amount of *N,N*-diethyl aniline are added to the reaction mixture (Fig. 3.22) [35]. Primary, secondary, and even tertiary amides **52** participate in the thionation to give the corresponding thioamides **53**. The reaction of amides having aryl and primary and secondary alkyl groups on the carbonyl carbon atom is complete within 6 h, while the tertiary alkyl group on that carbon retards the reaction and requires more than one night to give the corresponding thioamides in moderate yield. Berzelius reagent **49** has ten sulfur atoms, but less than three of them are introduced to the carbon atom of **52**. Functional compatibility of **49** is high [37–39], and the oxygen atom in amides **54** [37] and **56** [38] is selectively replaced with the sulfur atom to give **55** and **57**, even if the alkoxy carbonyl group is present in **54** and **56** (Fig. 3.23). Ultrasonication facilitates thionation using **49** (Fig. 3.24). This allows for the thionation of **58** [40] and **60** [41] at room temperature for shorter reaction time to give **59** and **61**. Again, functional groups such as alkoxy carbonyl and nitroso groups remain intact.

Fig. 3.22 Thionation of amides with Berzelius reagent **49**Fig. 3.23 Thionation of amides having some functional groups with **49**Fig. 3.24 Thionation of amides with **49** with ultrasonication

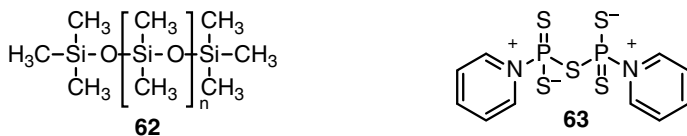
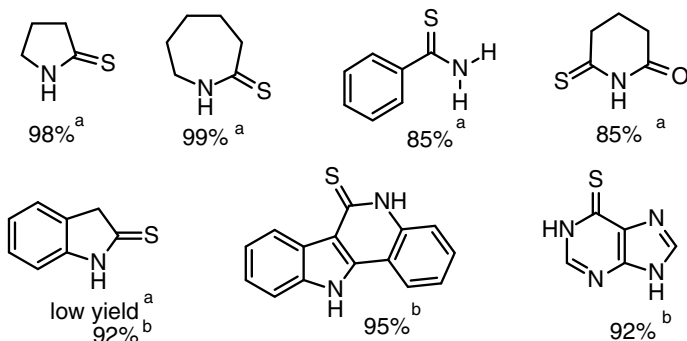


**Fig. 3.25** Structure of dimethicone **62** and pyridinium complex **63**



a in  $\text{CH}_3\text{CN}$ , reflux, b in dimethyl sulfone at 165–170 °C

**Fig. 3.26** Representative examples of thioamides and thiolactams prepared from amides and lactams using **63**

Dimethicone **62** (Fig. 3.25), which is one of the polysiloxanes, is used as a co-solvent in the thionation of aromatic amides using **49** [42]. With **62**, the yields of the products enhance to more than 84%, and several products are obtained almost quantitatively.

Pyridine reacts with **49** to give pyridinium complex **63** as a stable solid (m.p.: 167–169 °C) [43, 44]. The complex **63** highly efficiently thionates amides and lactams. Representative examples of the products derived from thionation using **63** are shown in Fig. 3.26. Dimethyl sulfone and acetonitrile are used as solvents at 165–170 °C and at reflux temperature, respectively, and the reaction is complete within 1 h.

A solid-supported **49** is prepared by grinding **49** and basic alumina in mortar and pestle to a fine homogeneous powder (Fig. 3.27) [45]. Thionation using the resulting powder under microwave irradiation conditions is complete within 5 min. In addition to  $\text{Al}_2\text{O}_3$ -supported **49**,  $\text{SiO}_2$ -supported **49** is prepared, and it is effective for the thionation of  $\beta$ -lactams [46].

Lawesson's reagent **50** is frequently used for the preparation of a wide range of thioamides. Because of ready availability, high efficiency, and high selectivity of **50**, the use of **50** is seen in the total synthesis of natural and unnatural products [47–52]. One of the representative examples is shown in Fig. 3.28 [52]. In many cases, the resulting thioamide moieties are reduced to the methylene group.



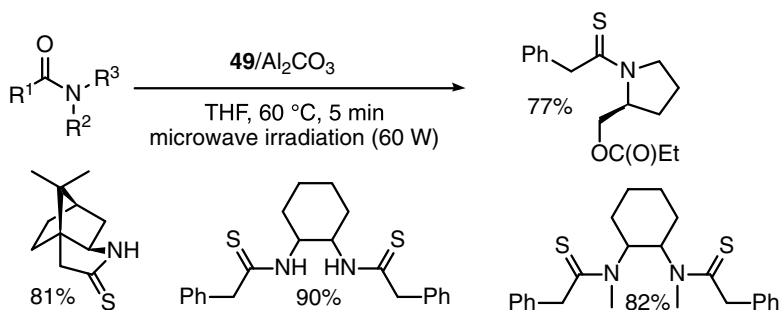


Fig. 3.27 Thionation using a solid-supported **49** under microwave irradiation

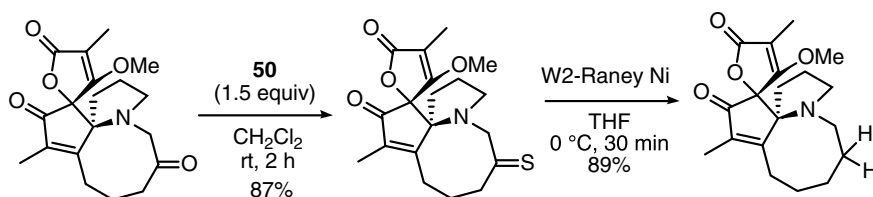


Fig. 3.28 Thionation using Lawesson's reagent **50** and reduction of the resulting thioamide moiety to a methylene group

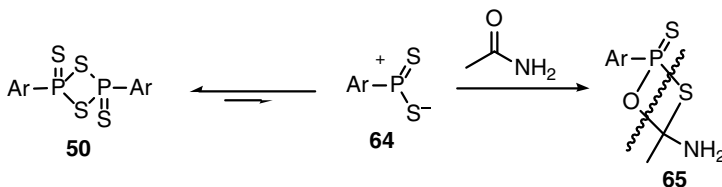


Fig. 3.29 Plausible reaction pathway of thionation using Lawesson's reagent **50**

The theoretical elucidation of the reaction pathway of thionation using **50** is shown in the literature [53]. The reagent **50** is in equilibrium with dithiophosphine ylide **64**, which reacts with amides to form four-membered cyclic intermediates **65**. Finally, cleavage of P–S and O–C bonds in **65** may give rise to the formation of thioamides (Fig. 3.29).

The reagent **50** thionates hemiaminals. In the reaction of hemiaminals **66** having a cyano group with **50**, the cyano group is converted to thioamide moieties in the product **67** (Fig. 3.30) [54]. Initially, thioamides **68** may be formed, which is in equilibrium with hemithioaminals **69**. Intramolecular addition of thiol groups in **69** to the cyano group may proceed to give imines **70**. Skeletal rearrangement of **70** gives the products **67**.

Ammonium phosphorodithioate **71** is also used for the thionation of aliphatic and aromatic amides (Fig. 3.31) [55]. The reaction is performed with toluene as a solvent.

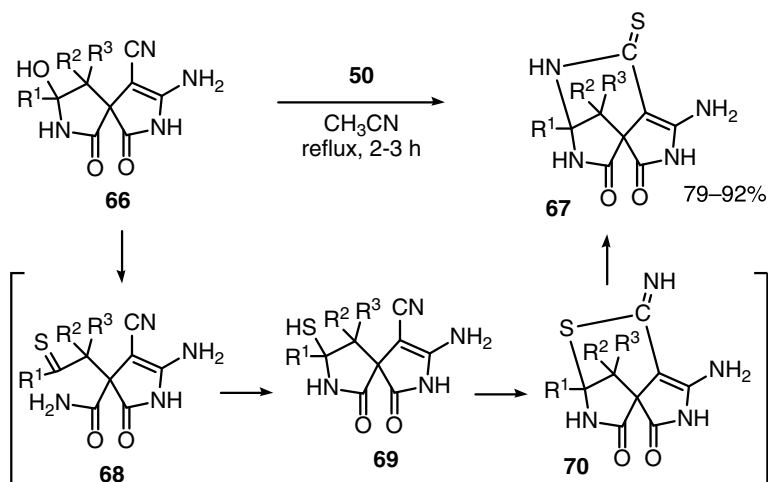


Fig. 3.30 Thionation of hemiaminals with **50** and subsequent cyclization

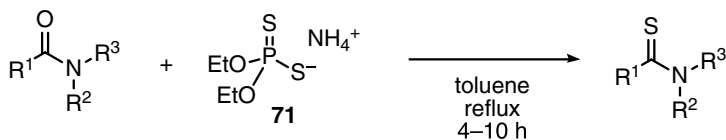
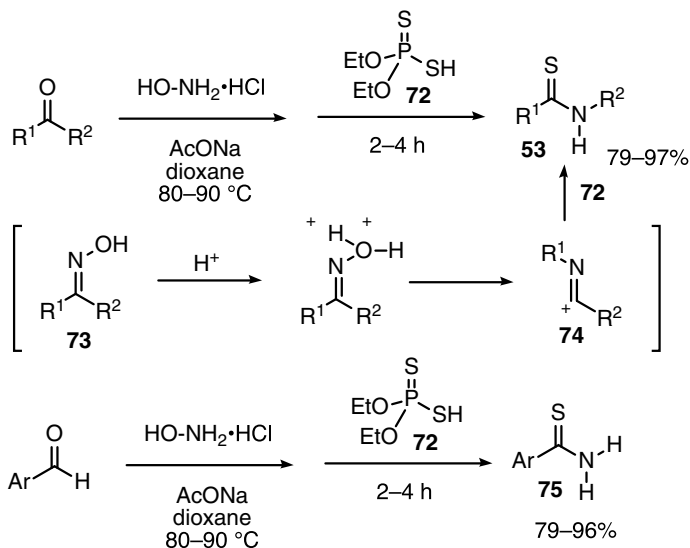


Fig. 3.31 Thionation of amides with ammonium phosphorodithioates

In other solvents such as dichloromethane, ethanol, THF, and water, no products are formed. The reaction is applicable to primary, secondary, and tertiary amides, and the substitution patterns on the nitrogen atom do not affect the efficiency of the reaction.

Phosphorodithioic acid **72** reacts with ketones and aldehydes and hydroxylamine hydrochloride to give secondary thioamides **53** and aromatic primary thioamides **75** (Fig. 3.32) [56]. In the reaction with ketones, the generated oximes undergo Beckmann rearrangement to form nitrilium cations **74**, to which **72** adds to give thioamides **53**. In the reaction with aldehydes, in situ generation of nitriles is postulated.

Carboxylic acids are converted to thioamides by reacting with ammonium phosphorodithioates **76**. In this case, ammonium moiety works as a nitrogen source (Fig. 3.33) [57]. A wide range of aliphatic and aromatic primary, secondary, and tertiary thioamides are formed. Salicylic acid (**77**) reacts with **76** to afford *O*-hydroxy benzthioamides **78a–78c**.



**Fig. 3.32** Thionation of ketones and aldehydes with hydroxylamine and phosphorodithioic acid

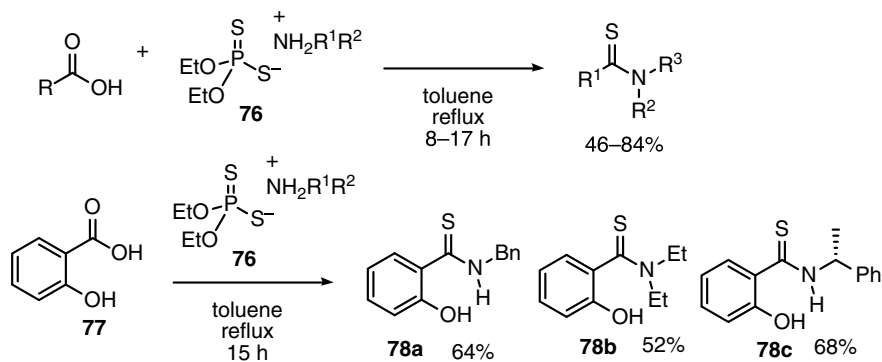


**Fig. 3.33** Thionation of carboxylic acids with ammonium phosphorodithioates

### 3.3.2 Thionation of Amides with Elemental Sulfur and Hydrochlorosilanes

Despite the fact that the reagents **49–51**, **71**, **72**, and **76** are highly powerful for the direct thionation of amides, phosphorus-containing by-products are always formed, and their separation is cumbersome in some cases. As phosphorus-free thionation, the combination of hydrochlorosilanes, amines, and elemental sulfur is developed (Fig. 3.34) [58]. The reaction of thiophene amides with HSiCl<sub>3</sub>, DABCO, and elemental sulfur proceeds in toluene at 115 °C to give thioamides **79** in high yields [59].

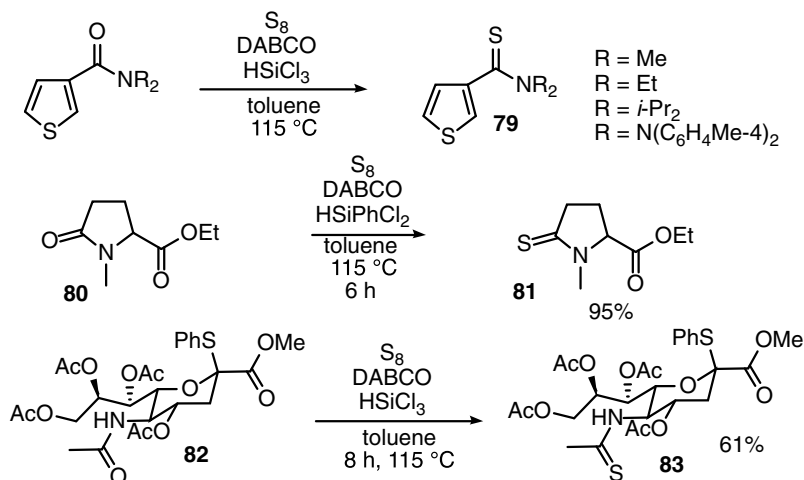


**Fig. 3.34** Thionation of amides with chlorohydrosilane, amines, and elemental sulfur

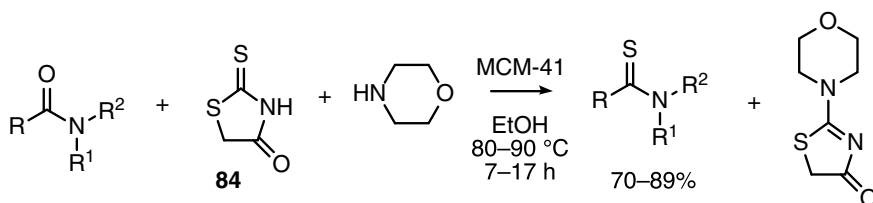


**Fig. 3.35** Thionation of amides with rhodanine

Amides having alkoxy carbonyl groups such as **80** and **82** participate in the reaction to give **81** and **83**. In the substrate **82**, six carbonyl groups are present, but amide moiety is selectively converted to thioamide moiety. Triphenylsilylthiol (Ph<sub>3</sub>SiSH) can convert DMF and acetamide to the corresponding thioamides [60].

### 3.3.3 Thionation of Amides with Rhodanine

Rhodanine **84** undergoes thionation of amides in the presence of mesoporous silica MCM-41 (Fig. 3.35) [61]. The reaction is applicable to a range of amides.

### 3.4 Addition of Thionating Agents to Nitriles

The addition of hydrogen sulfide to nitriles formally gives primary thioamides. Instead of hydrogen sulfide, other thionating agents such as Lawesson's reagent **50** [62], thioacetic acid [63], ammonium sulfide [64], dithiophosphoric acid **72** [64], and sodium sulfide [65, 66] are used in combination with  $\text{BF}_3 \cdot \text{Et}_2\text{O}$  and  $\text{CaH}_2$  in toluene– $\text{Et}_2\text{O}$ , pyridine, dioxane, DMF, and  $[\text{DBUH}][\text{OAc}]$  (Fig. 3.36). The reaction time and temperature are dependent on each reaction condition, but in most cases, aromatic and aliphatic primary thioamides are obtained in reasonable yields. Among reaction conditions A–G, the combination of  $\text{Na}_2\text{S} \cdot 9\text{H}_2\text{O}$  and  $[\text{DBUH}][\text{OAc}]$  (reaction condition G) [66] appears to facilitate the conversion of nitriles to thioamides, the most quickly. In the reaction with  $\text{CS}_2$  and  $\text{Na}_2\text{S} \cdot 9\text{H}_2\text{O}$  (reaction condition E) [64], sodium trithiocarbonate ( $\text{Na}_2\text{SC}(\text{S})\text{S}$ ) is generated. This enables the conversion of per-*O*-acetylated D-galactopyranosyl nitrile **85** and per-*O*-acetylated D-mannopyranosyl nitrile **87** to *C*-glycosyl thioamide **86** and glycal thioamide **88**, respectively. Examples of gram-scale synthesis of thioamides are described [65].

Copper-catalyzed reaction of acrylonitrile **89** with dimethyl formamide and elemental sulfur at 110 °C proceeds to give either aromatic thioamides **15** or acrylamide **2** depending on the absence or presence of pentanal (Fig. 3.37) [67]. Without pentanal, aryl radicals may generate and react with in situ formed *N,N*-dimethyl thioformamide, whereas in the presence of pentanal, arylmethyl radicals

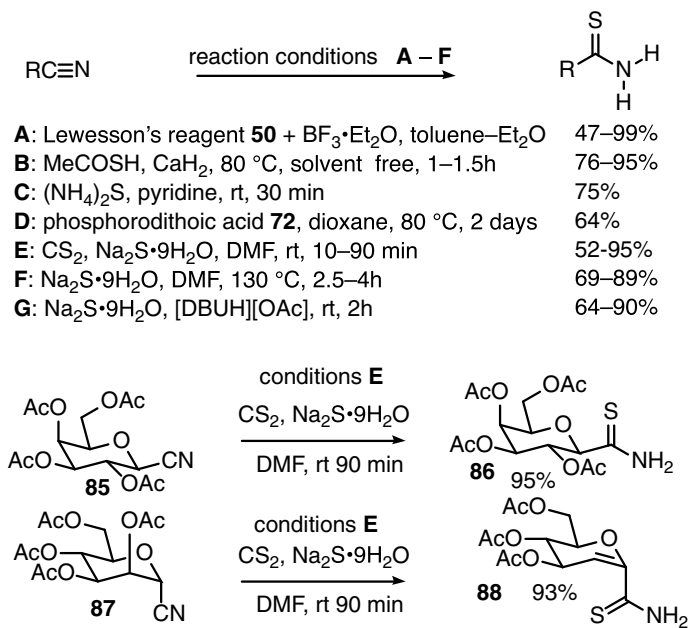
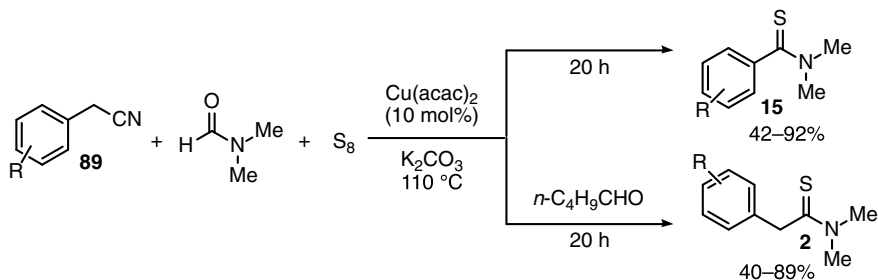


Fig. 3.36 Addition of thionating agents to nitriles



**Fig. 3.37** Copper-catalyzed thionation of arylacetonitriles

may generate. Although the role of pentanal is ambiguous, the reaction of phenylpropionitrile under the identical conditions with pentanal gives thioamides derived from the replacement of a cyano group with a dimethylthiocarbonyl group.

## 3.5 Thiocarbonyl Compounds as a Starting Material

### 3.5.1 Addition to Isothiocyanates

Isothiocyanates (general formula:  $\text{R-N}=\text{C}=\text{S}$ ), which are prepared from primary amines and carbon disulfides, are readily available precursors of secondary thioamides. The carbon atom attached to nitrogen and sulfur atoms is susceptible to attacks of carbon nucleophiles.

Imine **90** [68] and enamine **92** [69] react with aryl isothiocyanates to give  $\alpha,\beta$ -unsaturated secondary thioamides **91** and **93** (Fig. 3.38).

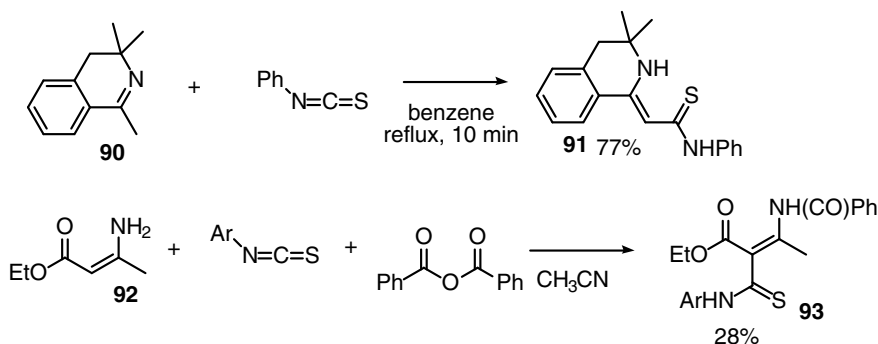


**Fig. 3.38** Addition of imines and enamines to isothiocyanates

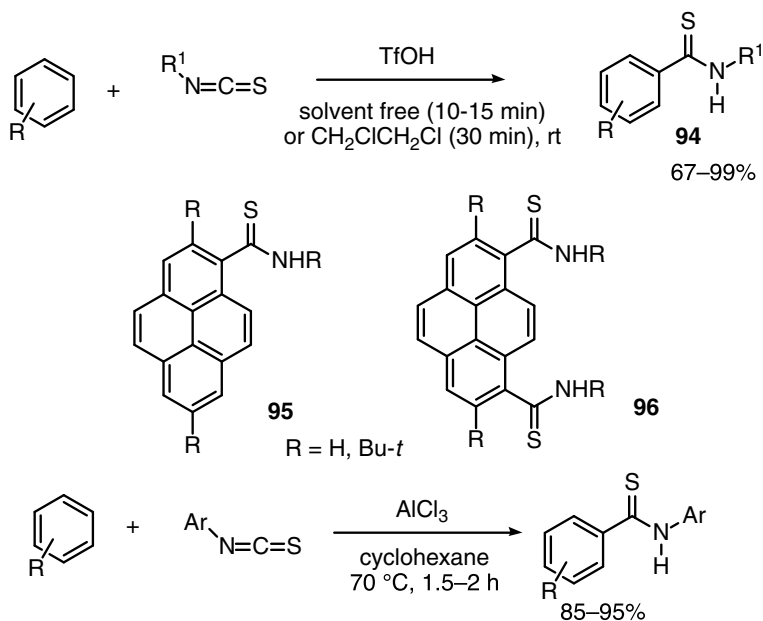


**Fig. 3.39** Friedel–Crafts reaction between isothiocyanates and arenes

Friedel–Crafts reactions between arenes and isothiocyanates have been known, but the reaction is sluggish. To facilitate the reaction, acids are optimized as an additive. Triflic acid [70–73] and aluminum chloride [74] are effective (Fig. 3.39). In the former case, not only aromatic but also aliphatic isothiocyanates are used. Nevertheless, only arenes having electron-donating groups are shown. As heteroarenes, thiophenes participate in the reaction, and the reaction selectively takes place at the 2-position of thiophenes. The Friedel–Crafts reaction of pyrenes also proceeds to give the products **95** and **96** [71–73]. The photophysical properties of some of the products are elucidated.

Organometallic reagents such as organolithium and organocopper reagents add to the carbon atom of isothiocyanates to give secondary thioamides (Fig. 3.40) [75, 76]. The development of chemistry of organolithium reagents enables us to use a wide variety of the reagents including optically active species. Deprotonation of *N*-Boc pyrrolidine **97** under Beak's reaction conditions followed by the addition of isothiocyanates affords thioamides **98**, wherein a chiral carbon atom is attached to the carbon atom of thiocarbonyl groups with high enantiomeric excess. Addition of organolithium reagents to optically active isothiocyanate **99** gives thioamides **100**. Chirality in **99** retains during the reaction. Higher reactivity of  $\text{N}=\text{C}=\text{S}$  compared with that of an alkoxy carbonyl group is proved by reacting Gilman reagent **101** with **102** to selectively furnish thioamide **103**. The use of metal acetylides can give rise to the formation of acetylenic thioamides [77]. Insertion of isothiocyanates to  $\text{Ar-Pd}$

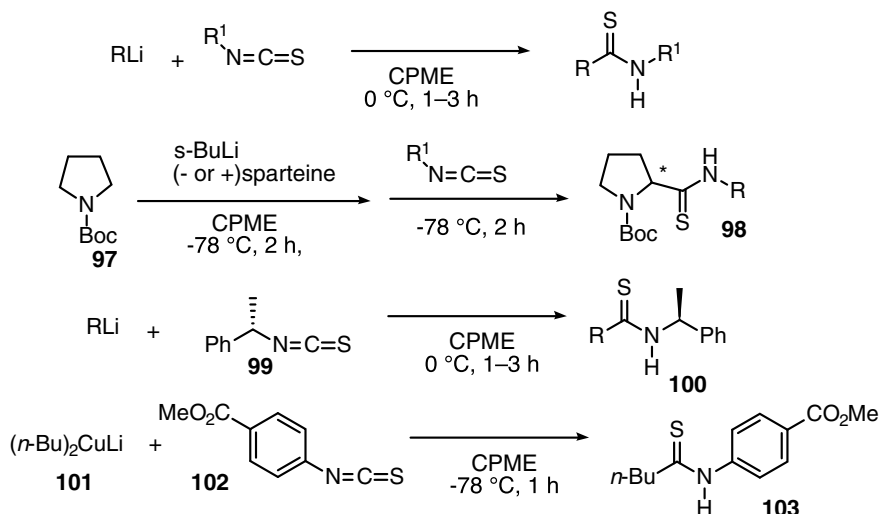


Fig. 3.40 Addition of organometallic reagents to isothiocyanates

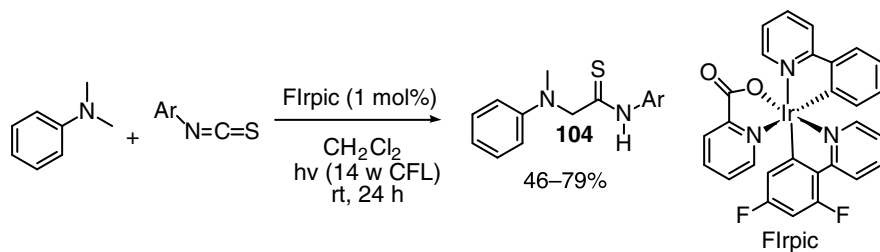


Fig. 3.41 Addition of *N,N*-dimethylaniline to aromatic isothiocyanates under the irradiation of visible light

bonds in situ generated from Pd complexes and aromatic carboxylic acids is also demonstrated to give aromatic thioamides [78].

*N,N*-Dimethyl aniline reacts with aryl isothiocyanates in the presence of 1 mol% of Flrpic under the irradiation of visible light to give  $\alpha$ -amino thioacetamides **104** (Fig. 3.41) [79]. The reaction may involve  $\alpha$ -aminoalkyl radicals, which then undergoes radical addition selectively to the carbon atom in the N=C=S moiety.

### 3.5.2 Addition to Other Thiocarbonyl Compounds

The compounds having C=S groups such as primary thioamides, thiourea, thiocarbonyl chlorides, dithioic acid esters, and thiuram disulfides are used as a starting



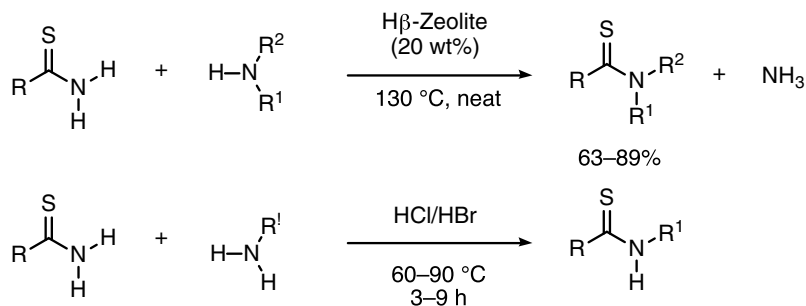


Fig. 3.42 Transthioamidation

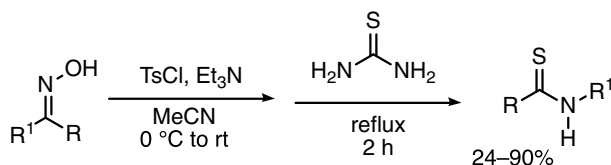
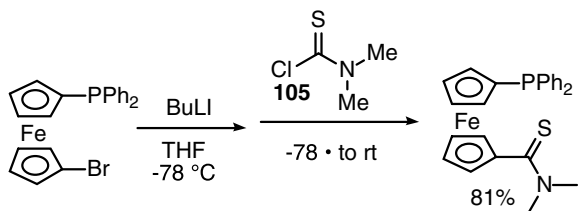


Fig. 3.43 Addition of thiourea to oxime sulfonates

Fig. 3.44 Thiocarbamylation of organolithium reagents



material to afford thioamides. Thiobenzaldehyde generated from benzylthiol is also converted to thioamides.

Transthioamidation of primary thioamides is mediated by H $\beta$ -zeolite at 130 °C to give secondary and tertiary thioamides (Fig. 3.42) [80]. Alternatively, HCl/HBr is used in the reaction with primary amines [81]. Secondary amines remain intact under these reaction conditions. Transthioamidation of thioacetamide with a range of amines is achieved by using heterobimetallic lanthanide alkoxide such as Nd<sub>2</sub>Na<sub>8</sub>(OCH<sub>2</sub>CF<sub>3</sub>)<sub>14</sub>(THF)<sub>6</sub> [82].

Thiourea reacts with oxime sulfonates derived from oximes and tosyl chlorides to give secondary amines (Fig. 3.43) [83]. Similarly to the reaction in Fig. 3.32, the reaction proceeds through Beckmann rearrangement.

Thiocarbamylation of organolithium reagents is achieved with thiocarbamoyl chloride **105** (Fig. 3.44) [84].

Thiocarbonylation of amines with dithioic acid esters is a well-known reaction to give thioamides (Fig. 3.45). A range of amines and dithioic acid esters are available. Some of the examples are shown in Fig. 3.45. The reaction is generally performed at

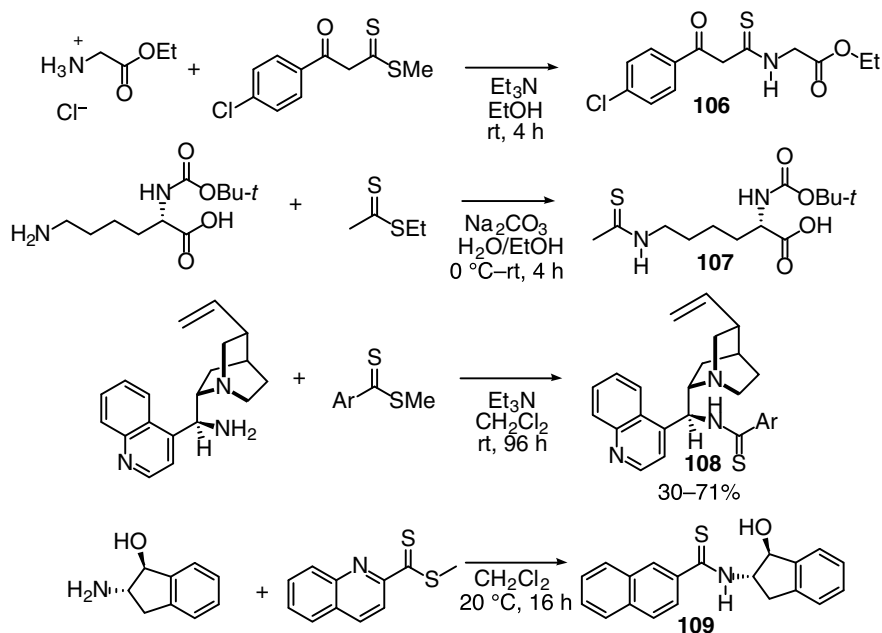


**Fig. 3.45** Thiocarbonylation of amines with dithioic acid esters

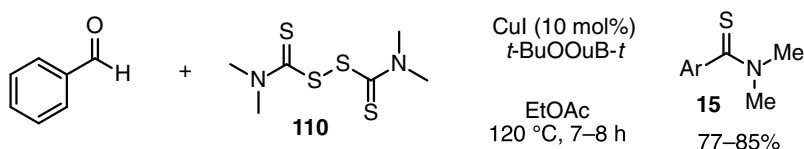


**Fig. 3.46** Copper-catalyzed reaction of aromatic aldehydes with thiuram disulfide and di(*tert*butyl) peroxide

room temperature. The reaction time depends on the substituents attached to the carbon atom of a thiocarbonyl group. The reaction of aliphatic dithioic acids with amino acids is complete within 4 h to give the products **106** [85] and **107** [86]. Arylthiocarbonylation of *epi*-cinchonidine and aminoalcohols is achieved with aromatic dithioic acid esters to give the corresponding thioamides **108** [87] and **109** [88].

Tetramethylthiuram disulfide (**110**) is used for the oxidative thiocarbonylation of aromatic aldehydes in the presence of catalytic amounts of copper iodide (Fig. 3.46) [89]. As an oxidant, di(*tert*butyl) peroxide efficiently works.

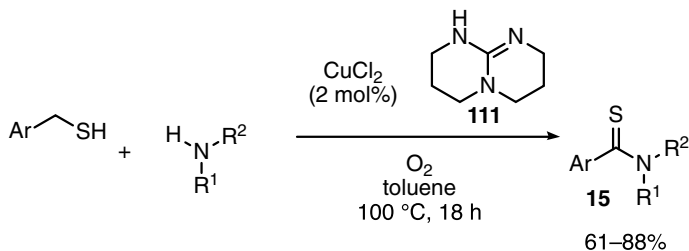


Fig. 3.47 Reaction of benzylthiol with secondary amines under O<sub>2</sub> atmosphere

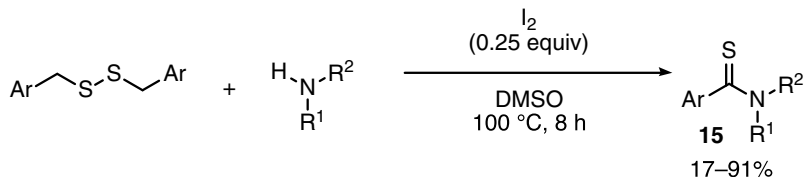


Fig. 3.48 Reaction of bis(arylmethyl) sulfides with amines

### 3.6 Thiols, Sodium Sulfides, and Disulfide as a Sulfur Source

Benzylthiols react with secondary amines under oxygen atmosphere to give aromatic tertiary thioamides **15**. The reaction is performed in the presence of a catalytic amount of copper(II) chloride and 1,5,7-triazabicyclo[4.4.0]dec-5-ene (**111**) (Fig. 3.47) [90]. Initially, thiobenzaldehydes may generate via disulfides formed by the oxidation of benzylthiol. Secondly, oxidative amination of thiobenzaldehydes may take place to furnish **15**. Likewise, dibenzyl disulfides are used as a source of a thiocarbonyl group (Fig. 3.48) [91]. In this case, primary and secondary amines are used to give **15**. <sup>1</sup>H NMR experiments of the reaction mixture suggest the in situ generation of thiobenzaldehyde.

Sodium sulfide hydrate is available as a sulfur source. The reaction of alkynyl bromides **112** with amines and Na<sub>2</sub>S·9H<sub>2</sub>O gives arylthioacetamides. Aromatic and aliphatic alkynyl bromides are used. Primary and secondary amines participate in the reactions, although aniline does not form the corresponding thioamides (Fig. 3.49) [92]. Ynamines **113** may initially generate from **112** and amines. The intermediates **113** resonate iminium salts **114**. Sulfide anion may attack the carbon atom next to the nitrogen atom in **114** to form enethiolates. Sodium sulfide hydrate is incorporated into aldehydes with amines derived from formamides in the presence of an oxidant (Fig. 3.50) [93]. A broad range of combinations of aldehydes and formamides are available to give a range of thioamides. The reaction is carried out in water, and similarly to the Willgerodt–Kindler reaction of aldehydes, iminium salts are postulated to generate in situ.



## 3.7 Summary

This chapter has introduced the preparative methods for a wide variety of thioamides. Because of the increasing importance of thioamides in synthetic chemistry, biology-related, and material-related scientific fields, synthetic methods will continuously be developed. Ready treatment of reagents for the introduction of the sulfur atom without nasty smelling, functional group compatibility of reagents, easier ways to isolate the resulting thioamides, and lesser amounts of by-products, which have to be frequently handled as wastes, are the key issues to be addressed in the future development of synthetic methods.

## References

1. T. Murai, in *Topics in Current Chemistry*, vol. 251. (2005), p. 247
2. E. Schaumann, *Comprehensive Org. Synth. II* **2**, 411 (2014)
3. C. Willgerodt, *Ber.* **20**, 2467 (1887)
4. D.L. Priebbenow, C. Bolm, *Chem. Soc. Rev.* **42**, 7870 (2013)
5. M.M. Mojtahedi, T. Alishiri, M.S. Abaee, *Phosphorus, Sulfur, Silicon* **2011**, 186 (2010)
6. D.S. Rekunge, C.K. Khatri, G.U. Chaturbhuj, *Monatsh. Chem.* **148**, 2091 (2017)
7. I. Radfar, S. Abbasi, M.K. Miraki, E. Yazdani, M. Karimi, A. Heydari, *ChemistrySelect* **3**, 3265 (2018)
8. J.E. Valdez-Rojas, H. Ríos-Guerra, A.L. Ramírez-Sánchez, G. García-González, C. Álvarez-Toledano, J.G. López-Cortés, R.A. Toscano, J.G. Penieres-Carrillo, *Can. J. Chem.* **90**, 567 (2012)
9. T.B. Nguyen, P. Retailleau, *Green Chem.* **19**, 5371 (2017)
10. N. Paul, R. Sathishkumar, C. Anuba, *RSC Adv.* **3**, 7445 (2013)
11. S.P. Pathare, P.S. Chaudhari, K.G. Akamanchi, *Appl. Cat. A.* **425–426**, 125 (2012)
12. H. Saeidian, S. Vahdati-Khajehi, H. Bazghosha, Z. Mirjafary, *J. Sulfur Chem.* **35**, 700 (2014)
13. Z. Mirjafary, L. Ahmadi, M. Moradib, H.X. S, *RSC Adv.* **5**, 78038 (2015)
14. P.S. Chaudhari, S.D. Salim, R.V. Sawant, K.G. Akamanchi *Green Chem.* 1707 (2010)
15. Z. Yin, B. Zheng, *J. Sulfur Chem.* **34**, 527 (2013)
16. Z. Yin, B. Zheng, F. Ai, *Phosphorus, Sulfur, and Silicon* **188**, 1412 (2013)
17. C.K. Khatri, D.S. Rekunge, G.U. Chaturbhuj, *New J. Chem.* **40**, 10412 (2016)
18. C.K. Khatri, A.S. Mali, G.U. Chaturbhuj, *Monatsh. Chem.* **148**, 1463 (2017)
19. S.D. Fazylov, O.A. Nurkenov, Z.S. Akhmetkarimova, D.R.R.J. Zhienbaeva, *Gen. Chem.* **82**, 781 (2012)
20. H. Xu, H. Deng, Z. Li, H. Xiang, X. Zhou, *Eur. J. Org. Chem.* 7054 (2013)
21. B. Eftekhari-Sis, S.V. Khajeh, S.M. Amini, M. Zirak, M. Saraei, *J. Sulfur Chem.* **34**, 464 (2013)
22. M. Papa, I. Chiarotto, M. Feroci, *ChemistrySelect* **2**, 3207 (2017)
23. W. Liu, C. Chem, H. Liu, *Beilstein J. Org. Chem.* **11**, 1721 (2015)
24. T. Guntreddi, R. Vanjari, K.N. Singh, *Org. Lett.* **16**, 3624 (2014)
25. S. Kumar, R. Vanjari, T. Guntreddi, K.N. Singh, *Tetrahedron* **2016**, 72 (2012)
26. M. Milen, A. Abranyi-Balogh, A. Dancso, G. Keglevich, *J. Sulfur Chem.* **33**, 33 (2012)
27. P. Gisbert, I.M. Pastor, *Synthesis* **50**, 3031 (2018)
28. M. Patra, J. Hess, B. Konatschnig, G. Gasser, *Organometallics* **32**, 6098 (2013)
29. B. Kurpil, B. Kumru, T. Heil, M. Antonietti, A. Savateev, *Green Chem.* **20**, 838 (2018)
30. T.B. Nguyen, M.Q. Tran, L. Ermolenko, A. Al-Mourabit, *Org. Lett.* **16**, 310 (2014)
31. K. Xu, Z. Li, F. Cheng, Z. Zuo, T. Wang, M. Wang, L. Liu, *Org. Lett.* **20**, 2228 (2018)
32. X. Li, Q. Pan, R. Hu, X. Wang, Z. Yang, S. Han, *Asian J. Org. Chem.* **5**, 1353 (2016)

33. J. Liu, S. Zhao, X. Yan, Y. Zhang, S. Shao, K. Zhuo, Y. Yue, *J. Asian, Org. Chem.* **6**, 1764 (2017)
34. T. Guntreddi, R. Vanjari, N. Singh, *Tetrahedron* **70**, 3887 (2014)
35. C.-H. Yang, G.-J. Li, C.-J. Gong, Y.-M. Li, *Tetrahedron* **71**, 637 (2015)
36. T. Ozturk, E. Ertas, O. Mert, *Chem. Rev.* **110**, 3419 (2010)
37. K. Manzor, F. Kelleher, *Tetrahedron Lett.* **57**, 5237 (2016)
38. S.S. Syeda, S. Jakkraj, G.I. Georg, *Tetrahedron Lett.* **56**, 3454 (2015)
39. N. Wang, J. Liu, C. Wang, L. Bai, X. Jiang, *Org. Lett.* **20**, 292 (2018)
40. K. Inami, Y. Ono, S. Kondo, I. Nakanishi, K. Ohkubo, S. Fukuzumi, M. Mochizuki, *Bioorg. Med. Chem.* **23**, 6733 (2015)
41. G. Prabhu, G. Nagendra, N.R. Sagar, R. Pal, T.N.G. Row, V.V. Sureshbabu, *Asian J. Org. Chem.* **5**, 127 (2016)
42. D. Cho, J. Ahn, K.A. De Castro, H. Ahn, H. Rhee, *Tetrahedron* **66**, 5583 (2010)
43. J. Bergman, B. Pettersson, V. Hasimbegovic, P.H. Svensson, *J. Org. Chem.* **76**, 1546 (2011)
44. N. Kingi, J. Bergman, *J. Org. Chem.* **81**, 7711 (2016)
45. H.R. Lagiakos, A. Walker, M.-I. Aquilar, P. Perlmutter, *Tetrahedron Lett.* **52**, 5131 (2011)
46. M. Zarei, *J. Sulfur Chem.* **34**, 370 (2013)
47. J.E. Sears, T.J. Barker, D.L. Boger, *Org. Lett.* **17**, 5460 (2015)
48. A. Margalef, T. Slagbrand, F. Tinnis, H. Adolffsson, M. Diéguez, O. Pamies, *Adv. Synth. Catal.* **358**, 4006 (2016)
49. M.S. Kirillova, M.E. Muratore, R. Dorel, A.M. Echavarren, *J. Am. Chem. Soc.* **138**, 3671 (2016)
50. J. Li, W. Zhang, F. Zhang, Y. Chen, A. Li, *J. Am. Chem. Soc.* **139**, 14893 (2017)
51. S. Lee, M. Bae, J. In, J.H. Kim, S. Kim, *Org. Lett.* **19**, 254 (2017)
52. S. Fujita, K. Nishikawa, T. Iwata, T. Tomiyama, H. Ikenaga, K. Matsumoto, M. Shindo, *Chem. Eur. J.* **24**, 1539 (2018)
53. L. Legnani, L. Toma, P. Caramella, M.A. Chiacchio, S. Giofre, I. Delso, T. Tejero, P. Merino, *J. Org. Chem.* **81**, 7733 (2016)
54. S.V. Fedoseev, M.Y. Belikov, O.V. Ershov, V.A. Tafeenko, *Chem. Heterocycl. Compd.* **53**, 1045 (2017)
55. B. Kaboudin, L. Malekzadeh, *Synlett* 2807 (2011)
56. A.K. Yadav, V.P. Srivastava, D.S. Yadav, *Tetrahedron Lett.* **53**, 7113 (2012)
57. B. Kaboudin, V. Yarahmadi, J. Kato, T. Yokomatsu, *RSC Adv.* **3**, 6435 (2013)
58. F. Shibahara, R. Sugiura, T. Murai, *Org. Lett.* **11**, 3064 (2009)
59. T. Yamauchi, F. Shibahara, T. Murai, *Org. Lett.* **17**, 5392 (2015)
60. R.N. Arias-Ugarte, H.K. Sharma, K.H. Pannell, *Appl. Organometal. Chem.* **30**, 510 (2016)
61. S. Ray, A. Bhaumik, R.J. Butcher, C. Mukhopadhyay, *Tetrahedron Lett.* **54**, 2164 (2013)
62. M. Nagl, C. Panuschka, A. Barta, Schmid, W. *Synthese*, 4012 (2008)
63. K.A. Mohammed, V.P. Jayashankara, N.P. Rai, K.M. Raju, P.N. Arunachalam, *Synthesis* 2338 (2009)
64. R.G. Hall, *Synth. Commun.* **44**, 3456 (2014)
65. T. Ghosh, A. Si, A.K. Misra, *Chem. Sel.* **2**, 1366 (2017)
66. X.T. Cao, H. Yang, H. Zheng, P. Zhang, *Heterocycles* **96**, 509 (2018)
67. Y. Qu, Z. Li, H. Xiang, X. Zhou, *Adv. Synth. Catal.* **355**, 3141 (2013)
68. O.V. Surikova, A.G. Mikhailovskii, *Russ. J. Org. Chem.* **50**, 1306 (2014)
69. T.N. Trinh, A. McCluskey, *Tetrahedron Lett.* **57**, 3256 (2016)
70. B.V. Varun, A. Sood, K.R. Prabhu, *RSC Adv.* **4**, 60798 (2014)
71. A. Wrona-Piotrowicz, R. Zakrzewski, A.B. Brosseau, A. Makal, K. Wozniak, *RSC Adv.* **4**, 56003 (2014)
72. A. Wrona-Piotrowicz, J. Zakrzewski, T. Gajda, A. Makal, A. Brosseau, R. Métivier, *Beilstein J. Org. Chem.* **11**, 2451 (2015)
73. A. Wrona-Piotrowicz, M. Witalewska, J. Zakrzewski, A. Makal, *Beilstein J. Org. Chem.* **13**, 1032 (2017)

74. K. Kumar, D. Konar, S. Goyal, M. Gangar, M. Chouhan, R.K. Rawal, V.A. Nair, *ChemistrySelect* **1**, 3228 (2016)
75. V. Pace, Castoldi, L.; Monticelli, S.; Safranek, S.; Roller, A.; Langer, T.; Holzer, W. *Chem. Eur. J.* 2015, **21**, 18966
76. V. Pace, S. Monticelli, K. Vega-Hernández, L. Castoldi, *Org. Biomol. Chem.* **14**, 7848 (2016)
77. H. Adams, H. Hodson, M.J. Morris, G.A. Venting, *Tetrahedron Lett.* **57**, 1328 (2016)
78. A. Noor, J. Li, G.N. Khairallah, Z. Li, H. Ghari, A.J. Canty, A. Ariaifard, P.S. Donnelly, A.J. O'Hair, *Chem. Commun.* **53**, 3854 (2017)
79. H. Zhou, P. Lu, X. Gu, P. Li, *Org. Lett.* **15**, 5646 (2013)
80. S.N. Rao, D.C. Mohan, S. Adimurthy, *RSC Adv.* **5**, 95313 (2015)
81. U. Pathak, S. Bhattacharyya, S. Mathur, *RSC Adv.* **5**, 4484 (2015)
82. H. Sheng, R. Zeng, W. Wang, S. Luo, Y. Feng, J. Liu, W. Chen, M. Zhu, Q. Guo, *Adv. Synth. Catal.* **359**, 302 (2017)
83. L.-F. L, N. An, H.-J. Pi, J. Ying, W. Du, W.-P. Deng, *Synlett* 979 (2011)
84. T.A. Fernandes, H. Solarova, I. Cisarova, F. Uhlik, M. Sticha, P. Stepnicka, *Dalton Trans.* **44**, 3092 (2015)
85. S. Prasanth, M. Varughese, N. Joseph, P. Mathew, T.K. Manojkumar, C.J. Sudarsanakumar, *Mo. Stru.* **1081**, 366 (2015)
86. H. Xiong, N.M. Reynolds, C. Fan, M. Englert, D. Hoyer, S.J. Millar, D. Söll, *Angew. Chem. Int. Ed.* **55**, 4083 (2016)
87. Y. Singjunla, M. Pigeaux, R. Laporte, J. Baudoux, J. Rouden, *Eur. J. Org. Chem.* 4319 (2017)
88. A. Sellme, H. Stangl, M. Beyer, E. Grünstein, M. Leonhardt, H. Pongratz, H. Eichhornm, S. Elz, B. Striegl, Z. Jenei-Lanzl, S. Dove, R.H. Straub, O.H. Krämer, S. Mahboobi, *J. Med. Chem.* **61**, 3454 (2018)
89. H.-Y. Zeng, M. Wang, H.-Y. Peng, Y. Cheng, Z.-B. Dong, *Synthesis* **50**, 644 (2018)
90. X. Wang, J. Miran, S. Lim, H.-Y. Jang, *J. Org. Chem.* **79**, 7256 (2014)
91. S. Chen, Y. Li, J. Chen, X. Xu, L. Su, Z. Tang, C.-T. Au, R. Qiu, *Synlett* **77**, 2339 (2016)
92. Y. Sun, H. Jiang, W. Wu, W. Zenga, J. Lia, *Org. Biomol. Chem.* **12**, 700 (2014)
93. J. Wei, Y. Li, X. Jiang, *Org. Lett.* **18**, 340 (2016)
94. H.-Z. Li, W.-J. Xue, A.-X. Wu, *Tetrahedron* **70**, 4645 (2014)
95. Z. Zhou, J.-T. Yu, Y. Zhou, Y. Jiang, J. Cheng, *Org. Chem. Front.* **4**, 413 (2017)

# Chapter 4

## Reaction of Thioamides



Toshiaki Murai

**Abstract** Thioamides react with a wide range of electrophiles, nucleophiles, radical species, and so on. Reactive sites in thioamides are also broad. The sulfur atom in the C=S group accepts electrophiles and nucleophiles, which is in a marked contrast to the reaction patterns of amides. Not only one molecule but also two molecules of organometallic reagents are introduced to the carbon atom of the C=S group. The reduction of the C=S group to methylene groups and oxidation of the C=S group to the C=O group are also important fundamental processes. The  $\alpha$ -protons to the C=S group are more acidic than those in amides, and the generated enols and enolates react at the  $\alpha$ -carbon atoms or sulfur atoms depending on the electrophiles used. The nitrogen atom in primary and secondary thioamides also works as nucleophiles. The C=S group is used as directing groups for transition metal-catalyzed functionalizations.

**Keywords** Oxidation · Reduction · Carbon nucleophiles · Heteroatom nucleophiles · Transition metal-catalyzed reactions

### 4.1 Introduction

Thioamides are generally more reactive than ordinary amides and participate in most reactions which can be achieved with amides. In addition, thioamides show unique reactions mainly because of the less polar C=S bonds, greater contribution of the sulfur atom to the LUMO of the C=S group, and higher acidity of the protons on the nitrogen atom and at the position  $\alpha$  to the C=S group. In this chapter, characteristic reactions of thioamides with a wide range of reagents are described, although only a few examples of the asymmetric reactions and reactions leading to the formation of heterocycles are shown.

---

T. Murai (✉)  
Department of Chemistry and Biomolecular Science, Faculty of Engineering, Gifu University,  
Yanagido, Gifu 501-1193, Japan  
e-mail: [mtoshi@gifu-u.ac.jp](mailto:mtoshi@gifu-u.ac.jp)



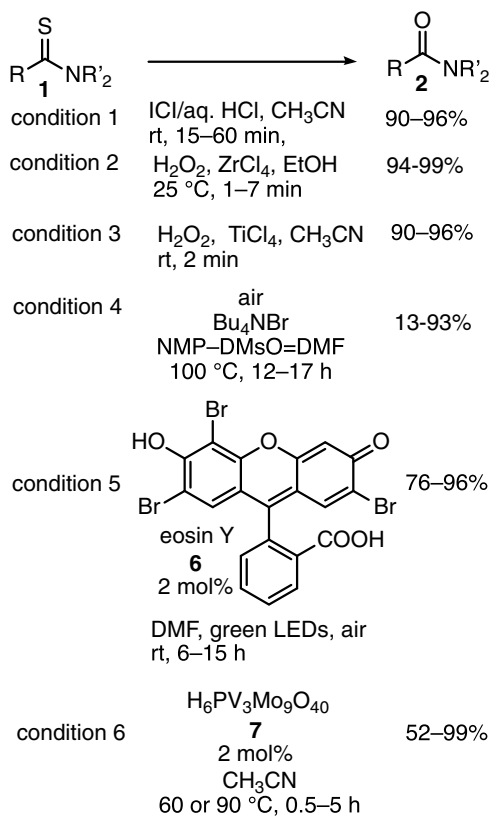
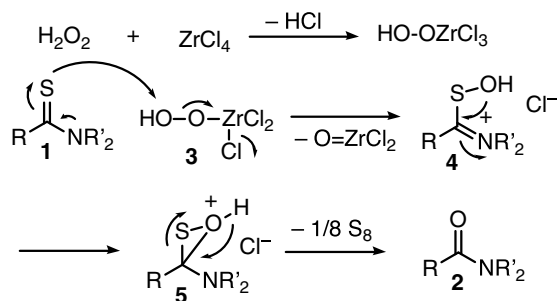
## 4.2 Oxidation of Thioamides

Thioamides **1** are readily converted to amides **2** by using a range of oxidants (Fig. 4.1). Oxidation with the combination of ICl and aqueous hydrochloric acid is complete within 1 h at room temperature (condition 1) [1]. Hydrogen peroxide (H<sub>2</sub>O<sub>2</sub>) converts **1–2** in the presence of zirconium tetrachloride (ZrCl<sub>4</sub>) (condition 2) [2]. It only needs less than 7 min to finish the reaction. Initially, H<sub>2</sub>O<sub>2</sub> reacts with ZrCl<sub>4</sub> to generate zirconium peroxide **3**, which then may react with **1** to form thioiminium salts **4** (Fig. 4.2). The salts **4** undergo intramolecular cyclization to give the intermediates **5**. The extrusion of the sulfur atom from **5** may give rise to the formation of **2**. In place of ZrCl<sub>4</sub>, titanium chloride (TiCl<sub>4</sub>) is employed as a reaction mediator (condition 3) [3]. Only two minutes are necessary to completely finish the reaction. The conversion of **1–2** is carried out under the air in the presence of tetrabutylammonium bromide in a mixed solvent of NMP-DMSO-DMF (condition 4) [4], although *N*-aryl aromatic secondary thioamides **1** are only used as a starting material. As another metal-free method, eosin Y (**6**) is used as a organophotoredox catalyst (condition 5) [5]. Under the irradiation of green LEDs (535 nm), aerobic oxidation of **1** proceeds to give the corresponding **2** in good to high yields. A range of **1** including aliphatic and aromatic derivatives, and secondary and tertiary derivatives participate in the oxidation. Phosphovanadomolybdic acid **7** catalyzes the oxidation of secondary and tertiary thioamides **1** to amides **2**, and the molecular oxygen is used as the terminal oxidant (condition 6) [6]. After the reaction, elemental sulfur is isolated. The use of a mixed solvent of acetonitrile and deuterated water gives the <sup>18</sup>O-labeled amides with the about 75% content of <sup>18</sup>O as a product.

Elimination of hydrogen sulfide from primary thioamides **8** gives rise to the formation of nitriles **9** (Fig. 4.3). To perform the reaction, amorphous manganese dioxide is used under the air (condition 1) [7]. Aromatic, heteroaromatic, and aliphatic nitriles **9** are obtained from **8**. Hydroxy and *tert*-butoxycarbonyl groups and halogens tolerate the reaction conditions. Indium triflate (In(OTf)<sub>3</sub>) catalyzes the formation of aromatic nitriles **9** from aromatic primary thioamides **8** in the presence of excess *N*-methyl *N*-trimethylsilyl trifluoromethylamide (**10**) (condition 2) [8].

The  $\alpha$ -position of C=S group of aryl thioacetamides **11** is oxidized to give  $\alpha$ -keto thioamides **12** in the presence of copper catalyst under oxygen atmosphere (Fig. 4.4) [9]. The reaction is complete within 3 h, and the elongation of the reaction time to 30 h facilitates further oxidation to give the  $\alpha$ -keto amides as a product. The reaction of **11** with a base and copper salt may form thioenolates **13**, which is in equilibrium with keto form **14**. The keto form **14** reacts with molecular oxygen at the position  $\alpha$  to the C=S group to result in the formation of **12** via **15**. Alkaline hydrolysis of the resulting product **12a** proceeds smoothly at reflux or under the irradiation of microwave to give glyoxalic acid **16** (Fig. 4.5).

Oxidation of polycyclic aromatic *N*-ethoxycarbonyl thioamides **17** with oxone or hydrogen peroxide takes place to give thioamide *S*-oxides **18** as thermally stable products, which are purified by the column chromatography on silica gel (Fig. 4.6) [10]. The structure of one of *S*-oxides **18** is disclosed by X-ray analyses. The oxygen

**Fig. 4.1** Oxidation of thioamides to amides**Fig. 4.2** Plausible reaction pathway using H<sub>2</sub>O<sub>2</sub> and ZrCl<sub>4</sub>

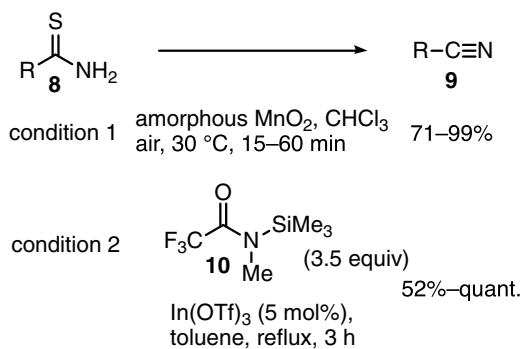


**Fig. 4.3** Conversion of primary thioamides to nitriles

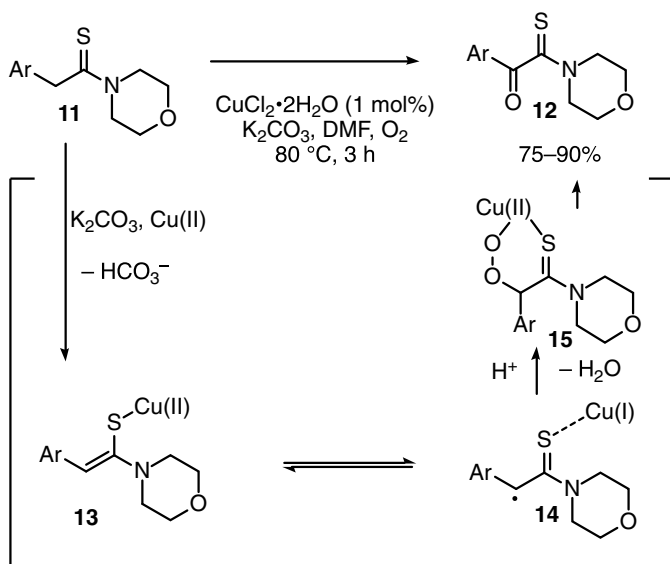


**Fig. 4.4** Oxidation of  $\alpha$ -position of C=S group

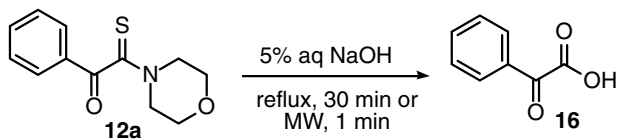


**Fig. 4.5** Alkaline hydrolysis of  $\alpha$ -keto thioamides

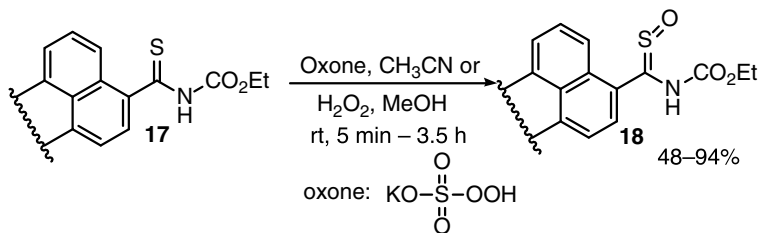


Fig. 4.6 Oxidation of polycyclic aromatic thioamides to *S*-oxides

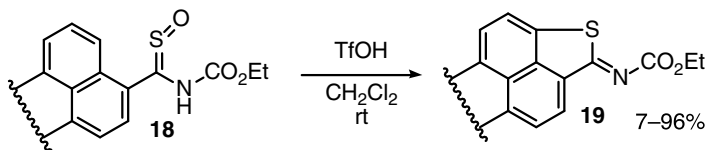


Fig. 4.7 Intramolecular cyclization of *S*-oxides

atom is oriented at the trans position of the aromatic group through the C=S bonds, and the C=S bonds and hydrogen atom are located in the cis position through C–N bonds. The acid-catalyzed cyclization of **18** gives naphthothiophenes **19** (Fig. 4.7).

### 4.3 Reaction at the Nitrogen Atom of Thioamides

Secondary thioamides can react at the nitrogen atom to form tertiary thioamides. For example, allylation at the nitrogen atom of secondary thioamides **20** is achieved by reacting with paraformaldehyde (**21**) and styrenes **22** in the presence of aluminum triflate ( $\text{Al}(\text{OTf})_3$ ) (Fig. 4.8) [11]. The reaction is extended to thiolactam **24**. Mechanistically, thiolactam **24** may react with **21** catalyzed by  $\text{Al}(\text{OTf})_3$  to generate iminium salt **26**, which is then nucleophilically attacked by **22** to form the intermediate **27**. The deprotonation from **27** may give **25**.

*N*-Benzoylation of thioacetamide (**28**) was achieved by reacting 2-naphthol (**29**) and aryl aldehydes **30** (Fig. 4.9) [12]. The reaction is catalyzed by ferric hydrogen sulfate ( $\text{Fe}(\text{HSO}_4)_3$ ) in dichlorobenzene. In the reaction,  $\text{Fe}(\text{HSO}_4)_3$ -catalyzed condensation reaction of **29** and **30** generates ortho-quinone methides **32**. Nucleophilic attack of the nitrogen atom in **28** to **32** may proceed to give the products **31**. Despite the fact that the sulfur atom is a more powerful nucleophilic atom than the nitrogen atom, the nitrogen atom selectively participates in the attack.

Acylation of polyfluoroalkylthioamides **33** takes place at the nitrogen atom at room temperature to give *N*-acyl thioamides **35** (Fig. 4.10) [13]. The product **35** derived from trifluoroacetamide is not isolated, but undergoes self-dimerization to

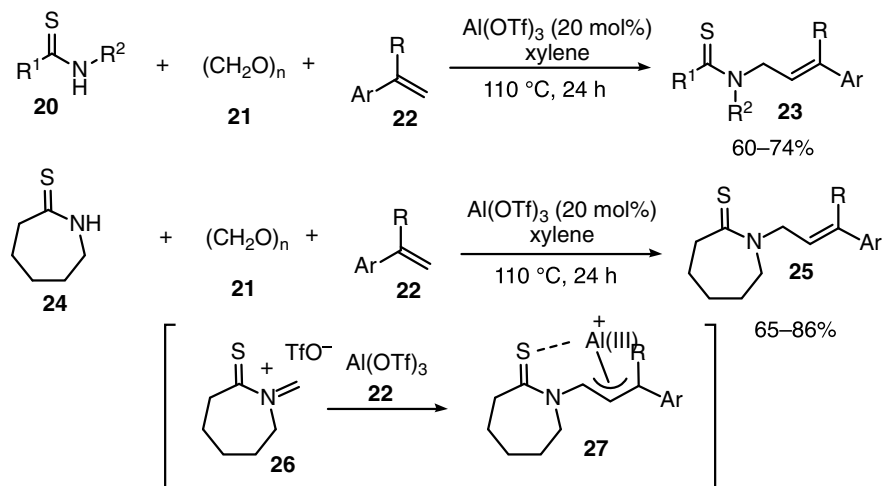


Fig. 4.8 *N*-Allylation of secondary thioamides

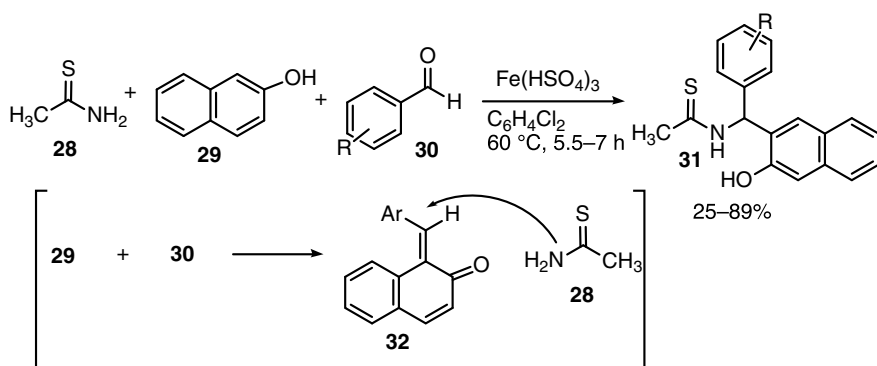


Fig. 4.9 *N*-Benzylation of thioacetamide

give 1,3-dithietane **36** as a stereoisomeric mixture. In contrast, the acylation of **33** with acid chloride **37** requires higher temperature to give *N*-acyl thioamides **38**.

#### 4.4 Reaction at the Carbon Atom of Thioamides

A range of nucleophiles react with thioamides at the carbon atom of C=S group.

The reduction of C=S group in thioamides to a methylene group has been used for the total synthesis of biologically relevant compounds. Raney Ni is often used as a reducing agent [14–16]. Alternatively, methylation of thioamide **39** with Meerwein's salt ( $\text{Me}_3\text{OBF}_4$ ) followed by the reduction with sodium borohydride ( $\text{NaBH}_4$ )

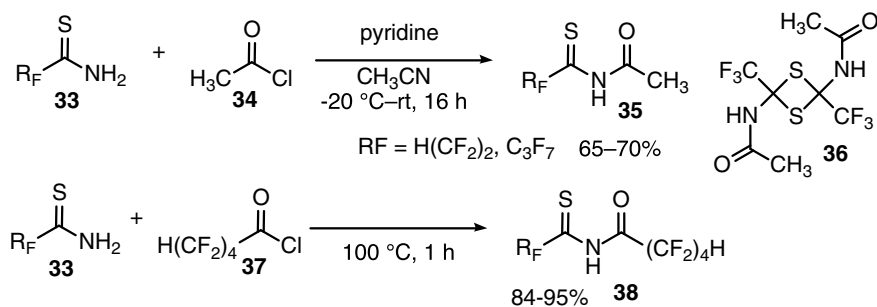


Fig. 4.10 Acylation of polyfluoroalkanethioamide

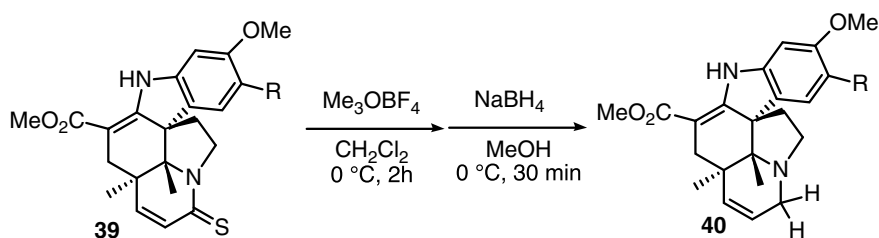
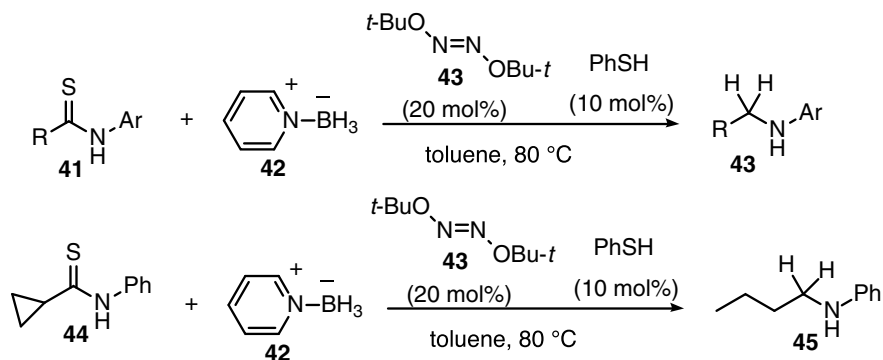


Fig. 4.11 Reduction of thioamide with  $\text{NaBH}_4$

gives the product **40** (Fig. 4.11) [17, 18]. The reduction of thioamides under the radical reaction conditions is also developed (Fig. 4.12) [19]. The treatment of *N*-aryl thioamides **41** with pyridine-borane **42** in the presence of di-*tert*-butyl hyponitrite (**43**) and benzenethiol (PhSH) gives arylamines **43**. In the reaction of the thioamide having a cyclopropyl group, the ring opening of a cyclopropyl group also proceeds to give *N*-phenyl butylamine (**45**). This result is indicative of the generation of radical species at the carbon atom of  $\text{C}=\text{S}$  group. Reductive sequential cyclization is achieved under the similar radical reaction conditions. Instead of **42**, borate **47** and instead of **43** azoisobutyronitrile (AIBN) (**48**) are used. Some of the examples are shown in Fig. 4.13. In these examples, thioamides **46**, **50**, and **52** are converted to the ring-fused heterocycles **49**, **51** and carbocycle **53**, although the stereoselectivity of the reaction is not high.

The reduction of secondary thioamide **54a** with excess hydrosilane in the presence of a catalytic amount of iron complex **55** affords imine **56** as a product (Fig. 4.14) [20, 21]. The use of triethylsilane and dimethylphenylsilane gives **56** along with an amine, whereas the use of methylphenylsilane and triphenylsilane selectively leads to **56**. The catalytic cycles involves several intermediates. One of them is carbene iron complexes. In fact, in the mixture of **54** and iron complex **57**, carbene iron complexes **58** are detected by NMR spectra, and the complex **58** is isolated by the reaction with triphenylsilane (Fig. 4.15).



**Fig. 4.12** Reduction of thioamides under radical conditions

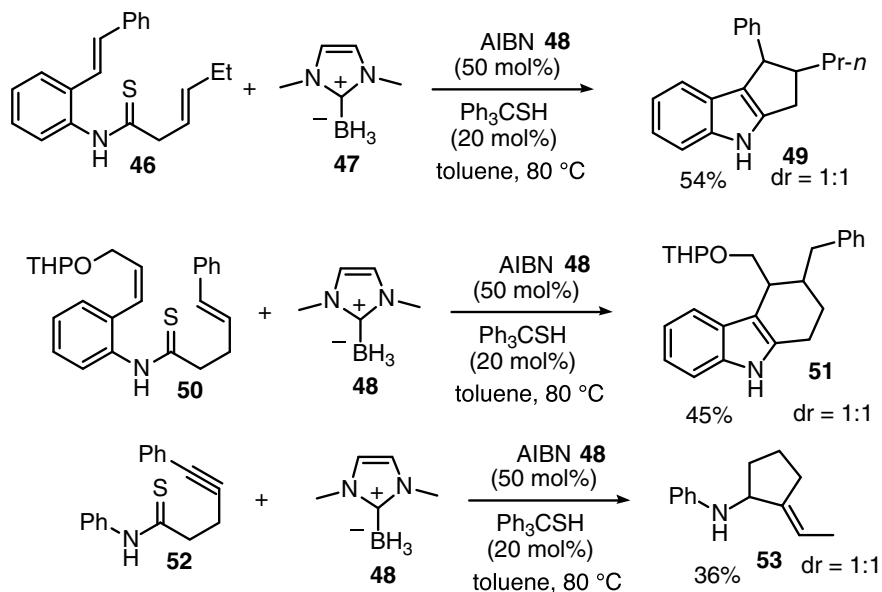


**Fig. 4.13** Reductive cyclization of thioamides

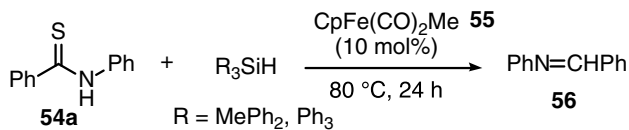


**Fig. 4.14** Reduction of thioamide **54a** with sodium borohydride

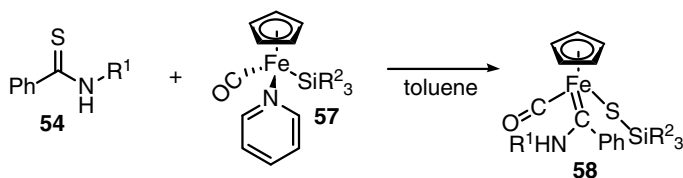


Fig. 4.15 Preparation of carbene iron complexes

## 4.5 Reaction of Thioamides with Organometallic Reagents Leading to the Formation of Amines

A range of organometallic reagents add to thioamides. Among them, the addition of excess Grignard reagents to thioformamides **59** proceeds at room temperature to give tertiary amines **60** (Fig. 4.16) [22]. Unlike the reaction of formamides, which gives aldehydes as a product, products involving C=S group are not observed. The use of 1,2-dichloroethane as a solvent is more effective compared with the use of Et<sub>2</sub>O and THF. Addition of two different Grignard reagents is also achieved to give unsymmetrically substituted amines **61**. As first Grignard reagents to be added, aryl Grignard is desirable. Otherwise, tertiary amines **60** are also formed. In place of the Grignard reagents, organolithium reagents are used as the first organometallic reagents to be added (Fig. 4.17) [23–25]. In this case, the products, in which two molecules of lithium reagents are incorporated, are not formed even with excess lithium reagents. The stereochemical outcome of the reaction is elucidated. The addition of phenyl sulfanylmethyl lithium (**62**) to thioformamide **59a** followed by the addition of Grignard reagents gives **63** with moderate-to-high stereoselectivity [24]. Alkynyl Grignard reagents generally show high diastereoselectivity, whereas the reaction of aryl Grignard reagents forms the products in low yields with moderate selectivity. The reaction of optically active thioformamide **59b** also proceeds stereoselectively to form the products **64** [25].

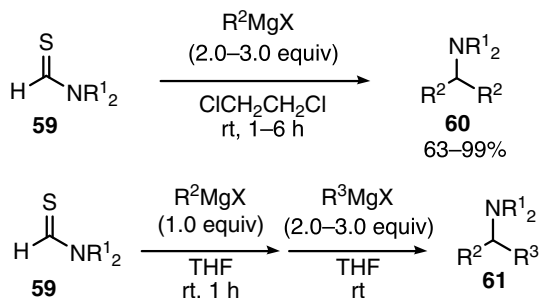
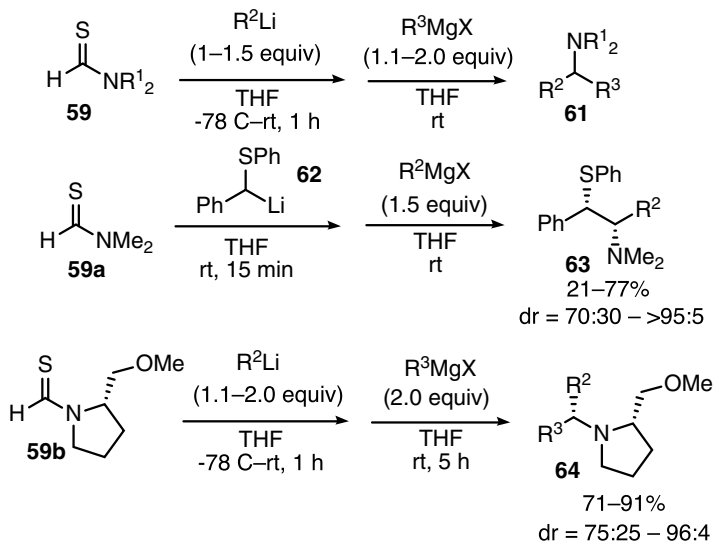
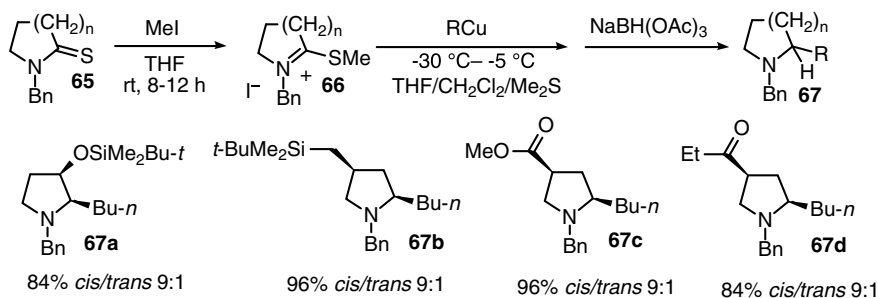


Fig. 4.16 Addition of Grignard reagents to thioformamides





**Fig. 4.17** Sequential addition of organolithium and Grignard reagents to thioformamides



**Fig. 4.18** Reaction of thioiminium salts **66** with organocupper reagents and metal hydride

In contrast to the reaction of thioformamides, the reaction of thioamides with organolithium and Grignard reagents is sluggish. Therefore, the preactivation of thioamides with electrophilic reagents is carried out [26]. Thioiminium salts **66** derived from thiolactams **65** react with organocupper reagents and sodium triacetoxyborohydride to give cyclic amines **67** (Fig. 4.18) [27]. The reaction shows high diastereo- and chemo-selectivity as proved by the preparation of **67a–67d**. Instead of methyl iodide, methyl triflate is used as a methylating agent [28]. In that case, methylation is complete within a minute.

Titanium-mediated reductive alkylation of thioamides **68** gives tertiary amines **69**. The reaction is applicable to aliphatic thioformamides, thioamides, and thiolactams (Fig. 4.19) [29, 30]. Initially, ligand exchange reaction of titanium isopropoxide ( $Ti(OPr-i)_4$ ) with **68** proceeds to give complexes **70**, which is in equilibrium with

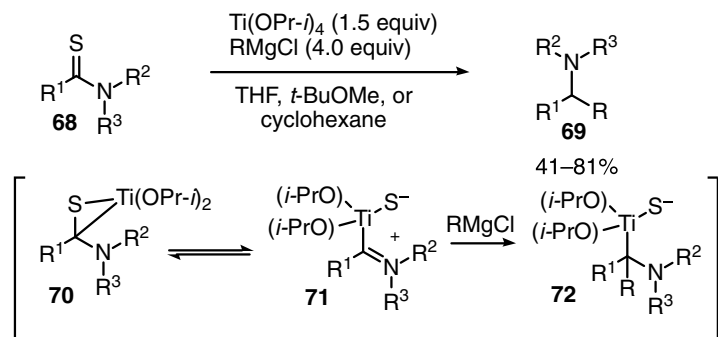


Fig. 4.19 Titanium-mediated reductive alkylation of thioamides

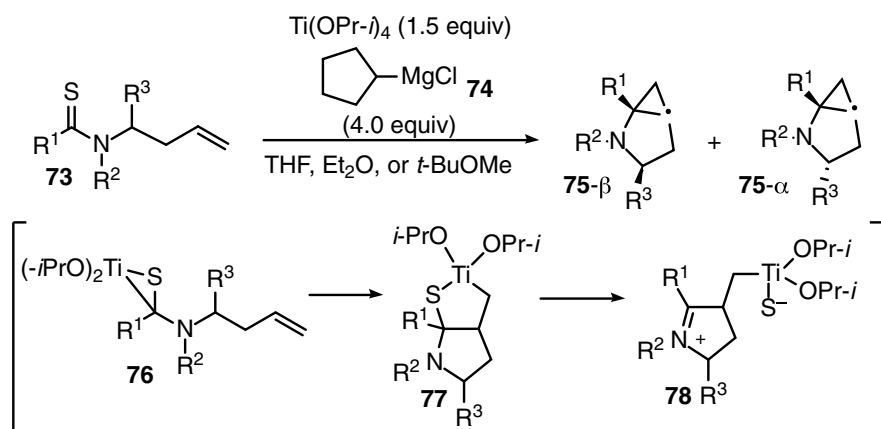


Fig. 4.20 Titanium-mediated cyclization of *N*-3-ethenyl thioamides

metallic iminium salts **71**. The addition of Grignard reagents to **71** generates **72** followed by the hydrolysis to afford the products **69**. In the Ti-mediated reaction of *N*-3-ethenyl thioamides **73** with cyclopentyl Grignard reagent, cyclopropanes **75** are formed with good selectivity of **75-β** (Fig. 4.20) [31]. On the basis of mechanistic elucidation, the initially formed complexes **76** undergoes intramolecular cyclization to generate titanacycles **77** followed by the ring opening to cyclic iminium salts **78** followed by the cyclization to give the products **75**.

## 4.6 Alkenylation of C=S Group in Thioamides

The reaction of thioamides with  $\alpha$ -halocarbonyl compounds has been known as Eschenmoser coupling reaction leading to the formation of enaminones. To facilitate the coupling reaction, the ultrasonic bath is used for the reaction (Fig. 4.21) [32].

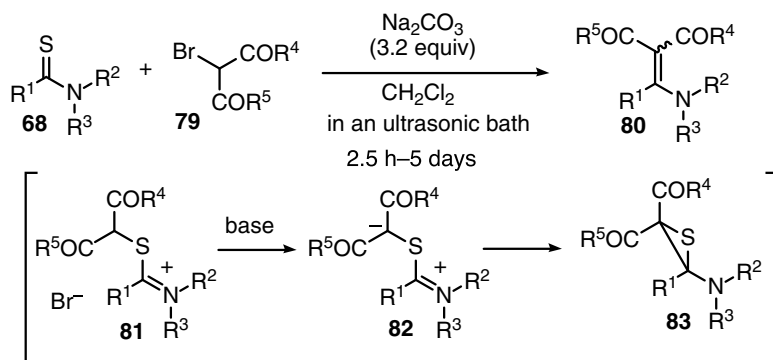


Fig. 4.21 Eschenmoser coupling reaction in an ultrasonic bath

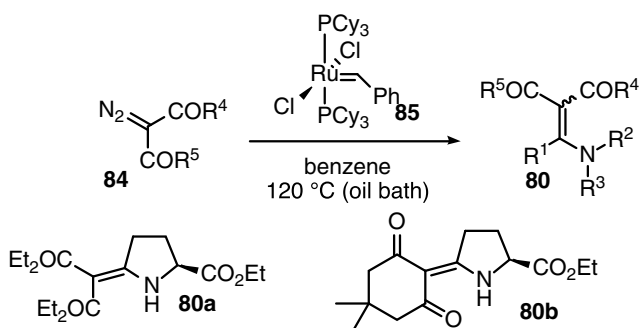


Fig. 4.22 Ru-catalyzed Eschenmoser coupling reaction

Primary and tertiary thioamides, secondary and tertiary thiolactams **68** are used to give the corresponding products **80**. Initially, alkylation at the sulfur atom of **68** with **79** takes place to give iminium salts **81**. The deprotonation from **81** generates the intermediates **82**, which then undergo intramolecular cyclization to give thiiranes **83**. The extrusion of the sulfur atom from **83** affords the products **80**. Ru-catalyzed alkenylation of the C=S group in thioamides is developed (Fig. 4.22) [33, 34]. Diazomalonates are used as a methylene precursor. Catalytic activity of several Ru complexes is tested, and Grubbs first-generation catalyst **85** is the most catalytically active. During the reaction, the stereochemistry of the asymmetric center remains intact to give the products such as **80a** and **80b**. As similar alkenylation reactions, the catalytic activity of copper salts is also examined, and the use of copper (I) trifluoromethanesulfonate toluene complex ((CuOTf)<sub>2</sub>•Tol) in dichloromethane is the most effective [35, 36].

## 4.7 Imidation of Thioamides

Nitrogen nucleophiles react with thioamides, and the C=S groups in thioamides are converted to the C=N groups. Excess silver salts are treated with secondary thioamides **20** and primary and secondary amine derivatives at 25 °C to give the corresponding amidines **86** and **87** (Fig. 4.23) [37]. Sulfonyl azides participate in the reaction with thioamides **68** and thiolactams under reflux in ethanol or in water at room temperature to form *N*-sulfonyl amidines **88** in high yields (Fig. 4.24) [38–40]. Initially, the sulfur atom of thioamides **68** adds to the nitrogen atom of sulfonyl azides to generate intermediates **89**, which then undergoes intramolecular cyclization to form the intermediates **90**. The elimination of nitrogen and sulfur atoms from **90** leads to the formation of **88**. The reaction of thioamides having functional groups such as cyano and carbonyl groups is also elucidated [40]. Copper-mediated self-dimerization takes place to give *N*-thioacyl amidines **91** (Fig. 4.25) [41]. Zinc-catalyzed ring opening of aziridines with thioamides **92** also gives amidines **93** (Fig. 4.26). The sulfur atom attacks to the benzylic carbon atom of aziridines to generate the intermediates **94**, which then undergo the intramolecular cyclization to form **95**. The elimination of thiirane **95** gives **93** (Fig. 4.27) [42].

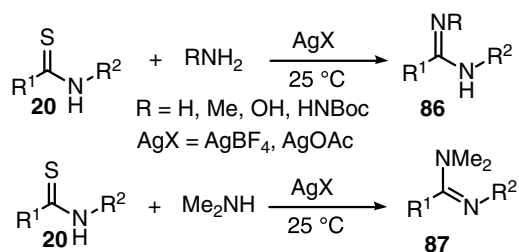


Fig. 4.23 Imidation of secondary thioamides

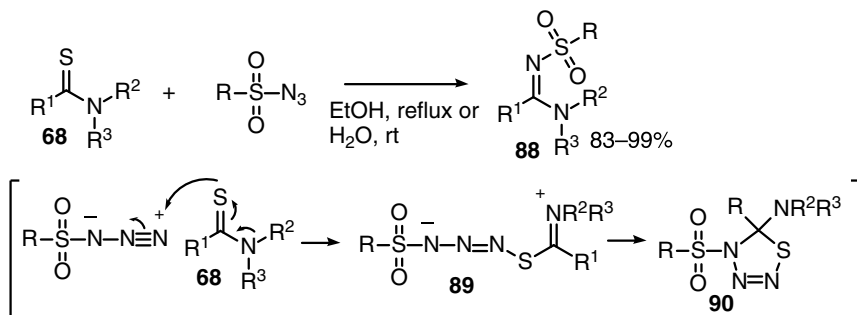


Fig. 4.24 Reaction of thioamides with sulfonyl azides

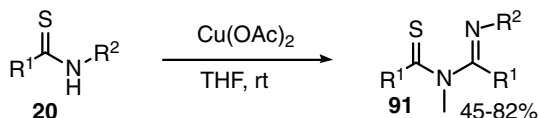


Fig. 4.25 Self-dimerization of thioamides

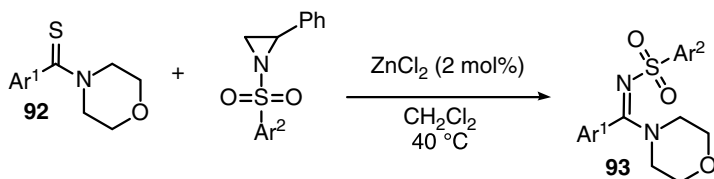


Fig. 4.26 Ring opening of aziridines with thioamides

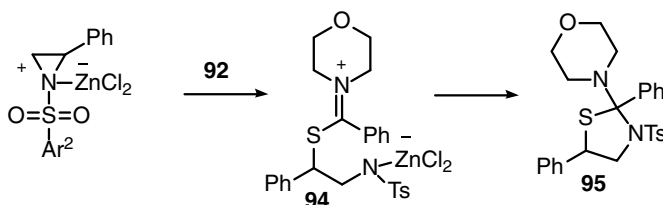


Fig. 4.27 Plausible reaction pathway to **93**

## 4.8 Reaction of Thioamides with Carboxylates

As oxygen nucleophiles, carboxylate silver salts of amino acids are added to thioamides **96** derived from amino acids to form imides **98**, which are further converted to dipeptides (Fig. 4.28) [43, 44]. The detail of the reaction pathway has been disclosed on the basis of DFT calculations. Nucleophilic addition of carboxylates **97** to thioamides **96** may initially take place to form **99**. The elimination of the sulfur atom as  $\text{Ag}_2\text{S}$  from **99** proceeds to give imidates **100**. Finally, **100** undergo  $O$ - $sp^2N$  1,3-acyl migration to give the imides **98**.

## 4.9 Reaction of Thioamides with Trialkyl Phosphites

The reaction of polyfluoroalkylthioamides **101** with trialkyl phosphites **102** gives alkenes **103** (Fig. 4.29) [45, 46]. In contrast to the reaction of **101**, trifluoroacetamide **104** gives  $N,P$ -acetal **105** as a product. The reaction pathway of the reaction between polyfluoroalkylthioamides **101** and phosphites **102** is elucidated by quantum chemical (DFT and MP2) calculations [47]. The results have suggested that the initial step

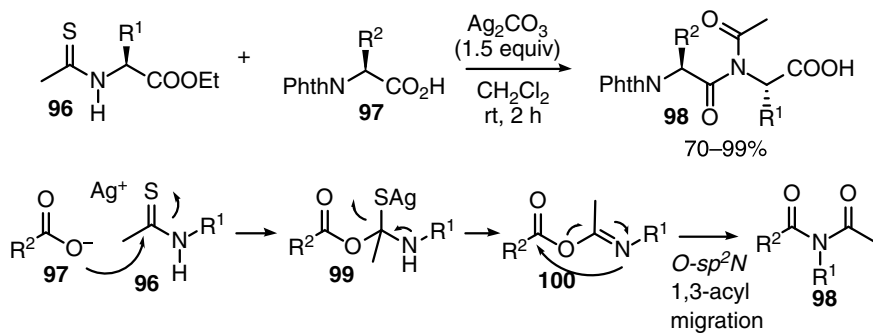


Fig. 4.28 Reaction of thioamides with carboxylates

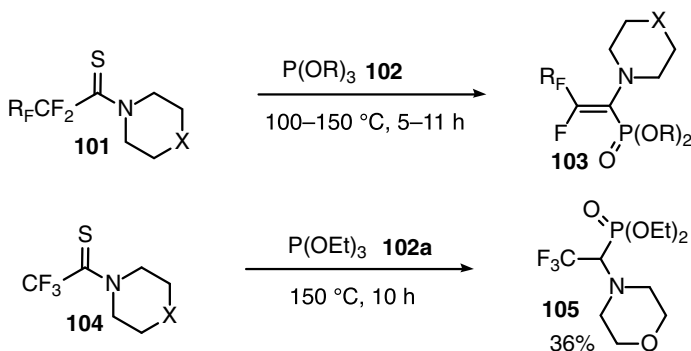
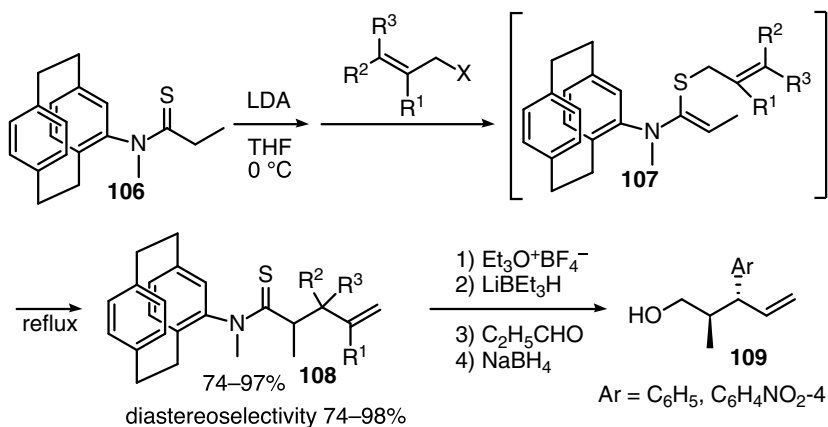


Fig. 4.29 Reaction of polyfluoroalkylthioamides with trialkyl phosphites

is the nucleophilic attack of the phosphorus atom of **102** to the carbon atom of C=S group in thioamides.

## 4.10 Reaction at the $\alpha$ -Position of Thioamides

Acidity of protons  $\alpha$  to the C=S groups in thioamides is higher than that of the corresponding protons in amides. As a result, the generation and reaction of thioenolates from thioamides have long been developed. The deprotonation from *N*-methyl-*N*-([2.2]paracyclophan-4-yl)thioamide **106** followed by the addition of allylic halides gives  $\gamma$ ,  $\delta$ -unsaturated thioamides **108** with high diastereoselectivity [48]. Allylation of thioenolates takes place on the sulfur atom to generate allylic vinyl sulfides **107**, which then undergo thio-Claisen rearrangement to form **108** (Fig. 4.30). Some of the resulting products are converted to enantiomerically enriched primary alcohols **109**. The details of the structures and conformations of thioamides, and plausible



**Fig. 4.30** Reaction of thioenolates from thioamides with allylic halides

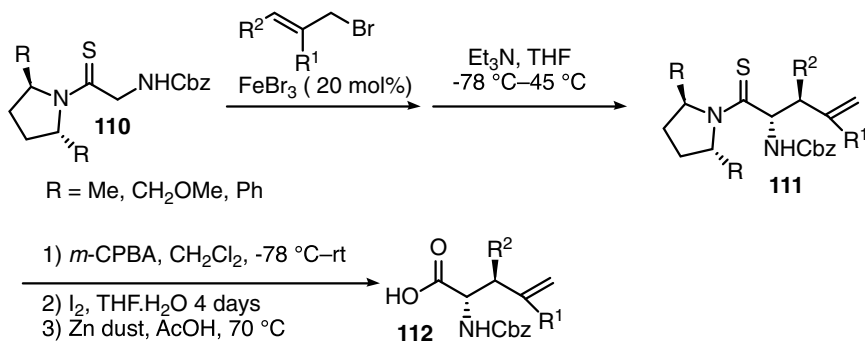


**Fig. 4.31** Reaction of iron-catalyzed allylation of thioamides

reaction pathways are elucidated on the basis of NMR experiments and theoretical calculations.

Iron-catalyzed allylation of thioamides **110** followed by the treatment with a base gives **111** (Fig. 4.31) [49]. The conversion of the resulting products **111** to amino acids **112** is further achieved.

The generation of the dianion **114** from secondary thioamide **113** is also the known reaction. The dianion **114** reacts with terpenones such as (1*R*)-(+)-camphor, (–)-menthone, (1*R*)-(–)-fenchone, (*R*)-(–)-carvone, and β-ionone to give β-hydroxy thioamides (Fig. 4.32) [50].

The reaction of β-ketothioamides **116** with aldehydes and enaminonitriles **117** in the presence of one equiv of acetic acid takes place to give 1,4-dihydropyridines **118** (Fig. 4.33) [51]. The β-ketothioamides **116** is in equilibrium with enol forms **119**, and Michael addition of **119** to iminium salts **120** generated from aldehydes and **117** proceeds to generate the intermediates **121** followed by the intramolecular cyclization to form **122**. Dehydration from **122** leads to **118**.

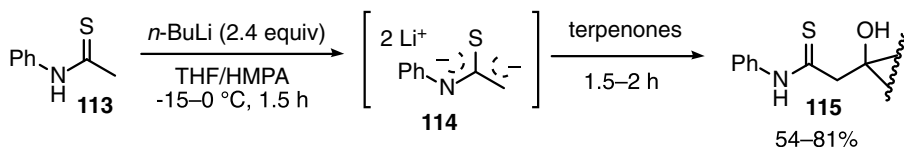


Fig. 4.32 Reaction of dianion generate from secondary thioamide with terpenones

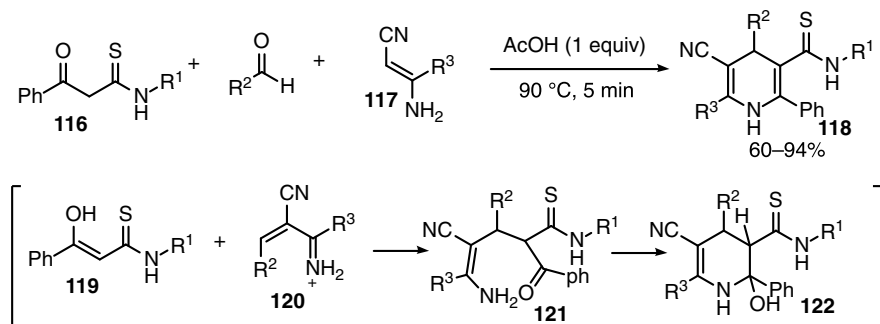


Fig. 4.33 Reaction of  $\beta$ -ketothioamides with aldehydes and enaminonitriles

## 4.11 Reaction of Carbanions Generated from Thioamides

Several types of carbanions are generated and used for the carbon–carbon bond-forming reactions (Fig. 4.34) [52]. As a base, lithium diisopropylamide (LDA),  $n\text{-BuLi}$ , and  $\text{sec-BuLi}$  are necessary, but these organolithium reagents do not work as carbon nucleophiles. In addition to these examples, the deprotonation of  $N$ -arylmethyl secondary thioamides **123** takes place at  $0\text{ }^\circ\text{C}$  to generate thioamide dianions **124**, which is the carbanions adjacent to the nitrogen atom (Fig. 4.35) [53]. Generation of those carbanions is carried out at very low temperature with or without additives. In contrast, the generation of **124** is achieved at  $0\text{ }^\circ\text{C}$  within 15 min. The addition of a range of electrophiles to **124** proceeds smoothly to give the corresponding products. In the reaction with imines as an electrophile,  $N$ -thioacyl 1,2-diamines **125** are formed as a product. Thioformamides are also used as an electrophile to **124** to form 5-amino-2-thiazolines **125** [54].

Lithiation of  $N$ -thiopivaloylazetid-3-ol takes place at the carbon atom adjacent to the nitrogen atom, and the subsequent trapping with electrophiles gives the products **128** (Fig. 4.36) [55]. As electrophiles, alkyl halides, allyl bromide, stannyl chloride, aldehydes, and methyl cyano formate (Mander's reagent) are used. Thiocarbonyl group-directed lithiation is proved by the deprotonation from **129** and **131** [56]. The treatment of **129** and **131** with  $\text{sec-BuLi}$  and methyl iodide forms **130** and **132**. The NMR studies and computational studies support the higher stable rotamers around a C–N single bond are those shown as **129** and **131**. Asymmetric lithiation of  $N$ -thiopivaloyl azetidine **133** and pyrrolidine is carried out in the presence of optically active amines such as (–)-sparteine (**134**), (+)-sparteine surrogate, and 1,2-



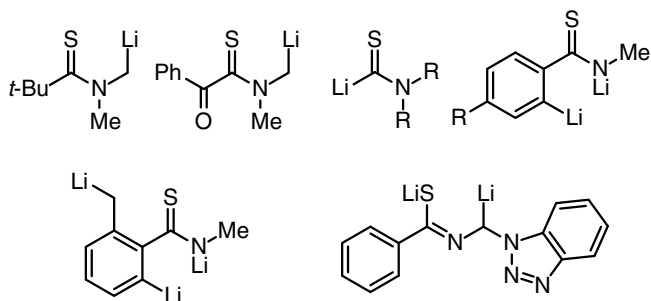


Fig. 4.34 Carbanions generated from thioamides

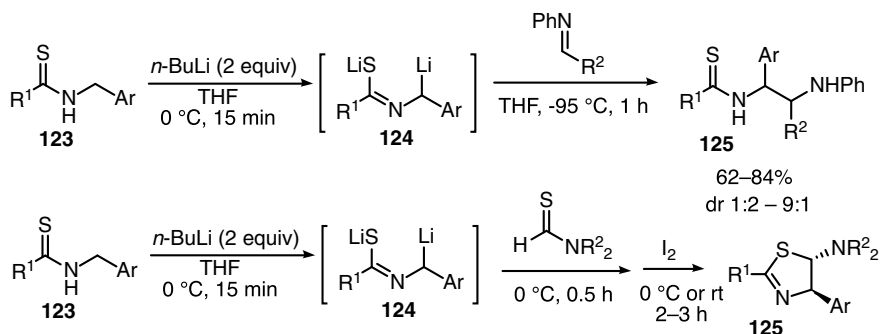


Fig. 4.35 Reaction of thioamide dianions generated from secondary thioamides

diamino cyclohexanes [57]. For example, the deprotonation from **133** in the presence of **134** and the addition of electrophiles give the products **136** with moderate-to-good enantioselectivity (Fig. 4.37). Experimental studies on the postulated lithiated intermediate **135** suggest that **135** is configurationally unstable at  $-78\text{ }^{\circ}\text{C}$  in THF and  $\text{Et}_2\text{O}$ , and the dynamic resolution of interconverting diastereomeric lithiated species **135** may take place to give predominantly one of enantiomers of **136**.

## 4.12 Reaction at the Sulfur Atom of Thioamides

Arylmethylation of aromatic thioamides **137** selectively takes place at the sulfur atom to generate thioiminium salts **138** (Fig. 4.38) [58]. Hydrolysis of **138** gives thioic acid *S*-arylmethyl esters **139**. The sulfur atom in primary thioacetamide **140** nucleophilically attacks pyridinium salts **141** to generate **142** as an intermediate (Fig. 4.39) [59]. Further stirring at low temperature gives indolizines **143** and thioxopyridines **144**.

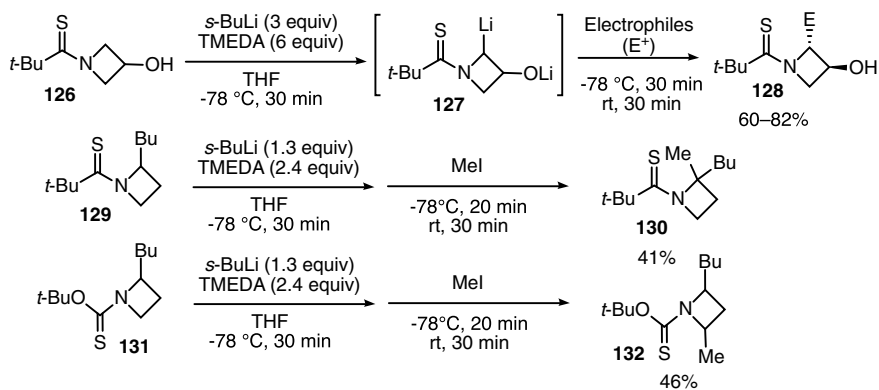
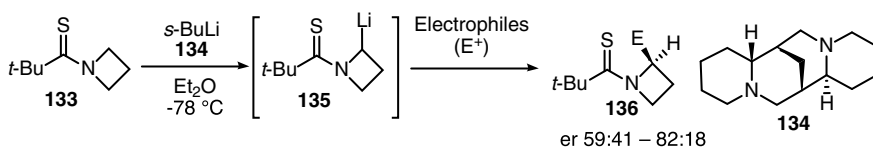
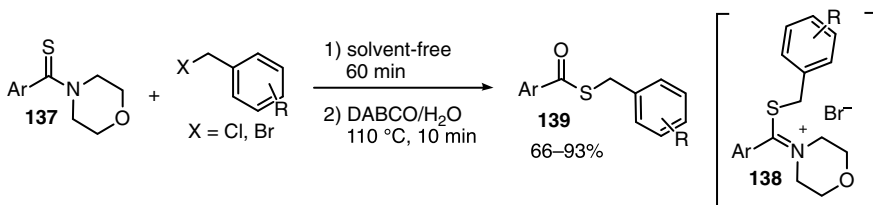
Fig. 4.36 Lithiation of *N*-thiopivaloyl azetidinesFig. 4.37 Asymmetric lithiation of *N*-thiopivaloyl azetidines

Fig. 4.38 Arylmethylation of thioamides

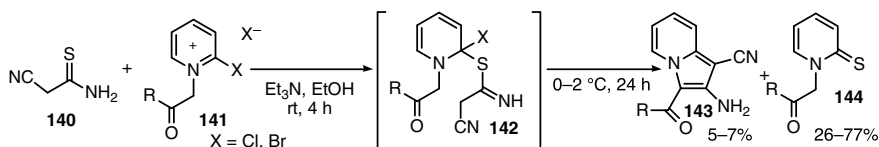
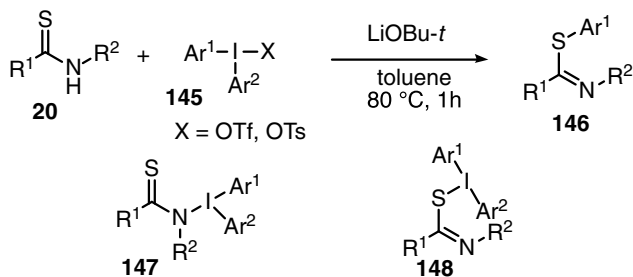


Fig. 4.39 Reaction of primary thioamide with pyridinium salts



**Fig. 4.40** Arylation of secondary thioamides with diaryliodonium salts

S-Arylation of secondary thioamides **20** giving thioimides **146** is achieved by reacting **20** with diaryliodonium salts **145** (Fig. 4.40) [60], while the reaction of thiolactams gives the *N*-arylated products. Initially, deprotonation from **20** may occur, and the ligand exchange reaction of **145** proceeds to give intermediates **147** and/or **148**. [2,3]-Rearrangement of aryl groups in **147** or [1,2]-rearrangement of aryl groups in **148** along with the elimination of aryl iodides affords **146**.

### 4.13 Transition Metal-Catalyzed Reactions of Thioamides

Organosulfur compounds have been believed to be a poison to transition metal complexes. As a result, thioamides were not considered to be substrates for transition metal-catalyzed reactions. In contrast, these situations have changed by choosing appropriate combinations of transition metals, ligands, and additives.

$\alpha$ -Arylation of thioamides **149** is catalyzed by Pd complex to give the products **150** (Fig. 4.41) [61]. The reaction is specific to thioamides, and a similar reaction using amides does not produce the corresponding products. A plausible catalytic cycle is shown in Fig. 4.42. Oxidative addition of aryl halides to Pd(0) takes place to form Pd(II) species **151**. The substitution reaction at the palladium atom with thioamides generates palladium thioenolates **152**, which is in equilibrium with keto forms **153**. Reductive elimination from **153** gives rise to the formation of **150**.

Pd-catalyzed  $\alpha$ -allylation of thioamides **149** is also achieved by using allylic acetate as a substrate and diphenylphosphinobutane (dppb) as a ligand (Fig. 4.43) [62]. The reaction is performed with THF as a solvent at room temperature. A range of phosphine ligands are elucidated for Pd-catalyzed asymmetric  $\alpha$ -allylation of thioamides **155** (Fig. 4.44) [63]. Among them, (*R*)-DM-BINAP shows better diastereoselectivity and higher enantiomeric excess of the major products **156**. Pd-catalyzed reaction of thioamides **157** with 1,4-benzoquinone (**158**) takes place at the position  $\alpha$  to the C=S group of **157** to give the products **159** having a tetra-substituted carbon atom (Fig. 4.45) [64]. Coordination of **157** and **158** to Pd(0) generates intermediates **160**. Further addition of PivOH to **160** forms intermediates **161**. Deprotonation at

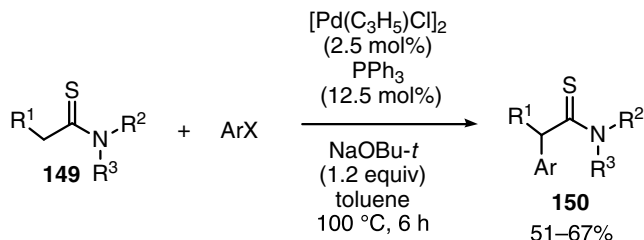


**Fig. 4.41** Pd-catalyzed  $\alpha$ -arylation of thioamides

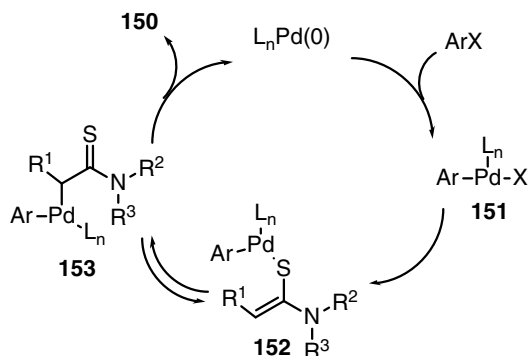


**Fig. 4.42** Plausible catalytic cycle of Pd-catalyzed  $\alpha$ -arylation of thioamides

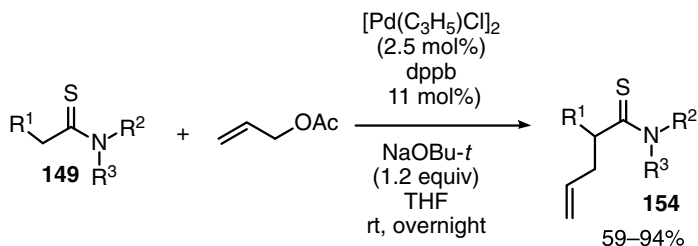


**Fig. 4.43** Pd-catalyzed  $\alpha$ -allylation of thioamides

the carbon  $\alpha$  to the C=S group and the formation of carbon–palladium bond give intermediates **162**. Reductive elimination from **162** results in the formation of **159** (Fig. 4.46).

Transition metal-catalyzed C–H functionalization of aromatic compounds is one of the hot topics in synthetic chemistry. Such reactions using C=S group in thioamides as a directing group are developed. Rh-catalyzed reaction of aromatic thioamides **163** with terminal alkenes proceeds to give the products **164** (Fig. 4.47) [65]. Thioamides **163** may initially coordinate to Rh(III) species to generate **165** (Fig. 4.48). Deprotonation and metalation proceeds in **165** to form rhodacycle **166**. Insertion of alkenes to the carbon–rhodium bond in **166** generates **167**. The subsequent dehydrometalation

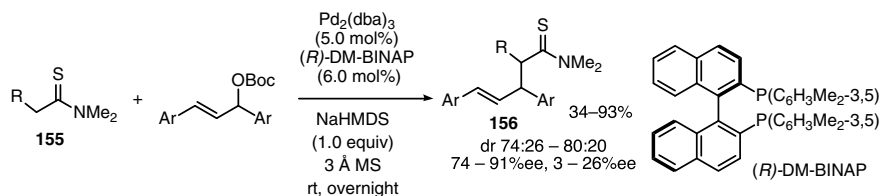


**Fig. 4.44** Pd-catalyzed asymmetric  $\alpha$ -allylation of thioamides

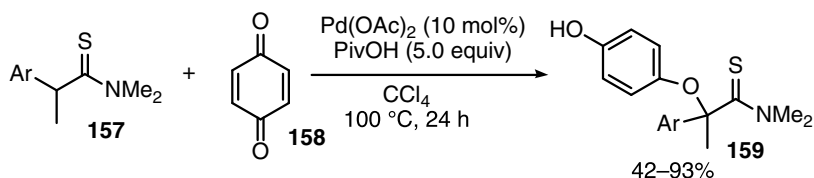


**Fig. 4.45** Pd-catalyzed *p*-hydroxyphenyloxylation of thioamides

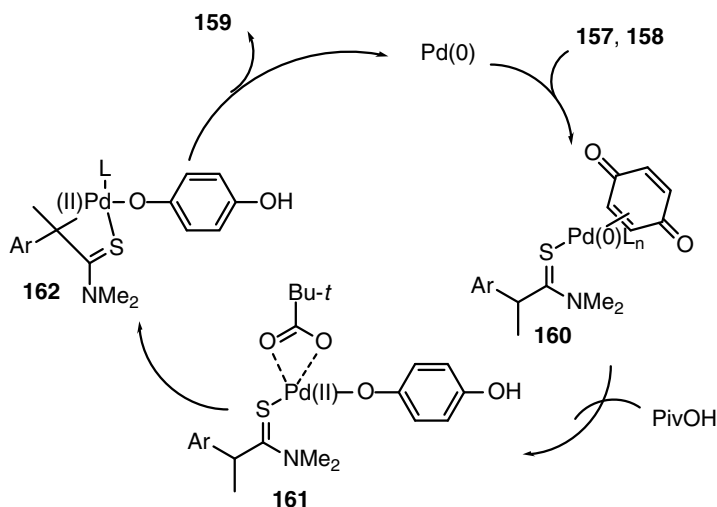


**Fig. 4.46** Proposed reaction pathway for the Pd-catalyzed *p*-hydroxyphenyloxylation of thioamides

from **167** gives the final products **164** and Rh(I) species. Oxidation of Rh(I) species generates Rh(III) species. The use of internal alkynes triggers annulative coupling between **163** and alkynes to give indenones **168** (Fig. 4.49). Thienyl thioamides **169** [66] and **171** [67] are used as starting materials for Pd-catalyzed arylation reactions (Fig. 4.50). Phenanthroline works as an effective bidentate ligand. Aryl groups are site-selectively introduced to the 2-position of **169** and the 3-position of **171**. The formation of palladacycle **173** is suggested to initially occur. Pd-catalyzed arylation at the ortho position of aromatic thioamides **174** is achieved by using boronic acids as

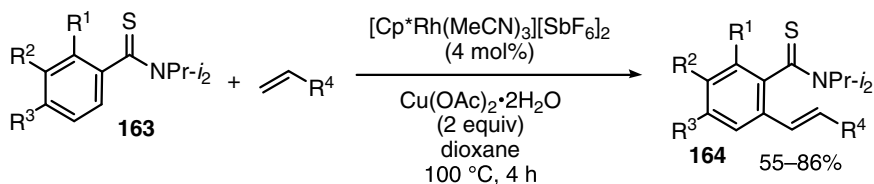


Fig. 4.47 Pd-catalyzed alkenylation of aromatic thioamides

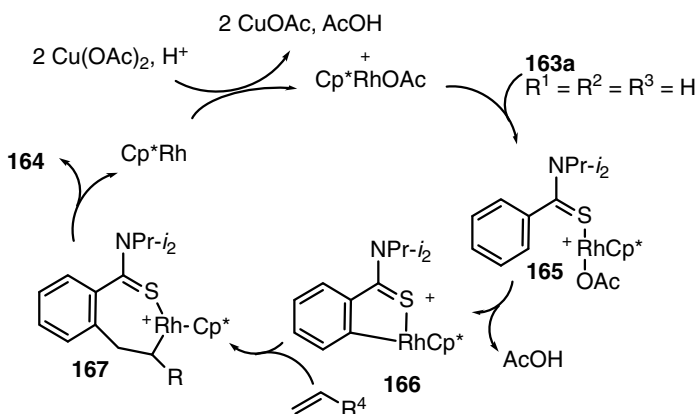


Fig. 4.48 Plausible reaction pathway of Pd-catalyzed alkenylation of aromatic thioamides

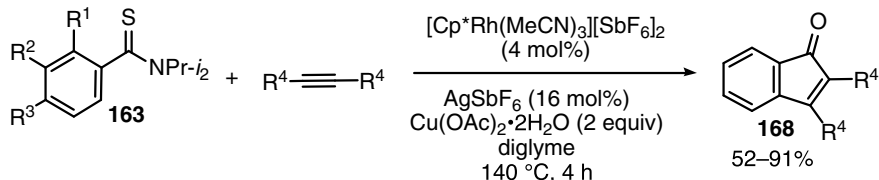


Fig. 4.49 Pd-catalyzed reaction of aromatic thioamides with internal alkynes

a coupling partner (Fig. 4.51) [68]. Similarly to the reactions in Figs. 4.48–4.50, the formation of paradicycles, transmetalation, and reductive elimination is proposed. Generated Pd(0) species is oxidized with 1,4-benzoquinone.

Pd-Catalyzed  $\alpha$ -C( $sp^3$ )-H arylation of thioamides **176** and **178** is developed with boronic acids as a coupling partner and 1,4-benzoquinone as an oxidant (Fig. 4.52) [69]. The thiocarbonyl groups remain intact even in the presence of an oxidant. Heteroaromatic substituents are also introduced to the carbon atom next to the nitrogen atom by using heteroarylboronic acids. Asymmetric Pd-catalyzed  $\alpha$ -C( $sp^3$ )-H arylation of 2,4,6-tris(isopropyl)benzthioamides **180** is achieved with phosphoric acid having an 9-anthracenyl group **181** as an asymmetric anionic ligand (Fig. 4.53) [70].

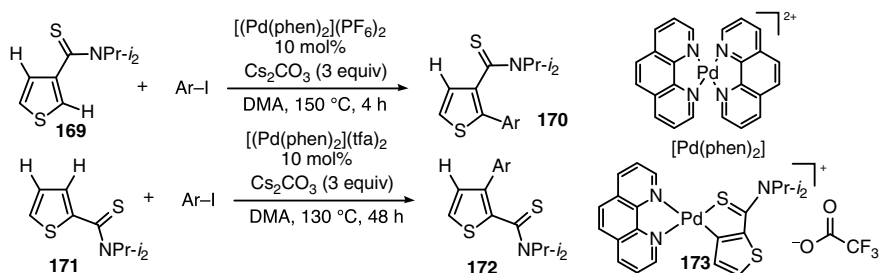


Fig. 4.50 Pd-catalyzed arylation of thienylthioamides with aromatic iodides

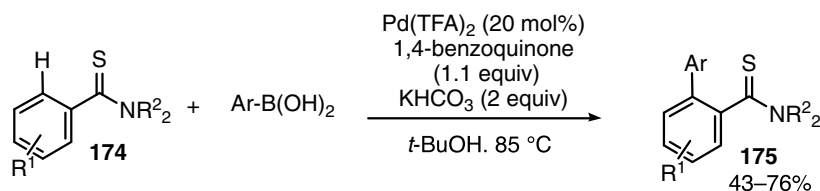


Fig. 4.51 Pd-catalyzed arylation of aromatic thioamides

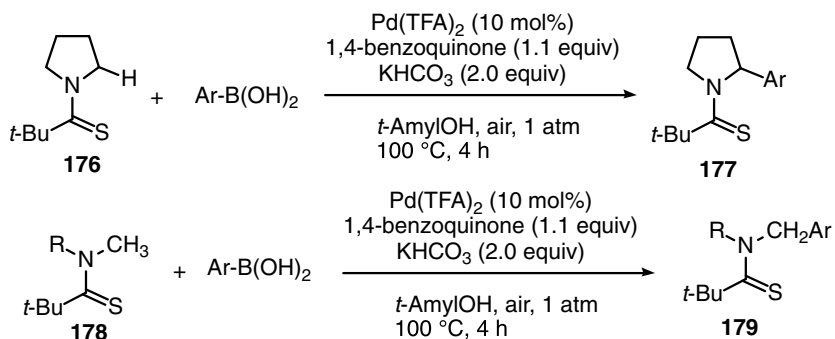


Fig. 4.52 Pd-catalyzed arylation of thioamides

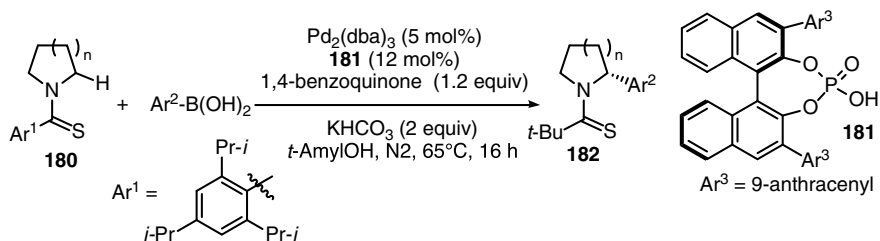


Fig. 4.53 Asymmetric Pd-catalyzed arylation of thioamides

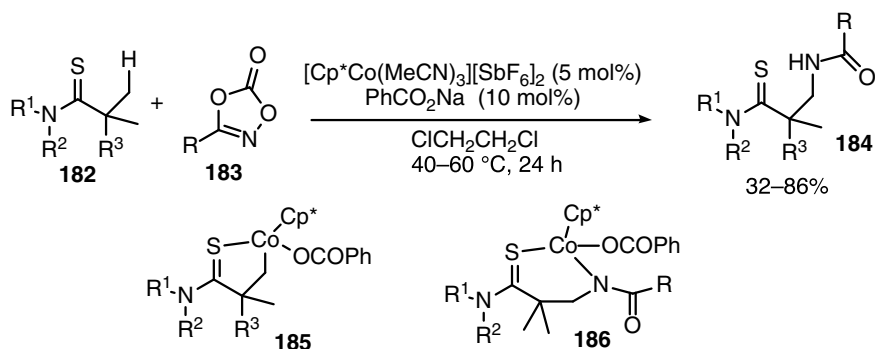


Fig. 4.54 Co-catalyzed amidation of thioamides with dioxazolones

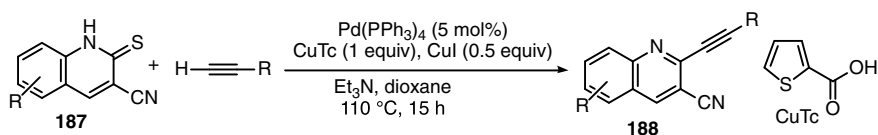


Fig. 4.55 Pd-catalyzed alkynylation of 3-cyano-2-mercaptoquinolines

C(sp<sup>3</sup>)-H amidation of a methyl group on the nitrogen atom of thioamides **182** is catalyzed by Co(III) complex with dioxazolones as a coupling partner to give the products **184** (Fig. 4.54) [71]. The detailed studies on the reaction pathway are carried out with experiments and theoretical calculations. On the basis of these results, the formation of intermediates **185** is suggested. Coordination of the nitrogen atom in **183** to the cobalt center in **185**, and the subsequent migratory insertion of the nitrogen atom to the carbon–cobalt bond may generate intermediates **186**. Finally, the protonation of **186** may lead to the formation of the final products **184**.

Desulfurative Sonogashira coupling reaction is achieved by using cyclic thioamides **187**, terminal alkynes, palladium catalyst, thienylcarboxylic acid copper salt (CuTc), and copper iodide to give the products **188** (Fig. 4.55) [72]. The alkynyl group is introduced to the carbon atom of C=S group, and the sulfur atom in **187** is eliminated as hydrogen sulfide.

## 4.14 Summary

The present chapter has described characteristic reactions of thioamides. The stepwise conversion of amides to thioamides followed by the reduction is readily applicable methods for the construction of the methylene group in the total synthesis of natural products and biologically relevant compounds. A wide variety of carbon–carbon forming reactions are developed by using the electrophilic characters of the



carbon atom of the C=S group, and carbanions are generated from thioamides. Availability of thioamides for transition metal-catalytic reactions is proved, and the C=S group has worked as directing groups. Because of the easiness of the handling and reactivity of thioamides, new synthetic reactions using them will be further developed.

## References

1. M. Nasr-Esfahani, M. Montazerzohori, M. Moghadam, I. Mohammadpoor-Baltork, S. Moradi, *J. Sulfur Chem.* **30**, 17 (2009)
2. K. Bahrami, M.M. Khodaei, Y. Tirandaz, *Synthesis*, 369 (2009)
3. K. Bahrami, M.M. Khodaei, V. Shakibaian, D. Khaledian, B.H. Yousefi, *J. Sulfur Chem.* **33**, 155 (2012)
4. K. Inamoto, M. Shiraishi, K. Hiroya, T. Doi, *Synthesis*, 3087 (2010)
5. A.K. Yadav, V.P. Srivastava, L.D.S. Yadav, *New J. Chem.* **37**, 4119 (2013)
6. N. Xu, X. Jin, K. Suzuki, K. Yamaguchi, N. Mizuno, *New J. Chem.* **40**, 4865 (2016)
7. K. Yamaguchi, K. Yajima, N. Mizuno, *Chem. Commun.* **48**, 11247 (2012)
8. T. Mineno, Y. Takebe, C. Tanaka, S. Mashimo, *Int. J. Org. Chem.* **4**, 49052 (2014)
9. F.M. Moghaddam, Z. Mirjafari, H. Saeidian, M.J. Javan, *Synlett*, 892 (2008)
10. M. Witalewska, A. Wrona-Piotrowicz, A. Makal, J. Zakrzewski, *J. Org. Chem.* **2018**, 83 (1933)
11. B. Xu, X. Zhong, X.-C. Wang, Z.J. Quan, *Synlett* **27**, 2237 (2016)
12. H. Eshghi, G.H. Zohuri, S. Damavandi, *Synth. Commun.* **42**, 516 (2012)
13. S.S. Mykhaylychenko, N.V. Pikun, Y.G. Shermolovich, *J. Fluorine Chem.* **140**, 76 (2012)
14. Y. Chen, W. Zhang, L. Ren, J. Li, A. Li, *Angew. Chem. Int. Ed.* **57**, 952 (2018)
15. S. Fujita, K. Nishikawa, T. Iwata, T. Tomiyama, H. Ikenaga, K. Matsumoto, M. Shindo, *Eur. J.* **24**, 1539 (2018)
16. W. Zhang, M. Ding, J. Li, Z. Guo, M. Lu, Y. Chen, L. Liu, Y.-H. Shen, A.J. Li, *Am. Chem. Soc.* **140**, 4227 (2018)
17. N. Wang, J. Liu, C. Wang, L. Bai, X. Jiang, *Org. Lett.* **20**, 292 (2018)
18. E.L. Campbell, C.K. Skepper, K. Sankar, K.K. Duncan, D.L. Boger, *Org. Lett.* **15**, 5306 (2013)
19. Y.-J. Yu, F.-L. Zhang, J. Heng, J.-H. Hei, W.-T. Deng, Y.-F. Wang, *Org. Lett.* **20**, 24 (2018)
20. K. Fukumoto, A. Sakai, K. Hayasaka, H. Nakazawa, *Organometallics* **32**, 2889 (2013)
21. K. Fukumoto, A. Sakai, T. Murai, H. Nakazawa, *Heteroatom Chem.* **25**, 607 (2014)
22. T. Murai, K. Ui, J. Narengerile, *Org. Chem.* **74**, 5703 (2009)
23. T. Murai, F.J. Asai, *Am. Chem. Soc.* **129**, 780 (2007)
24. T. Murai, F.J. Asai, *Org. Chem.* **73**, 9518 (2008)
25. T. Murai, N.J. Mutoh, *Org. Chem.* **81**, 8131 (2016)
26. A. Mercedes, N. Llor, J. Hidalgo, C. Escolano, J. Bosch, *J. Org. Chem.* **68**, 1919 (2003)
27. P. Mateo, J.E. Cinqualbre, M.M. Mojzes, K. Schenk, P. Renaud, *J. Org. Chem.* **82**, 12318 (2017)
28. T. Murai, R. Toshio, Y. Mutoh, *Tetrahedron* **62**, 6312 (2006)
29. E. Augustowska, A. Boiron, J. Deffit, Y. Six, *Chem. Commun.* **48**, 5031 (2012)
30. F. Hermant, E. Urbańska, S.S. de Mazancourt, T. Maubert, E. Nicolas, Y. Six, *Organometallics* **33**, 5643 (2014)
31. F. Hermant, E. Nicolas, Y. Six, *Tetrahedron* **70**, 3924 (2014)
32. N.D. Koduri, B. Hileman, J.D. Cox, H. Scott, P. Hoang, A. Robbins, K. Bowers, L. Tsebaot, K. Miao, M. Castaneda, M. Coffin, G. Wei, T.D.W. Claridge, K.P. Roberts, S. Hussaini, *RSC Adv.* **3**, 181 (2013)
33. N.D. Koduri, H. Scott, B. Hileman, J.D. Cox, M. Coffin, L. Glicksberg, S.R. Hussaini, *Org. Lett.* **14**, 440 (2012)
34. N.D. Koduri, Z.G. Wang, K. Cooley, T.M. Lemma, K. Miao, M. Nguyen, B. Frohock, M. Castaneda, H. Scott, D. Albinescu, S.R.J. Hussaini, *Org. Chem.* **79**, 7405 (2014)

35. L. Mohammadi, M.A. Zolfigol, M. Ebrahimi, K.P. Roberts, S. Ansari, T. Azadbakht, S.R. Hussaini, *Cat. Commun.* **102**, 44 (2017)
36. A. Pal, N.D. Koduri, Z. Wang, E.L. Quiroz, A. Chong, M. Vuong, N. Rajagopal, M. Nguyen, K.P. Roberts, S.R. Hussaini, *Tetrahedron Lett.* **58**, 586 (2017)
37. A. Okano, R.C. James, J.G. Pierce, J. Xie, D.L. Boger, *J. Am. Chem. Soc.* **134**, 8790 (2012)
38. M. Aswad, J. Chiba, T. Tomohiro, Y. Hatanaka, *Chem. Commun.* **49**, 10242 (2013)
39. L. Dianova, V. Berseneva, T. Beryozkina, I. Efimov, M. Kosterina, O. Eltsov, W. Dehaen, V. Bakulev, *Eur. J. Org. Chem.* 6917 (2015)
40. M. Aswad, J. Chiba, T. Tomohiro, Y. Hatanaka, *Tetrahedron Lett.* **57**, 1313 (2016)
41. J.-S. Li, Y. Xue, P.-Y. Li, Z.-W. Li, C.-H. Lu, W.-D. Liu, H.-L. Pang, D.-H. Liu, M.-S. Lin, B.-B. Luo, W. Jiang, *Res. Chem. Intermed.* **41**, 2235 (2015)
42. K. Hajibabaei, H. Zali-Boeini, *Synlett* **25**, 2044 (2014)
43. A. Pourvali, J.R. Cochrane, C.A. Hutton, *Chem. Commun.* **50**, 15936 (2014)
44. C.A. Hutton, J. Shang, U. Wille, *Chem. Eur. J.* **22**, 3163 (2016)
45. S.S. Mykhaylychenko, N.V. Pikun, Y.G. Shermolovich, *Tetrahedron Lett.* **52**, 4788 (2011)
46. N.V. Pikun, S.S. Mykhaylychenko, E.B. Rusanov, Y.G. Shermolovich, *Russ. J. Org. Chem.* **49**, 1572 (2013)
47. A.B. Rozhenko, S.S. Mykhaylychenko, N.V. Pikun, Y. Shermolovich, J. Leszczynski, *Int. J. Quantum Chem.* **114**, 241 (2014)
48. B. Jiang, L. Han, Y.-L. Li, X.-L. Zhao, Y. Lei, D.-Q. Xie, J.Z.H. Zhang, *J. Org. Chem.* **77**, 1701 (2012)
49. Z. Liu, S.J. Mehta, K.-S. Lee, B. Grossman, H. Qu, X. Gu, G.S. Nichol, V.J. Hruby, *J. Org. Chem.* **77**, 1289 (2012)
50. T.S. Jagodziński, J.G. Sośnicki, E. Struck, *Phosphorus Sulfur Silicon* **191**, 290 (2016)
51. M. Li, K.-N. Sun, L.-R. Wen, *RSC Adv.* **6**, 21535 (2016)
52. T. Murai, *Pure Appl. Chem.* **82**, 541 (2010)
53. F. Shibahara, S. Kobayashi, T. Maruyama, T. Murai, *Chem. Eur. J.* **19**, 304 (2013)
54. K. Yamaguchi, T. Murai, S. Hasegawa, Y. Miwa, S. Kutsumizu, T. Maruyama, T. Sasamori, N. Tokitoh, *J. Org. Chem.* **80**, 10742 (2015)
55. D.M. Hodgson, C.I. Pearson, A.L.J. Thompson, *Org. Chem.* **78**, 1098 (2013)
56. K.E. Jackson, C.L. Mortimer, B.X. Mortimer, J.M. McKenna, T.D.W. Claridge, R.S. Paton, D.M.J. Hodgson, *Org. Chem.* **80**, 9838 (2015)
57. P.J. Rayner, J.C. Smith, C. Denneval, P. O'Brien, P.A. Clarke, A.J. Horanb, *Chem. Commun.* **52**, 1354 (2016)
58. H.Z. Boeini, A. Zali, *Synth. Commun.* **41**, 2421 (2011)
59. N.M. Tverdokhle, G.É.I. Khoroshilov, *Chem. Heterocycl. Compd.* **51**, 56 (2015)
60. P. Villo, G. Kervelfors, B. Olofsson, *Chem. Commun.* **54**, 8818 (2018)
61. H. Yu, X. Liu, L. Dian, Q. Yang, B. Rong, A. Gao, B. Zhao, H. Yang, *Tetrahedron Lett.* **54**, 3060 (2013)
62. B. Rong, L. Ding, H. Yu, Q. Yang, X. Liu, D. Xu, G. Li, B. Zhao, *Tetrahedron Lett.* **54**, 6501 (2013)
63. B. Rong, Q. Yang, Y. Liu, H. Xu, Y. Hu, X. Cheng, B. Zhao, *Tetrahedron Lett.* **56**, 595 (2015)
64. G. Song, Z. Zheng, Y. Wang, X. Yu, *Org. Lett.* **18**, 6002 (2016)
65. Y. Yokoyama, Y. Unoh, R.A. Bohmann, T. Satoh, K. Hirano, C. Bolm, M. Miura, *Chem. Lett.* **44**, 1104 (2015)
66. T. Yamauchi, F. Shibahara, T. Murai, *Org. Lett.* **17**, 5392 (2015)
67. F. Shibahara, Y. Asai, T. Murai, *Asian J. Org. Chem.* **7**, 1323 (2018)
68. K.-X. Tang, T.C.-M. Wang, T.-H. Gao, C. Pan, L.-P. Sun, *Org. Chem. Front.* **4**, 2167 (2017)
69. J.E. Spangler, Y. Kobayashi, P. Verma, D.-H. Wang, J.-Q. Yu, *J. Am. Chem. Soc.* **137**, 11876 (2015)
70. P. Jian, P. Verma, G. Xia, J.-Q. Yu, *Nature Chem.* **9**, 140 (2017)
71. P.W. Tan, A.M. Mak, M.B. Sullivan, D.J. Dixon, J. Seayad, *Angew. Chem. Int. Ed.* **56**, 16550 (2017)
72. Y. Wu, Y. Xing, J. Wang, Q. Sun, W. Kong, F. Suzenet, *RSC Adv.* **5**, 48558 (2015)

# Chapter 5

## Asymmetric Synthesis Using Thioamides



Naoya Kumagai and Masakatsu Shibasaki

**Abstract** Following the preceding chapter in which synthesis and transformation of thioamides were introduced, this chapter provides an overview of state-of-the-art asymmetric catalysis to elicit the hidden reactivity of thioamide functionality, thereby engaging thioamide substrates in catalytic transformations to produce more elaborate thioamide compounds. The designed catalytic systems, comprising a soft Lewis acid and Brønsted base, chemoselectively activate thioamides in both a nucleophilic and electrophilic fashion, leading to a number of bimolecular reactions rendered catalytic and enantioselective. The last section showcases the synthetic application of these catalytic processes to demonstrate their practical utility.

**Keywords** C–C bond formation · Asymmetric catalysis · Enantioselective · Soft-soft interaction · Synthetic application

### 5.1 Introduction

As described in the preceding chapters, a thioamide is a readily accessible functional group that is widely utilized in organic synthesis. This chapter specifically focuses on enantioselective reactions featuring the thioamide functionality as a key functional group to drive the reaction of interest. Particular emphasis is placed on enantioselective catalysis, where the soft Lewis basic nature of the thioamide functionality dictates the catalyst design to achieve chemoselective interactions sufficient to promote the reaction in a highly stereoselective fashion. The inert reactivity of amides, the closest analog of thioamides, in these catalytic systems illustrates that these tailor-made catalytic systems for thioamides are highly chemoselective and compatible with common hard Lewis basic functionalities. Catalytic enantioselective

---

N. Kumagai (✉) · M. Shibasaki (✉)  
Institute of Microbial Chemistry (BIKAKEN), Tokyo, 3-14-23 Kamiosaki, Shinagawa-Ku, Tokyo 141-0021, Japan  
e-mail: [nkumagai@bikaken.or.jp](mailto:nkumagai@bikaken.or.jp)

M. Shibasaki  
e-mail: [mshibasa@bikaken.or.jp](mailto:mshibasa@bikaken.or.jp)

© Springer Nature Singapore Pte Ltd. 2019  
T. Murai (ed.), *Chemistry of Thioamides*,  
[https://doi.org/10.1007/978-981-13-7828-7\\_5](https://doi.org/10.1007/978-981-13-7828-7_5)

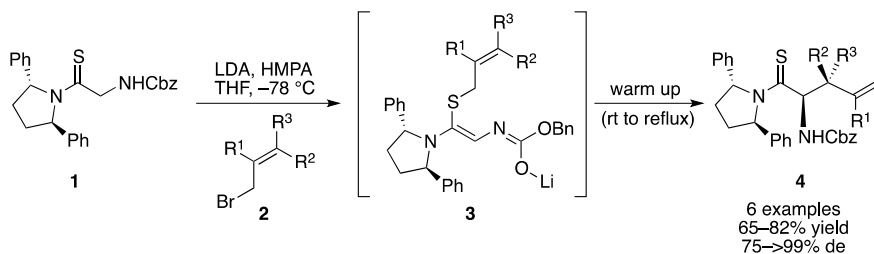
tive reactions offer a powerful strategy for producing value-added enantioenriched synthons, which are further leveraged by the capability of thioamides to undergo diverse functional group transformations [1]. Indeed, the catalytic enantioselective reactions introduced in this chapter are extensively utilized in enantioselective total syntheses of biologically active natural products as well as active pharmaceutical ingredients (APIs). These are briefly overviewed in the latter part of this chapter.

## 5.2 Enantioselective Reactions Using Thioamides

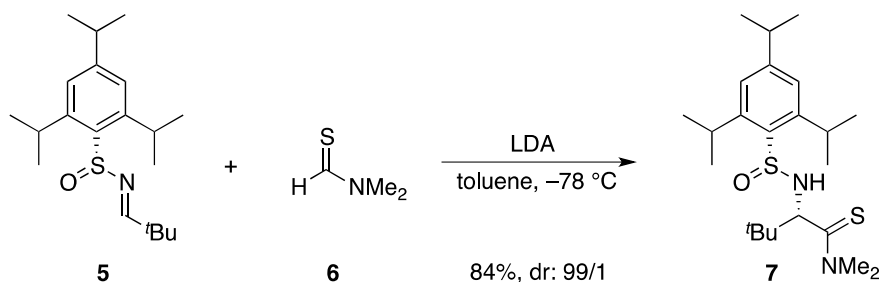
### 5.2.1 Auxiliary Approach

Surprisingly, enantioselective reactions utilizing thioamide compounds have not been extensively explored and only a few reaction settings are reported in the literature. Hruby et al. demonstrated a smooth chirality transfer of chirally decorated thioamide **1** to provide unnatural  $\alpha$ -amino acid derivatives (Scheme 5.1) [2]. With (2*R*,5*R*)-2,5-diphenylpyrrolidine-appended thioacetamide **1** bearing an NHCbz group at the  $\alpha$ -position as the substrate of choice, successive treatment with lithium diisopropylamide (LDA) and allylic bromides **2** at  $-78^\circ\text{C}$  in THF gives *S*-allylated intermediate **3**. Simply warming the reaction mixture to room temperature (then to THF reflux) leads to the breakdown of **3** to afford **4** with excellent control of the enantioselectivity via a thio-Claisen rearrangement. Dianion formation is proposed, and a slight excess of LDA (3.2 eq) is recommended. Facile transformation of **4** into the corresponding amide is achieved via the *S*-methylation/hydride reduction/Pinnick oxidation sequence.

Reeves et al. employed auxiliary appended *N*-sulfinyl aldimines **5** as electrophiles with a thiocarbamoyl anion generated from thioformamide **6** (Scheme 5.2) [3]. Although this reaction was principally developed for formamides, the conditions were equally effective for thioformamide **6**, potentially providing a range of unnatural  $\alpha$ -amino acid derivatives.



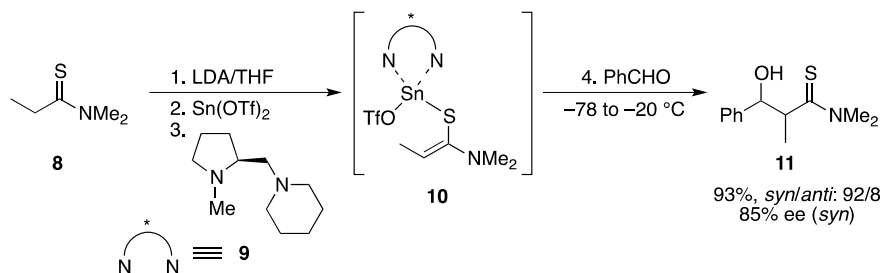
**Scheme 5.1** Thio-Claisen rearrangement of homochiral thioamide **1**



**Scheme 5.2** Addition of thiocarbamoyl anion generated from **6** to homochiral *N*-sulfinyl aldimine **5**

### 5.2.2 Chiral Lewis Acid Approach

The use of chiral Lewis acids obviates the additional procedures required for covalent linking and the removal of chiral molecular units. Chiral Lewis acid catalysis plays a pivotal role in this regard, where chiral Lewis acids interact with substrates and subsequent reactions proceed under a chiral environment to deliver enantioenriched products [4, 5]. Because thioamides belong to the carbonyl class of functional groups, enolization was attempted in diastereoselective aldol reactions by Yoshida et al. in 1980 [6, 7]. The observed diastereoselectivity suggested the in situ generation of *Z*-configured enolate, and these studies were followed by diastereoselective aldol reactions using *S*-silyl ketene *N,S*-acetals derived from thioamides [8–10]. It took nearly a decade to achieve an enantioselective version of the aldol reaction with strategic use of a chiral Lewis acid. Mukaiyama et al. reported the effectiveness of a chiral Sn(II) complex as a chiral Lewis acid to control the enantioselectivity of this important carbon-carbon bond-forming reaction (Scheme 5.3) [11]. The *Z*-enolate generated from thioamide **8** and LDA is successively treated with Sn(OTf)<sub>2</sub> and chiral diamine **9** to produce the Sn(II)-enolate of thioamide **10**, which is coupled with benzaldehyde to forge a carbon-carbon single bond with stereocontrol (85% ee) exerted by proximal chiral ligand **9**. Although this work pioneered the use of an external chiral element to drive enantioselectivity in thioamide reactions, stoichiometric amounts of bases and the chiral Sn(II) complex were essential. It took another two decades to witness that enantioselective thioamide reactions were rendered catalytic, as detailed in the following section.



**Scheme 5.3** Enantioselective aldol reaction of thioamide **8** using stoichiometric amounts of base and chiral Lewis acid

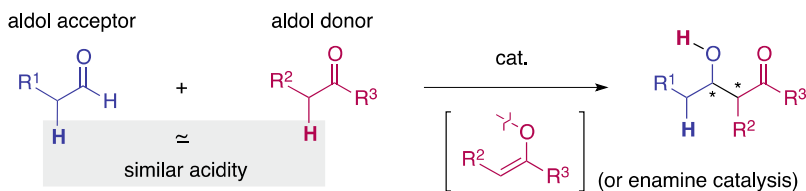
## 5.3 Catalytic Enantioselective Reactions of Thioamides

### 5.3.1 Use of Thioamides as Pronucleophiles

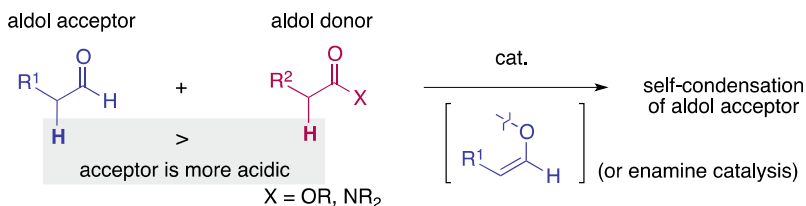
Catalytic enantioselective reactions have gained popularity as a powerful tool in synthetic organic chemistry, as this class of reactions offers the most efficient means of producing enantioenriched high-value chiral building blocks. Given the well-established synthetic protocol of thioamides as well as the capability for diverse functional group transformation, chiral synthons bearing the thioamide functionality have particular utility in enantioselective syntheses of biologically active natural products and active pharmaceutical ingredients (APIs).

As discussed in the previous section, however, catalytic turnover remained unrealized in enantioselective reactions of thioamides. Furthermore, the total efficiency of the reaction was deteriorated by the mandatory use of more than stoichiometric amounts of achiral activating reagents. In this context, Shibasaki et al. reported that thioamides exhibit enhanced reactivity in the presence of chiral Cu(I) complexes, which is rendered catalytic in terms of a chiral source and base for activation. The general concept is outlined in Fig. 5.1c; the Cu(I) complex is characterized by its soft Lewis acidic nature and tendency to interact with the soft Lewis basic thioamide functionality [12–14]. This strategy was inspired by research directed toward direct aldol chemistry [15–20], in which aldol acceptors (commonly aldehydes, electrophiles) and aldol donors (commonly aldehydes or ketones, pronucleophiles) are coupled in a truly catalytic fashion. To manifest this direct aldol scheme, chemoselective enolization of less acidic aldol donors in the presence of aldol acceptors (aldehydes) bearing highly acidic  $\alpha$ -protons is essential. This mismatched acidity scale presents a large hurdle to achieve this rather simple reaction, severely limiting the scope of direct aldol reactions to relatively acidic aldol donors, e.g., aldehydes, ketones, and active methylene-type compounds (Fig. 5.1a) [21–24]. More commonly used carbonyl-type synthons, e.g., esters and amides, remain elusive as aldol donors in catalyst-driven reactions due to the reluctance to enolize and generally lead to self-condensation of aldehydes (Fig. 5.1b). In this context, thioamides (Fig. 5.1c) are promising aldol

(a) Direct aldol reaction of acceptors and donors of small acidity difference.



(b) Direct aldol reaction of acceptors and donors of large acidity difference.



(c) Direct aldol reaction of thioamides as aldol acceptors, inverted acidity by soft-soft interaction.

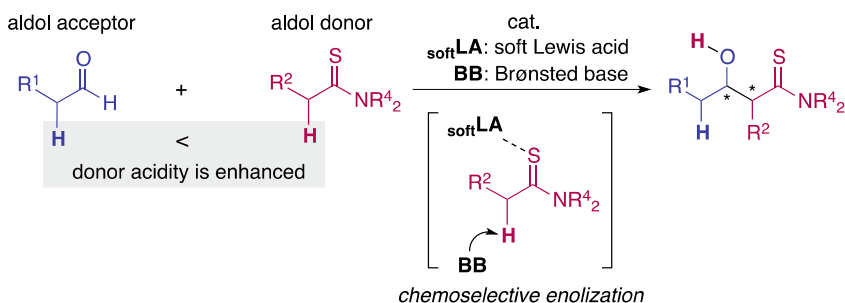


**Fig. 5.1** Direct aldol reaction using various aldol donors

donors because (1) chemoselective activation of thioamides can be achieved by taking advantage of their soft Lewis basic nature; (2) excessive activation of hard Lewis basic aldehydes (aldol acceptors) can be avoided; (3) soft-soft interactions with a soft Lewis acidic catalyst can invert the enolization kinetics to enable the exclusive enolization of the thioamide; and (4) thioamides are in a carboxylic acid oxidation state and multifaceted transformations are possible after the enantioselective reactions. Based on this blueprint, a cooperative catalytic system comprising a soft Lewis acid and a Brønsted base was developed [4, 5, 13, 25–28], allowing for general and tractable direct aldol reactions for organic synthesis.

In 2009, Shibasaki et al. reported a direct catalytic enantioselective aldol reaction of thioamide based on the strategy discussed above (Scheme 5.4) [29]. Chiral biphosphine ligand (*R,R*)-Ph-BPE is uniquely effective in combination with [Cu(CH<sub>3</sub>CN)<sub>4</sub>]PF<sub>6</sub>, which activates thioacetamide **13** as the chiral soft Lewis acid and promotes enolization in combination with Li-phenoxide **14** (first-generation catalyst). **14** is relatively basic among phenoxide derivatives due to the electron-donating

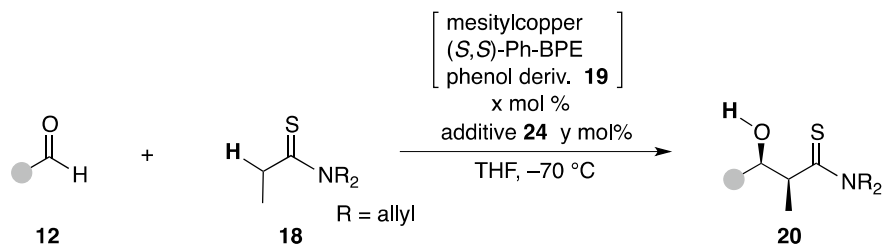




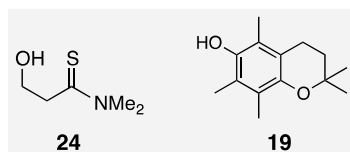
firmly that the influence of the chiral environment of the Cu(I)-complex overrides the intrinsic chirality of **16**.

The synthetic utility of this direct aldol reaction is significantly expanded by incorporating thiopropionamide **18** as a viable pronucleophile. Given the privileged nature of the propionate unit in natural products, decent control of the stereoselectivity by direct aldol reactions enables expeditious access to a myriad of useful enantioenriched synthons. Initial attempts to control the stereoselectivity by simple extrapolation of the above-mentioned optimized conditions for thioacetamides **13** to the reactions of thiopropionamide **18** resulted in unexpectedly poor stereoselectivity [30]. Re-evaluation of the reaction conditions revealed that **18** is more reactive than **13**, likely due to higher enolization aptitude, and undergoes a rapid retro-aldol reaction, which is efficiently suppressed by changing the solvent from DMF to the less polar THF with a concomitant decrease in the reaction rate. The forward and reverse reaction rates are attenuated by the addition of hard Lewis basic phosphine oxide in a concentration-dependent manner, suggesting that the hard Lewis acidic Li cation perturbs the overall reaction rate and the equilibrium of the intermediate species. Based on this hypothesis, a Li-free catalyst was developed and proved to be a more active catalyst with the additional bonus of an easy-preparation protocol (Scheme 5.5) [31]. This second-generation catalyst was prepared by mixing mesitylcopper [32–34], (*S,S*)-Ph-BPE, and 2,2,5,7,8-pentamethylchromanol **19**, with the liberation of mesitylene (the opposite absolute configuration of product **20** was due to the *S*-catalyst) (Fig. 5.2). Initially in the catalytic cycle, the thus-formed phosphine-ligated Cu(I)-phenoxide **21** serves as the soft Lewis acid/Brønsted base cooperative catalyst to affect enolization of thioamides **18**. Subsequent addition of the Cu(I)-enolate **22** to aldehydes **12** affords Cu(I)-aldolate **23**, which functions as the cooperative catalyst to drive the following catalytic cycle (blue arrow), or abstracts a proton from **19** to regenerate Cu(I)-phenoxide **21**. Additionally, the identification of this more reactive catalyst revealed that erosion of the enantioselectivity due to the retro reaction (red arrow) becomes more obvious as the steric bulk is increased. To prevent reentry of the aldol products into the catalytic cycle (en route to a retro reaction), dummy product **24** was devised as an additive to competitively bind to the catalyst, thereby kinetically retarding the problematic retro reaction. Basically, when the aldehydes possess two methylene groups before branching, the steric hindrance has little effect and the aldol products are obtained in high *syn* and enantioselectivity, even after an extended reaction time (Scheme 5.5). In contrast, when the aldehyde branching occurs closer to the formyl group, enantioselectivity decreases as a function of the reaction time, which can be effectively suppressed by dummy product **24**. The unexpectedly close kinetics of the back and forth reactions is characteristic of direct aldol chemistry of thioamides. Diverse transformation of the thioamide moiety supports the synthetic utility of this direct aldol protocol [30].

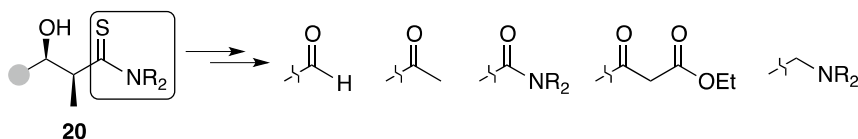
Intriguingly,  $\alpha$ -vinyl thioacetamide pronucleophile **25** bearing an  $\alpha$ -vinyl group exhibits different behavior (Scheme 5.6) [35]. The second-generation catalyst comprising mesitylcopper/(*R,R*)-Ph-BPE/phenol derivative **19** competently promotes the reaction, albeit with significantly eroded stereoselectivity. The structure of the phenol derivatives determines the stereoselectivity; while a less coordinative phenol deriva-



selected examples		cat. (x mol%)	additive <b>24</b> (y mol%)	time (h)	yield (%)	<i>syn/anti</i>	ee (%)
$\alpha$ -branch [ <b>24</b> essential]		1	0	24	89	>20/1	90
		1	0	48	95	>20/1	72
		1	2	48	96	>20/1	95
$\beta$ -branch [ <b>24</b> essential]		3	0	48	99	3/1	20
		3	6	48	96	>20/1	89
$\gamma$ -branch [ <b>24</b> can be omitted]		3	0	48	>99	>20/1	94
		3	3	48	>99	>20/1	98
$\gamma$ -branch [ <b>24</b> can be omitted]		5	0	48	96	>20/1	97
		5	5	72	83	>20/1	97



#### functional group transformation



**Scheme 5.5** Direct catalytic enantioselective aldol reaction of thiopropionamide **18**

tive, e.g., **19**, gives poor stereoselectivity, a more coordinative phenol derivative, e.g., *p*-methoxyphenol **26**, affords the aldol product in the expected absolute configuration with high stereoselectivity. The pendant vinyl group of **25** likely coordinates to Cu(I) at the stage of Cu(I)-enolate **29'**, which may lead to aldol addition via the less stereoselective open transition state **30'** (Fig. 5.3). By employing less coordinative **26** (catalyst **28**), undesired vinyl coordination is suppressed and the reaction via cyclic transition state **30** is operative from the enolate Cu(I)-enolate **29**. Indeed, the effect

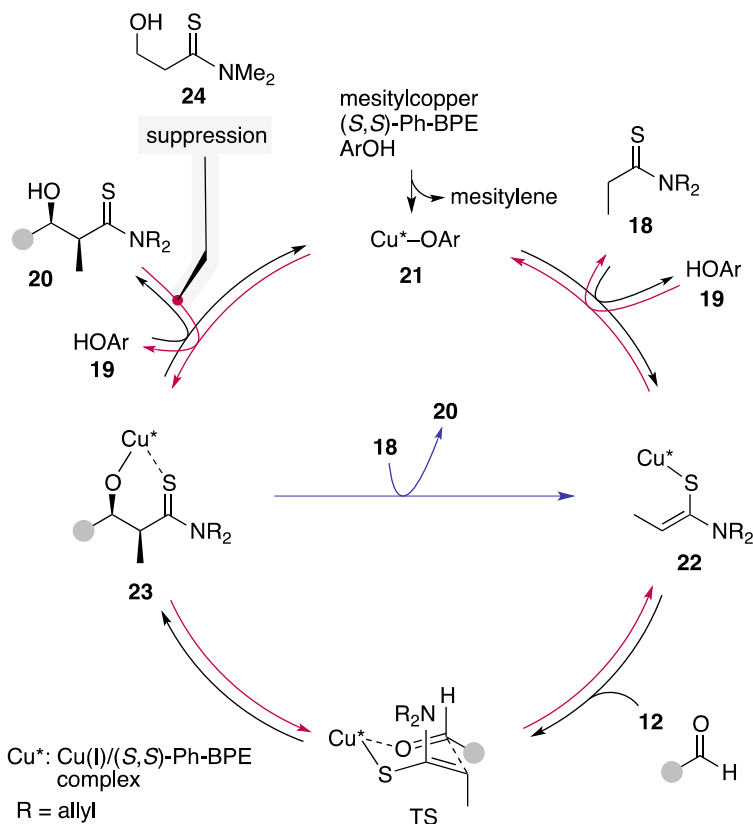
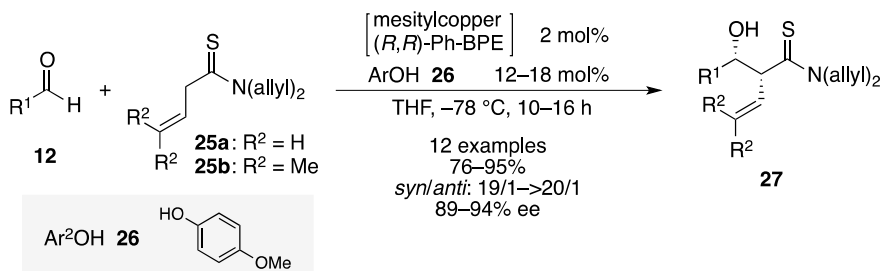


**Fig. 5.2** Plausible catalytic cycle of aldol reaction using thiopropanamide **18**



**Scheme 5.6** Direct catalytic enantioselective aldol reaction of  $\alpha$ -vinylated thioacetamide **25**

of **26** is enhanced by increasing the loading, and the coordination of **26** with the vinyl group is likely competitive.

The diastereo- and enantioselective aldol reactions discussed above consistently give *syn*-products as the kinetic products, implying that an in situ-formed

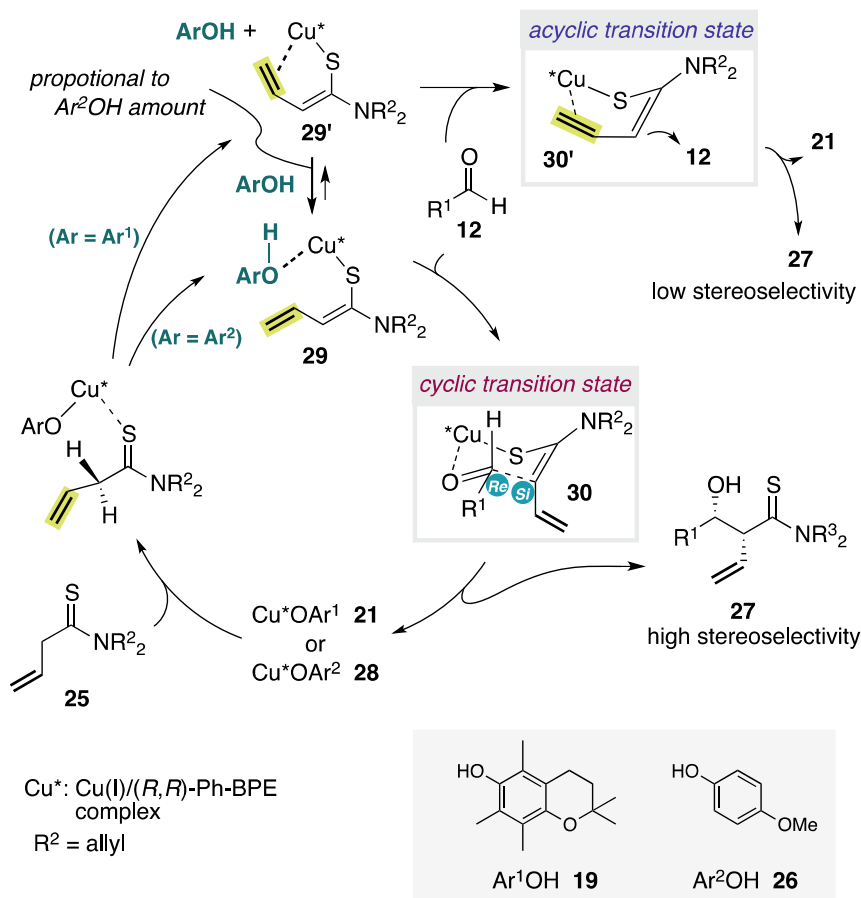
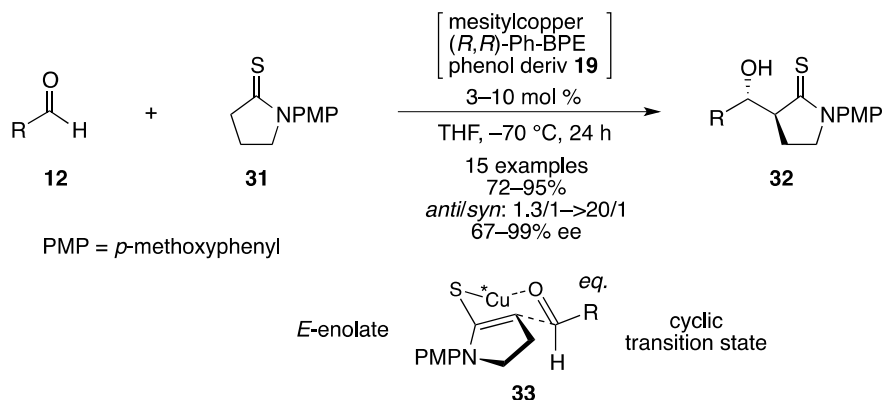


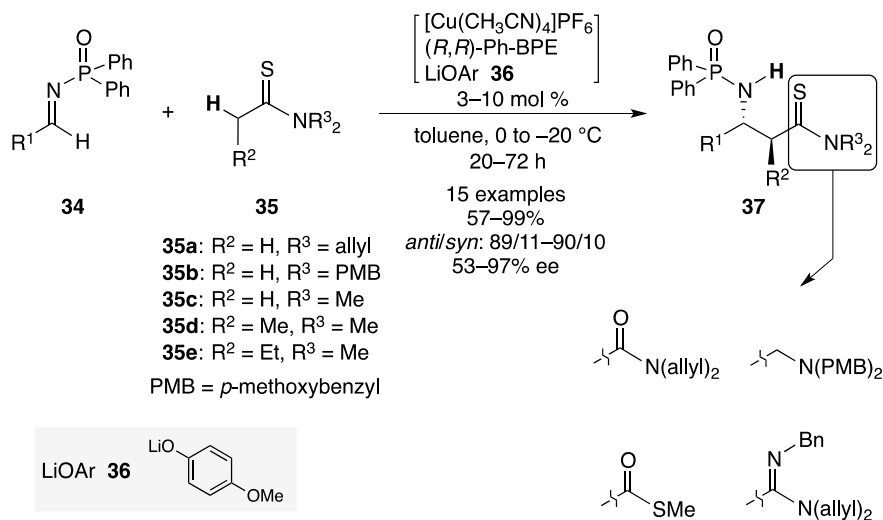
**Fig. 5.3** Plausible catalytic cycle of aldol reaction using  $\alpha$ -vinylated thioacetamide **25**

*Z*-configured enolate and cyclic transition state are involved. Although this stringent *Z*-selectivity is presumably due to the steric repulsion of two alkyl groups on the thioamide nitrogen and unlikely surpassed, the use of conformationally-restricted thioactam pronucleophile **31** exclusively generates the *E*-configured enolate en route to *anti*-aldol products **32** via transition state model **33** (Scheme 5.7) [36]. Six-membered  $\delta$ -valerolactam can also be utilized, although the stereoselectivity is decreased.

Expanding the scope of viable electrophilic partners further broadened the synthetic utility of the direct enolization of thioamide pronucleophiles. Aldimines are an obvious lateral extension from aldehyde electrophiles to achieve Mannich-type reactions, furnishing  $\beta$ -amino (thio)carbonyl products. In general, retro reactions are less prominent, particularly in the case of activated aldimines, e.g., *N*-diphenylphosphinoyl (Dpp) imines **34**, and the first-generation catalyst prepared from  $[\text{Cu}(\text{CH}_3\text{CN})_4]\text{PF}_6/(\text{R},\text{R})\text{-Ph-BPE}/\text{LiOAr}$  **36** promotes the desired reaction with

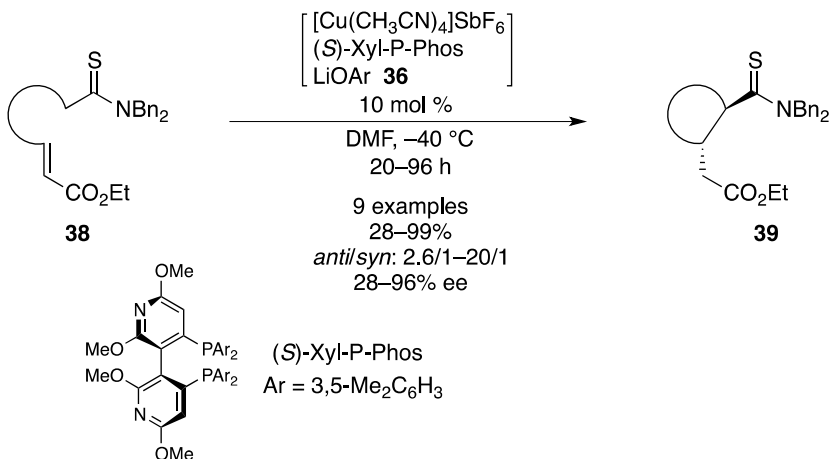


**Scheme 5.7** Direct catalytic enantioselective aldol reaction of  $\alpha$ -vinylated thioacetamide **31**

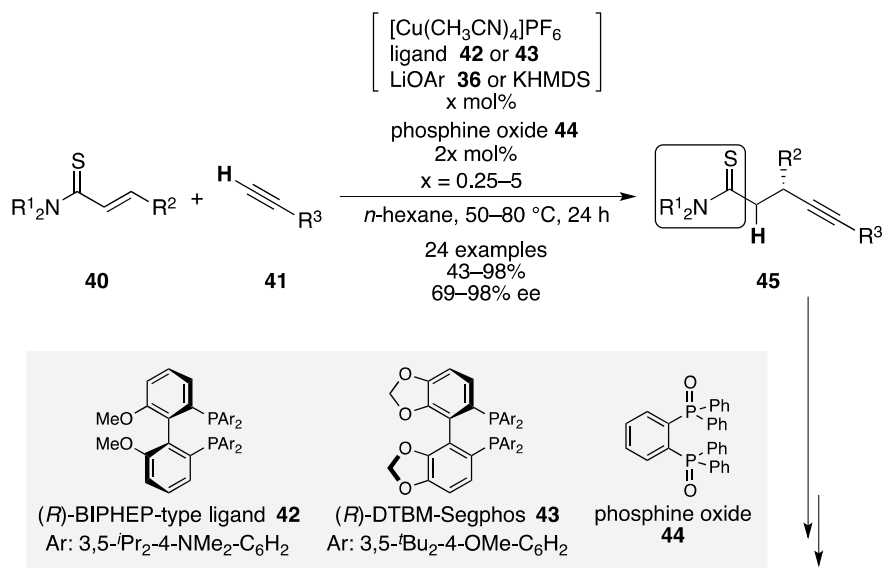


**Scheme 5.8** Direct catalytic enantioselective Mannich-type reaction of *N*-diphenylphosphinoyl imines **34** and thioamides **35**

various thioamides **35** (Scheme 5.8) [37]. Most of the reported examples used thioacetamides **35a–c** for non-diastereoselective reactions with 3 mol% of catalyst, delivering the products **37** ( $\text{R}^2 = \text{H}$ ) with generally high enantioselectivity. The reactions of thiopropanamide **35d** and thiobutyramide **35e** require higher catalyst loading (10 mol%), and enantioselectivity is significantly decreased. *anti*-Diastereoselection implies that a different transition state is operative from the *Z*-enolate due to the distinct coordination pattern of imine **34**. The diverse transformations of the thioamide moiety and easy removal of the Dpp group on the nitrogen highlight the synthetic utility of these enantioenriched products.



**Scheme 5.9** Direct catalytic enantioselective intramolecular conjugate addition



**Scheme 5.10** Direct catalytic enantioselective conjugate addition of terminal alkynes **41** to  $\alpha,\beta$ -unsaturated thioamides **40**

Thioamide enolates have the capability to react in a conjugate-type addition manifold. Although the scope is relatively limited and only intramolecular reactions are attainable, this reaction is an important new entry for the collection of catalytic enantioselective reactions of thioamides. Contrasting with the aforementioned reactions, where Ph-BPE is uniquely effective as a chiral ligand in combination with a Cu(I) cation, a biaryl-type chiral bisphosphine ligand (*S*)-Xyl-P-Phos is optimal and can be applied to the first-generation catalyst format with  $[\text{Cu}(\text{CH}_3\text{CN})_4]\text{SbF}_6^-$  and LiOAr **36** (Scheme 5.9) [38]. 5-Exo-trigonal cyclization is generally higher yielding than a 6-exo-trigonal reaction, and stereoselectivity is relatively dependent on subtle differences in the substrate structures and functional groups. An intermolecular version was achieved by taking advantage of the dual activation strategy, as summarized in the following section.

### 5.3.2 Use of Thioamides as Electrophiles

In addition to the utility of thioamides as pronucleophiles, conjugation of the thioamide functionality with a double bond provides moderately electron-deficient olefins as electrophiles that can be specifically activated by chiral soft Lewis acids with a soft-soft interaction. To make the best use of the cooperative catalytic system associated with a Brønsted base catalyst, the nucleophilic counterparts are in situ-generated to achieve perfect atom economy. Shibasaki et al. reported a direct catalytic enantioselective conjugate addition of soft Lewis basic terminal alkynes **41** to  $\alpha,\beta$ -unsaturated thioamides **40**, where the soft Lewis acid Cu(I) complex exhibits dual functions to activate both the pronucleophile and the electrophile (Scheme 5.10) [39, 40]. The standard first-generation catalyst,  $[\text{Cu}(\text{CH}_3\text{CN})_4]\text{PF}_6^-$ /chiral phosphine ligand/LiOAr **36**, acts to couple these two substrates in an enantioselective fashion, and more common biaryl-type ligands are optimal. Neither the Cu(I) complex nor LiOAr **36** can solely promote the reaction; these two catalytic elements cooperatively convert terminal alkyne **41** into the Cu(I)-alkynylide, the active nucleophile, while the vacant coordination site of Cu(I)-alkynylide directs nearby  $\alpha,\beta$ -unsaturated thioamides **40** to forge a carbon-carbon bond. In general, the reaction of aromatic alkynes proceeds with high enantioselectivity using BIPHEP-type ligand **42**, but additional use of phosphine oxide **44** boosts the reaction rate to reach completion with 0.25–1 mol% of catalyst loading. The observed kinetic isotope effect (with deuterated **41**) indicates that Cu(I)-alkynylide formation is presumably the rate-determining step, which is accelerated by the enhanced basicity of LiOAr **36** through the coordination of hard Lewis basic phosphine oxide **44**. Silylated alkynes require more sterically demanding ligand **43** and the stronger KHMDS base to afford the corresponding products. In a competitive study using chalcone, a typical and inherently more electrophilic conjugate addition acceptor,  $\alpha,\beta$ -unsaturated thioamides **40** exclusively react, confirming the highly chemoselective nature of the current catalytic system. As discussed in the previous section, mechanistic considerations raise the possibility that the reaction is promoted by a second-generation-type catalytic cycle. As delineated in Fig. 5.4,

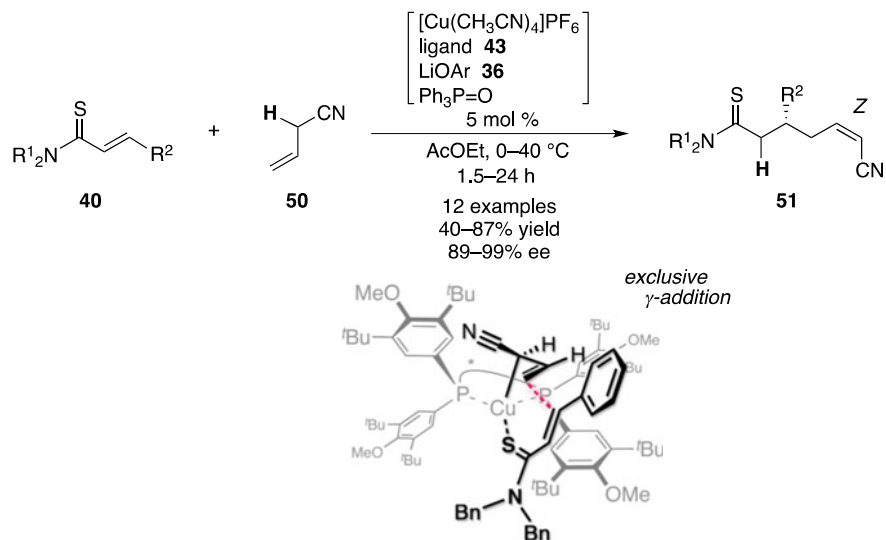
cycle A, the first-generation catalyst promotes the reaction from the top to cyclic transition state **47** in a clockwise manner, though the subsequent Cu(I)-thioamide enolate species **48** warrants deeper inspection. **48** contains two characteristic units, a soft Lewis acidic Cu(I) cation with a vacant coordination site and a Brønsted basic thioamide enolate unit, implying that **48** potentially acquires the requisite functionality as the cooperative catalyst in this specific reaction. The second-generation catalytic system, without LiOAr **36**, avoids quenching **48** by in situ-generated ArOH **26** and directly promotes the following catalytic cycle. Indeed, the simplified catalytic system, mesitylcopper and ligand **42**, is a competent catalyst to promote the reaction via the efficient proton exchange mechanism shown in **49**, incorporating the next terminal alkyne into the catalytic cycle with simultaneous liberation of product **45**. The thioamide moiety of the product is successfully transformed into a variety of functional groups for further synthetic elaboration (Scheme 5.10).

The powerful dual activation mechanism is also emulated in the reaction using allyl cyanide **50** as a soft Lewis basic pronucleophile (Scheme 5.11) [41]. While the  $\alpha$ -proton of **50** is not sufficiently acidic to catalytically generate the corresponding carbanion under mild basic conditions, the combined use of a soft Lewis acid and suitable Brønsted base efficiently renders this elusive task. A similar type of first-generation catalyst promotes the coupling reaction of **50** with  $\alpha,\beta$ -unsaturated thioamides **40**, which are activated in near proximity of the Cu(I)-cyanocarbanion in an asymmetric environment of ligand **43**. The exclusive formation of  $\gamma$ -adduct **51** is intriguing, because the Cu(I) complex binds to the  $\alpha$ -position of **50** and the  $\gamma$ -carbon approaches the  $\beta$ -position of the coordinated **40** in a cyclic transition state. The beneficial effect of triphenylphosphine oxide is likely due to the enhanced Brønsted basicity of LiOAr, which accelerates the reaction.

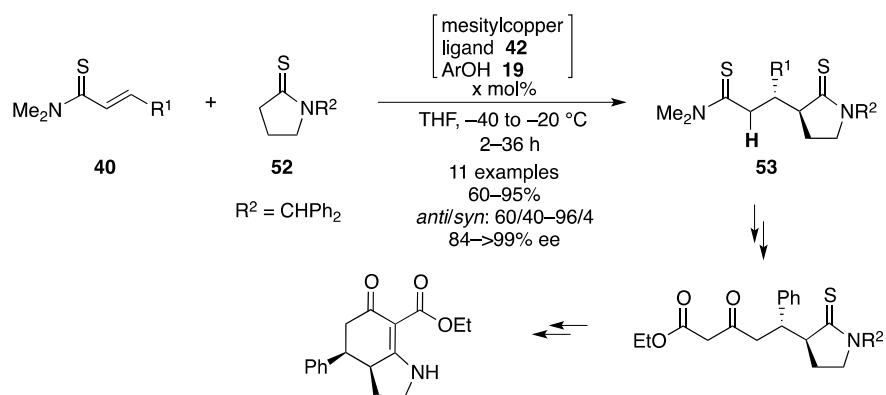
Further application of this strategy enables the intermolecular version of conjugate addition, which is not manifested in the ester-thioamide combination outlined in Scheme 5.9. The coexistence of a saturated thioamide (pronucleophile) and  $\alpha,\beta$ -unsaturated thioamides **40** in the context of a soft Lewis acid/Brønsted base cooperative catalytic system provides a dual activation mechanism to render intermolecular conjugate addition in an enantio- and diastereoselective fashion (Scheme 5.12) [42]. The second-generation catalyst prepared from mesitylcopper/ligand **42**/2,2,5,7,8-pentamethylchromanol **19** performed best to couple *N*-benzhydryl-protected thiobutylolactam **52** and  $\alpha,\beta$ -unsaturated thioamides **40**. The reaction favors *anti*-diastereoselectivity, while valerothiolactam gives the *syn*-adduct with a different chiral phosphine ligand. Sequential transformation of the thiolactam and thioamide moieties enables the productive transformation of enantioenriched products, as demonstrated by the construction of an optically active azabicyclo[4.3.0] skeleton.

In addition to the dual activation strategy discussed above, the activation of  $\alpha,\beta$ -unsaturated thioamides **40** proved sufficiently powerful to produce enantioenriched chiral building blocks by taking advantage of the specific soft-soft interaction. In general,  $\alpha,\beta$ -unsaturated carboxylic acid derivatives suffer from intrinsically low electrophilicity toward nucleophilic reaction partners, while enals and enones readily furnish the corresponding conjugate addition products. Therefore, the development of





**Scheme 5.11** Direct catalytic enantioselective addition of allyl cyanide **50** to  $\alpha,\beta$ -unsaturated thioamides **40**



**Scheme 5.12** Direct catalytic enantioselective conjugate addition of thiolactam **52** to  $\alpha,\beta$ -unsaturated thioamides **40**

catalytic enantioselective reactions of  $\alpha,\beta$ -unsaturated thioamides **40**, i.e., carboxylic acid derivatives, contributes to reinforce the chemists' toolbox for producing enantioenriched specialty chemicals. Indeed, relatively active pronucleophiles serve as suitable substrates for soft Lewis acid/Brønsted base cooperative catalysis. Thiophenol **54** is a pronucleophile in this category, and a second-generation catalyst comprising mesitylcopper/ligand **43** without the phenol component, the simplest catalytic system shown in Fig. 5.4, was effective (Scheme 5.13) [43]. Thereby, the intermediate Cu(I)-thioamide enolate functions as a cooperative catalyst to deprotonate **54** to pro-

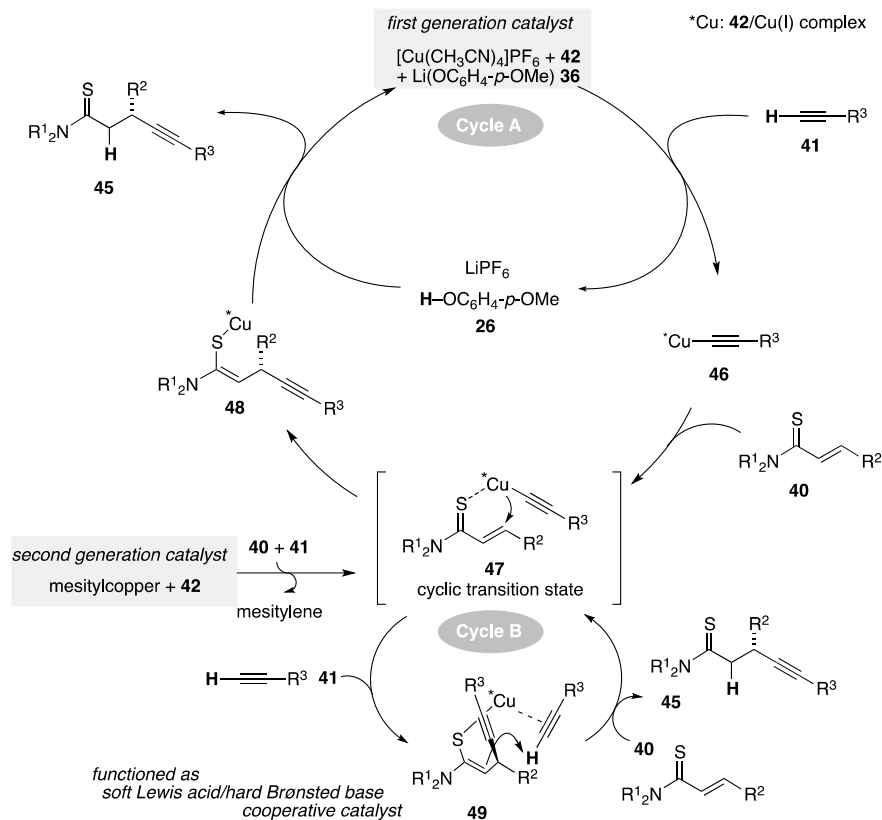
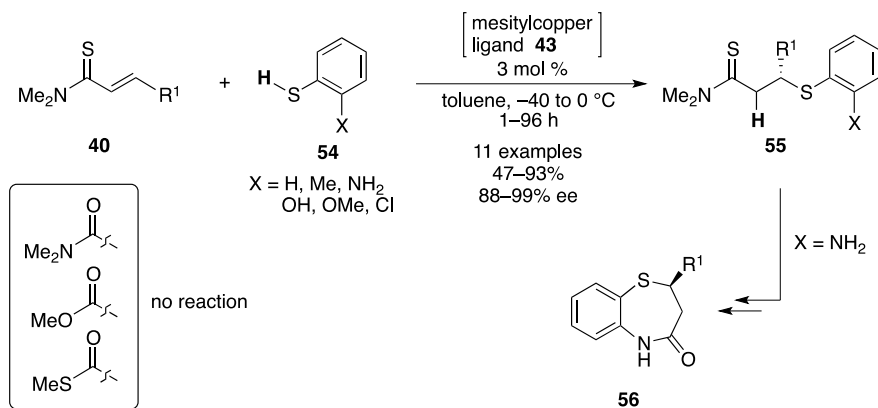


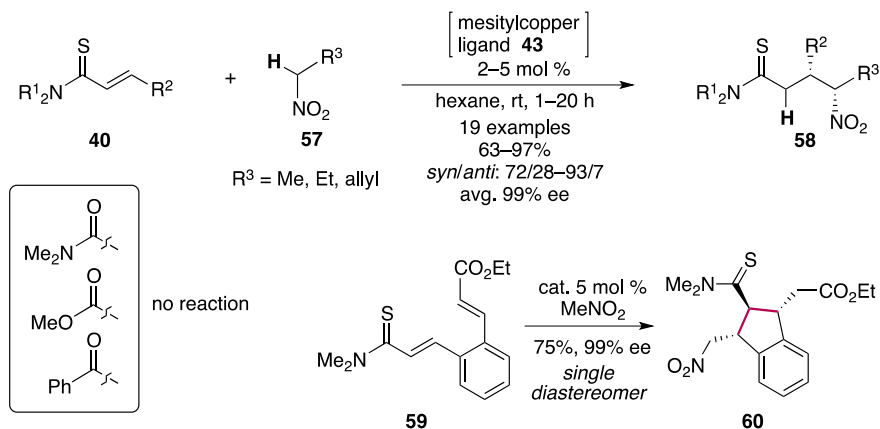
**Fig. 5.4** Plausible reaction mechanisms operating in the first-generation and second-generation catalytic systems

mote the catalysis. Free amino and phenol functionalities on the thiophenol are tolerated, presumably due to the significantly higher nucleophilicity of the thiolate anion. The inertness of structurally related unsaturated olefins bearing amide, ester, and thioesters underscores the significance of the specific soft-soft interaction between the thioamide and the Cu(I) complex. The product derived from 2-aminothiophenol is particularly useful in terms of medicinal chemistry; alkylative activation of the thioamide moiety of **55** gives rise to the construction of 1,5-benzothiazepine skeleton **56**, a privileged core structure of pharmaceuticals. Successful incorporation of 2-mercaptoethanol is also noteworthy, affording the corresponding product bearing a pendant 2-hydroxyethyl group with high enantioselectivity. The identical catalytic system can be directly applied to the conjugate addition of nitroalkanes **57** (Scheme 5.14) [44]. The reaction can be run conveniently at room temperature and with excellent enantioselectivity. In most cases, 4-nitrobut-1-ene is used, affording the product with a synthetically useful allyl group ( $\text{R}^3 = \text{allyl}$ ). Similarly, the catalytic system is exclusive for thioamide activation, which is advantageous in terms of

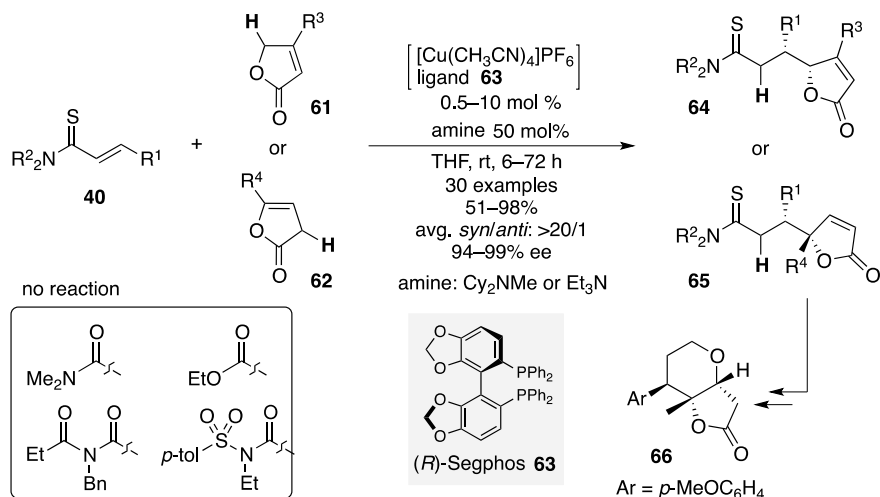


**Scheme 5.13** Direct catalytic enantioselective conjugate addition of thiophenols **54** to  $\alpha,\beta$ -unsaturated thioamides **40**

functional group tolerance for more complicated substrates. Intriguingly, for the specific case of  $\alpha,\beta$ -unsaturated thioamide **59** installed with  $\alpha,\beta$ -unsaturated ester, initial nitroalkane addition proceeds at the  $\beta$ -position of thioamide, and the intermediate Cu(I)-thioamide enolate undergoes subsequent intramolecular conjugate addition to the  $\alpha,\beta$ -unsaturated ester, furnishing trisubstituted indane **60** as a single diastereomer in 99% ee. Butenolides **61** and  $\alpha$ -angelica lactones **62** are another class of compatible pronucleophiles for  $\alpha,\beta$ -unsaturated thioamides **40**, where slightly modified first-generation catalysts with sterically less congested chiral ligand **63** effectively afford the corresponding optically active compounds as densely functionalized chiral building blocks (Scheme 5.15) [45]. Although LiOAr bases are competent to promote this reaction in a highly stereoselective manner, conversion remains moderate even after an extended reaction time. Considering the enolization-prone property of these pronucleophiles, a stoichiometric amount of inexpensive tertiary amines can be used instead of LiOAr bases, leading to the optimized conditions shown in Scheme 5.15. Diastereoselectivity and enantioselectivity are uniformly high in all cases examined, and the convenient room temperature protocol is advantageous. As opposed to the  $\alpha,\beta$ -unsaturated amide and ester, the corresponding imide and sulfonimide fail to promote the reaction under the cooperative catalysis. Of note, consecutive tri- and tetrasubstituted stereogenic centers are constructed in the reaction of  $\alpha$ -angelica lactones **62**, whose product **65** can be transformed into bicyclic compound **66** as a single diastereomer via a reduction/intramolecular conjugate addition sequence.



**Scheme 5.14** Direct catalytic enantioselective conjugate addition of nitroalkanes **57** to  $\alpha,\beta$ -unsaturated thioamides **40**



**Scheme 5.15** Direct catalytic enantioselective conjugate addition of butenolides **61** or  $\alpha$ -angelicalactones **62** to  $\alpha,\beta$ -unsaturated thioamides **40**

## 5.4 Utility in Enantioselective Synthesis of Natural Products and Biologically Active Compounds

As overviewed in Sect. 5.5.3, thioamides serve as useful starting materials for catalytic enantioselective reactions as both pronucleophiles and electrophiles, producing diverse sets of chiral building blocks bearing suitable functional handles for further elaboration. This chapter illustrates the collection of biologically active nat-

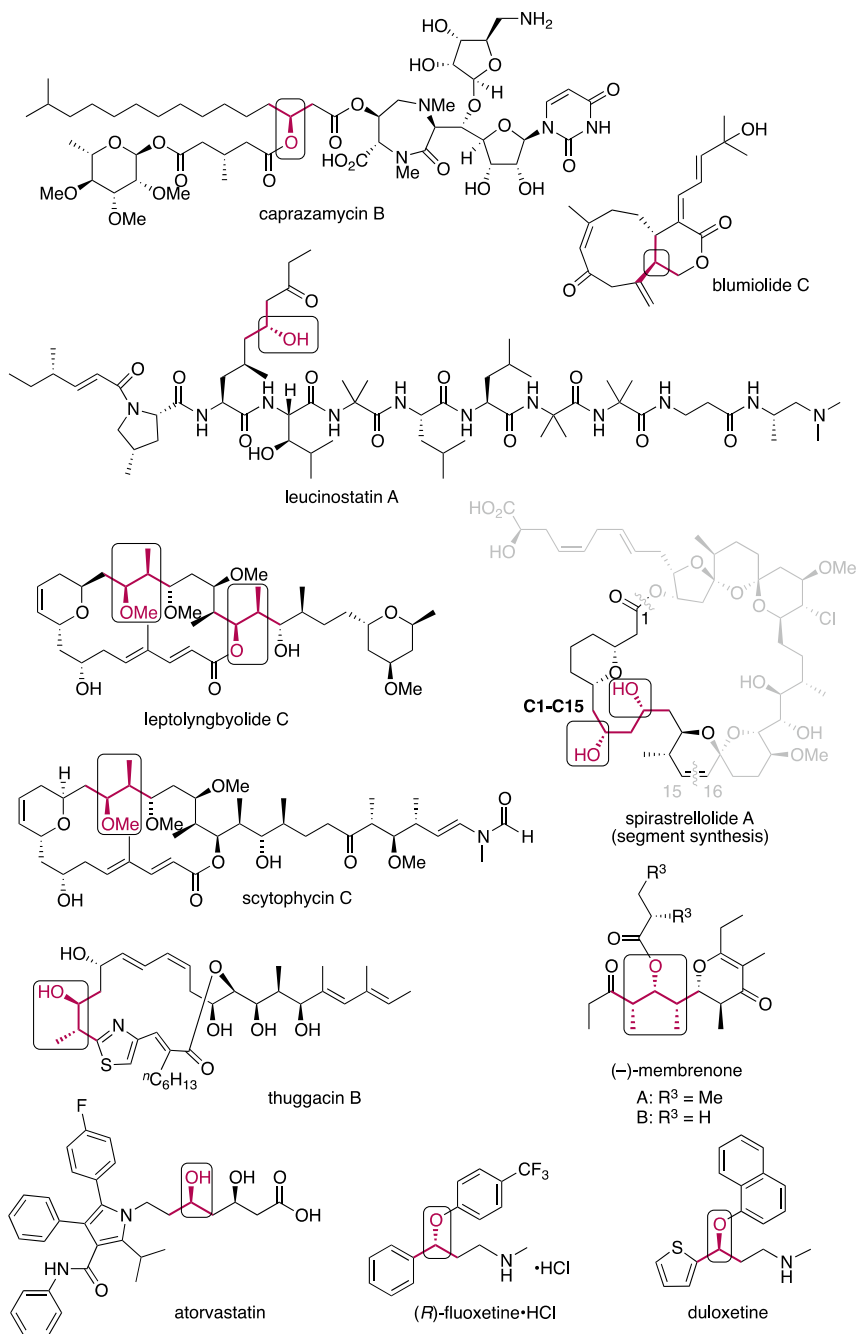


**Fig. 5.5** Natural products and APIs synthesized by direct catalytic asymmetric aldol reaction of thioamides

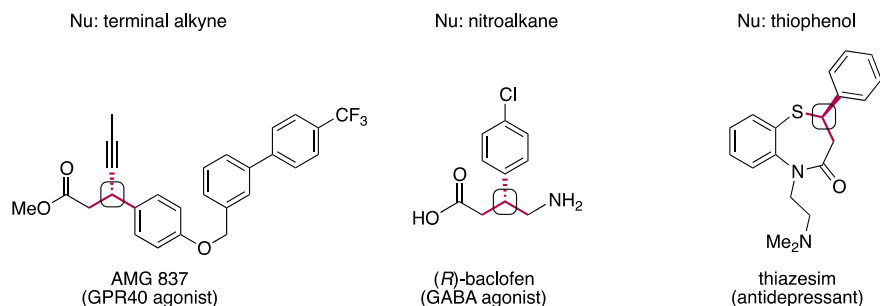


**Fig. 5.6** APIs synthesized by catalytic asymmetric reactions of  $\alpha,\beta$ -unsaturated thioamides as electrophiles

ural products as well as APIs that can be accessed by synthetic strategies based on the enantioselective catalysis of thioamides.

As the Evans aldol strategy gained unparalleled popularity in the synthetic chemistry community [46–48], aldol products unquestionably contain the necessary structural elements for synthesizing complicated synthetic targets. Reliable stereocontrol is also an issue for streamlined stereoselective synthesis without nonproductive stereoinversion processes. One drawback of the Evans aldol strategy is the stoichiometric use of chiral materials and bases to promote the reaction, which can be avoided by the direct aldol strategy empowered by the unique properties of the thioamide functionality and cooperative catalysis. As demonstrated by Shibasaki et al., the thioamide aldol reaction can be applied to a number of enantioselective syntheses (Fig. 5.5). Thioacetamide pronucleophiles are used in the natural products caprazamycine B (anti-tuberculosis) [49, 50], leucinostatin A (anti-tumor) [51, 52], spirastrellolide (anti-tumor, segment synthesis of C1–C15) [53], as well as APIs atorvastatin (anti-hypercholesterolemia) [54, 55], fluoxetine (antidepressant) [56], and duloxetine (antidepressant) [57]. Thiopropionamide pronucleophiles are even more effective for constructing propionate units and introducing a methyl group at the stereogenic center with precise stereocontrol, allowing for streamlined synthesis of leptolyngbyolide B (cytotoxin) [58], scytophycin C (anti-tumor) [59], thuggacin B [60], and membrenone A and B [61], the last of which showcases the iterative aldol strategy to construct consecutive propionate units in a highly stereoselective fashion. The enantioenriched product derived from  $\alpha$ -vinylated thioacetamide is particularly useful for constructing a cyclic architecture, e.g., blumiolide C [35], where the pendant vinyl group serves as a handle for ring-closing metathesis. Besides their role as pronucleophiles,  $\alpha,\beta$ -unsaturated thioamides offer additional utility as electrophiles to accept various nucleophiles under stringent stereocontrol (Fig. 5.6). APIs bearing a  $\beta$ -branched carboxylic acid units are suitable synthetic targets, as demonstrated by the synthesis of AMG 837 (GPR40 agonist) [39, 40, 62] and baclofen (GABA agonist) [44] by the catalytic enantioselective addition of a terminal alkyne and a nitroalkane, respectively. 2-Aminothiophenol addition is quite useful for rapidly con-

structing the 1,5-benzothiazepine ring system as exemplified by the enantioselective synthesis of thiazesim (antidepressant) [43].

## 5.5 Future Outlook

Thioamides comprise a very attractive class of compounds with distinctive chemical properties, e.g., soft Lewis basicity, that can be effectively exploited for chemoselective activation. Chemoselectivity is a fundamental, but sometimes overwhelming, factor for determining the overall efficiency of synthetic processes; high chemoselectivity promises orthogonal reactivity in an ensemble of multiple functional groups, and functional groups that are inert but become active solely in the presence of a specific trigger are highly useful in many synthetic processes. Thioamides are such a functional group, where a soft Lewis acid complex serves as a key to unlock hidden reactivity to render catalytic reactions in a highly enantioselective fashion. This favorable property is further leveraged by the easy preparation and the capability for multifaceted transformation. The synthetic demonstrations illustrated in the previous section showcases the utility of the stereocontrolled construction of molecules of interest. Further sophistication of catalytic systems will allow these catalytic processes to be functional in future pilot plant syntheses of high-value specialty chemicals.

## References

1. T.S. Jagodziński, *Chem. Rev.* **103**, 197–227 (2003)
2. Z. Liu, H. Qu, X. Gu, B.J. Min, J. Nyberg, V.J. Hruby, *Org. Lett.* **10**, 4105–4108 (2008)
3. J.T. Reeves, Z. Tan, M.A. Herbage, Z.S. Han, M.A. Marsini, Z. Li, G. Li, Y. Xu, K.R. Fandrick, N.C. Gonnella, S. Campbell, S. Ma, N. Grinberg, H. Lee, B.Z. Lu, C.H. Senanayake, *J. Am. Chem. Soc.* **135**, 5565–5568 (2013)
4. H. Yamamoto, K. Futatsugi, *Angew. Chem. Int. Ed.* **44**, 1924–1942 (2005)
5. H. Yamamoto, K. Ishihara, *Acid Catalysis in Modern Organic Synthesis* (Wiley-VCH; Wiley, Weinheim, 2008)
6. Y. Tamaru, T. Harada, S.-I. Nishi, M. Mizutani, T. Hioki, Z.-I. Yoshida, *J. Am. Chem. Soc.* **102**, 7806–7808 (1980)
7. Y. Tamaru, T. Hioki, Z. Yoshida, *Tetrahedron Lett.* **25**, 5793–5796 (1984)
8. C. Goasdoué, N. Goasdoué, M. Gaudemar, *J. Organomet. Chem.* **208**, 279–292 (1981)
9. C. Goasdoué, N. Goasdoué, M. Gaudemar, *Tetrahedron Lett.* **24**, 4001–4004 (1983)
10. C. Goasdoué, N. Goasdoué, M. Gaudemar, *J. Organomet. Chem.* **263**, 273–281 (1984)
11. N. Iwasawa, T. Yura, T. Mukaiyama, *Tetrahedron* **45**, 1197–1207 (1989)
12. N. Kumagai, *Chem. Pharm. Bull.* **59**, 1–22 (2011)
13. N. Kumagai, M. Shibasaki, *Angew. Chem. Int. Ed.* **50**, 4760–4772 (2011)
14. N. Kumagai, M. Shibasaki, *Isr. J. Chem.* **52**, 604–612 (2012)
15. B. Alcaide, P. Almendros, *Eur. J. Org. Chem.* **2002**, 1595–1601 (2002)
16. R. Mahrwald, *Modern Aldol Reactions* (Wiley-VCH, Weinheim, 2004)
17. W. Notz, F. Tanaka, C.F. Barbas III, *Acc. Chem. Res.* **37**, 580–591 (2004)
18. S. Mukherjee, J.W. Yang, S. Hoffmann, B. List, *Chem. Rev.* **107**, 5471–5569 (2007)

19. B.M. Trost, C.S. Brindle, *Chem. Soc. Rev.* **39**, 1600–1632 (2010)
20. R. Mahrwald, *Modern Methods in Stereoselective Aldol Reactions* (Wiley-VCH, Weinheim, 2013)
21. Y.M.A. Yamada, N. Yoshikawa, H. Sasai, M. Shibasaki, *Angew. Chem. Int. Ed. Engl.* **36**, 1871–1873 (1997)
22. N. Yoshikawa, Y.M.A. Yamada, J. Das, H. Sasai, M. Shibasaki, *J. Am. Chem. Soc.* **121**, 4168–4178 (1999)
23. B. List, R.A. Lerner, C.F. Barbas III, *J. Am. Chem. Soc.* **122**, 2395–2396 (2000)
24. B.M. Trost, H. Ito, *J. Am. Chem. Soc.* **122**, 12003–12004 (2000)
25. M. Shibasaki, N. Yoshikawa, *Chem. Rev.* **102**, 2187–2209 (2002)
26. M. Kanai, N. Kato, E. Ichikawa, M. Shibasaki, *Synlett* **2005**, 1491–1508 (2005)
27. D.H. Paull, C.J. Abraham, M.T. Scerba, E. Alden-Danforth, T. Lectka, *Acc. Chem. Res.* **41**, 655–663 (2008)
28. R. Peters, *Cooperative Catalysis* (Wiley-VCH, Weinheim, 2015)
29. M. Iwata, R. Yazaki, Y. Suzuki, N. Kumagai, M. Shibasaki, *J. Am. Chem. Soc.* **131**, 18244–18245 (2009)
30. M. Iwata, R. Yazaki, I.H. Chen, D. Sureshkumar, N. Kumagai, M. Shibasaki, *J. Am. Chem. Soc.* **133**, 5554–5560 (2011)
31. Y. Bao, N. Kumagai, M. Shibasaki, *Chem. Sci.* **6**, 6124–6132 (2015)
32. T. Tsuda, T. Yazawa, K. Watanabe, T. Fujii, T. Saegusa, *J. Org. Chem.* **46**, 192–194 (1981)
33. E.M. Meyer, S. Gambarotta, C. Floriani, A. Chiesi-Villa, C. Guastinit, *Organometallics* **8**, 1067–1079 (1989)
34. M. Stollenz, F. Meyer, *Organometallics* **31**, 7708–7727 (2012)
35. J. Cui, A. Ohtsuki, T. Watanabe, N. Kumagai, M. Shibasaki, *Chem. Eur. J.* **24**, 2598–2601 (2018)
36. D. Sureshkumar, Y. Kawato, M. Iwata, N. Kumagai, M. Shibasaki, *Org. Lett.* **14**, 3108–3111 (2012)
37. Y. Suzuki, R. Yazaki, N. Kumagai, M. Shibasaki, *Angew. Chem. Int. Ed.* **48**, 5026–5029 (2009)
38. Y. Suzuki, R. Yazaki, N. Kumagai, M. Shibasaki, *Chem. Eur. J.* **17**, 11998–12001 (2011)
39. R. Yazaki, N. Kumagai, M. Shibasaki, *J. Am. Chem. Soc.* **132**, 10275–10277 (2010)
40. R. Yazaki, N. Kumagai, M. Shibasaki, *Chem. Asian J.* **6**, 1778–1790 (2011)
41. Y. Yanagida, R. Yazaki, N. Kumagai, M. Shibasaki, *Angew. Chem. Int. Ed.* **50**, 7910–7914 (2011)
42. N. Majumdar, A. Saito, L. Yin, N. Kumagai, M. Shibasaki, *Org. Lett.* **17**, 3362–3365 (2015)
43. T. Ogawa, N. Kumagai, M. Shibasaki, *Angew. Chem. Int. Ed.* **51**, 8551–8554 (2012)
44. T. Ogawa, S. Mouri, R. Yazakinaoya, N. Kumagai, M. Shibasaki, *Org. Lett.* **14**, 110–113 (2012)
45. L. Yin, H. Takada, S. Lin, N. Kumagai, M. Shibasaki, *Angew. Chem. Int. Ed.* **53**, 5327–5331 (2014)
46. D.A. Evans, E. Vogel, J.V. Nelson, *J. Am. Chem. Soc.* **101**, 6120–6123 (1979)
47. D.A. Evans, J. Bartroli, T.L. Shih, *J. Am. Chem. Soc.* **103**, 2127–2129 (1981)
48. D.A. Evans, *Aldrichimica Acta* **15**, 23–32 (1982)
49. P. Gopinath, T. Watanabe, M. Shibasaki, *J. Org. Chem.* **77**, 9260–9267 (2012)
50. H. Abe, P. Gopinath, G. Ravi, L. Wang, T. Watanabe, M. Shibasaki, *Tetrahedron Lett.* **56**, 3782–3785 (2015)
51. H. Abe, H. Ouchi, C. Sakashita, M. Kawada, T. Watanabe, M. Shibasaki, *Chem. Eur. J.* **23**, 11792–11796 (2017)
52. H. Abe, M. Kawada, C. Sakashita, T. Watanabe, M. Shibasaki, *Tetrahedron* **74**, 5129–5137 (2018)
53. Y. Sahara, J. Cui, M. Furutachi, J. Chen, T. Watanabe, M. Shibasaki, *Synthesis* **49**, 69–75 (2016)
54. Y. Kawato, M. Iwata, R. Yazaki, N. Kumagai, M. Shibasaki, *Tetrahedron* **67**, 6539–6546 (2011)
55. Y. Kawato, S. Chaudhary, N. Kumagai, M. Shibasaki, *Chem. Eur. J.* **19**, 3802–3806 (2013)
56. Iwata M, Yazaki R, Kumagai N, Shibasaki M, *Tetrahedron: asymmetry* **21**:1688–1694 (2010)



57. Y. Suzuki, M. Iwata, R. Yazaki, N. Kumagai, M. Shibasaki, *J. Org. Chem.* **77**, 4496–4500 (2012)
58. J. Cui, M. Morita, O. Ohno, T. Kimura, T. Teruya, T. Watanabe, K. Suenaga, M. Shibasaki, *Chem. Eur. J.* **23**, 8500–8509 (2017)
59. J. Cui, T. Watanabe, M. Shibasaki, *Tetrahedron Lett.* **57**, 446–448 (2016)
60. A. Matsuzawa, C.R. Opie, N. Kumagai, M. Shibasaki, *Chem. Eur. J.* **20**, 68–71 (2014)
61. K. Alagiri, S. Lin, N. Kumagai, M. Shibasaki, *Org. Lett.* **16**, 5301–5303 (2014)
62. R. Yazaki, N. Kumagai, M. Shibasaki, *Org. Lett.* **13**, 952–955 (2011)

# Chapter 6

## Synthesis of Heterocycles from Thioamides



Hong Yan and Hai-Chao Xu

**Abstract** This chapter has reviewed recent developments from the year 2000 on the synthesis of heterocycles from thioamides. Heterocycles are ubiquitous motifs that play critical roles in chemistry and biology. Thioamides, owing to their easy availability and versatile reactivity in ionic and radical reactions, have become useful synthons in the synthesis of various heterocycles.

**Keywords** Thioamide · Heterocycle · Cyclization

### 6.1 Introduction

Heterocycles are prevalent in natural products, bioactive compounds, and materials. As a result, the development of efficient methods for their synthesis from easily available materials is an important research focus for organic chemists [1–3]. Among numerous methods for their synthesis, those starting from thioamides have been extensively studied [4]. Thioamides are valuable building blocks for synthesis because of their versatile reactivities. While the carbon atom of the thiocarbonyl is electrophilic, the sulfur atom of the thiocarbonyl and the nitrogen atom of the thioamide moiety are nucleophilic. In addition to ionic reactions, thioamides can be converted to thioamide radicals and participate in radical reactions. Moreover, thioamides bearing an electron-withdrawing substituent at the  $\alpha$ -position introduce additional sites for functionalization [5, 6]. Therefore, thioamides have been employed for the synthesis of a host of heterocycles, especially those containing sulfur and/or nitrogen atoms. Since a comprehensive review on the synthesis of heterocycles from thioamides has been published in 2003 [4], we have focused on the more recent results in this area from 2000 with occasionally mentioning earlier results from a historical point of view.

---

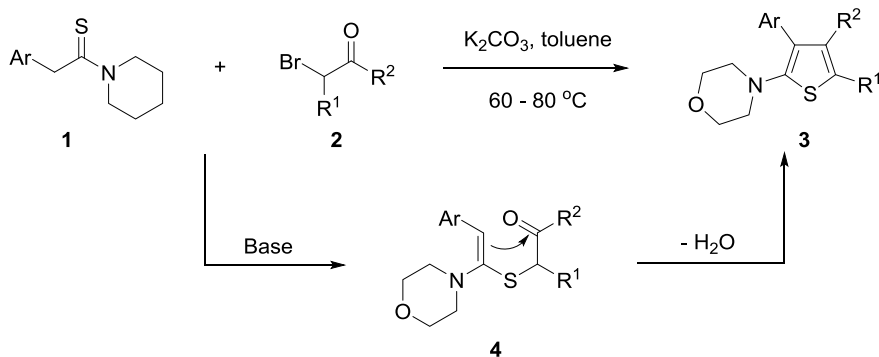
H. Yan · H.-C. Xu (✉)  
College of Chemistry and Chemical Engineering,  
Xiamen University, Xiamen, People's Republic of China  
e-mail: [haichao.xu@xmu.edu.cn](mailto:haichao.xu@xmu.edu.cn)

## 6.2 Synthesis of Heterocycles with One Heteroatom

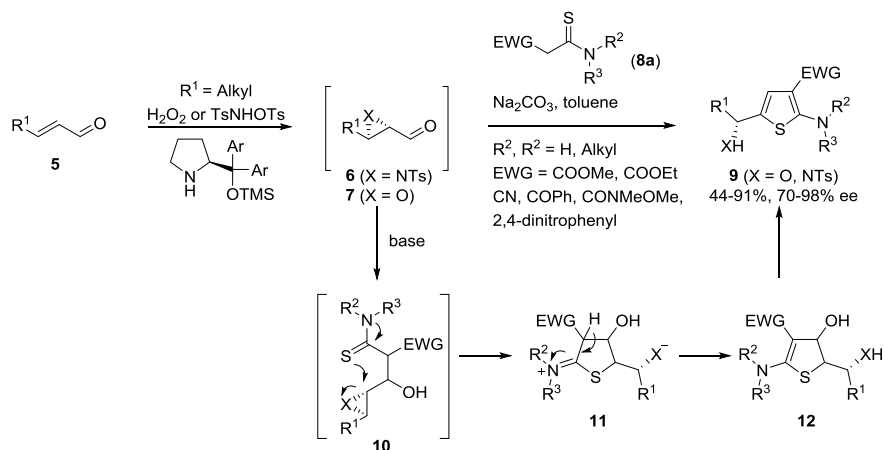
### 6.2.1 *S*-Heterocycles

Thiophenes are prepared through the annulation of thioamides bearing an active  $\alpha$ -methylene moiety with a variety of electrophilic compounds. The intermolecular cyclization of primary or secondary thioamides with  $\alpha$ -halo ketones affords thiazole derivatives [7, 8]. However, tertiary thioamides afford different types of products. For example, aryl thiomorpholides **1**, which bear an aryl group at the  $\alpha$ -position, react with  $\alpha$ -halo ketones **2** to generate highly substituted thiophenes **3** (Scheme 6.1) [9–12]. The reactions first form the intermediate **4**, which undergoes intramolecular dehydration to furnish the thiophene product. Besides  $\alpha$ -halo ketones, aldehydes bearing  $\alpha$ -leaving groups such as aziridine (**6**) or epoxy (**7**) groups undergo intermolecular dehydrative annulation with activated thioamides **8a** to produce thiophenes **9** (Scheme 6.2) [13]. In this case, the aziridines and epoxides were prepared in one pot from  $\alpha,\beta$ -unsaturated aldehydes **5** via an organocatalytic asymmetric reaction. Under basic conditions, thioamide **8a** adds to the aldehyde carbonyl to give **10**, which undergoes intramolecular nucleophilic cyclization/ring opening of three-membered ring to give five-membered *S*-heterocycle **11**. Aromatization through proton shift and dehydration affords thiophene **9**. The reaction of 2-ynals **13** with activated thioamides **8b** in alcoholic solvent produces 2,3,5-trisubstituted 2-aminothiophenes **14** (Scheme 6.3) [14]. Mechanistically, thioamide **8b** first condenses with aldehyde **13** to give **16**, which undergoes intramolecular cyclization followed by conjugate addition to afford the final thiophene **14**.

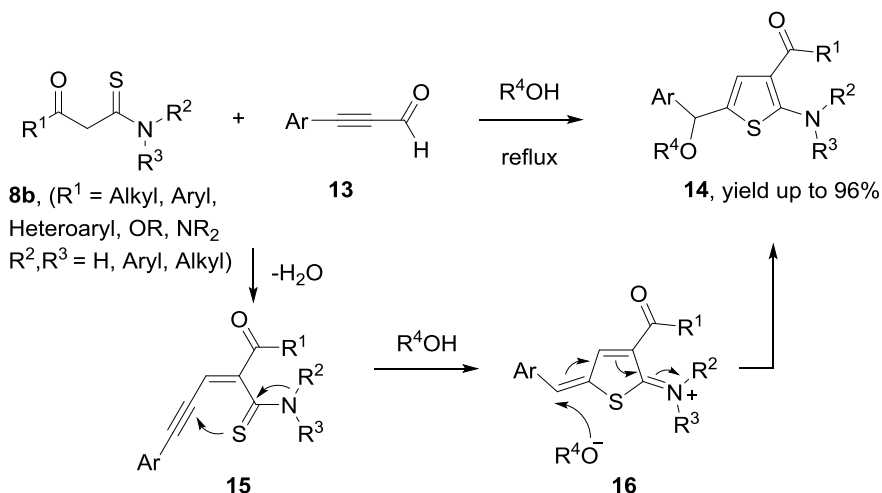
4-Dimethylaminopyridine (DMAP)-mediated annulation of  $\beta$ -ketothioamides **8c** with 1,4-naphthoquinone (**17**) affords naphtho[2,3-*b*]thiophenes **18** (Scheme 6.4) [15]. The reactions are proposed to proceed via Michael addition to give 1,4-dihydroxynaphthalene **19**. Oxidation of **19** affords 1,4-naphthoquinone **20**, which



**Scheme 6.1** Synthesis of thiophenes via annulations of thioamides and  $\alpha$ -halo ketones



Scheme 6.2 Synthesis of optically active thiophenes

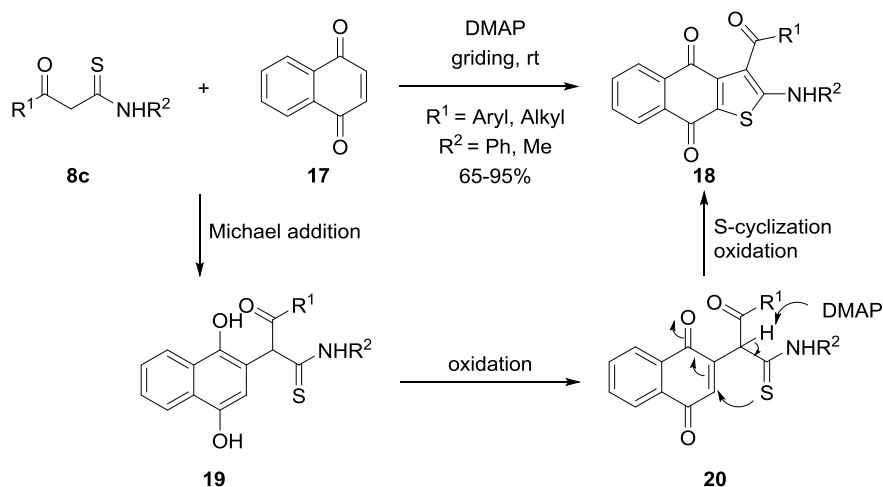


Scheme 6.3 Synthesis of thiophenes from 2-ynals

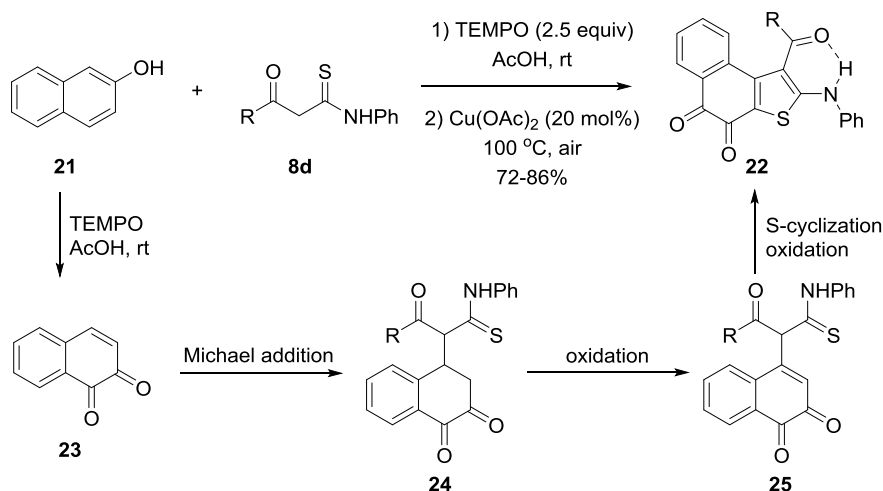
undergoes *S*-cyclization and further oxidation to give **18**. Although not mentioned by the authors, air is probably the terminal oxidant for this oxidative annulation reaction.

1,2-Naphthoquinone **23** generated through TEMPO-mediated oxidation of  $\beta$ -naphthol (**21**) reacts under air in the presence of a copper catalyst with  $\beta$ -ketothioamides **8d** to afford naphtho[2,1-*b*]thiophene-4,5-diones **22** (Scheme 6.5) [16]. The mechanism is similar to that of 1,4-naphthoquinone and involves Michael addition, oxidation, *S*-cyclization, and further oxidative aromatization.

2,3-Dichloro-5,6-dicyanobenzoquinone (DDQ, **26**) reacts with  $\beta$ -ketothioamides **8e** via ring cleavage to afford 2,3-dicyanothiophenes **27**. The reactions first undergo



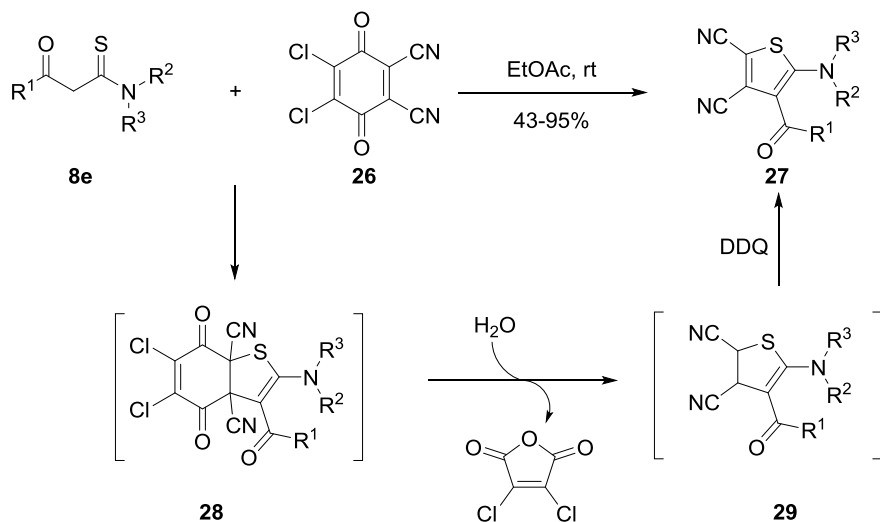
**Scheme 6.4** Synthesis of thiophenes from  $\beta$ -ketothioamides and 1,4-naphthoquinone



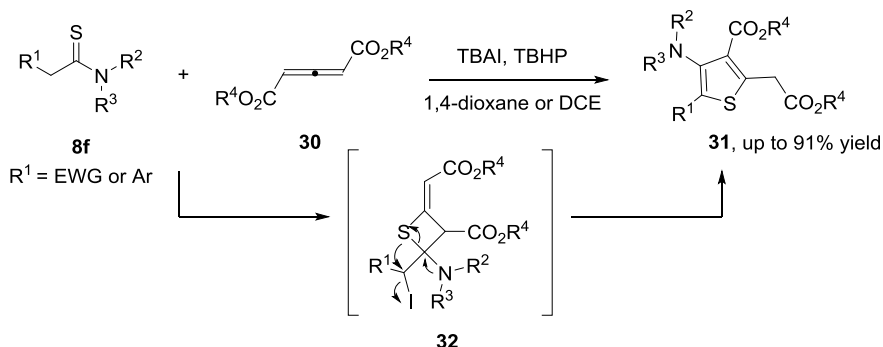
**Scheme 6.5** Synthesis of thiophenes from  $\beta$ -ketothioamides and  $\beta$ -naphthol

annulation to afford bicyclic intermediate **28**, which reacts with  $\text{H}_2\text{O}$  to afford **29**. Dehydrogenation of **29** with DDQ furnishes thiophene **27**. DDQ serves both as a reactant and as an oxidant (Scheme 6.6) [17].

Thioamides **8f** bearing an electron-withdrawing group or aryl group at the  $\alpha$ -position undergo oxidative annulation with electron-deficient allenes **30** to afford 3-aminothiophenes **31** (Scheme 6.7) [18, 19]. The reactions are proposed to proceed through 1,2-sulfur migration via the four-membered ring intermediate **32**.



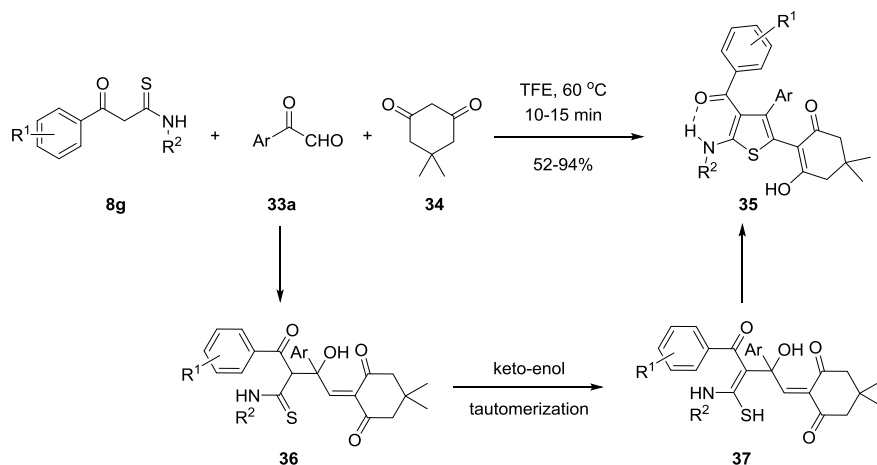
**Scheme 6.6** Annulation of  $\beta$ -ketothioamides and DDQ via ring cleavage



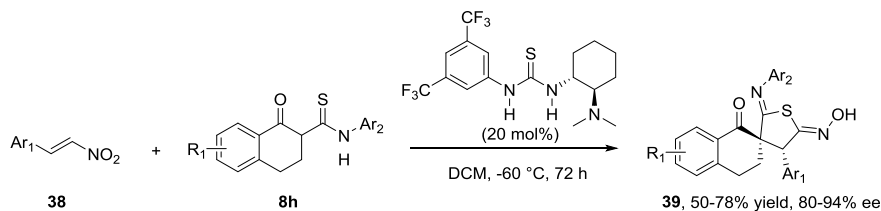
**Scheme 6.7** Oxidative annulation of thioamides with electron-deficient allenes

A three-component annulation of  $\beta$ -ketothioamides **8g** with arylglyoxals **33a** and 5,5-dimethyl-1,3-cyclohexanedione (**34**) in CF<sub>3</sub>CH<sub>2</sub>OH (TFE) generated rapidly ( $\leq 15$  min) tetrasubstituted thiophenes **35**. The reactions are proposed to proceed through Knoevenagel condensation of **34** with **33a** to generate an  $\alpha,\beta$ -unsaturated ketone, which undergoes addition reaction with **8g** at the aryl carbonyl group to give **36**. Tautomerization of **36** gives **37**, which undergoes dehydrative cyclization to afford the final thiophene product (Scheme 6.8) [20].

Annulation of  $\beta$ -keto thioamides **8h** with nitroalkenes **38** catalyzed by Takemoto's organocatalyst affords optically active spiroannulated dihydrothiophenes **39** (Scheme 6.9) [21].



**Scheme 6.8** Synthesis of thiophenes via three-component reactions

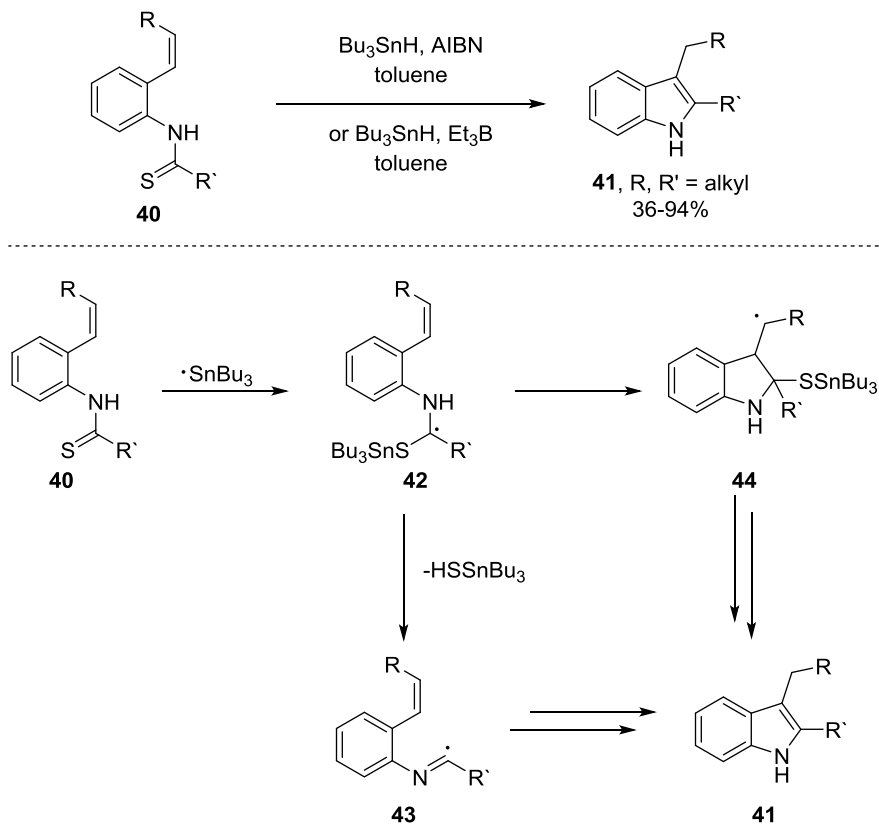


**Scheme 6.9** Synthesis of optically active spiroannulated dihydrothiophenes

## 6.2.2 *N*-Heterocycles

Fukuyama and coworkers have developed a radical cyclization reaction of 2-alkenylthioanilides **40** to prepare 2,3-disubstituted indoles **41** using  $\text{Bu}_3\text{SnH}$  and a radical initiator such as AIBN or  $\text{BEt}_3$  (Scheme 6.10) [22]. The reaction efficiency is affected by the configuration of the alkene with the *cis*-alkene being superior to the *trans* isomer. The reaction is proposed to proceed through the addition of tin radical to the thioamide moiety to form a  $\text{sp}^3$  carbon radical **42** or a  $\sigma$ -type imidoyl radical **43** after the loss of  $\text{Bu}_3\text{SnSH}$ . Further radical cyclization of the C-radical intermediate furnishes 2,3-disubstituted indoles **41**. This method has been successfully applied to the synthesis of indole alkaloids, such as catharanthine [23], vinblastine [24, 25], and strychnine [26]. Recently, Wang and coworkers reported that Lewis base–boryl radicals ( $\text{LB-BH}_2\cdot$ ) generated from  $\text{LB-BH}_3$  also promoted the desulfurizative cyclization of thioamides **45**, leading to the formation of various N-heterocycles **46** (Scheme 6.11) [27].

Building on the early work of the groups of Kanaoka and Machida on the photochemical reactions of thioamides [28], Padwa and coworkers studied the intramolec-

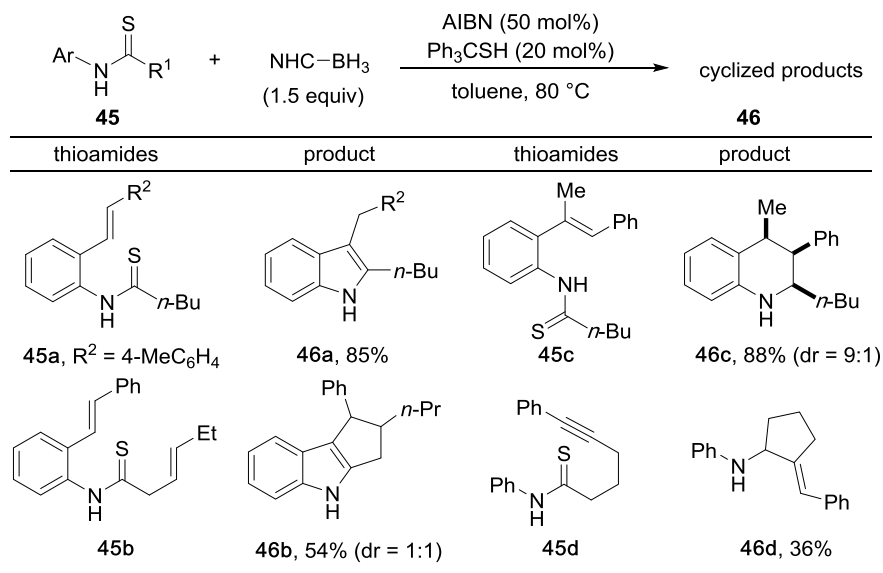


**Scheme 6.10** Synthesis of 2,3-disubstituted indoles via radical cyclization of 2-alkenylthioamides

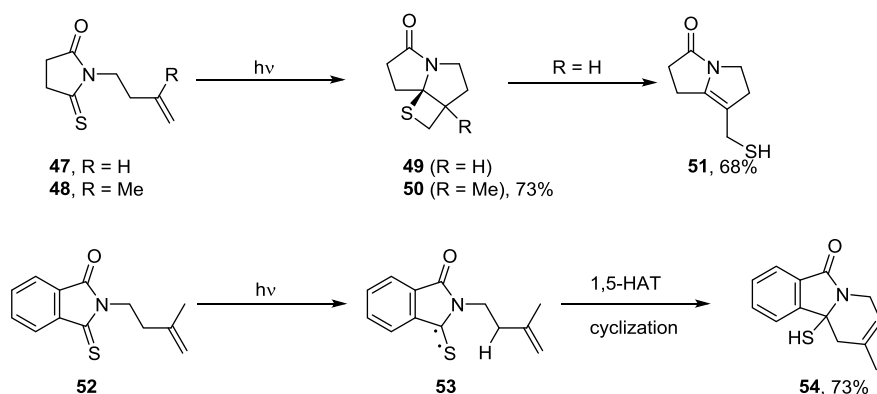
ular photochemical reactions of *N*-alkenyl-substituted thioamides. The thioxopyrrolidinones **47** and **48** underwent intramolecular [2+2]-photocycloaddition to afford spirocyclic heterocycles **49** and **50**, respectively. **49** undergoes further ring opening to furnish fused pyrrolizinone **51**. In contrast, irradiation of **52** afforded **54**, which was derived from hydrogen atom transfer (HAT) from the  $n-\pi^*$  triplet excited state **53** (Scheme 6.12) [29, 30].

Ethyl 2-(3-aryl-3-oxopropanethioamido)acetates **55** are converted into ketene-*N,S*-acetals **56** in good yields by the treatment with alkyl iodide in the presence of  $\text{K}_2\text{CO}_3$  in acetone. The reactions of **56** under Vilsmeier–Haack conditions afford smoothly the tetrasubstituted pyrrole derivatives **57** in excellent yields (Scheme 6.13) [31]. The reaction is proposed to proceed through sequential C- and O-iminoalkylations to afford the intermediate **58**. Reaction of **58** with chloride ion affords vinyl chloride **59**, which cyclizes to give iminium salt **60**. Hydrolysis of **60** affords the final pyrrole **57**.



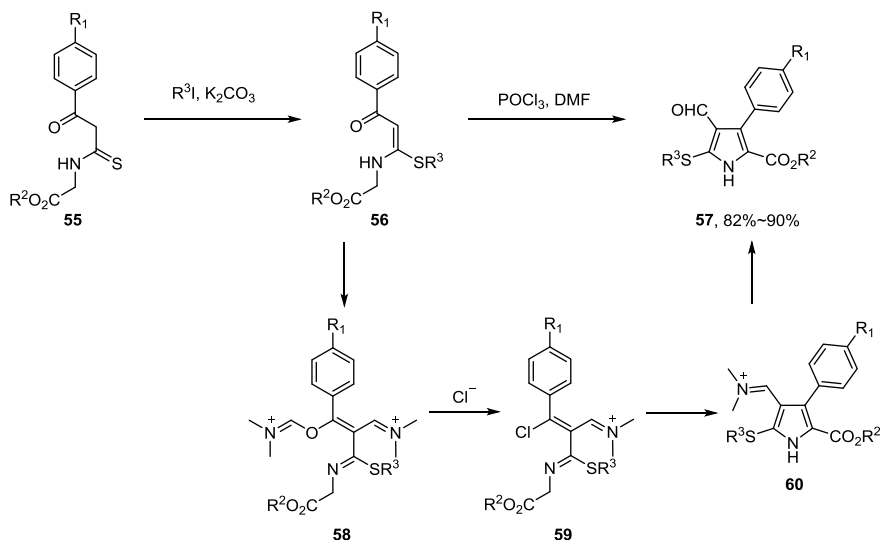
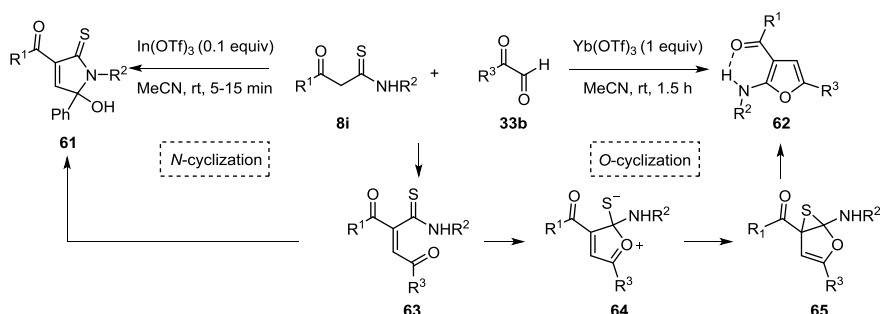


**Scheme 6.11** NHC-BH<sub>3</sub>-mediated intramolecular cyclization of thioamides



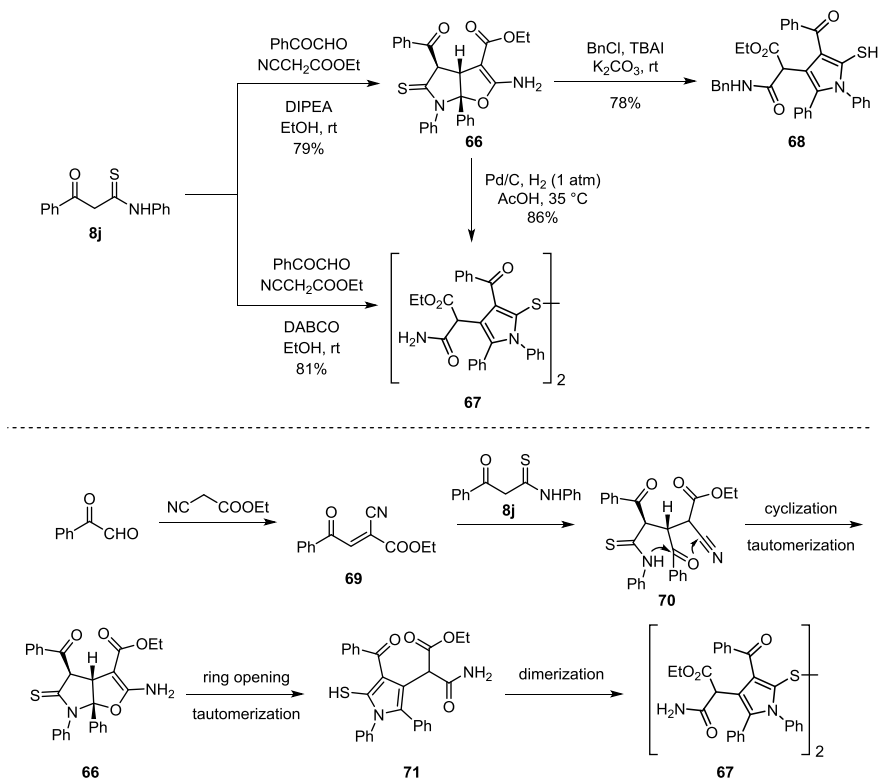
**Scheme 6.12** Intramolecular photocycloaddition of *N*-alkenyl-substituted thioamides

The reaction of secondary  $\beta$ -kethioamides **8i** with arylglyoxal **33b** in the presence of a catalytic amount of In(OTf)<sub>3</sub> afforded in 5–15 min pyrrol-2-thiones **61** with good yields [32]. In contrast, the reactions with 1 equiv of Yb(OTf)<sub>3</sub> and longer reaction time furnished 2-aminofurans **62** (Scheme 6.14) [33]. Primary and tertiary  $\beta$ -kethioamides are not suitable substrates for the latter reactions. Mechanistically, the two substrates **8i** and **33b** undergo condensation and N-cyclization via the intermediate **63** to afford the kinetic product **61**. Compound **61** opens up in the presence

**Scheme 6.13** Synthesis of tetrasubstituted pyrroles**Scheme 6.14** Lewis acid-promoted annulations of  $\beta$ -ketothioamides with phenylglyoxals

of  $Yb(OTf)_3$  to give back **63**, which undergoes *O*-cyclization and desulfurization via intermediates **64** and **65** to afford the furan product **62**.

In a three-component reaction of  $\beta$ -ketothioamides **8j**, glyoxals, and ethyl cyanoacetate, a series of furo[2,3-*b*]pyrrole derivatives **66** are obtained in moderate to good yields when *N*-ethyldiisopropylamine (DIPEA) is used as the base (Scheme 6.15) [34]. The bicyclic heterocycle **66** can be converted to disulfide **67** when treated with  $Pd/C$  under  $H_2$  atmosphere or to mercaptopyrrole **68** by reaction with  $BnCl$ . The disulfide is also formed directly from the three-component coupling when 1,4-diazabicyclo[2.2.2]octane (DABCO) is employed as the base under air [35]. Mechanistically, Michael addition of **8j** onto  $\alpha,\beta$ -unsaturated ketone **69**, which is derived from the condensation of phenylglyoxal with ethyl cyanoacetate, affords **70**. Biscyclization of **70** followed by tautomerization furnishes **66**. Ring opening

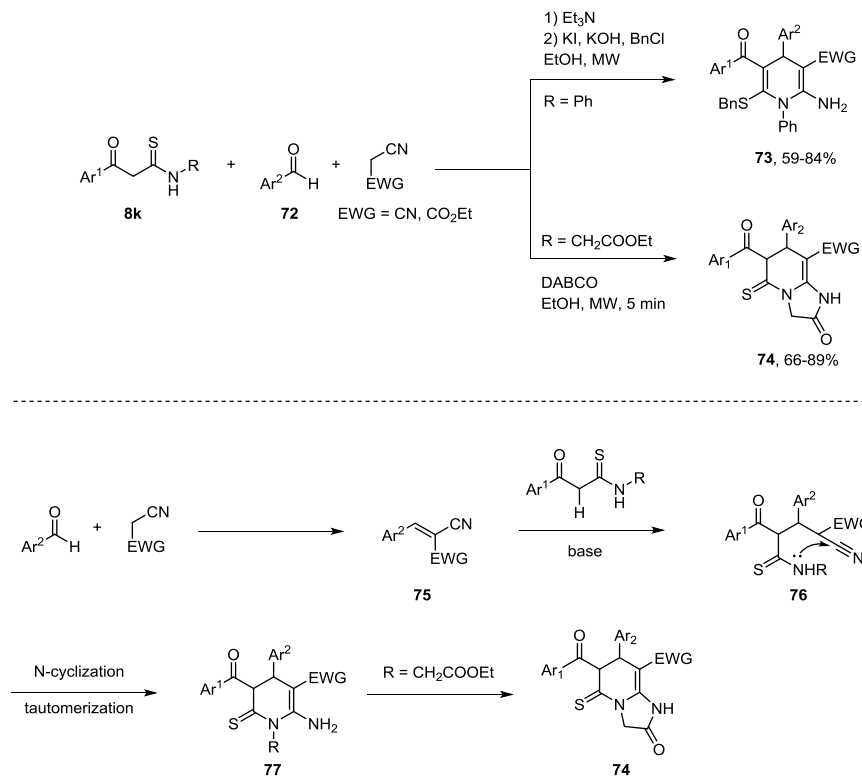
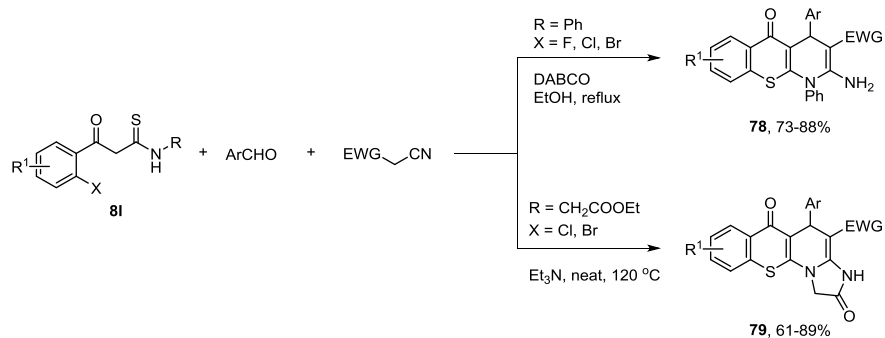


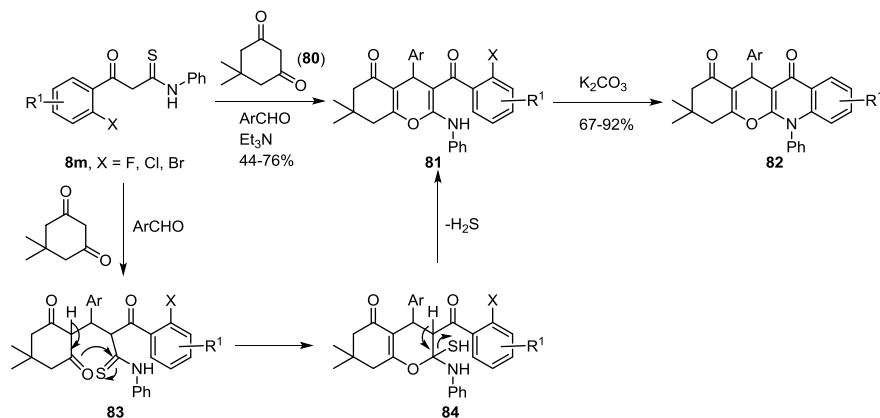
**Scheme 6.15** Three-component reaction of  $\beta$ -ketothioamides, phenylglyoxals, and 2-cyanoacetates

of the O-heterocyclic ring followed by tautomerization gives **71**, which undergoes oxidative dimerization to afford disulfide **67**.

The microwave-assisted three-component reaction of  $\beta$ -ketothioamides **8k**, aldehydes **72**, and malononitrile or ethyl cyanoacetate via a one-pot two-step process afforded hexasubstituted 1,4-dihydropyridine scaffolds **73**. The reaction mechanism involves Knoevenagel condensation of the aldehyde and nitrile to give **75**, which undergoes Michael addition with **8k** to afford **76**. Cyclization and tautomerization furnish **77**, which are alkylated with BnCl in the second step to afford the final product **73** (Scheme 6.16) [36]. Moreover, when  $\beta$ -ketothioamides bearing an ester group on the nitrogen atom were employed, bicyclic N-heterocycles **74** were afforded through further intramolecular cyclization of **77** [37].

$\beta$ -Ketothioamides **8l** bearing an aryl halide ring reacted with arylaldehydes and acetonitriles that contain an electron-withdrawing group at the  $\alpha$ -position to afford polycyclic heterocycles **78** and **79** through intramolecular S<sub>N</sub>Ar reaction of the thio-carbonyl with the aryl halide moiety (Scheme 6.17) [38–41].  $\beta$ -Ketonitriles can be replaced with Meldrum's acid to form similar tricyclic heterocycles [42]. The use

**Scheme 6.16** Synthesis of 1,4-dihydropyridine via three-component reactions**Scheme 6.17** Three-component synthesis of thiochromeno[2,3-*b*]pyridines



**Scheme 6.18** Three-component synthesis of chromeno-[2,3-*b*]quinoline

of 5,5-dimethyl-1,3-cyclohexanedione **80**, on the other hand, afforded desulfurized tetrahydrobenzo[*b*]pyrans **81** with Et<sub>3</sub>N as the base (Scheme 6.18) [43]. Further intramolecular S<sub>N</sub>Ar reaction of **81** promoted by K<sub>2</sub>CO<sub>3</sub> furnished the tetracyclic chromeno-[2,3-*b*]quinoline frameworks **82**. The three-component coupling reaction initially affords **83**, which undergoes intramolecular addition onto the thiocarbonyl to furnish **84**. Elimination of H<sub>2</sub>S from **84** produces the O-heterocycle **81**.

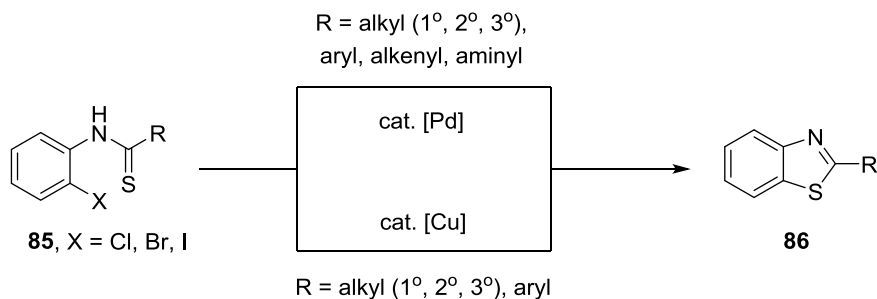
## 6.3 Heterocycles with Two Heteroatoms

### 6.3.1 *S,N*-Heterocycles

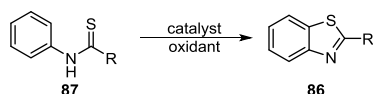
The benzothiazole scaffold is prevalent in bioactive compounds including commercial drugs such as dercitin, stelletamine, and kuanoniamine [44]. Among various approaches to synthesize benzothiazoles, the condensation of *o*-aminothiophenols with aldehydes, nitriles, carboxylic acids, esters, and acyl chlorides has been extensively studied [45]. While these methods provided efficient access to the targeted benzothiazoles, limited availability of the starting *o*-aminothiophenols makes the development of alternative methods necessary.

Transition metal-catalyzed cyclization of *o*-halothiobenzanilide derivatives **85** has been developed for the synthesis of 2-substituted benzothiazoles **86** (Scheme 6.19) [46–52].

The oxidative cyclization of *N*-aryl thioamides **87** is an attractive method for the synthesis of benzothiazoles because prefunctionalization of the substrate is unnecessary (Scheme 6.20). The pioneering work of synthesizing benzothiazoles via oxidative cyclization of thiobenzanilides dates to 1886 when Jacobson reported the cyclization using potassium ferricyanide as the oxidant [53]. Later in 1901, Hugershoff



**Scheme 6.19** Transition metal-catalyzed cyclization of *o*-halothiobenzanilide



Entry	Catalyst	Oxidant	R	Ref.
1	-	Dess-Martin periodinane	aryl	56, 57
2	-	DDQ	aryl	58, 59
3	-	CAN	aryl	57
4	-	Mn(OAc) <sub>3</sub>	aryl, benzoyl	60
5	-	DABCO tribromide	aryl	61
6	-	NBS	aryl	62
7	-	chloranil	<sup>t</sup> Bu, aryl	63
8	-	AIBN	aryl	64
9	FeCl <sub>3</sub>	Na <sub>2</sub> S <sub>2</sub> O <sub>8</sub>	<sup>t</sup> Bu, Bn, aryl, aminyl	65
10	aryl iodide	oxone	alkyl (1°, 2°, 3°), aryl	66
11	[Pd]	CuI	aryl, aminyl	67
12	PdCl <sub>2</sub>	O <sub>2</sub>	aryl, aminyl	68
13	Ru(bpy) <sub>3</sub> (PF <sub>6</sub> ) <sub>2</sub>	O <sub>2</sub>	aryl	69
14	Ru(bpy) <sub>3</sub> (PF <sub>6</sub> ) <sub>2</sub> / Co <sup>III</sup> (dmgH) <sub>2</sub> PyCl	-	alkyl (2°, 3°), aryl	72

**Scheme 6.20** Oxidative annulation of *N*-aryl thioamides to prepare benzothiazoles

achieved similar cyclizations with bromine as the oxidant [54, 55]. Building on these pioneering works, many other chemical oxidants have been found to promote these cyclization reactions including Dess–Martin periodinane [56, 57], DDQ [58, 59], CAN [57], Mn(OAc)<sub>3</sub> [60], DABCO tribromide [61], NBS [62], chloranil [63], and AIBN [64]. Conditions that employ a catalyst and a terminal oxidant have also been reported. For example, in 2012, Lei and coworkers reported that the combination of a catalytic amount of FeCl<sub>3</sub> and a stoichiometric Na<sub>2</sub>S<sub>2</sub>O<sub>8</sub> promotes efficiently the cyclization of *N*-aryl thioamides and thioureas [65]. In 2014, Punniyamurthy and coworkers reported a metal-free method employing aryl iodide as catalyst and oxone as the terminal oxidant to promote the cyclization of thioamides [66]. Both 2-aryl- and 2-alkyl-substituted benzothiazoles are accessible under these conditions.

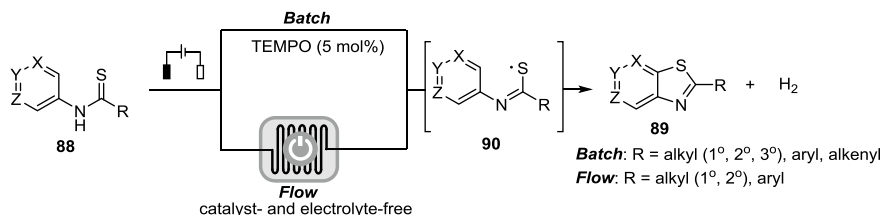
Oxygen is a green oxidant because water is usually generated as the by-product. In 2008, Doi and coworkers reported the synthesis of 2-aryl-substituted benzothiazoles

via Pd-catalyzed C–S bond formation process in the presence of 0.5 equiv of CuI and 2 equiv of Bu<sub>4</sub>NBr [67]. In 2010, the same research group reported that CuI could be replaced by oxygen as the terminal oxidant [68]. Under these conditions, the reactions are suitable for the synthesis of 2-aryl- and 2-aminobenzothiazoles. In 2012, Li and coworkers reported a visible light-promoted cyclization using Ru-based photocatalyst under aerobic conditions for the synthesis of 2-aryl-substituted benzothiazoles [69]. It is important to use a low concentration of oxygen (5%) to avoid desulfurization of the thioamide, which is a common side reaction for the oxidative cyclization of thioamides.

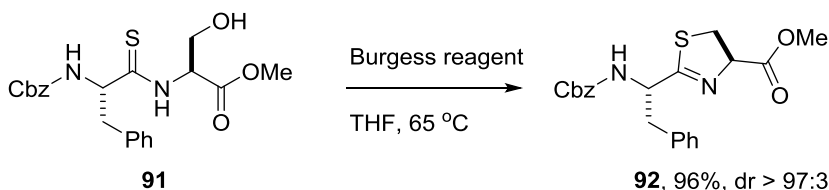
The use of stoichiometric chemical oxidants in organic synthesis creates potential safety hazards for large-scale production and often imposes a considerable amount of waste on the environment. In addition, the use of chemical oxidants reduces functional group compatibility. An ideal approach for the dehydrogenative reactions is through H<sub>2</sub> evolution, which obviates the need for chemical oxidants and proton acceptors [70, 71]. In this context, Lei and Wu reported an elegant oxidant-free photochemical cyclization of *N*-aryl thioamides, employing Ru(bpy)<sub>3</sub><sup>3+</sup> as the photocatalyst and Co<sup>III</sup>(dmgH)<sub>2</sub>PyCl as a proton-reduction catalyst [72]. Hydrogen gas is generated as the only theoretical by-product. Despite these significant advances, 2-alkyl-substituted benzothiazoles and thiazolopyridines remain difficult to access probably because the corresponding thioamides are usually prone to desulfurization.

Organic electrochemistry, which employs electric current to promote oxidation and reduction reactions, is a green and enabling synthetic tool [73, 74]. The combination of anodic oxidation and cathodic proton reduction provides a general approach for achieving dehydrogenative reactions through H<sub>2</sub> evolution. Electrooxidative cyclization of thiobenzanilides to prepare benzothiazoles was first reported in 1974 by Tabaković et al. [75, 76]. Notably, both 2-aryl- and 2-alkyl-substituted benzothiazoles are accessible by this method. However, a divided cell and high electrode potential (1.5–1.8 V) are needed. Recently, Xu and coworkers reported an electrochemical method for cyclization of *N*-aryl thioamides **88**, employing 2,2,6,6-tetramethylpiperidine-*N*-oxyl radical (TEMPO,  $E_{p/2} = 0.62$  V vs. SCE) as the redox catalyst (Scheme 6.21) [77]. These reactions are conducted conveniently in an undivided cell and provide efficient access to a host of benzothiazoles and thiazolopyridines bearing 2-aryl or 2-alkyl substituents. Under these electrochemical conditions, the reactions proceed through the cyclization of a thioamide radical **90** to form the C–S bond. At almost the same time, Lei et al. [78] disclosed an electrochemical cyclization of thioureas and thioamides using direct electrolysis. These conditions provide efficient access to 2-amino-, 2-aryl-, and 2-tertiary alkyl-substituted benzothiazoles. *N*-phenyl cyclohexylthioamide afforded a low yield of 20%.

Thiazoline scaffold exists in many cyclopeptide alkaloids [79–82]. Intramolecular cyclodehydration of hydroxythioamide is an efficient way to construct the thiazoline ring. This transformation can be achieved using diethylaminosulfur trifluoride (DAST), TsCl/Et<sub>3</sub>N, SOCl<sub>2</sub> as well as under Mitsunobu conditions [82–85]. However, many of these conditions cause epimerization at the  $\alpha$ -position of the thioamide [80]. The use of Burgess reagent allows the reactions to proceed under neutral conditions with minimum epimerization as illustrated with the stereoselective cyclization



**Scheme 6.21** Electrochemical synthesis of benzothiazoles



**Scheme 6.22** Synthesis of thiazoline via intramolecular cyclization of hydroxythioamide

of **91** (Scheme 6.22) [79–82, 86]. The protocol has been utilized in total synthesis of lissoclinamide **7** [81] and yersiniabactin [79]. The cyclodehydration of hydroxy thioamides is also applicable to the synthesis of larger heterocycles 5,6-dihydro-4*H*-[1, 3]thiazines [87, 88].

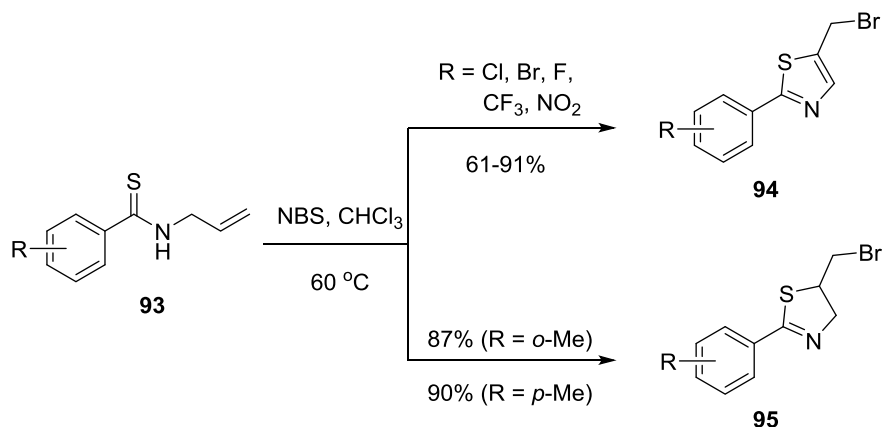
The cyclization of *N*-allylthioamides to thiazolines has been achieved using electrophilic halogenation reagents (Scheme 6.23). Interestingly, cyclization of *N*-allylbenzothioamides **93** in the presence of NBS provides either 5-(bromomethyl)thiazoles **94** or thiazolines **95**, depending on the phenyl substituents [89]. While thiazolines are obtained from the substrates bearing electron-donating groups, substrates bearing electron-withdrawing groups reacted to give thiazoles. The reaction of *N*-allylthioamides **96** with  $\text{PhI}(\text{OAc})_2$  and  $\text{Ts}_2\text{NH}$  afforded thioamination product **97** (Scheme 6.24) [90]. Mechanistically, these cyclization reactions generally proceed through activation of the alkene with the electrophilic halogen reagents, followed by the nucleophilic cyclization with the thioamide moiety.

In 2015, Nicewicz and coworkers reported the synthesis of thiazolines via photoredox-catalyzed cyclization of *N*-allylthioamides employing the Fukuzumi catalyst, 9-mesityl-*N*-methylacridinium salt ( $\text{MesAcrBF}_4$ ) (Scheme 6.25) [91]. The reactions are proposed to proceed through thioamidyl radical cyclization onto the alkene to form the new C–S bond.

The reaction of 2-chloro-2-cyclopropylideneacetates **98** with thioamides **99** afforded 5-spirocyclopropane-annulated thiazoline-4-carboxylates **100** [92]. The reaction involves Michael addition and nucleophilic substitution via the intermediate **101** (Scheme 6.26).

Phosphine-catalyzed intermolecular annulation of 2-alkynoates **102** with thioamides **99** affords thiazolines **103** (Scheme 6.27) [93]. The reaction of alkynoate bearing a Me at  $\text{R}^1$  position afforded a mixture of stereo- and regioisomers.

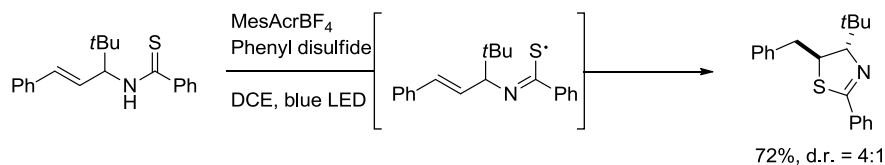




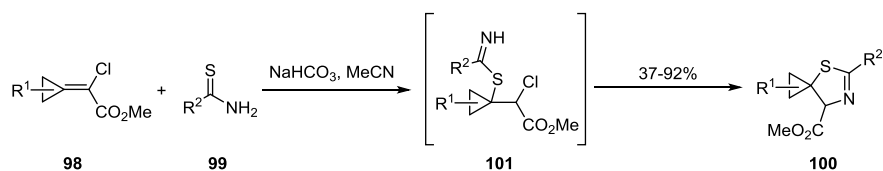
**Scheme 6.23** Cyclization of *N*-allylthioamides with NBS



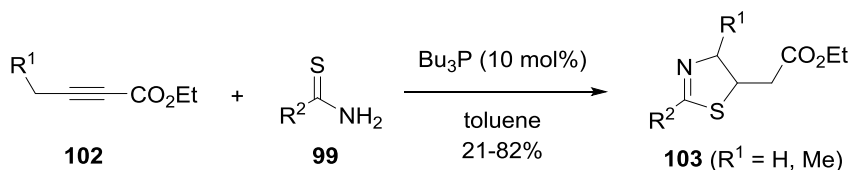
**Scheme 6.24** Cyclization of *N*-allylthioamides with  $\text{Ts}_2\text{NH}$



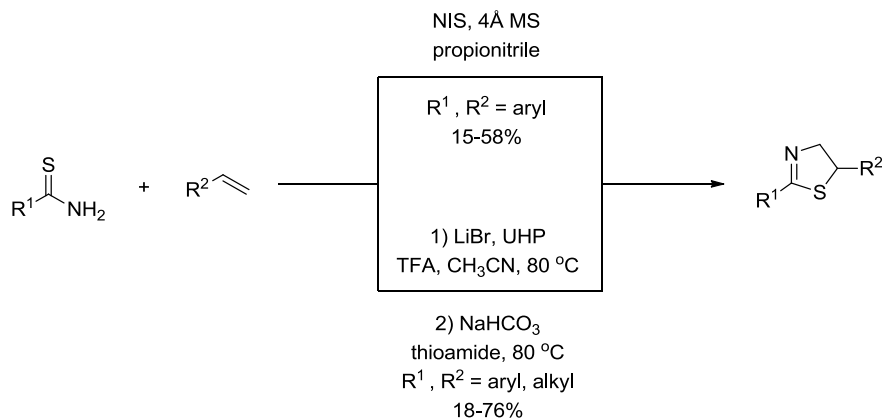
**Scheme 6.25** Photoredox-catalyzed cyclization of *N*-allylthioamides



**Scheme 6.26** Annulation of 2-chloro-2-cyclopropylideneacetates with thioamides



**Scheme 6.27** Phosphine-catalyzed annulation of 2-alkynoates with thioamides

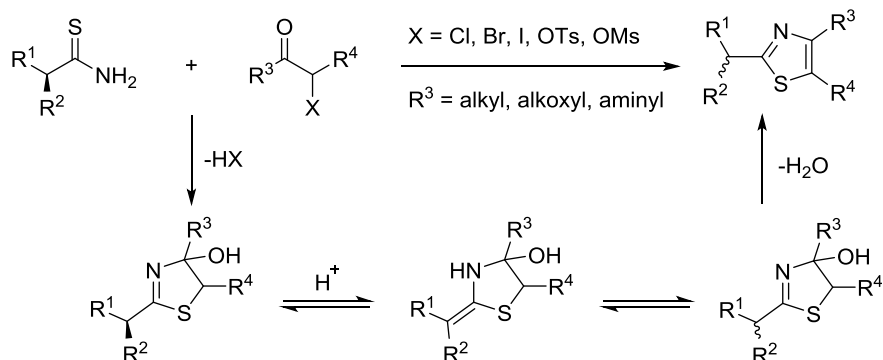


**Scheme 6.28** Annulation of thioamides with alkenes

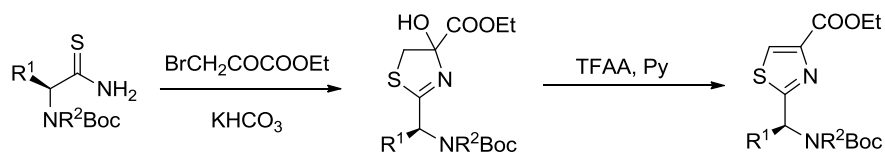
Thiazolines are also prepared by the annulation of thioamides with styrenyl alkenes and in an isolated example with tri-*O*-benzyl-D-glucal in the presence of *N*-iodo-succinimide (NIS) (Scheme 6.28) [94, 95]. Under these conditions, alkyl alkenes are not suitable for the annulation reaction. This limitation has been overcome by a two-step, one-pot protocol involving alkene dibromination using in situ generated Br<sub>2</sub> from LiBr and urea hydrogen peroxide (UHP), followed by base-promoted annulation with thioamide [96]. While styrenyl alkenes reacted with good regioselectivity, a mixture of regioisomers was usually formed using electron-deficient or alkyl alkenes.

The Hantzsch condensation of  $\alpha$ -haloketones with thioamides is among the most reliable methods for the synthesis of thiazoles (Scheme 6.29) [7, 97–112]. This method is now not limited to  $\alpha$ -halo ketones, and  $\alpha$ -halo amide [113, 114] and  $\alpha$ -halo esters [115–120] are also suitable substrates under modified conditions, leading to form 2-amino or 2-alkoxy thiazoles, respectively. The classic Hantzsch reaction generates one equivalent acid, which causes epimerization for amino acid-derived thioamides. The racemization problem has been addressed by the Holzapfel–Meyers–Nicolaou modification. Under the modified conditions, the reaction is carried out using a two-step procedure, involving condensation under basic conditions to form a hydroxythiazoline intermediate, followed by dehydration using trifluoroacetic anhydride and a pyridine base (Scheme 6.30) [7, 121–123]. In addition to the intermolecular reactions, intramolecular Hantzsch condensation has been reported for the synthesis of the macrocyclic compound IB-01211 (Scheme 6.31) [124, 125].

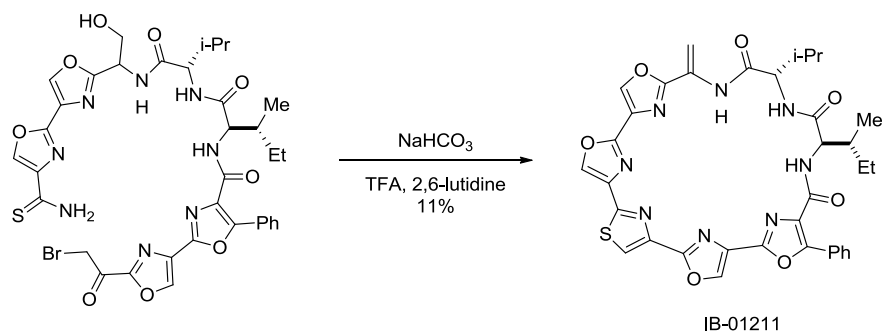
The condensation of thioamides with other two carbon donors has been developed for the synthesis of thiazoles. For example, the condensation with propargylic alcohols **105** has been reported by several research groups using acid catalysts to afford thiazoles **106** (Scheme 6.32) [126–129]. These reactions are proposed to proceed through a propargylic (**107**) or allenic (**108**) cation intermediate. The synthesis of thiazoles has also been achieved through the condensation of thioamides



**Scheme 6.29** Synthesis of thiazoles via Hantzsch condensation



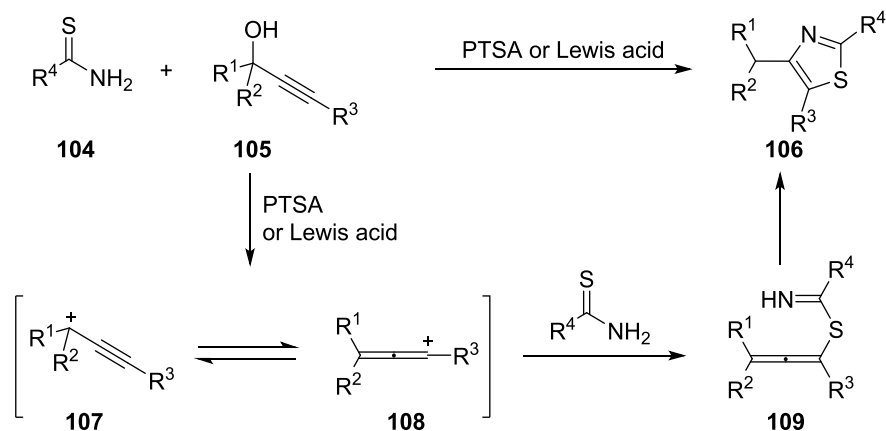
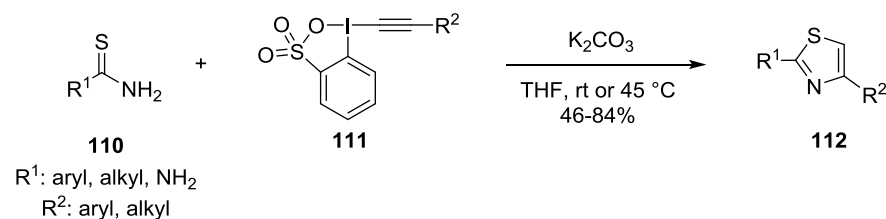
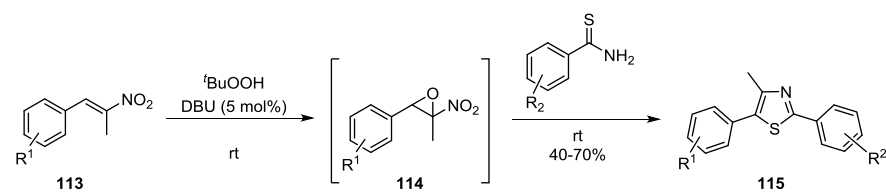
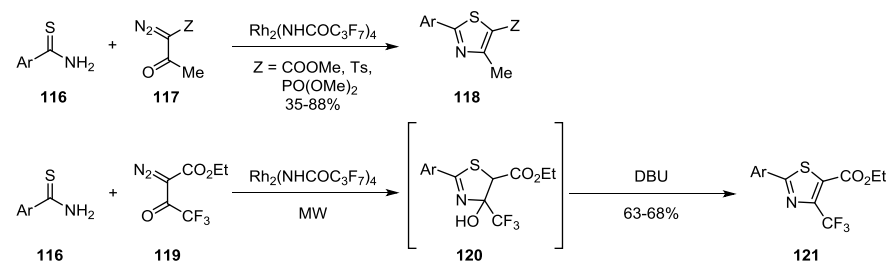
**Scheme 6.30** Synthesis of thiazoles via Holzzapfel–Meyers–Nicolaou modification

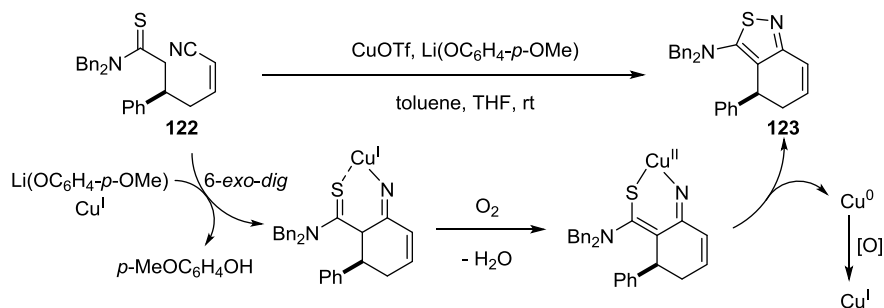


**Scheme 6.31** Synthesis of IB-01211

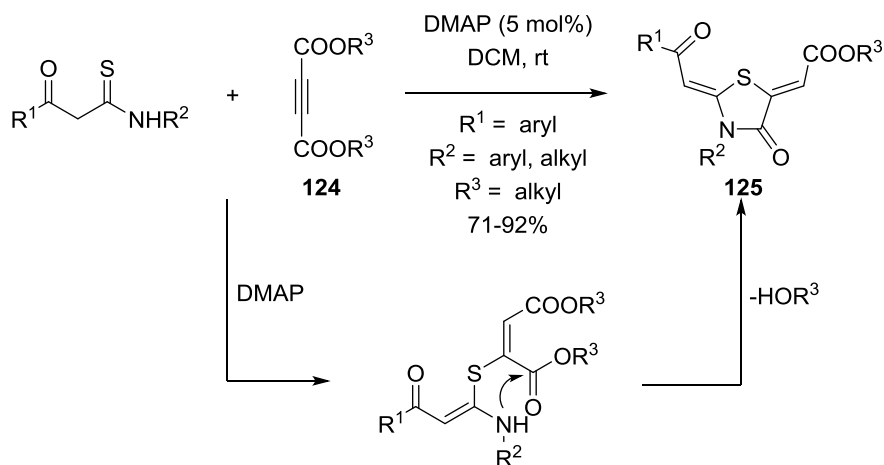
**110** with alkynylidonium reagents **111** (Scheme 6.33) [130, 131], or epoxide **114** formed in situ from nitro-olefins **113** with the *t*-BuOOH/DBU (Scheme 6.34) [132]. Rh-catalyzed coupling of arylthioamides **116** with  $\alpha$ -diazocarbonyl compounds **117** under microwave irradiation or heating led to the formation of thiazole-5-carboxylates, thiazole-5-phosphonates, and thiazole-5-sulfones **118** [133]. This protocol has later been extended to the synthesis of trifluoromethylthiazoles **121** from diazo compounds **119** (Scheme 6.35) [134].

In 2011, Kumagai and Shibasaki and coworkers reported Cu-catalyzed asymmetric conjugate addition of allyl cyanide to  $\alpha,\beta$ -unsaturated thioamides. The resulting thioamides **122** underwent Cu-catalyzed aerobic [3+2] annulation to form isothia-

**Scheme 6.32** Synthesis of thiazoles from propargylic alcohols**Scheme 6.33** Synthesis of thiazoles from alkynyl iodonium reagents**Scheme 6.34** Synthesis of thiazoles from nitro-olefins**Scheme 6.35** Rh-catalyzed cyclization of arylthioamides with  $\alpha$ -diazocarbonyl compounds



**Scheme 6.36** Cu-catalyzed [3+2] cycloaddition to form isothiazoles



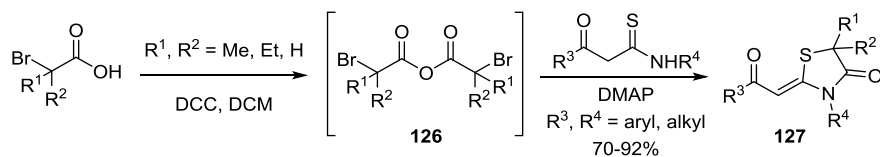
**Scheme 6.37** Cycloaddition of  $\beta$ -ketothioamides with electron-deficient alkynes

zoles **123** (Scheme 6.36) [135]. In the latter reaction, Cu plays dual roles as a soft Lewis acid and a redox catalyst to forge the C–C and S–N bonds.

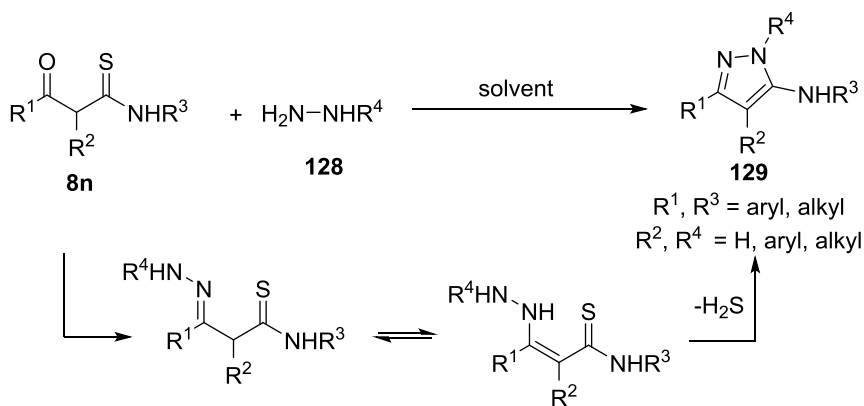
1,3-Thiazolidin-4-ones are prepared through DMAP-catalyzed annulation of  $\beta$ -ketothioamides with biselectrophiles such as electron-deficient alkynes **124** (Scheme 6.37) or  $\alpha$ -halocarboxylic anhydrides **126** generated in situ from the corresponding carboxylic acids (Scheme 6.38) [136–139]. Both reactions were proposed to form the C–S bond first between the thioamide and the biselectrophile and then the C–N bond via intramolecular cyclization.

### 6.3.2 *N,N*-Heterocycles

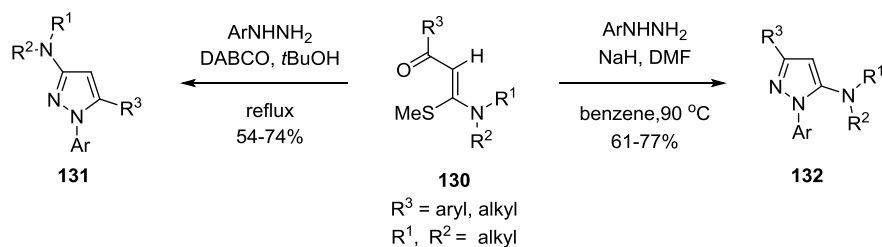
The cyclocondensation of  $\beta$ -ketothioamides **8n** with hydrazines **128** affords 5-aminopyrazole derivatives **129** (Scheme 6.39) [140–144]. When  $\alpha$ -oxoketene N,S-



**Scheme 6.38** Cycloaddition of  $\beta$ -kethioamides with  $\alpha$ -halocarboxylic anhydride



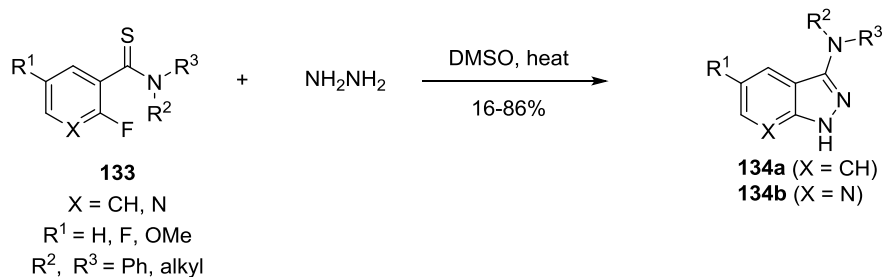
**Scheme 6.39** Synthesis of pyrazoles via cyclocondensation of hydrazines with  $\beta$ -kethioamides



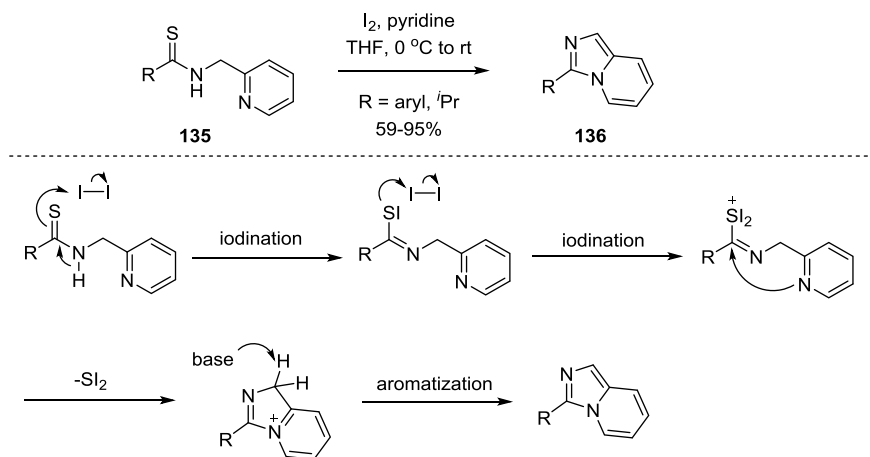
**Scheme 6.40** Base-controlled cyclization of hydrazines with  $\beta$ -kethioamides

acetals **130** are used as substrates, both 3-aminopyrazoles **131** and 5-aminopyrazoles **132** can be obtained selectively depending on the base employed (Scheme 6.40) [144]. In addition, the *o*-fluoroaryl thioamides **133** undergo cyclization with hydrazine to afford 3-aminoindazoles **134a** and 3-amino-7-azaindazoles **134b** (Scheme 6.41) [140].

2-Azaindolizines **136** are rapidly generated in high yields via iodine-promoted intramolecular cyclization of *N*-pyridylmethylthioamides **135** [145]. A plausible mechanism proposed by the authors involves double iodination of the thioamide, followed by nucleophilic substitution and aromatization (Scheme 6.42).



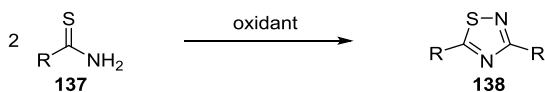
**Scheme 6.41** Cyclization of *o*-fluoro aryl thioamides with hydrazine



**Scheme 6.42** Synthesis of 2-azaindolines from *N*-pyridylmethylthioamide

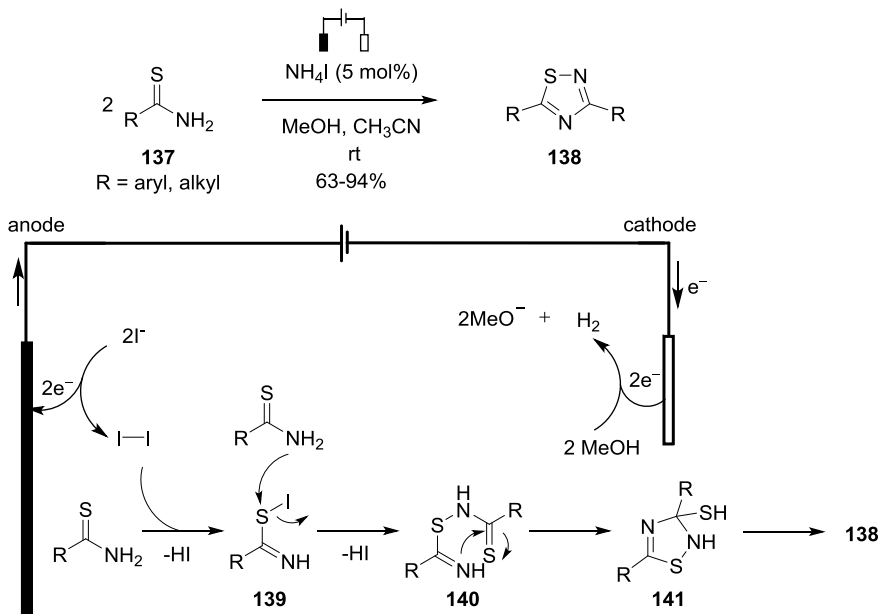
## 6.4 Heterocycles with Three Heteroatoms

Oxidative dimerization of primary thioamides **137** affords 3,5-disubstituted 1,2,4-thiadiazoles **138** (Scheme 6.43). A variety of oxidants have been employed to promote this transformation, including hypervalent iodines [146–149], I<sub>2</sub>/O<sub>2</sub> [150], copper salt [151], DDQ [152], H<sub>6</sub>PV<sub>3</sub>Mo<sub>9</sub>O<sub>40</sub> [153], CAN [154], oxone [155], eosin Y/air [156], tribromide salt [157, 158], and DMSO in combination of electrophilic reagents [159–161]. Electrochemistry has also been shown to promote this transformation using NH<sub>4</sub>I as the redox mediator (Scheme 6.44) [162]. No oxidizing reagents are needed under the electrochemical conditions. Under these conditions, iodide is oxidized at the anode to generate I<sub>2</sub>, which reacts with the thioamide to give intermediate **139**. Nucleophilic substitution by another thioamide molecule followed by cyclization affords intermediate **141**, which loses one molecule of H<sub>2</sub>S to give the final thiadiazole.



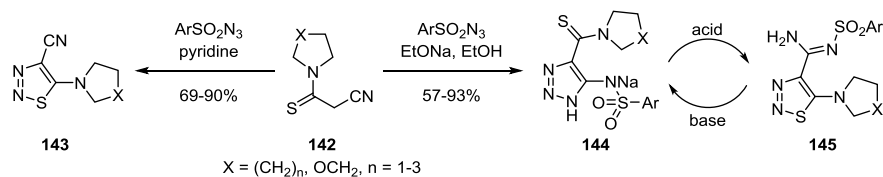
Entry	Oxidant	R	Ref.
1	hypervalent iodines	aryl, alkyl	146-149
2	I <sub>2</sub> /O <sub>2</sub>	aryl, alkyl, aminyl	150
3	Cu(OTf) <sub>2</sub>	aryl, alkyl, aminyl	151
4	DDQ	aryl, alkyl	152
5	H <sub>6</sub> PV <sub>3</sub> Mo <sub>9</sub> O <sub>40</sub>	aryl, alkyl	153
6	CAN	aryl, alkyl	154
7	oxone	aryl, alkyl	155
8	eosin Y/air	aryl, alkyl	156
9	tribromide salt	aryl	157, 158
10	DMSO-electrophilic reagents	aryl	159-161

**Scheme 6.43** Synthesis of 1,2,4-thiadiazoles via oxidative dimerization of thioamides

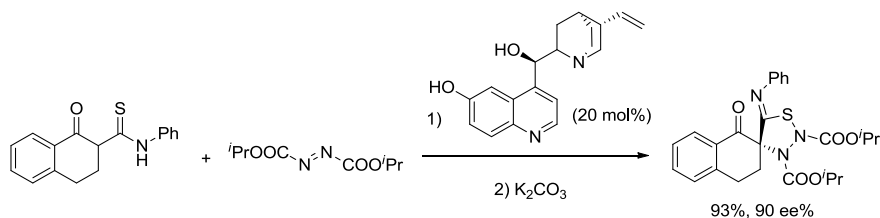


**Scheme 6.44** Electrochemical synthesis of 1,2,4-thiadiazoles via dimerization of thioamides

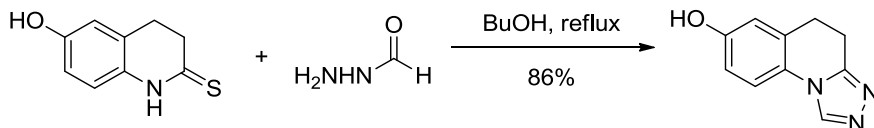




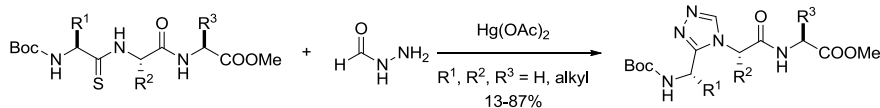
**Scheme 6.45** Synthesis of 1,2,3-thiadiazoles from 2-cyanothioacetamide and sulfonyl azides



**Scheme 6.46** Synthesis of optically active spiroannulated 1,2,3-thiadiazoles



**Scheme 6.47** Synthesis of 1,2,4-triazole from thioamides and acylhydrazines



**Scheme 6.48** Construction of 1,2,4-triazole core with thiopeptide

The reaction of 2-cyanothioacetamides **142** with sulfonyl azides in pyridine affords 4,5-functionalized 1,2,3-thiadiazoles **143** (Scheme 6.45). In contrast, the reaction in the presence of NaOEt in EtOH furnished 1,2,3-triazoles **144** as the products. **144** can be converted to 5-amino-1,2,3-thiadiazole-4-carboximidamides **145** under acidic conditions. Under basic conditions, **145** can be transformed back to **144** [163].

Under aerobic conditions, the organocatalytic [3+2] annulation of  $\beta$ -keto thioamides with azodicarboxylates furnishes 1,2,3-thiadiazole derivatives in high yields and high enantioselectivities (Scheme 6.46) [164].

The cyclocondensation of thioamides or S-alkyl thioimide with acylhydrazines at high temperatures yields 1,2,4-triazole derivatives (Scheme 6.47) [165–172]. In the presence of mercury(II) acetate [173, 174] or silver benzoate [175], the reactions proceed at room temperature and are compatible with thiopeptide as substrates (Scheme 6.48).

## 6.5 Summary

This chapter has summarized the synthetic applications of thioamides in the preparation of heterocycles published since 2000. The thioamide moiety is a versatile functional group and can participate in various transformations. Particularly, thioamides bearing an  $\alpha$ -electron-withdrawing group possess several nucleophilic and electrophilic centers, which make these compounds powerful building blocks for annulation reactions. Because of their versatile reactivities, thioamides have been extensively used for the synthesis of various N-, O-, and S-heterocycles through cyclization or annulation reactions. In recent years, radical reactions of thioamides have been attracting increasing interests and this direction deserves more investigation in the future. With the introduction of greener and more efficient methods for the preparation of thioamides, the synthetic utility of thioamides is expected to be further expanded.

## References

1. D.K. Dalvie, A.S. Kalgutkar, S.C. Khojasteh-Bakht, R.S. Obach, J.P. O'Donnell, *Chem. Res. Toxicol.* **15**, 269 (2002)
2. T. Eicher, S. Hauptmann, A. Speicher (eds.), *The Chemistry of Heterocycles* (Wiley-VCH, Weinheim, 2003)
3. Z. Jin, *Nat. Prod. Rep.* **26**, 382 (2009)
4. T.S. Jagodziński, *Chem. Rev.* **103**, 197 (2003)
5. V.N. Britsun, A.N. Esipenko, M.O. Lozinskii, *Chem. Heterocycl. Compd.* **44**, 1429 (2008)
6. W.-S. Guo, L.-R. Wen, M. Li, *Org. Biomol. Chem.* **13**, 1942 (2015)
7. E. Aguilar, A.I. Meyers, *Tetrahedron Lett.* **35**, 2473 (1994)
8. M. Hasegawa, A. Nakayama, S. Yokohama, T. Hosokami, Y. Kurebayashi, T. Ikeda, Y. Shimoto, S. Ide, Y. Honda, N. Suzuki, *Chem. Pharm. Bull.* **43**, 1125 (1995)
9. F. Matloubi Moghaddam, H. Zali Boinee, *Tetrahedron* **60**, 6085 (2004)
10. H.Z. Boeini, *Helv. Chim. Acta* **92**, 1268 (2009)
11. M.F. Mechelke, A.I. Meyers, *Tetrahedron Lett.* **41**, 4339 (2000)
12. C. Heyde, I. Zug, H. Hartmann, *Eur. J. Org. Chem.* **2000**, 3273 (2000)
13. L.K. Ransborg, Ł. Albrecht, C.F. Weise, J.R. Bak, K.A. Jørgensen, *Org. Lett.* **14**, 724 (2012)
14. X. Luo, L.-S. Ge, X.-L. An, J.-H. Jin, Y. Wang, P.-P. Sun, W.-P. Deng, *J. Org. Chem.* **80**, 4611 (2015)
15. G. Shukla, G.K. Verma, A. Nagaraju, R.K. Verma, K. Raghuvanshi, M.S. Singh, *RSC Adv.* **3**, 13811 (2013)
16. D. Yadav, G. Shukla, M.A. Ansari, A. Srivastava, M.S. Singh, *Tetrahedron* **74**, 5920 (2018)
17. Z.-L. Wang, H.-L. Li, L.-S. Ge, X.-L. An, Z.-G. Zhang, X. Luo, J.S. Fossey, W.-P. Deng, *J. Org. Chem.* **79**, 1156 (2014)
18. T. Han, X. Luo, *Org. Biomol. Chem.* **16**, 8253–8257 (2018)
19. T. Han, Y. Wang, H.-L. Li, X. Luo, W.-P. Deng, *J. Org. Chem.* **83**, 1538 (2018)
20. L.-R. Wen, T. He, M.-C. Lan, M. Li, *J. Org. Chem.* **78**, 10617 (2013)
21. X.-M. Zeng, C.-Y. Meng, J.-X. Bao, D.-C. Xu, J.-W. Xie, W.-D. Zhu, *J. Org. Chem.* **80**, 11521 (2015)
22. H. Tokuyama, T. Yamashita, M.T. Reding, Y. Kaburagi, T. Fukuyama, *J. Am. Chem. Soc.* **121**, 3791 (1999)
23. M.T. Reding, T. Fukuyama, *Org. Lett.* **1**, 973 (1999)

24. C. Schneider, *Angew. Chem. Int. Ed.* **41**, 4217 (2002)
25. S. Yokoshima, T. Ueda, S. Kobayashi, A. Sato, T. Kuboyama, H. Tokuyama, T. Fukuyama, J. Am. Chem. Soc. **124**, 2137 (2002)
26. Y. Kaburagi, H. Tokuyama, T. Fukuyama, J. Am. Chem. Soc. **126**, 10246 (2004)
27. Y.-J. Yu, F.-L. Zhang, J. Cheng, J.-H. Hei, W.-T. Deng, Y.-F. Wang, *Org. Lett.* **20**, 24 (2018)
28. M. Machida, K. Oda, E. Yoshida, Y. Kanaoka, *J. Org. Chem.* **50**, 1681 (1985)
29. A. Padwa, M.N. Jacquez, A. Schmidt, *Org. Lett.* **3**, 1781 (2001)
30. A. Padwa, M.N. Jacquez, A. Schmidt, *J. Org. Chem.* **69**, 33 (2004)
31. P. Mathew, C.V. Asokan, *Tetrahedron* **62**, 1708 (2006)
32. G.K. Verma, G. Shukla, A. Nagaraju, A. Srivastava, M.S. Singh, *Tetrahedron Lett.* **55**, 5182 (2014)
33. M. Li, X.-J. Kong, L.-R. Wen, *J. Org. Chem.* **80**, 11999 (2015)
34. N.-N. Man, J.-Q. Wang, L.-M. Zhang, L.-R. Wen, M. Li, *J. Org. Chem.* **82**, 5566 (2017)
35. C.-X. Li, R.-J. Liu, K. Yin, L.-R. Wen, M. Li, *Org. Biomol. Chem.* **15**, 5820 (2017)
36. M. Li, Z. Zuo, L. Wen, S. Wang, *J. Comb. Chem.* **10**, 436 (2008)
37. M. Li, T. Li, K. Zhao, M. Wang, L. Wen, *Chin. J. Chem.* **31**, 1033 (2013)
38. L. Wen, C. Ji, Y. Li, M. Li, *J. Comb. Chem.* **11**, 799 (2009)
39. L.-R. Wen, Y.-J. Shi, G.-Y. Liu, M. Li, *J. Org. Chem.* **77**, 4252 (2012)
40. L.-R. Wen, J.-H. Sun, M. Li, E.-T. Sun, S.-S. Zhang, *J. Org. Chem.* **73**, 1852 (2008)
41. M. Li, H. Cao, Y. Wang, X.-L. Lv, L.-R. Wen, *Org. Lett.* **14**, 3470 (2012)
42. L.-R. Wen, C. Ji, M. Li, H.-Y. Xie, *Tetrahedron* **65**, 1287 (2009)
43. M. Li, Y.-L. Hou, L.-R. Wen, F.-M. Gong, *J. Org. Chem.* **75**, 8522 (2010)
44. G.P. Gunawardana, F.E. Koehn, A.Y. Lee, J. Clardy, H.Y. He, D.J. Faulkner, *J. Org. Chem.* **57**, 1523 (1992)
45. N.P. Prajapati, R.H. Vekariya, M.A. Borad, H.D. Patel, *RSC Adv.* **4**, 60176 (2014)
46. C. Benedí, F. Bravo, P. Uriz, E. Fernández, C. Claver, S. Castellón, *Tetrahedron Lett.* **44**, 6073 (2003)
47. M.D. Vera, J.C. Pelletier, *J. Comb. Chem.* **9**, 569 (2007)
48. Y. Cheng, Q. Peng, W. Fan, P. Li, *J. Org. Chem.* **79**, 5812–5819 (2014)
49. G. Evindar, R.A. Batey, *J. Org. Chem.* **71**, 1802 (2006)
50. E.A. Jaseer, D.J.C. Prasad, A. Dandapat, G. Sekar, *Tetrahedron Lett.* **51**, 5009 (2010)
51. H.C. Ma, X.Z. Jiang, *Synlett* **2008**, 1335 (2008)
52. J.H. Spatz, T. Bach, M. Umkehrer, J. Bardin, G. Ross, C. Burdack, J. Kolb, *Tetrahedron Lett.* **48**, 9030 (2007)
53. P. Jacobson, *Chem. Ber.* **19**, 1067 (1886)
54. A. Hugershoff, *Chem. Ber.* **34**, 3130 (1901)
55. A. Hugershoff, *Chem. Ber.* **36**, 3121 (1903)
56. D.S. Bose, M. Idrees, *J. Org. Chem.* **71**, 8261 (2006)
57. N.K. Downer-Riley, Y.A. Jackson, *Tetrahedron* **64**, 7741 (2008)
58. D.S. Bose, M. Idrees, *Tetrahedron Lett.* **48**, 669 (2007)
59. D.S. Bose, M. Idrees, B. Srikanth, *Synthesis* **2007**, 819 (2007)
60. X.-J. Mu, J.-P. Zou, R.-S. Zeng, J.-C. Wu, *Tetrahedron Lett.* **46**, 4345 (2005)
61. F. Matloubi Moghaddam, H. Zali Boeini, *Synlett* **2005**, 1612 (2005)
62. F.M. Moghaddam, D. Zargarani, *J. Sulfur Chem.* **30**, 507 (2009)
63. V. Rey, S.M. Soria-Castro, J.E. Argüello, A.B. Peññory, *Tetrahedron Lett.* **50**, 4720 (2009)
64. N.K. Downer, Y.A. Jackson, *Org. Biomol. Chem.* **2**, 3039 (2004)
65. H. Wang, L. Wang, J. Shang, X. Li, H. Wang, J. Gui, A. Lei, *Chem. Commun.* **48**, 76 (2012)
66. S.K. Alla, P. Sadhu, T. Punniyamurthy, *J. Org. Chem.* **79**, 7502 (2014)
67. K. Inamoto, C. Hasegawa, K. Hiroya, T. Doi, *Org. Lett.* **10**, 5147 (2008)
68. K. Inamoto, C. Hasegawa, J. Kawasaki, K. Hiroya, T. Doi, *Adv. Synth. Catal.* **352**, 2643 (2010)
69. Y. Cheng, J. Yang, Y. Qu, P. Li, *Org. Lett.* **14**, 98 (2012)
70. S. Tang, L. Zeng, A. Lei, *J. Am. Chem. Soc.* **140**, 13128 (2018)
71. S. Tang, Y. Liu, A. Lei, *Chem* **4**, 27 (2018)

72. G. Zhang, C. Liu, H. Yi, Q. Meng, C. Bian, H. Chen, J.-X. Jian, L.-Z. Wu, A. Lei, *J. Am. Chem. Soc.* **137**, 9273 (2015)
73. M. Yan, Y. Kawamata, P.S. Baran, *Chem. Rev.* **117**, 13230 (2017)
74. Y. Jiang, K. Xu, C. Zeng, *Chem. Rev.* **118**, 4485 (2018)
75. M. Laćan, K. Jakopčić, V. Rogić, S. Damoni, O. Rogić, I. Tabaković, *Synth. Commun.* **4**, 219 (1974)
76. I. Tabaković, M. Trkovnik, M. Batušić, K. Tabaković, *Synthesis* **1979**, 590 (1979)
77. X.-Y. Qian, S.-Q. Li, J. Song, H.-C. Xu, *ACS Catal.* **7**, 2730 (2017)
78. P. Wang, S. Tang, A. Lei, *Green Chem.* **19**, 2092 (2017)
79. A. Ino, A. Murabayashi, *Tetrahedron* **57**, 1897 (2001)
80. P. Wipf, P.C. Fritch, *Tetrahedron Lett.* **35**, 5397 (1994)
81. P. Wipf, P.C. Fritch, *J. Am. Chem. Soc.* **118**, 12358 (1996)
82. P. Wipf, C.P. Miller, *Tetrahedron Lett.* **33**, 6267 (1992)
83. N. Galéotti, C. Montagne, J. Poncet, P. Jouin, *Tetrahedron Lett.* **33**, 2807 (1992)
84. N. Leflemme, P. Marchand, M. Gulea, S. Masson, *Synthesis* **2000**, 1143 (2000)
85. Y. Tamaru, T. Hioki, S. Kawamura, H. Satomi, Z. Yoshida, *J. Am. Chem. Soc.* **106**, 3876 (1984)
86. P. Wipf, C.P. Miller, S. Venkatraman, P.C. Fritch, *Tetrahedron Lett.* **36**, 6395 (1995)
87. P. Wipf, G.B. Hayes, *Tetrahedron* **54**, 6987 (1998)
88. N. Leflemme, P. Dallemagne, S. Rault, *Tetrahedron Lett.* **45**, 1503 (2004)
89. W. Zhou, S. Ni, H. Mei, J. Han, Y. Pan, *Tetrahedron Lett.* **56**, 4128 (2015)
90. H. Jeon, D. Kim, J.H. Lee, J. Song, W.S. Lee, D.W. Kang, S. Kang, S.B. Lee, S. Choi, K.B. Hong, *Adv. Synth. Catal.* **360**, 779 (2018)
91. P.D. Morse, D.A. Nicewicz, *Chem. Sci.* **6**, 270 (2015)
92. M.W. Nötzel, T. Labahn, M. Es-Sayed, A. de Meijere, *Eur. J. Org. Chem.* **2001**, 3025 (2001)
93. B. Liu, R. Davis, B. Joshi, D.W. Reynolds, *J. Org. Chem.* **67**, 4595 (2002)
94. S.S. Gratia, E.S. Vigneau, S. Eltayeb, K. Patel, T.J. Meyerhoefer, S. Kershaw, V. Huang, M. De Castro, *Tetrahedron Lett.* **55**, 448 (2014)
95. E.M. Reid, E.S. Vigneau, S.S. Gratia, C.H. Marzabadi, M.D. Castro, *Eur. J. Org. Chem.* **2012**, 3295 (2012)
96. N.-E. Alom, F. Wu, W. Li, *Org. Lett.* **19**, 930 (2017)
97. A. Hantzsch, J.H. Weber, *Chem. Ber.* **20**, 3118 (1887)
98. N.P. Belskaya, S.G. Sapozhnikova, V.A. Bakulev, O.S. Eltsov, P.A. Slepukhin, Z.J. Fan, *Chem. Heterocycl. Compd.* **45**, 844 (2009)
99. M.W. Breidenkamp, C.W. Holzapfel, R.M. Snyman, W.J. van Zyl, *Synth. Commun.* **22**, 3029 (1992)
100. J.S. Carter, D.J. Rogier, M.J. Graneto, K. Seibert, C.M. Koboldt, Z. Yan, J.J. Talley, *Bioorg. Med. Chem. Lett.* **9**, 1167 (1999)
101. Q.-Y. Chen, P.R. Chaturvedi, H. Luesch, *Org. Process Res. Dev.* **22**, 190 (2018)
102. T.J. Donohoe, M.A. Kabeshov, A.H. Rathi, I.E.D. Smith, *Org. Biomol. Chem.* **10**, 1093 (2012)
103. J. Du, F. Qu, D.-W. Lee, M.G. Newton, C.K. Chu, *Tetrahedron Lett.* **36**, 8167 (1995)
104. C.W. Holzapfel, G.R. Pettit, *J. Org. Chem.* **50**, 2323 (1985)
105. R.C. Kelly, I. Gebhard, N. Wicnienski, *J. Org. Chem.* **51**, 4590 (1986)
106. P. Mathew, M. Prasadha, C.V. Asokan, *J. Heterocycl. Chem.* **47**, 430 (2010)
107. R.J. Mathvink, J.S. Tolman, D. Chitty, M.R. Candelore, M.A. Cascieri, L.F. Colwell, L. Deng, W.P. Feeney, M.J. Forrest, G.J. Hom, D.E. MacIntyre, L. Tota, M.J. Wyvratt, M.H. Fisher, A.E. Weber, *Bioorg. Med. Chem. Lett.* **10**, 1971 (2000)
108. D.S. Nielsen, H.N. Hoang, R.-J. Lohman, F. Diness, D.P. Fairlie, *Org. Lett.* **14**, 5720 (2012)
109. U. Schmidt, R. Utz, A. Lieberknecht, H. Griesser, B. Potzolli, J. Bahr, K. Wagner, P. Fischer, *Synthesis* **1987**, 233 (1987)
110. H. Takayama, K. Kato, H. Akita, *Eur. J. Org. Chem.* **2006**, 644 (2006)
111. A. Tsuruoka, Y. Kaku, H. Kakinuma, I. Tsukada, M. Yanagisawa, K. Nara, T. Naito, *Chem. Pharm. Bull.* **46**, 623 (1998)

112. K. Umemura, T. Tate, M. Yamaura, J. Yoshimura, Y. Yonezawa, C.-G. Shin, *Synthesis* **1995**, 1423 (1995)
113. O. Uchikawa, T. Aono, *J. Heterocycl. Chem.* **31**, 1545 (1994)
114. O. Uchikawa, K. Fukatsu, M. Suno, T. Aono, T. Doi, *Chem. Pharm. Bull.* **44**, 2070 (1996)
115. L.K. Calderón Ortiz, H. Würfel, E. Täuscher, D. Weiß, E. Birckner, H. Görls, R. Beckert, *Synthesis* **46**, 126 (2014)
116. F.A.J. Kerdesky, J.H. Holms, J.L. Moore, R.L. Bell, R.D. Dyer, G.W. Carter, D.W. Brooks, *J. Med. Chem.* **34**, 2158 (1991)
117. R. Menzel, S. Kupfer, R. Mede, D. Weiß, H. Görls, L. González, R. Beckert, *Eur. J. Org. Chem.* **2012**, 5231 (2012)
118. E. Täuscher, L. Calderón-Ortiz, D. Weiß, R. Beckert, H. Görls, *Synthesis* **2011**, 2334 (2011)
119. S.K. Kim, J.-H. Kim, Y.C. Park, J.W. Kim, E.K. Yum, *Tetrahedron* **69**, 10990 (2013)
120. A. Reichelt, J.M. Bailis, M.D. Bartberger, G. Yao, H. Shu, M.R. Kaller, J.G. Allen, M.F. Weidner, K.S. Keegan, J.H. Dao, *Eur. J. Med. Chem.* **80**, 364 (2014)
121. M.W. Bredenkamp, C.W. Holzapfel, W.J. van Zyl, *Synth. Commun.* **20**, 2235 (1990)
122. K.C. Nicolaou, B.S. Safina, M. Zak, S.H. Lee, M. Nevalainen, M. Bella, A.A. Estrada, C. Funke, F.J. Zécree, S. Bulat, *J. Am. Chem. Soc.* **127**, 11159 (2005)
123. K.C. Nicolaou, M. Zak, B.S. Safina, A.A. Estrada, S.H. Lee, M. Nevalainen, *J. Am. Chem. Soc.* **127**, 11176 (2005)
124. D. Hernández, G. Vilar, E. Riego, L.M. Cañedo, C. Cuevas, F. Albericio, M. Álvarez, *Org. Lett.* **9**, 809 (2007)
125. D. Hernández, M. Altuna, C. Cuevas, R. Aligué, F. Albericio, M. Álvarez, *J. Med. Chem.* **51**, 5722 (2008)
126. G.C. Nandi, M.S. Singh, *J. Org. Chem.* **81**, 5824–5836 (2016)
127. X. Gao, Y.-M. Pan, M. Lin, L. Chen, Z.-P. Zhan, *Org. Biomol. Chem.* **8**, 3259 (2010)
128. M. Yoshimatsu, T. Yamamoto, A. Sawa, T. Kato, G. Tanabe, O. Muraoka, *Org. Lett.* **11**, 2952 (2009)
129. X. Zhang, W.T. Teo, P.W.H. Chan, *J. Org. Chem.* **75**, 6290 (2010)
130. Y. Ishiwata, H. Togo, *Synlett* **2008**, 2637 (2008)
131. P. Wipf, S. Venkatraman, *J. Org. Chem.* **61**, 8004 (1996)
132. K.M. Weiß, S. Wei, S.B. Tsogoeva, *Org. Biomol. Chem.* **9**, 3457 (2011)
133. B. Shi, A.J. Blake, W. Lewis, I.B. Campbell, B.D. Judkins, C.J. Moody, *J. Org. Chem.* **75**, 152 (2010)
134. M.A. Honey, R. Pasceri, W. Lewis, C.J. Moody, *J. Org. Chem.* **77**, 1396 (2012)
135. Y. Yanagida, R. Yazaki, N. Kumagai, M. Shibasaki, *Angew. Chem.* **123**, 8056 (2011)
136. V.A. Bakulev, V.S. Berseneva, N.P. Belskaia, Y.Y. Morzherin, A. Zaitsev, W. Dehaen, I. Luyten, S. Toppet, *Org. Biomol. Chem.* **1**, 134 (2003)
137. V.S. Berseneva, Y.Y. Morzherin, W. Dehaen, I. Luyten, V.A. Bakulev, *Tetrahedron* **57**, 2179 (2001)
138. G.K. Verma, G. Shukla, A. Nagaraju, A. Srivastava, K. Raghuvanshi, M.S. Singh, *RSC Adv.* **4**, 11640 (2014)
139. G.K. Verma, G. Shukla, A. Nagaraju, A. Srivastava, M.S. Singh, *Tetrahedron* **70**, 6980 (2014)
140. M.J. Burke, B.M. Trantow, *Tetrahedron Lett.* **49**, 4579 (2008)
141. N. Jelaiel, C. Comoy, B. Fernet, M.L. Efrat, Y. Fort, *Tetrahedron* **67**, 9440 (2011)
142. G.C. Nandi, M.S. Singh, H. Ila, H. Junjappa, *Eur. J. Org. Chem.* **2012**, 967 (2012)
143. L.-R. Wen, X.-J. Jin, X.-D. Niu, M. Li, *J. Org. Chem.* **80**, 90 (2015)
144. S. Peruncheralathan, A.K. Yadav, H. Ila, H. Junjappa, *J. Org. Chem.* **70**, 9644 (2005)
145. F. Shibahara, A. Kitagawa, E. Yamaguchi, T. Murai, *Org. Lett.* **8**, 5621 (2006)
146. E.A. Mamaeva, A.A. Bakibaev, *Tetrahedron* **59**, 7521 (2003)
147. P.C. Patil, D.S. Bhalerao, P.S. Dangate, K.G. Akamanchi, *Tetrahedron Lett.* **50**, 5820 (2009)
148. A.U.H.A. Shah, Z.A. Khan, N. Choudhary, C. Lohölter, S. Schäfer, G.P.L. Marie, U. Farooq, B. Witulski, T. Wirth, *Org. Lett.* **11**, 3578 (2009)
149. D.-P. Cheng, Z.-C. Chen, *Synth. Commun.* **32**, 2155 (2002)
150. J.-W. Zhao, J.-X. Xu, X.-Z. Guo, *Chin. Chem. Lett.* **25**, 1499 (2014)

151. Y. Sun, W. Wu, H. Jiang, *Eur. J. Org. Chem.* **2014**, 4239 (2014)
152. D. Cheng, R. Luo, W. Zheng, J. Yan, *Synth. Commun.* **42**, 2007 (2012)
153. K. Yajima, K. Yamaguchi, N. Mizuno, *Chem. Commun.* **50**, 6748 (2014)
154. G. Vanajatha, V.P. Reddy, *Tetrahedron Lett.* **57**, 2356 (2016)
155. A. Yoshimura, A.D. Todora, B.J. Kastern, S.R. Koski, V.V. Zhdankin, *Eur. J. Org. Chem.* **2014**, 5149 (2014)
156. V.P. Srivastava, A.K. Yadav, L.D.S. Yadav, *Synlett* **24**, 465 (2013)
157. H. Zali-Boeini, A. Shokrolahi, A. Zali, K. Ghani, *J. Sulfur Chem.* **33**, 165 (2012)
158. H. Zali Boeini, J. Iran. Chem. Soc. **6**, 547 (2009)
159. A.R. Khosropour, J. Noei, *Monatsh. Chem.* **141**, 649 (2010)
160. A.R. Khosropour, J. Noei, *J. Heterocycl. Chem.* **48**, 226 (2011)
161. H. Zali-Boeini, S.G. Mansouri, *Synth. Commun.* **45**, 1681 (2015)
162. Z.-Q. Wang, X.-J. Meng, Q.-Y. Li, H.-T. Tang, H.-S. Wang, Y.-M. Pan, *Adv. Synth. Catal.* **360**, 4043 (2018)
163. V.O. Filimonov, L.N. Dianova, K.A. Galata, T.V. Beryozkina, M.S. Novikov, V.S. Berseneva, O.S. Eltsov, A.T. Lebedev, P.A. Slepukhin, V.A. Bakulev, *J. Org. Chem.* **82**, 4056 (2017)
164. X.-M. Zeng, J.-W. Xie, *J. Org. Chem.* **81**, 3553 (2016)
165. C.N. Di Marco, S.D. Kuduk, *Synth. Commun.* **36**, 3377 (2006)
166. X.-Z. Guo, L. Shi, R. Wang, X.-X. Liu, B.-G. Li, X.-X. Lu, *Bioorg. Med. Chem.* **16**, 10301 (2008)
167. H. Klingele Marco, S. Brooker, *Eur. J. Org. Chem.* **2004**, 3422 (2004)
168. M. Sechi, F. Carta, L. Sannia, R. Dallochio, A. Dessi, R.I. Al-Safi, N. Neamati, *Antiviral Res.* **81**, 267 (2009)
169. X. Wen, S.-B. Wang, D.-C. Liu, G.-H. Gong, Z.-S. Quan, *Med. Chem. Res.* **24**, 2591 (2015)
170. Y. Wu, L.X. Ma, T.W. Niu, F.L. Meng, X. Cui, H.R. Piao, *Arch. Pharm. Chem. Life Sci.* **345**, 980 (2012)
171. H. Neunhoeffer, H. Hammann, *Liebigs Ann. Chem.* **1984**, 283 (1984)
172. S.A.D. Keczer, M.R. Masjedizadeh, S.Y. Wu, T. Lara-Jaime, K. Comstock, C. Dvorak, Y.Y. Liu, W. Berger, *J. Label. Compd. Radiopharm.* **49**, 1223 (2006)
173. D. Boeglin, S. Cantel, A. Heitz, J. Martinez, J.-A. Fehrentz, *Org. Lett.* **5**, 4465 (2003)
174. Y. Hitotsuyanagi, S. Motegi, H. Fukaya, K. Takeya, *J. Org. Chem.* **67**, 3266 (2002)
175. M. Bibian, A.-L. Blayo, A. Moulin, J. Martinez, J.-A. Fehrentz, *Tetrahedron Lett.* **51**, 2660 (2010)

# Chapter 7

## Thioamide-Based Transition Metal Complexes



Ken Okamoto, Junpei Kuwabara and Takaki Kanbara

**Abstract** This chapter reviews the synthesis of thioamide transition metal complexes and their structural features. The coordination chemistry of this group of ligands is unique due to their versatility of coordination states, such as monodentate, bridging, and chelating modes, including pincer ligands and scorpionate ligands. Further, some thioamide complexes can be used for applications in various areas such as chemical-sensor materials, tunable redox-potentials complexes, polymer hybrid luminescence materials, building blocks for multinuclear complexes, and catalysts for several coupling reactions.

**Keywords** Thioamide ligand · Coordination chemistry of thioamide · Thioamide-based pincer ligand · Thioamide-based scorpionate ligand · Material usage of thioamides with transition metals

### 7.1 Introduction

Thioamides (TAs) are more stable when compared to other thiocarbonyls such as thioic acid O-esters, thioketones, and thioaldehydes. Thus, TAs are increasingly being used as organosulfur ligands in coordination chemistry and organometallic chemistry. The coordination chemistry of TAs is unique due to their versatility of coordination states. To be specific, secondary TAs (*sec*-TAs) are better H bond donors than their corresponding secondary amides (*sec*-As) (Fig. 7.1a) [1]. This is due to the higher acidity of *sec*-TA compared to that of the corresponding amides (Fig. 7.1b) [2, 3]. The structure of *sec*-TA can be converted by the addition of inorganic and

---

K. Okamoto

Division of Chemical Engineering and Biotechnology, Department of Engineering for Future Innovation, National Institute of Technology, Ichinoseki College, Takanashi, Hagisho, Ichinoseki, Iwate 021-8511, Japan

J. Kuwabara · T. Kanbara (✉)

Tsukuba Research Center for Energy Materials Science (TREMS), Graduate School of Pure and Applied Sciences, University of Tsukuba, 1-1-1 Tennodai, Tsukuba, Ibaraki 305-8573, Japan  
e-mail: [kanbara@ims.tsukuba.ac.jp](mailto:kanbara@ims.tsukuba.ac.jp)

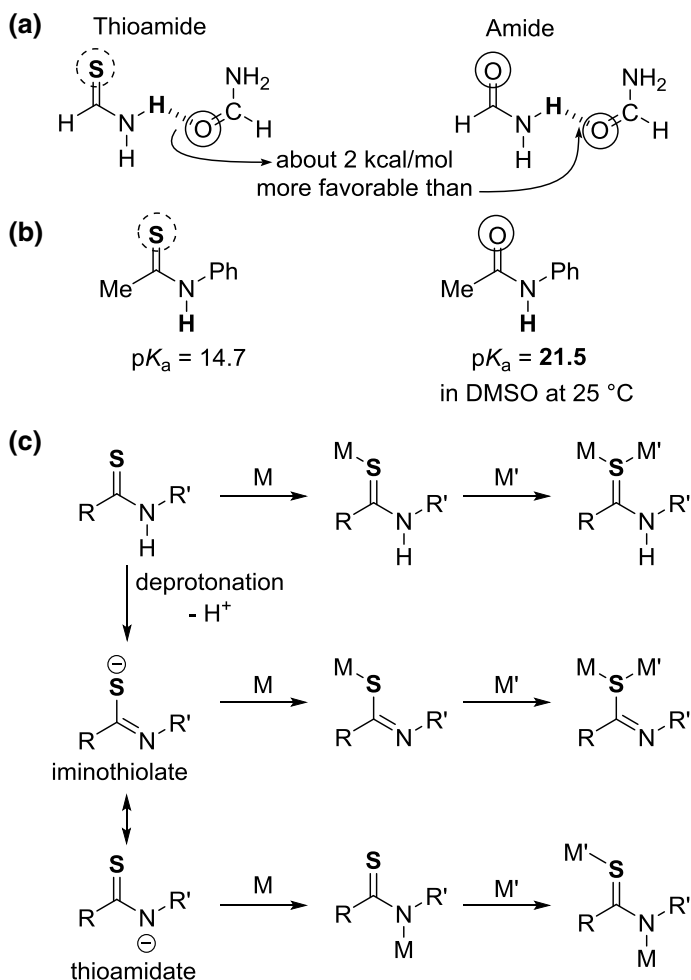


**Fig. 7.1** Basic physical properties of TAs and their corresponding amides. **a** Hydrogen bonding ability and **b** acidity, **c** the neutral and anionic forms of a secondary TA unit and possible coordination modes as a building block of a multinuclear metal complex ( $M = \text{metal ion}$ )

organic bases (Fig. 7.1c). As a result of deprotonation, TA is converted to a bridging ligand. In recent years, several studies showed the advantages of using multidentate TA-based transition metal complexes in a diverse range of fields, namely photochemistry, structural chemistry, catalyst development, polymer-based materials science, electrochemistry, and supramolecular chemistry.

This chapter describes the unique coordination states of TA ligands and TA derivatives with transition metals. Utilization of the coordination chemistry of TAs in various areas is also described. The discussion is divided into the following three sections—the coordination manner and structural features of mono and multiden-



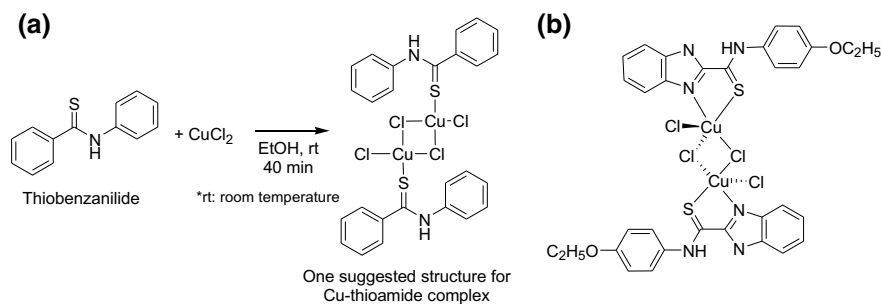
tate TA ligands, catalysts, and application of TA as directing groups and sorbent materials.

## 7.2 Transition Metal Complexes with Monodentate Thioamide Ligands

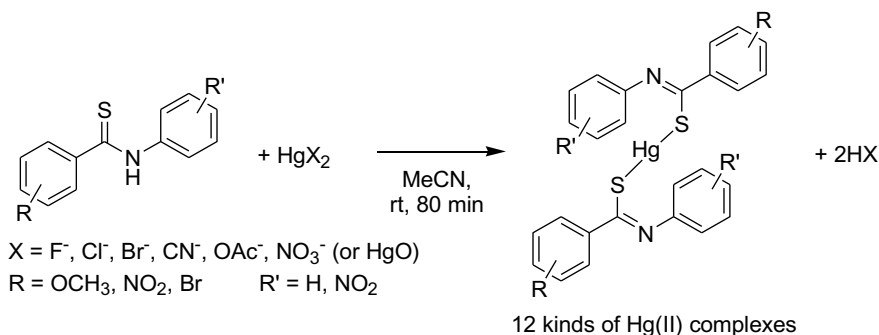
Thiobenzanilide and 2-mercaptopyridine are often used as monodentate ligands and also as starting materials for heterocycles and other types of ligands. The first example is a Cu complex with thiobenzanilide as a ligand [4]. The reaction of  $\text{CuCl}_2$  with the equivalent of thiobenzanilide in ethanol at room temperature produced a dark red precipitate. The obtained red product is stable in air and insoluble in organic solvents, except for dimethylsulfoxide (DMSO) and dimethylformamide (DMF). Although the structure is not clear due to the solubility of the Cu complex, Mirjafari and co-workers suggested possible structure and a redox system between precursor Cu(II) and Cu(I) (Scheme 7.1 a). A similar Cu(II) complex was determined by single-crystal X-ray diffraction (Scheme 7.1b) [5]. The geometry of the Cu(II) complex is distorted trigonal bipyramidal with two bridging chloride ions. Although the two molecules of Cu complexes are stabilized by bridging with a  $\text{Cl}^-$  ligand, the solution state of the Cu(I) or Cu(II) complexes might contain more complicated solvated states due to the donor ability of the solvent molecules.

Thiobenzanilide was also used in studies on coordination chemistry with Hg(II) for the development of novel antidotes [6]. In this study,  $^1\text{H}$  nuclear magnetic resonance ( $^1\text{H NMR}$ ), Raman, and infrared (IR) spectroscopic measurements were conducted to reveal the complexation of mercury with sulfur. The results show that the coordination mode is the iminothiolate form (Scheme 7.2).

The number of commercially available TAs is very limited. However, 2-mercaptopyridine is available in the market. 2-mercaptopyridine is a tautomer of cyclized TA (1*H*-pyridine-2-thione, hereinafter called pySH) [7]. Several transition metals with pySH have been widely studied in coordination chemistry, electrochem-



Scheme 7.1 TA-Cu complexes



**Scheme 7.2** Complexation reaction of thiobenzanilides with Hg(II) compounds

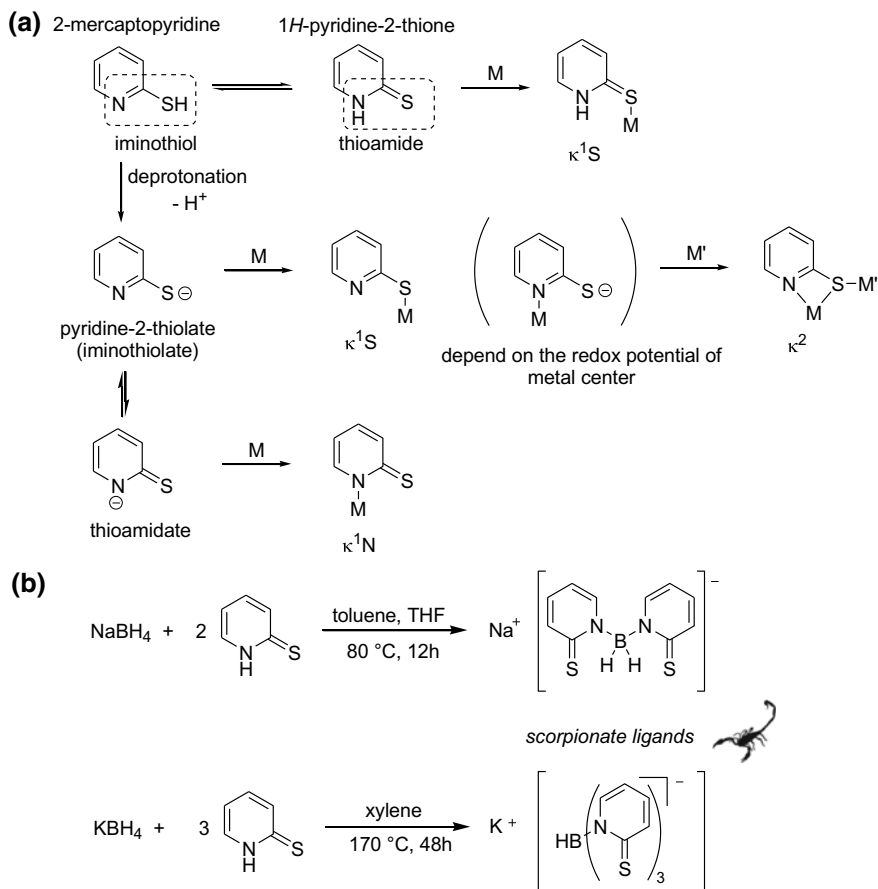
istry, and biochemistry. There are two series of possible coordination modes of pySH and deprotonated pySH ( $pyS^-$ ); however, the most reported transition metal complexes with pySH exhibit  $\kappa^1S$  coordination (Scheme 7.3a, cf. Fig. 7.1). The tautomerism on the ligand shows unique structural and electronic features. In this context, the Owen research group has reported an alkali metal salt of the “soft” scorpionate ligand, which is derived from the reaction of pySH with  $NaBH_4$  or  $KBH_4$  (Scheme 7.3b) [8]. The details of the scorpionate ligand will be described in the section on multidentate ligands.

Studies on the synthesis, characterization, and reactivity of Fe(II) complexes  $[Fe(II)(pySH)_4](OTf)_2$ ,  $[Fe(II)(pySH)_4](ClO)_4$ , and polymeric  $[Fe(II)(pyS)_2]_n$  of pySH ligands were reported by the Halder group [9]. The X-ray crystal structures of both Fe(II) complexes reveal a distorted tetrahedral geometry at the Fe(II) center. Interestingly, all the pyridine nitrogen atoms are protonated and thiolate ions are coordinated to the Fe(II) center. The structure of these Fe complexes resembles the active site of rubredoxin, which is a low-molecular weight iron-containing protein and participates in electron transfer in the biological system. On the other hand,  $Fe_2(CO)_9$  and 2,2'-dipyridyl disulfide (oxidized product of pySH) exhibit an octahedral geometry at the Fe(II) center, forming a 1D coordination polymer (Scheme 7.4).

The same Group 8 metal was used for the synthesis of a ruthenium complex  $[Ru(II) \text{ bis}(2,2'\text{-bipyridine})(pySH)(pyridine)](PF_6)_2$ ; the complex was characterized from its deprotonated form and investigated by electrochemical measurements [10]. Depending on the chemical acid–base conditions or the oxidation state of the metal center, the Ru(II) complex shows three reversible coordination modes of TA (Scheme 7.5).

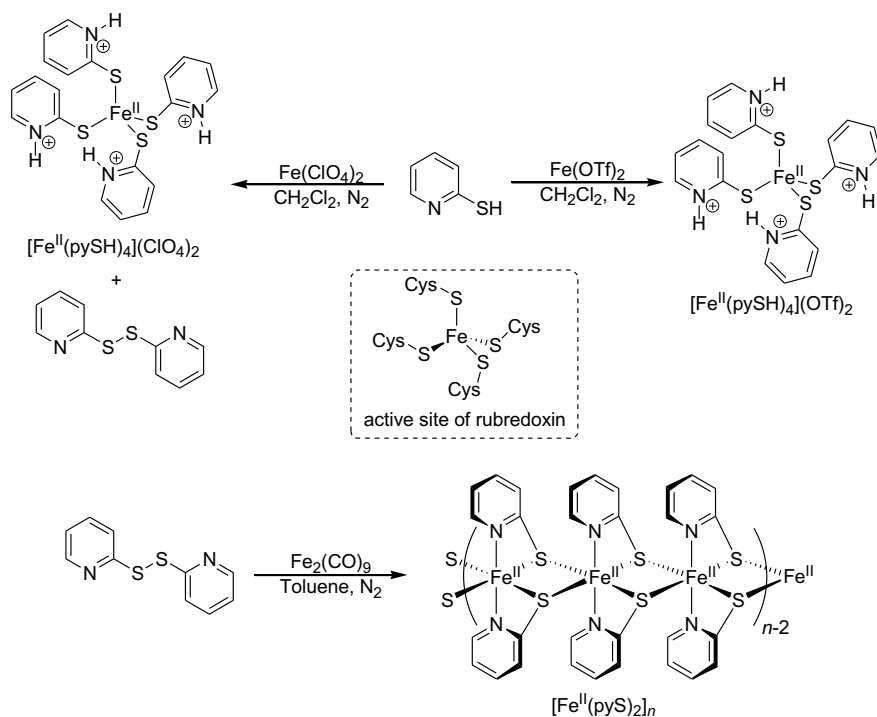
An intramolecular proton–hydride interaction was discovered by the Milstein group, the Crabtree group, and the Morris group independently [11–13]. Further investigations were conducted by the Morris group, and they reported a unique bifurcated hydrogen bonding interaction involving the hydride, a proton, nitrogen, and a fluorine atom of the tetrafluoroborate anion (Scheme 7.6) [14].

In all the above cases, the TA ligand does not undergo desulfurization. However, redox-driven desulfurization [15] and migratory metal insertion into the C=S bond

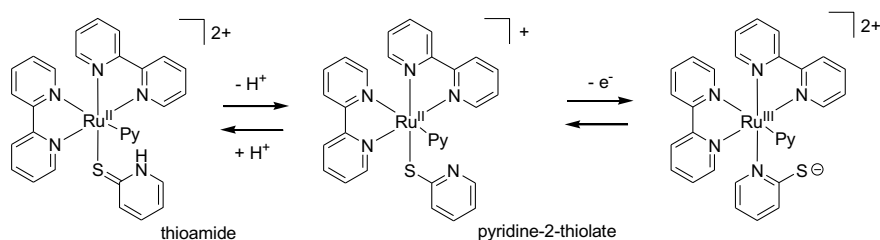


**Scheme 7.3** **a** Thiol/thione tautomeric equilibrium and possible coordination mode of pySH and pyS<sup>-</sup>, **b** syntheses of scorpionate ligand derived from pySH

[16, 17] were reported (Scheme 7.7a, b, respectively). For example, the Nakazawa group reported that several TAs and half-sandwich CpFe(CO)<sub>2</sub>Me with hydrosilanes undergo desulfurization and yield trimethylamine or the corresponding imines. Some of the key intermediates are isolated and characterized by single-crystal X-ray analysis. Therefore, it is necessary to evaluate the redox potential of the transition metal ion and the reaction conditions to monitor the target complex structure.



**Scheme 7.4** Synthesis of Fe(II) complexes with  $\kappa^1\text{S}$  and  $\kappa^3\mu^2$  coordination modes

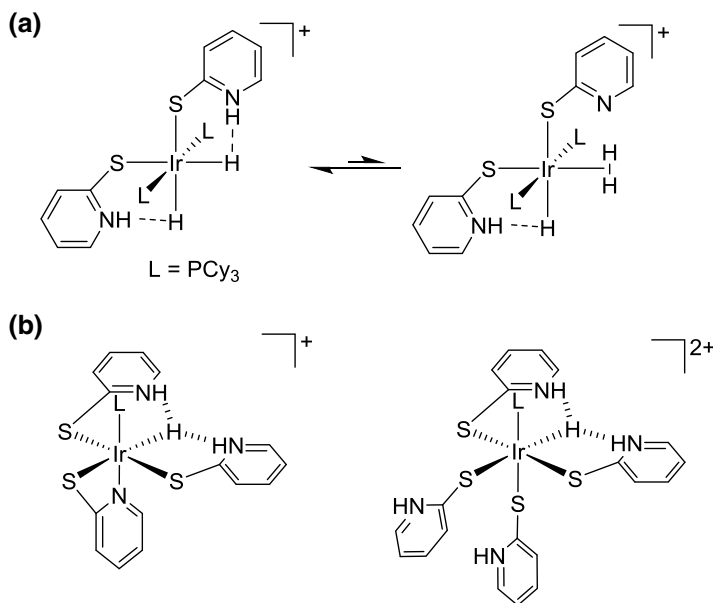


**Scheme 7.5** Electrochemical and/or acid–base stimuli-induced isomerization

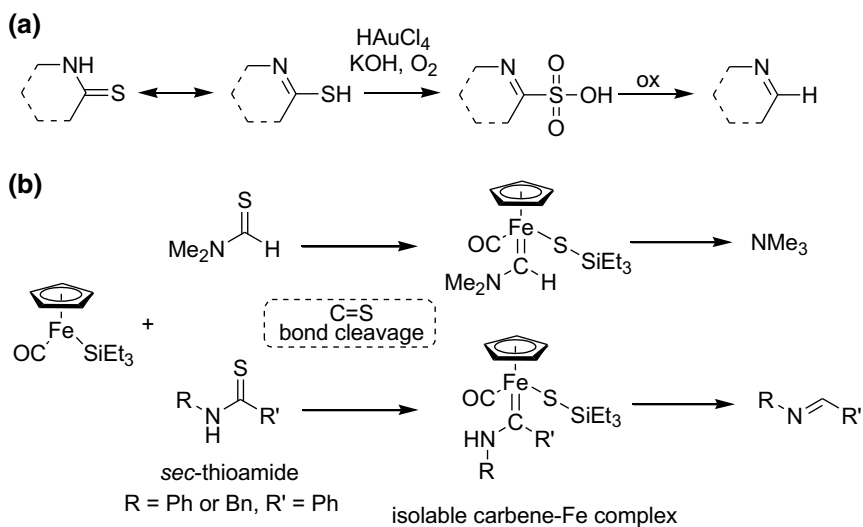
## 7.3 Transition Metal Complexes with Multidentate Thioamide Ligands

### 7.3.1 Bidentate Thioamide Ligands ( $N^3S$ , $C^3S$ , $B^3S$ , and $P^3S$ )

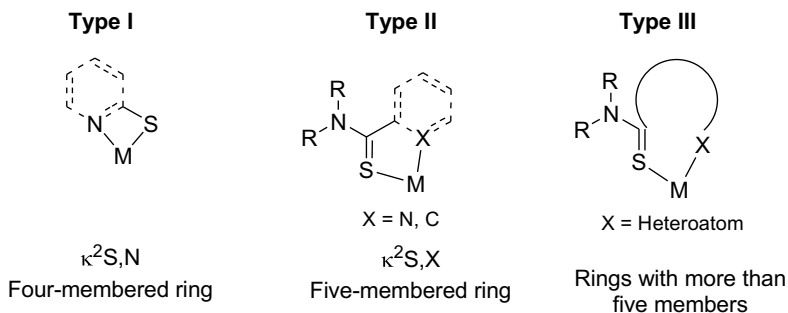
As depicted in Scheme 7.8, the coordination modes for a bidentate ligand can be classified into three types—a four-membered ring, five-membered ring, and rings



**Scheme 7.6** **a** Intramolecular H...H interaction and **b** proton-hydride interaction between Ir-H and N-H of the pySH metal center



**Scheme 7.7** Proposed desulfurization mechanism through the formation of **a** a sulfonate intermediate derivative or **b** a carbene complex



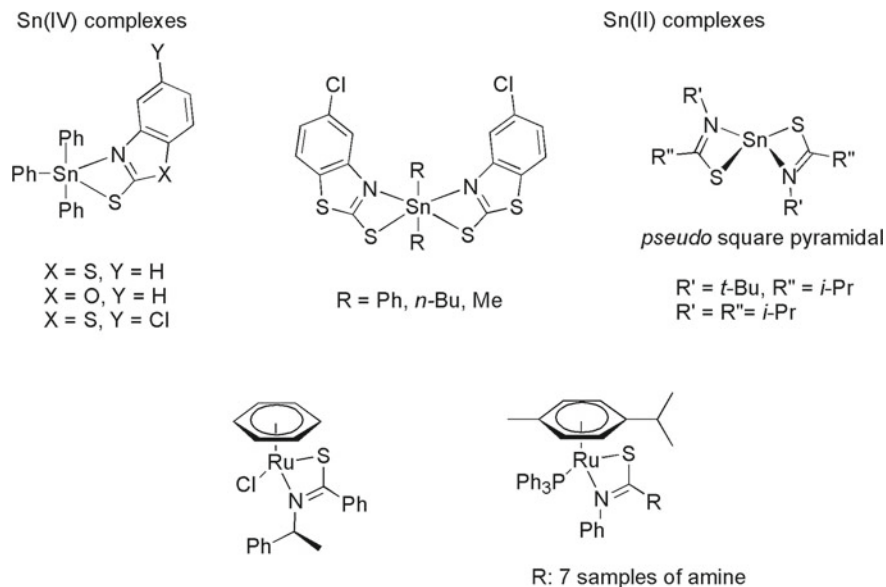
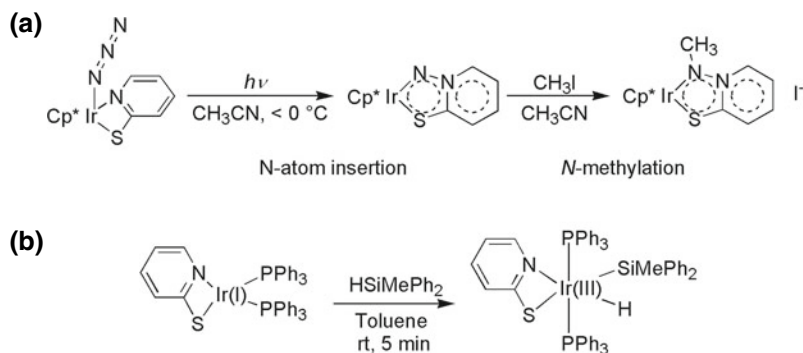
**Scheme 7.8** Coordination modes of bidentate ligands

with more than five members, including two coordination bonds with a transition metal center.

The number of type I complexes is very limited (Scheme 7.9). Six types of Sn(IV) complexes with heterocyclic TAs have been used for the peroxidation of oleic acid [18]. An analysis of the influence of these complexes on the peroxidation of oleic acid showed that the formation of reactive radicals caused the initiation of chain radical oxidation of the substrate. The influence of these complexes on the catalytic peroxidation of linoleic acid by the enzyme lipoxygenase (LOX) was also studied, and the results obtained were compared with those of cisplatin. In addition, all the Sn(IV) complexes were tested for in vitro cytotoxicity against *leiomyosarcoma* cells. On the other hand, TAs can be used as sources of sulfur in semiconducting materials. Hill's group reported two TA-based tin complexes [19]. Both Sn(II) complexes were used to grow thin films by aerosol-assisted chemical vapor deposition (AACVD). The films were analyzed by powder X-ray diffraction (PXRD), Raman spectroscopy, X-ray photoelectron spectroscopy (XPS), atomic force microscopy (AFM), and scanning electron microscopy (SEM). The films comprised primarily of the orthorhombic (herzenbergite) phase of SnS, which is contaminated by low levels of residual carbon (<5 at.%). These results demonstrate the potential of such simple thioamidate derivatives as single-source precursors in the fabrication of useful metal sulfide thin-film materials. Prior to this investigation, low-temperature and scalable synthesis of wurtzite ZnS anisotropic nanocrystals in air was studied [20]. Although the coordination structure was not clear, it was reported that a reaction between a zinc salt (nitrate or chloride) and thioacetamide and amines at 60 °C yields ZnS nanoplatelets or nanowires.

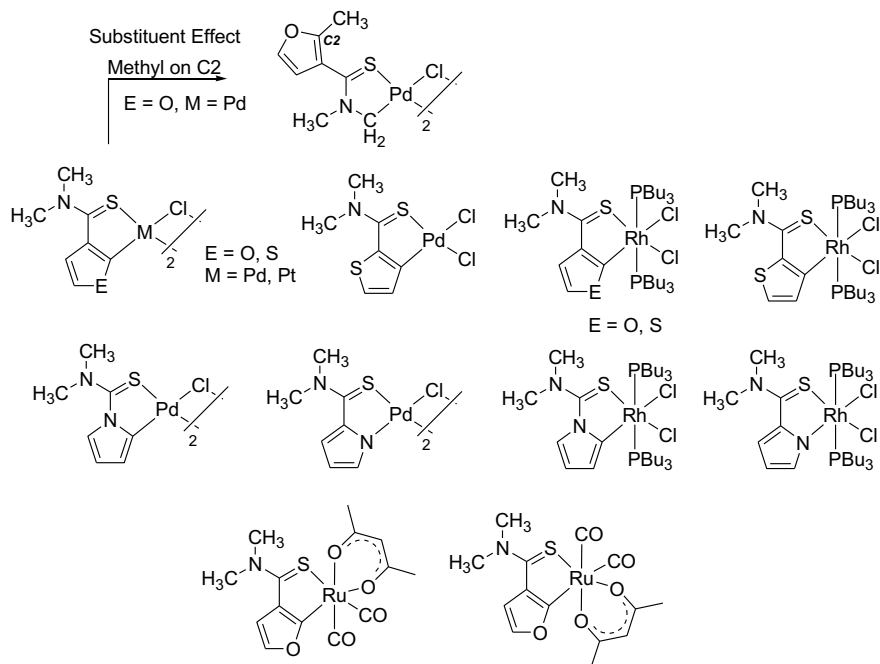
Brunner et al. analyzed a piano stool type Ru(II) complex by single-crystal XRD [21]. In addition, a series of four-membered Ru(II) complexes with different non-cyclic TA ligands were prepared and fully characterized by spectroscopic methods including NMR spectroscopy and electrospray mass spectrometry [22]. The solid-state structures of the two Ru complexes were determined by single-crystal XRD.

Bidentate anionic pyS-based Ir(I) complexes and their reactivity were investigated by three groups [23–25]. Suzuki et al. described that the unique photolysis

**Scheme 7.9** Type I: four-membered metal complexes with TAs**Scheme 7.10** **a** Photolysis and methylation of the (azido)(pyS)Ir complex, and **b** an example of oxidative addition to Ir(I)

of an (azido)(pyS)Ir(III) complex resulted in a pyridine-1-imido-2-thiolato complex (Scheme 7.10a) [23]. Further, the imido Ir(III) complex reacted with methyl iodide and yielded an *N*-methylated complex. On the other hand, Ogata and Toyota tested the reactivity of a (pyS)Ir(I) precursor with small molecules, such as  $\text{CHCl}_3$ , methyl diphenylsilane, acetic acid, and *p*-tolylacetylene (Scheme 7.10b). The corresponding Ir(III) complexes were obtained and were accompanied by the homolytic bond cleavage of small molecules [25].

## Nonoyama Group



**Scheme 7.11** TA-based five-membered metal complexes developed in the 1990s

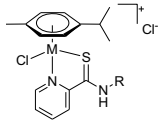
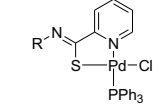
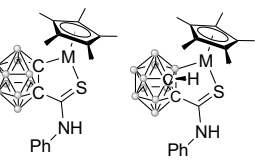
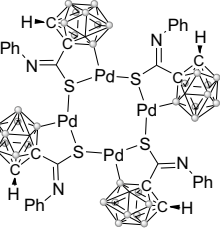
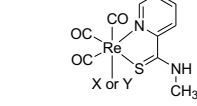
A number of studies addressed Type II complexes with a focus on Pd(II) complexes. Over the past two decades, C–H activation and the following C–C coupling reaction have emerged as hot topics for the green synthesis of organic products [26]. In reference to the C–H activation of TAs, pioneering investigations were conducted by the Nonoyama group on TA-based cyclometallation in the 1990s (Scheme 7.11) [27–33]. The number of reactions catalyzed by TA-based transition metal complexes increased in the twenty-first century. The details of the catalytic activity will be described in the next session.

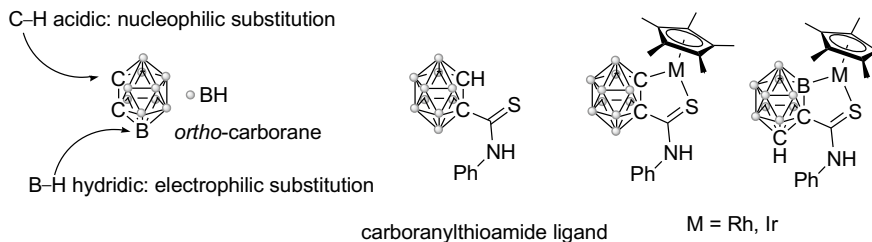
The characteristic structure of TA-based transition metal complexes and the transformation of ligand structures were also reported by several groups. Their structures and remarks are listed in Table 7.1. TA ligands were employed for research on carborane chemistry. Due to the rigidity and robustness of carboranes, they exhibit a series of structurally unique skeletons with excellent thermal and chemical stabilities [34]. As shown in Scheme 7.12, C–H or B–H activation on the carborane unit affords C<sup>∞</sup>S or B<sup>∞</sup>S half-sandwich Rh and Ir complexes bearing a carboranylthioamide ligand [35]. Following this report, Jin's group conducted further investigations on Ir and Pd complexes [36, 37].

Type III complexes are very rare. This is probably due to the structural strain caused due to the large ring size and ion size of the transition metals and

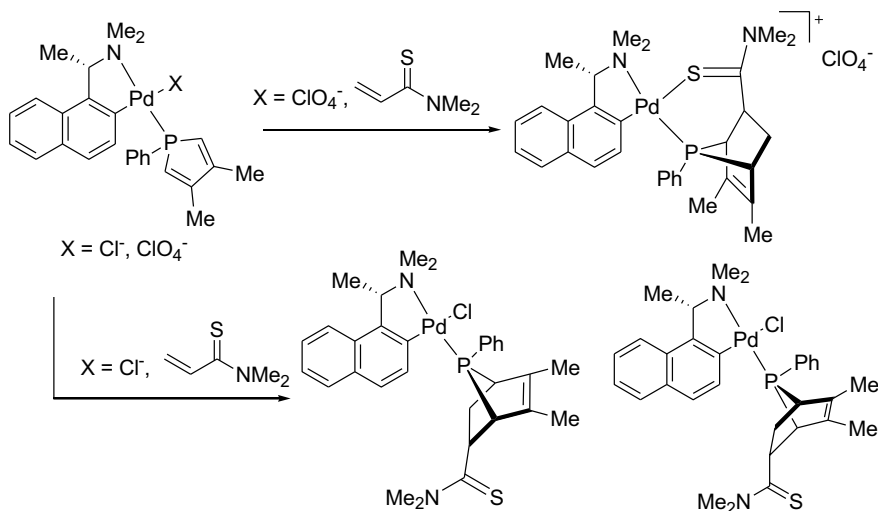


**Table 7.1** Various TA-based complexes with five-membered cycle(s)

Year [ref.]	Structure of the unique complex	Remarks
2013 [38]	 <p>M = Ru, Os R = C<sub>6</sub>H<sub>5</sub>, 4-FC<sub>6</sub>H<sub>4</sub>, 4-OHC<sub>6</sub>H<sub>4</sub>, 2,4,6-(Me)<sub>3</sub>C<sub>6</sub>H<sub>2</sub>.</p>	Organometallic anticancer compounds
2014 [39]	 <p>R = 3-MeC<sub>6</sub>H<sub>4</sub>, 2,4,6-(Me)<sub>3</sub>C<sub>6</sub>H<sub>2</sub>, benzyl, 4-BrC<sub>6</sub>H<sub>4</sub></p>	DNA/protein binding studies and cytotoxicity
2015 [35] 2017 [36]	 <p>M = Rh, Ir</p>	Site-selective activation of the B–H bond or the C–H bond
2017 [37]		B(4)–H activation of <i>o</i> -carboranyl TA
2018 [40]	 <p>Anionic: X = Cl<sup>-</sup>, Br<sup>-</sup>, I<sup>-</sup>, NCS<sup>-</sup> Neutral: Y = 3,5-dimethylpyrazole, imidazole (PF<sub>6</sub><sup>-</sup>)</p>	Lower cytotoxicity than cisplatin toward non-cancerous cells



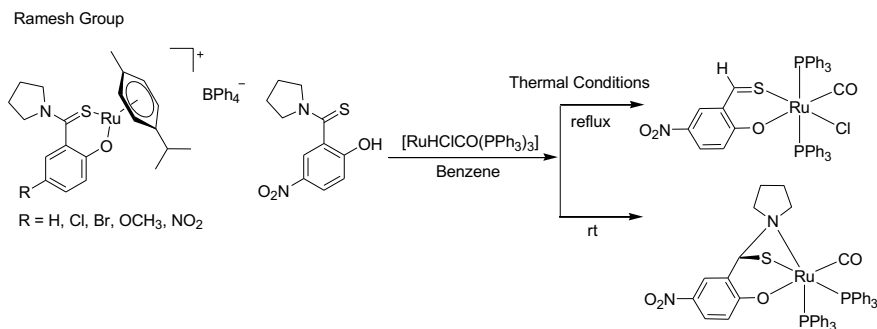
**Scheme 7.12** Carboranyl TA ligand and transition metal complexes



**Scheme 7.13** Reactivities of phosphine ligand with thioacrylamide

may be also attributed to the complexity of the ligand design. As depicted in Scheme 7.13, the intramolecular *exo*-endo-cycloaddition reaction between *N,N*-dimethylthioacrylamide and 3,4-dimethyl-1-phenylphosphole in the presence of Pd complex precursors yielded the corresponding stereospecific TA-substituted chiral/diastereomeric phosphanorbornenes [41].

The Ramesh group reported a family of Ru complexes (Scheme 7.14) [42, 43]. In one study, cationic half-sandwich complexes with O<sup>+</sup>S bidentate TA ligands have been synthesized and isolated as tetraphenylborate salts [42]. All the synthesized Ru(II) complexes are air stable, and they were comprehensively characterized by elemental analysis, spectral analysis, and X-ray diffraction. In the second study, the reaction of a TA-based ligand with [RuHCl(CO)(PPh<sub>3</sub>)<sub>3</sub>] afforded two structurally different Ru(II) complexes by varying the experimental reaction conditions [43]. Interestingly, the ligand behaves as a mono-anionic bidentate with O<sup>+</sup>S fashion under reflux conditions via C–N bond cleavage, while it acts as a di-anionic tridentate N<sup>+</sup>O<sup>+</sup>S donor at room temperature. The two synthesized Ru(II) complexes were



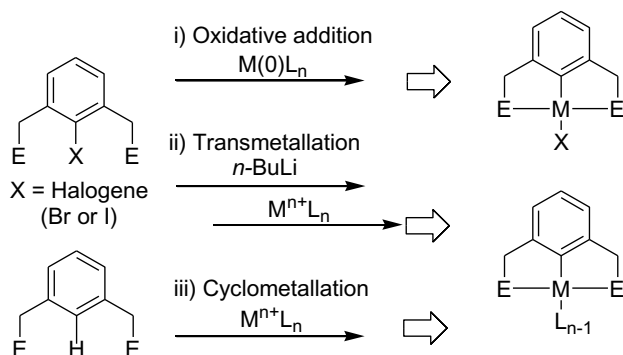
**Scheme 7.14** Ru(II) complexes with S<sup>O</sup> bidentate ligands

fully characterized. The solid-state molecular structures of the ligand and complexes were studied using single-crystal X-ray crystallography, which confirms the different coordination modes of the ligand with ruthenium ions and reveals the presence of a distorted octahedral geometry. Moreover, the cytotoxic effect of the Ru(II) complexes was examined on cancerous cell lines, such as HeLa and MCF-7, along with a cell viability assay against non-cancerous NIH-3T3 cells under *in vitro* conditions, and the results showed that the complexes exhibit significant anticancer activity.

### 7.3.2 Tridentate Thioamide Ligands (*Pincer Types and Scorpionate Types*)

Both pincer-type and scorpionate-type ligands are known as tridentate ligands. Generally, pincer-type ligands exhibit a meridional geometry and scorpionate-type ligands exhibit a facial geometry, respectively. However, there is no clear border between the two types of ligands, which sometimes means that the term “scorpionate” and “pincer” are used interchangeably in the same paper. For the sake of clarity, in this chapter, “pincer” refers to meridional geometry and “scorpionate” refers to facial coordination geometry.

A number of comprehensive reviews have already been conducted on the structural features of pincer ligands [44–46], catalytic properties of pincer complexes [47], and development of chemical sensors [48] using pincer complexes. In general, three methods are used for the preparation of pincer complexes (Scheme 7.15)—(i) oxidative addition using zero-valent metal precursors, (ii) transmetallation via lithiated pincer ligands, and (iii) direct cyclometallation assisted by chelation [49–51]. Of these three methods, the cyclometallation route is the most favorable, because it does not require any air-sensitive chemicals or a strictly inert atmosphere. In addition, cyclometallation enables a rapid construction of pincer complexes via C–H activation (or N–H activation). All the reported TA-based pincer complexes can be



**Scheme 7.15** General pincer complex preparation routes

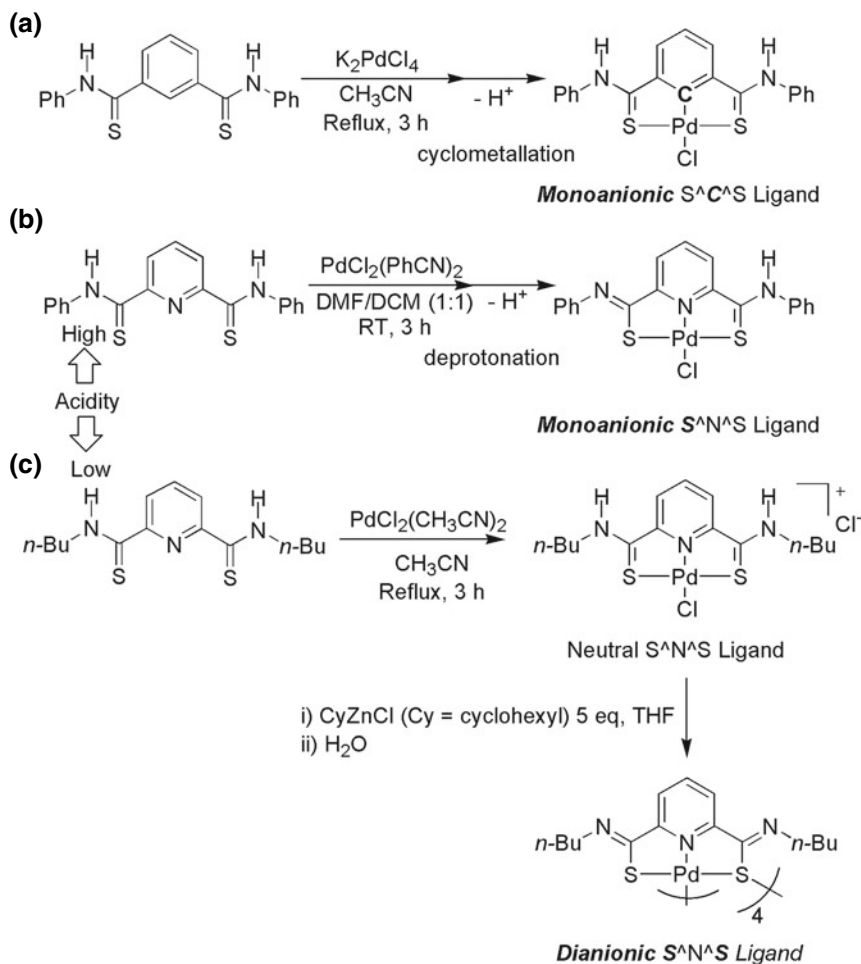
**Table 7.2** TA-based pincer complexes reported by the Kanbara research group

Year [ref.]	Coordination mode	Centered unit	Metal
2004 [52]	$S^{\wedge}C^{\wedge}S$	Phenyl	Pt(II)
2005 [53]	$S^{\wedge}C^{\wedge}S$	Phenyl	Pd(II)
2006 [54]	$S^{\wedge}N^{\wedge}S$	Pyrrolyl	Ni(II), Pd(II), Pt(II)
2010 [55, 56]	$S^{\wedge}C^{\wedge}S$	Azulenyl	Pd(II), Pt(II)
	$S^{\wedge}C^{\wedge}S$	Phenyl	Ni(II)
2011 [57, 58]	$S^{\wedge}C^{\wedge}S$	Phenyl	Ru(II)
	$S^{\wedge}N^{\wedge}S$	Pyrrolyl	Ru(II)
	$S^{\wedge}N^{\wedge}S$	Pyrrolyl	Cu(II)
2014 [59]	$S^{\wedge}N^{\wedge}S$	Pyridyl	Ru(II)

prepared by route (iii). This is probably due to the strong coordination ability of the two sulfur atoms with the transition metals.

The same applies to the C–H activation route of TA pincer ligands; the Nonoyama research group demonstrated the first example in 1995 [32, 33]. The Kanbara group explored a series of  $S^{\wedge}X^{\wedge}S$  pincer complexes (Table 7.2).

Charge versatility is a unique property of *sec*-TA-based pincer ligands. As shown in Scheme 7.16, the important feature of *sec*-TA-based pincer ligands is their ability to form a multivalent structure upon deprotonation of the *sec*-TA moiety. The phenyl-centered  $S^{\wedge}C^{\wedge}S$  ligand has a mono-anionic coordination mode. Alternatively, pyridyl-centered  $S^{\wedge}N^{\wedge}S$  ligands may exhibit mono-anionic coordination modes or neutral coordination modes, depending on the *N*-end substituents (Scheme 7.16b, c (top) for *N*-phenyl and *N*-butyl, respectively). The mono-anionic  $S^{\wedge}N^{\wedge}S$  coordination of pyridyl-centered *N*-phenyl TA can be related to the high acidity of the *sec*-TA moiety. In addition, further treatment of the cationic *N*-butyl TA-based  $S^{\wedge}N^{\wedge}S$  Pd(II) complex with an organometallic base can yield a di-anionic ligand structure (Scheme 7.16c, bottom) [60]. Therefore, both centered aromatics and *N*-end substituents should be carefully considered with respect to the selected metal center and the intended use.

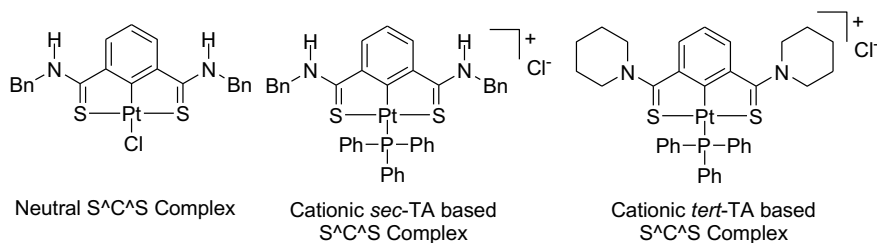


**Scheme 7.16** Complexation behavior of a **a** S<sup>C</sup>S ligand, **b** *N*-phenyl S<sup>N</sup>S ligand, and **c** *N*-alkyl S<sup>N</sup>S ligand with Pd(II) sources

Besides, the coordination mode of *sec*-TA-containing an asymmetrical S<sup>X</sup>E ligand [X=C or N and E=heteroatom (including sulfur)], the so-called hybrid-type pincer ligand, is also expected to yield regioselective S<sup>X</sup>E coordination structures. Odinets et al. reported asymmetrical S<sup>C</sup>S' pincer Pd(II) and Pt(II) complexes with *sec*-TA and phosphine sulfide moieties using a preparation method similar to that shown in Scheme 7.16a [61, 62]. In this context, solid-state cyclopalladation has been reported [63].

As described in several reviews, TA-based S<sup>C</sup>S pincer complexes with Pd(II) and Pt(II) show photoluminescence and electroluminescence properties [64]. In particular, for *sec*-TA-based pincer Pt(II) complexes, the presence of a coordinated

### Aggregates in Binary Solvent Mixtures



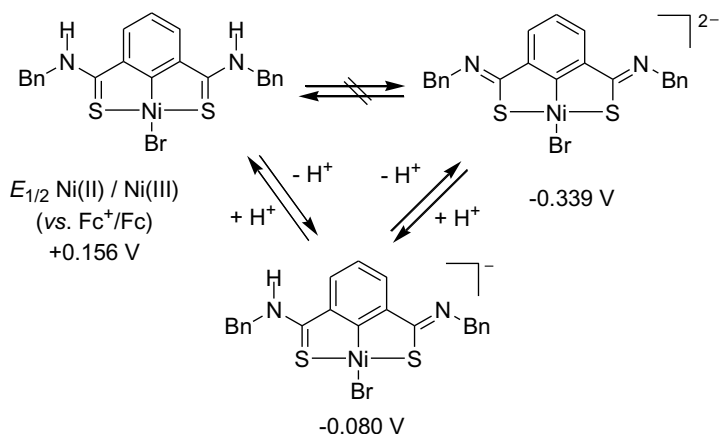
**Scheme 7.17** Structures of AIE-active complexes

*sec*-TA linkage in the pincer ligand worked as a reactive site upon the addition of bases and anions, resulting in modulating absorption and emission properties of the complexes [65]. In order to achieve a deeper understanding of the features of the *sec*-TA-based S<sup>C</sup>S pincer complexes, studies were conducted on the external stimuli-responsive photochemical behavior of *sec*-TA-based S<sup>X</sup>S (X=C or N) pincer complexes [66–68].

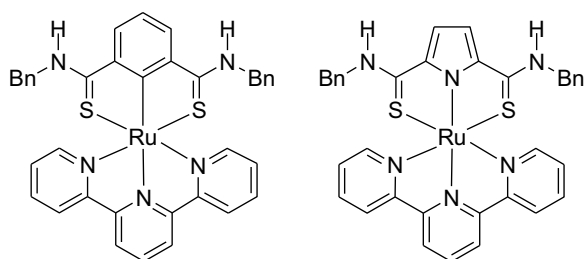
Aggregation-induced emission (AIE) has been widely recognized as a type of solid-state luminescence, and many efforts were made to understand this photo-physical behavior [69]. The AIE activity was evaluated in three different types of S<sup>C</sup>S Pt complexes, namely neutral *sec*-TA-based S<sup>C</sup>S Pt(II), cationic *sec*-TA-based S<sup>C</sup>S Pt, and cationic tertiary-TA-based complexes (Scheme 7.17) [70, 71]. Only the cationic *sec*-TA-based S<sup>C</sup>S Pt complex formed aggregates in various solvent systems, and the aggregates showed an AIE behavior.

Proton-coupled electron transfer (PCET)-active pincer complexes showed remarkable progress in small-molecule activation [72–76]. In the case of TA-based pincer complexes, deprotonation of *sec*-TA ligands is an option that can be considered for controlling the unit's electrochemical response (redox potential) and activating the metal center. The modulation of redox potential in the S<sup>C</sup>S Ni complexes was systematically investigated by the addition of external chemical stimuli (e.g., organic bases), because deprotonation of the TA group is expected to change the electron density of the Ni center by forming thioamidate and iminothiolate resonance structures (Scheme 7.18) [77]. In fact, deprotonation of the TA moiety led to a negative shift of the Ni(II)/Ni(III) redox potential by approximately 500 mV. Further, the effect of centered aromatic units on the redox potential of Ni(II)/(III) has been investigated [56].

Modulation of the electronic properties of *sec*-TA-based S<sup>X</sup>S (X=C or N) Ru pincer complexes (Scheme 7.19) has also been examined [57]. Both complexes showed a two-step deprotonation reaction with bases; this resulted in a shift in the centered metal redox couples to a lower potential (by 720 mV for S<sup>C</sup>S and 550 mV for S<sup>N</sup>S). These results are consistent with those obtained from the Ni pincer complexes. The Pourbaix diagram revealed that the *sec*-TA-based S<sup>C</sup>S Ru complex undergoes a one-proton/one-electron transfer process in the pH range of 5.83–10.35



**Scheme 7.18** Effect of deprotonation on the redox potential of *sec*-TA-based  $\text{S}^{\text{C}}\text{S}$  Ni complexes

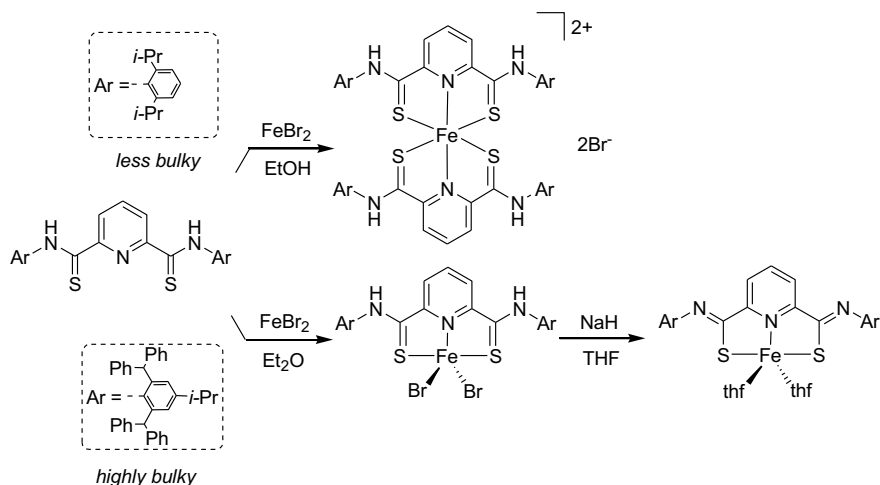


**Scheme 7.19** Structures of *sec*-TA-based  $\text{S}^{\text{C}}\text{S}$  and  $\text{S}^{\text{N}}\text{S}$  Ru complexes

and a two-proton/one-electron process at a pH above 10.35, indicating that the deprotonation/protonation of the complexes is related to the PCET process. Qiu and Liu et al. investigated similar structure of two-dimensional  $\text{S}^{\text{C}}\text{S}$  pincer Ru(II) complexes for the second-order nonlinear optical properties by density functional theory (DFT) calculations [78].

A deprotonated *sec*-TA-based  $\text{S}^{\text{N}}\text{S}$  Fe(II) complexes were reported by Masuda's research group (Scheme 7.20) [79, 80]. Deprotonation of the highly bulky *sec*-TA ligand activates the coordination sites, and the resulting THF-coordinated complex can be converted into new structures with several small molecules and ligands, such as CO, NO, NC-Ar, and 1,3-bis-(2,6-diisopropylphenyl)imidazol-2-ylidene (NHC ligand).

The family of soft scorpionate ligands, which are derived from cyclized thioamides, continues to increase in number. Not only pySH but also other cyclized thioamides can be used for the preparation of soft scorpionate ligands (Scheme 7.21a). The Owen group published numerous papers on the preparation of soft scorpionate ligands and their transition metal complexes (Scheme 7.21b) [8, 81–83]. As described in the section on carboranyl TA ligands, B–H activation is an interesting research



**Scheme 7.20** Synthesis and activation of the coordination sites of *sec*-TA-based S<sup>N</sup>CS Fe complexes

topic as metal–borane interactions are expected to be weak. If B–H activation does not occur, agostic B–H...metal interaction is the more dominant mechanism affecting the stability of the complexes (Scheme 7.21b, c) [84].

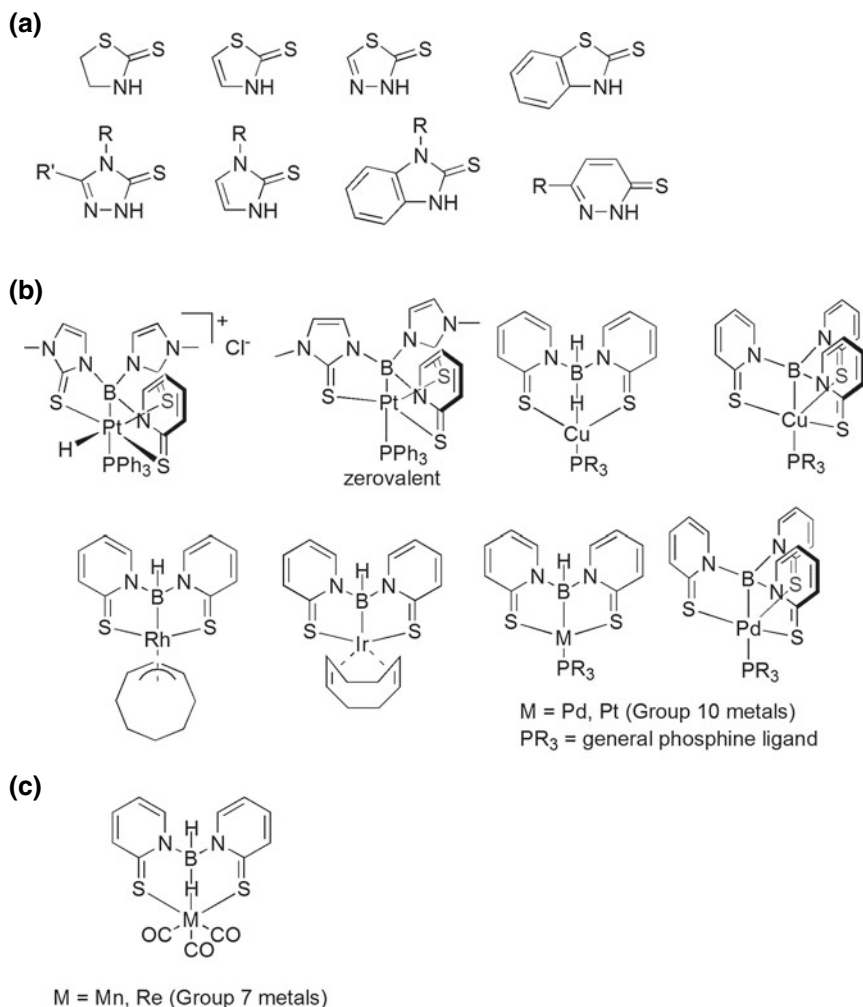
Compared to pincer complexes, the physical properties of scorpionate complexes have not been very thoroughly investigated. Baba and Nakano reported a high-spin Co(II) complex, [Co(II)(Tbz)<sub>2</sub>] (Tbz=hydrotris(2-mercaptobenzothiazolyl)borate), with an octahedral Co(II) core [85]. In addition, the magnetic properties and electronic spectrum of the cobalt(II) complex were studied and the ligand-field splitting and nephelauxetic effects of the complex were discussed.

### 7.3.3 Preparation of Multinuclear Complexes by Bridging with Thioamide Ligands

The aforementioned TA-based complexes were mainly based on single molecules with a few exceptions. However, the development of multistep redox systems and multispin control are also important for bioinorganic chemistry and materials science, for example, in metal organic frameworks.

In this section, initially, the bridging coordination mode of pySH will be reviewed. Deprotonated pySH plays an important role as a bridging ligand. Mainly, two types of complexes have been reported. The structures shown in Scheme 7.22 are called “lantern-shaped” and “half-lantern-shaped” complexes. Both types of binuclear complexes represent a topic of intense research not only from theoretical point of view

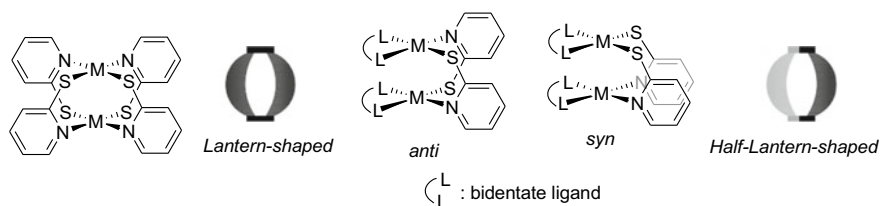




**Scheme 7.21** **a** Available cyclized thioamides for the preparation of soft scorpionate ligands, **b** representative structures of scorpionate complexes with pyS-based ligands, and **c** agostic complexes of Group 7 metals

but also due to their potential use in catalysis, biomedicine, and chemosensors for organic molecules and ions.

The Umakoshi group reported that the reactions of *cis*-PtCl<sub>2</sub>(NH<sub>3</sub>)<sub>2</sub> with pySH in dioxane and PtCl<sub>2</sub>(CH<sub>3</sub>CN)<sub>2</sub> with potassium 4-methylpyridine-2-thiolate in toluene yield lantern-shaped binuclear Pt complexes (Scheme 7.23a) [86]. Both Pt complexes react with CHCl<sub>3</sub> and result in binuclear Pt(III) complexes. Further, the Umakoshi group also reported mono, di, and tetranuclear Pd complexes with pySH [87]. The reaction of pySH with Pd<sub>3</sub>(CH<sub>3</sub>COO)<sub>6</sub> results in a binuclear Pd complex, while that



**Scheme 7.22** Two types of bridging mode of pySH for binuclear complexes

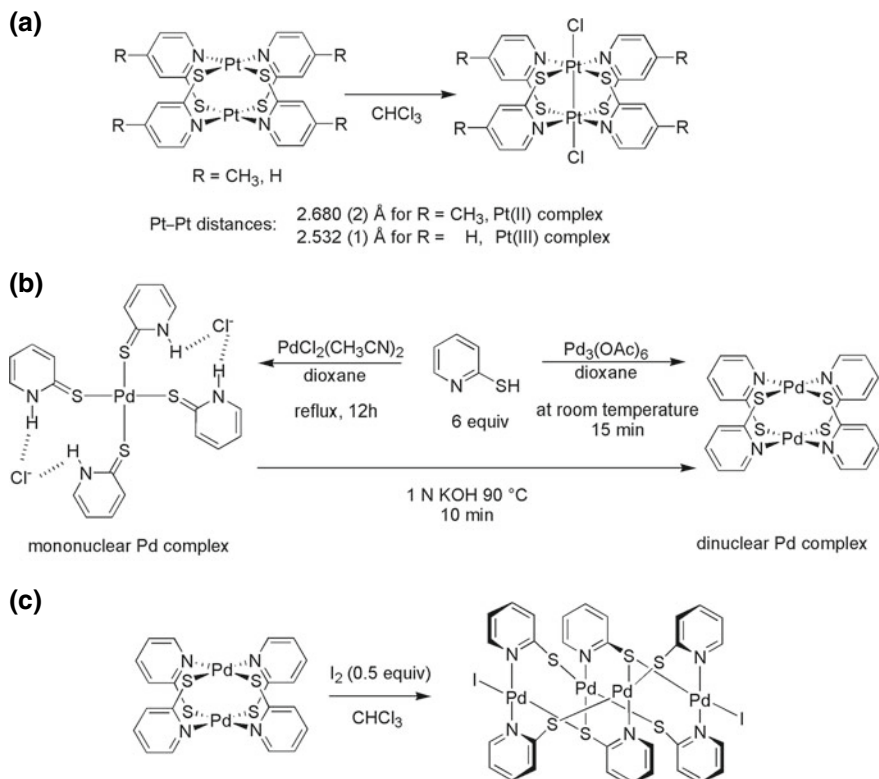
with  $\text{PdCl}_2(\text{CH}_3\text{CN})_2$  yields a mononuclear Pd complex. The cationic mononuclear Pd complex exhibits square planar coordination owing to the presence of four S atoms (Scheme 7.23b). All pyridine N atoms are protonated and linked to chloride ions by  $\text{N-H}\cdots\text{Cl}$  hydrogen bonds. Alkalinization of a mononuclear Pd complex yields a binuclear complex. Two Pd atoms in the binuclear complex are bridged by four ligands in such a way that two *cis*- $\text{PdS}_2\text{N}_2$  units are formed. The Pd–Pd distance is 2.677 (1) Å. Furthermore, the reaction of the binuclear Pd complex with iodine yields a tetranuclear complex (Scheme 7.23c), which exhibits a  $C_2$  symmetry.

A series of binuclear half-lantern-type Pt complexes bridged by pySH were reported by the Kato group (Scheme 7.24) [88, 89]. Subsequently, several groups applied pySH-type cyclized TA (cf. Scheme 7.21a) as a bridging ligand for the synthesis of binuclear complexes [90–92].

Similar complexation reactions were performed on a precursor Pt(II) complex with pySH by the Rashidi group [93]. As shown in Scheme 7.25a, the cycloplatinated(II) complexes of  $[\text{PtR}(\text{ppy})(\text{SMe}_2)]$  ( $\text{R}=\text{CH}_3$  or *p*- $\text{MeC}_6\text{H}_4$ , ppy: 2-phenylpyridine) with pySH (monodentate  $\kappa^1\text{S}$  complexes with the N–H pendant group) are formed along with a dimeric complex  $[\text{Pt}(\text{ppy})(\text{N}^*\text{S})]_2$ , resulting from the reductive elimination of R–H. The kinetics of these reactions were followed using UV–Vis spectroscopy and  $^1\text{H}$  NMR spectroscopy in different solvents, and the mechanisms were suggested for the related reactions. In this context, the reactivity of the half-lantern-shaped binuclear Pt complex with triphenylphosphine has been reported (Scheme 7.25b) [94].

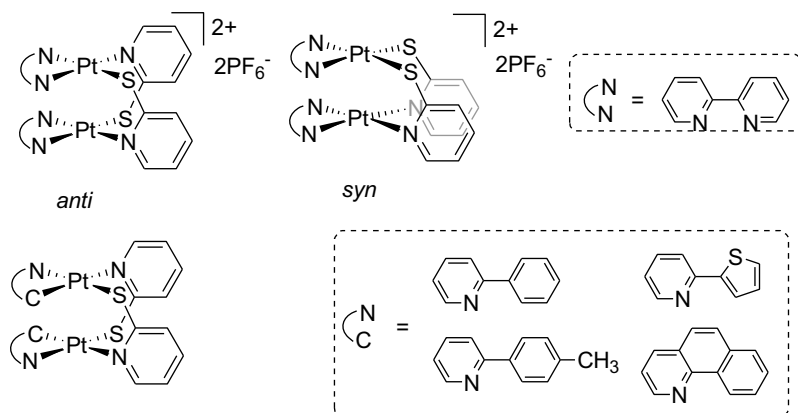
Very little literature is currently available on early transition metal complexes with TA ligands. In 2014 and 2017, bridged-lantern-, lantern-, and half-lantern-shaped multinuclear Mo complexes were reported (Scheme 7.26) [95, 96]. These complexes were further employed for optical analysis.

Other bridging TA ligand complexes are summarized in Table 7.3; several groups reported multinuclear Cu complexes. In most cases, the structural features were determined by single-crystal X-ray analysis. Kapoor et al. reported the structural and magnetic properties of two S- or Cl-bridged Cu complexes [97, 98]. Several pincer-type bridging TA ligands afforded the macrocyclic multinuclear complexes with Group 10 metals [58, 99] or assisted the dimeric complex structures with Cu(II) [58, 100] or Ru(II) cores [59]. In this context, unique examples of metal organic frameworks with TA ligands were reported [101]. Two 3D porous coordination net-

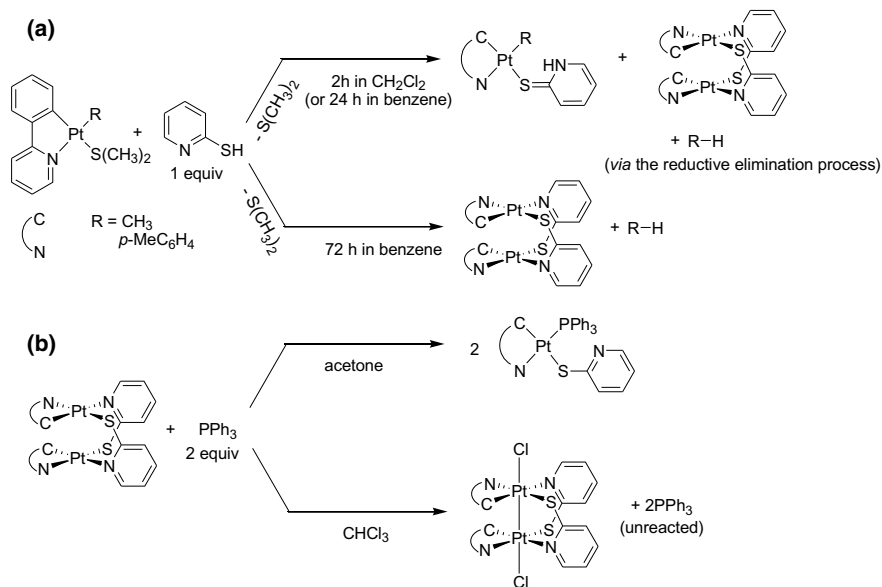


**Scheme 7.23** Lantern-shaped Pd and Pt complexes. **a** Pt(II) and Pt(III) complexes and **b** reaction of pySH and Pd<sub>3</sub>(OAc)<sub>6</sub> under various conditions: heating, no heating, and basic conditions, **c** formation of a tetranuclear Pd complex with I<sub>2</sub> as an oxidant

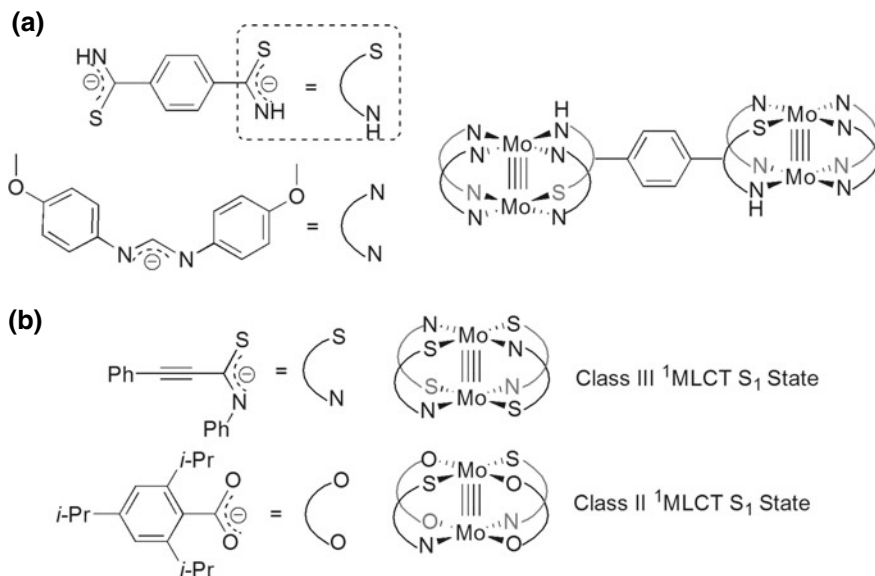
### Kato Group



**Scheme 7.24** Structures of half-lantern-shaped binuclear Pt complexes



**Scheme 7.25** a Reaction between pySH and the Pt(II) precursor complex under various conditions and b the reaction of a half-lantern-shaped binuclear Pt complex with  $\text{PPh}_3$  in common solvents



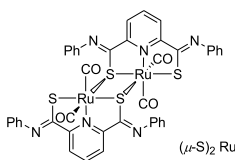
**Scheme 7.26** Bridged lantern-type and lantern-type Mo complexes

**Table 7.3** Various TA-based multinuclear complexes other than pySH-based complexes

Year [ref.]	Metal	Multinuclear complex
2001 [97]	Cu	<p>R = R' = Me      R = <i>n</i>-Bu, R' = <i>t</i>-Bu</p>
2004 [98]	Cu	<p>(<math>\mu</math>-S)<sub>2</sub> Cu<sub>2</sub> complex      (<math>\mu</math>-Cl)<sub>2</sub> Cu<sub>2</sub> complex</p>
2009 [99]	Pd	<p>(<math>\mu</math>-S)<sub>4</sub> Pd<sub>4</sub> complex (Pd<sub>4</sub>S<sub>4</sub> core)</p>
2011 [58]	Cu, Pt	<p>(<math>\mu</math>-S)<sub>2</sub> Cu<sub>2</sub> complex      (<math>\mu</math>-S)<sub>3</sub> Pt<sub>3</sub> complex (Pt<sub>3</sub>S<sub>3</sub> core)</p>
2011 [100]	Cu	<p>(<math>\mu</math>-S)<sub>2</sub> Cu<sub>2</sub> complex      (<math>\mu</math>-Cl)<sub>3</sub> Cu<sub>3</sub> complex</p>

(continued)

**Table 7.3** (continued)

Year [ref.]	Metal	Multinuclear complex
2014 [59]	Ru	 $(\mu\text{-S})_2 \text{Ru}_2$ complex

works were successfully constructed from a pyridine-substituted *N*-heterocyclic TA ligand. Of these, the Ni complex is composed of two identical interpenetrating coordination networks with a dia-topology and contains 1D microporous channels along the axis. Meanwhile, the Zn complex is assembled by 2D square-grid layers stacked in an eclipsed fashion to yield 1D large square channels along the b-axis. In particular, the Ni complex is capable of selectively detecting  $\text{Fe}^{3+}$  ions as a fluorescence “turn-off” sensor [101].

## 7.4 Applications of Thioamide Ligands and Complexes

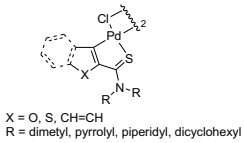
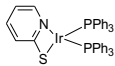
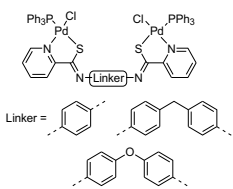
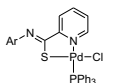
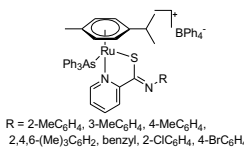
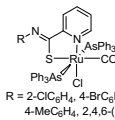
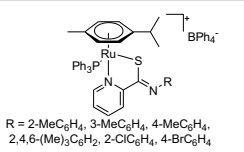
### 7.4.1 Catalytic Activities of Thioamide Complexes

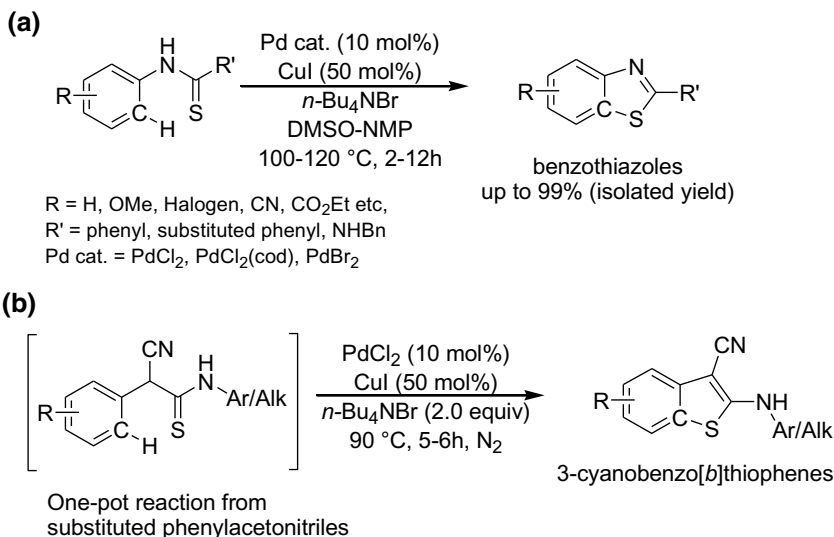
The number of reactions catalyzed by TA-based transition metal complexes is still small compared to the number of reactions catalyzed by phosphine-based-transition metal catalysts. Table 7.4 summarizes the structures of the complexes and the reactions. After Nonoyama’s pioneering efforts, a number of studies on the design and synthesis of furancarbothioamide-based palladacycles were reported [102]. These Pd complexes are thermally stable and not sensitive to air or moisture and can be applied effectively for the Mizoroki–Heck reaction of aryl halides with terminal olefins and in the Suzuki–Miyaura reaction of aryl halides with arylboronic acids. In another study, Ramesh et al. reported the synthesis and catalytic activity of TA-based Ru complexes [103]; the synthesized  $\text{N}^{\wedge}\text{S}$  Ru complexes worked as highly efficient catalysts for the synthesis of secondary or tertiary amides by the coupling of amines and alcohols at low catalyst loadings; a maximum yield of 97% was reported.

### 7.4.2 Thioamide Ligand as a Directing Group for C–H Functionalization

C–H functionalization of aromatic substrates has attracted attention as a route for atom- and step-economical syntheses. To conduct the regioselective cleavage and

**Table 7.4** Various TA-based complexes and their catalytic activities

Year [ref.]	Structure of the catalyst	Catalytic reaction	Remarks
2004 [102]	 <p>X = O, S, CH=CH R = dimethyl, pyrrolyl, piperidyl, dicyclohexyl</p>	Mizoroki–Heck and Suzuki–Miyaura	Aerobic conditions, leading to turnover numbers (TONs) of up to $1 \times 10^5$
2007 [25]		Terminal alkyne dimerization via C–H activation	<i>E</i> -selectivity
2011 [104]	 <p>Linker =</p>	Mizoroki–Heck	Binuclear complexes
2012 [105]		Suzuki–Miyaura	Electrically deactivated aromatics
2012 [106]	 <p>R = 2-MeC<sub>6</sub>H<sub>4</sub>, 3-MeC<sub>6</sub>H<sub>4</sub>, 4-MeC<sub>6</sub>H<sub>4</sub>, 2,4,6-(Me)<sub>3</sub>C<sub>6</sub>H<sub>2</sub>, benzyl, 2-ClC<sub>6</sub>H<sub>4</sub>, 4-BrC<sub>6</sub>H<sub>4</sub></p>	Oxidation of alcohols	Oxidation of a series of alcohols in the presence of <i>N</i> -methylmorpholine- <i>N</i> -oxide
2014 [103]	 <p>R = 2-ClC<sub>6</sub>H<sub>4</sub>, 4-BrC<sub>6</sub>H<sub>4</sub>, 4-MeC<sub>6</sub>H<sub>4</sub>, 2,4,6-(Me)<sub>3</sub>C<sub>6</sub>H<sub>2</sub></p>	Synthesis of amides	Aerobic conditions for the coupling of a wide range of amines and alcohols
2015 [4]	Thiobenzanilide + CuCl <sub>2</sub>	Azide-alkyne [3+2] Huisgen cycloaddition reaction	Mild reaction conditions, high yield
2016 [107]	 <p>R = 2-MeC<sub>6</sub>H<sub>4</sub>, 3-MeC<sub>6</sub>H<sub>4</sub>, 4-MeC<sub>6</sub>H<sub>4</sub>, 2,4,6-(Me)<sub>3</sub>C<sub>6</sub>H<sub>2</sub>, 2-ClC<sub>6</sub>H<sub>4</sub>, 4-BrC<sub>6</sub>H<sub>4</sub></p>	Transfer hydrogenation of ketones	Easy recovery of the catalyst and reuse at least three times



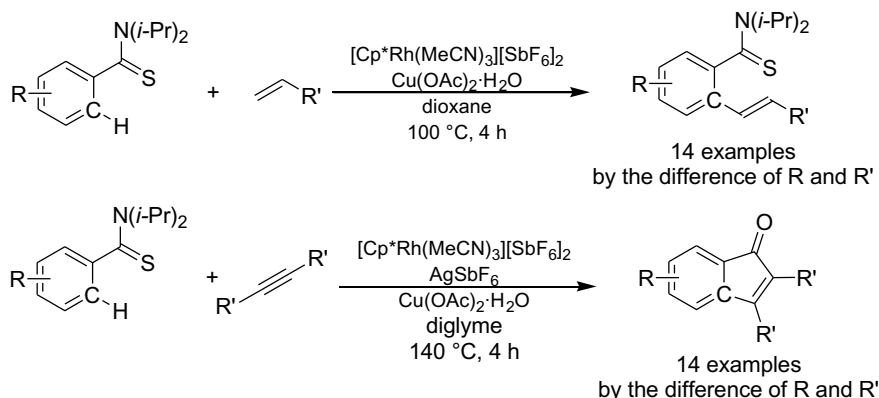
**Scheme 7.27** Intramolecular C–H functionalization and resulting C–S bond formation

functionalization of C–H bonds, several amides have been developed for use as directing groups in metal-catalyzed C–H functionalization, which induces *ortho*-C(sp<sup>2</sup>)–H bond cleavage followed by cyclometallation [108–110]. As described earlier, the TA group also induces C–H bond cleavage of aromatic substrates and forms cyclometallated transition metal complexes. However, the application of TA as the directing group in C–H functionalization reactions has been far less explored. This could be owing to its tight coordination with the metal centers of catalysts, which renders the following reaction less effective. Thiocarbonyl groups also directly react with phosphine, the catalyst, and the catalyst metals to yield the corresponding metal sulfides, which are catalytically inactive [111]. Alternatively, the cyclometallation of TAs was accompanied by C–S bond formation; catalytic intramolecular oxidative arylation led to benzothiazoles [112] and benzo[*b*]thiophenes [113] (Scheme 7.27). Furthermore, several recent studies on TA compounds revealed unique C–H functionalization reactions.

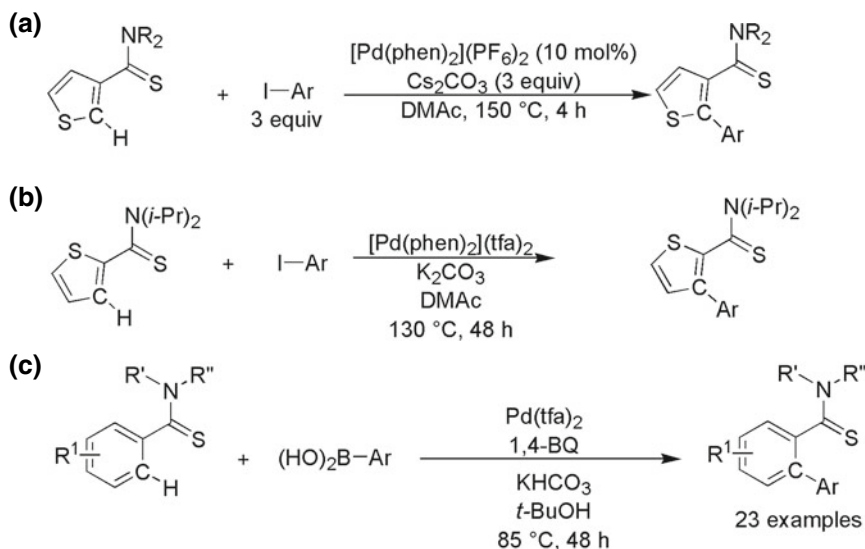
Rhodium-catalyzed direct coupling of benzothioamides with alkenes proceeded smoothly via *ortho*-C–H bond cleavage to yield the corresponding *ortho*-alkenylated products; aromatic TAs also couple with alkynes under similar conditions accompanied by desulfurization and C–N bond cleavage to produce indenone derivatives (Scheme 7.28) [114]. In these reactions, the TA group served as the directing group; coordination of the sulfur atom with a Rh(III) center and successive cyclorhodation would take place.

Pd-catalyzed direct C(sp<sup>2</sup>)–H bond arylation of thienyl TAs with aryl iodides was reported by Murai et al. (Scheme 7.29a, b) [115, 116]. Mechanistic studies revealed that the reaction started with the formation of Pd–bisthioamide complexes owing to





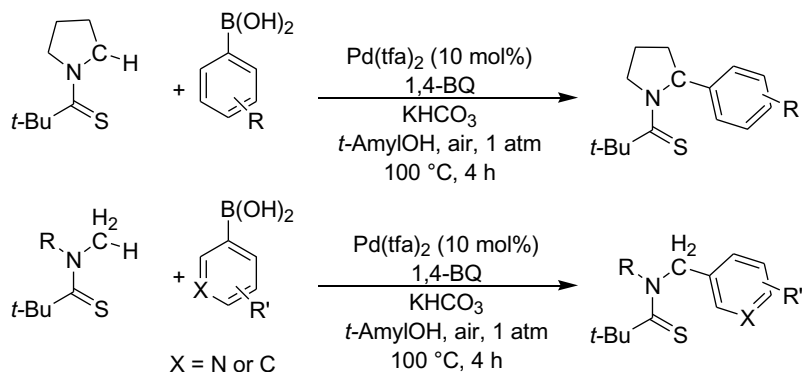
**Scheme 7.28** Intermolecular C–H functionalization and resulting C–C bond formation



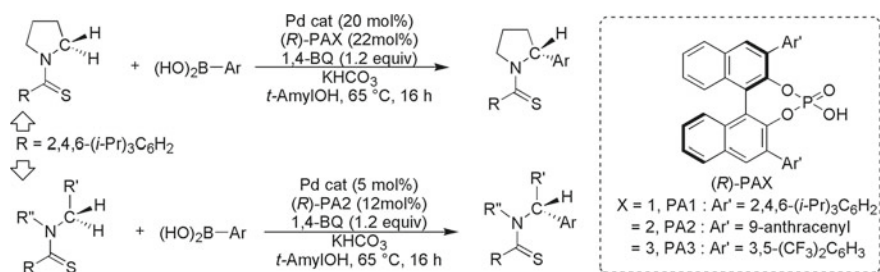
**Scheme 7.29** C–H arylation of thiophenes and benzenes directed by TA substituents

the strong coordination properties of the TA group. Pd-catalyzed arylation of benzothioamides with aryl boronic acids was also conducted by Tang et al. (Scheme 7.29c) [117]; reactions using TAs as the directing groups proceeded with a high functional group tolerance and resulted in good yields.

Taking inspiration from the cyclopalladation of *N*-alkylTAs, Pd-catalyzed  $\alpha$ -C(sp<sup>3</sup>)-H arylation of azacycles and *N*-methylamines with aryl boronic acids was also conducted (Scheme 7.30) [118]. Besides, the use of chiral phosphoric acids enabled enantioselective coupling of the  $\alpha$ -C(sp<sup>3</sup>)-H arylation reaction (Scheme 7.31) [119]. The arylated products can be readily deprotected by the cleavage of TA with methyl-



**Scheme 7.30**  $\alpha\text{-C}(\text{sp}^3)\text{-H}$  arylation of azacycles and *N*-methylamines directed by TA substituent



**Scheme 7.31** Enantioselective  $\alpha\text{-C}(\text{sp}^3)\text{-H}$  arylation of TAs using chiral ligand

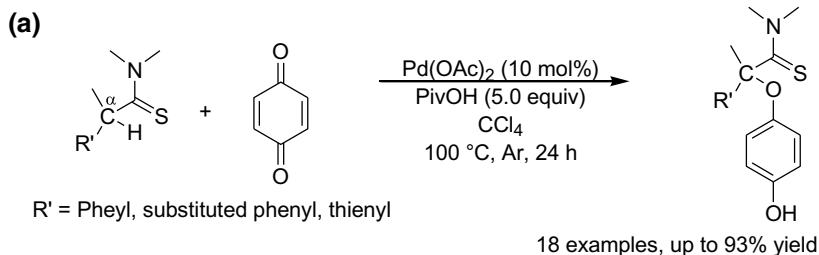
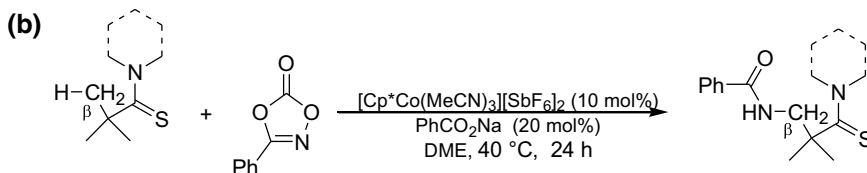
lithium to yield the corresponding amines after protection as Boc-carbamates, while TA can be converted to amides by oxidation with  $\text{Ag}(\text{I})$  salts.

$\text{Pd}$ -catalyzed *p*-hydroxyphenoxylation of benzylic  $\alpha\text{-C}(\text{sp}^3)\text{-H}$  bonds with 1,4-benzoquinone using TA as a directing group was reported by Yu et al. (Scheme 7.32a) [120]. The reaction proceeded at the  $\alpha\text{-C}(\text{sp}^3)\text{-H}$  site of TA rather than at the  $\beta\text{-C}(\text{sp}^3)\text{-H}$  site; this is due to the formation of an unusual four-membered palladacycle.

$\text{Co}(\text{III})$ -catalyzed amidation of TAs with di-oxazolones was also examined (Scheme 7.32b) [121]; the TA moiety served as an efficient directing group to facilitate the  $\text{C}(\text{sp}^3)\text{-H}$  activation of primary methyl groups. Computational studies supported the theory that the cyclometallation of  $\text{Cp}^*\text{Co}(\text{III})$  and TA proceeded by means of an external carboxylate-assisted concerted metallation/deprotonation reaction.

### 7.4.3 Sorption and Extraction Ability of Thioamide Ligands

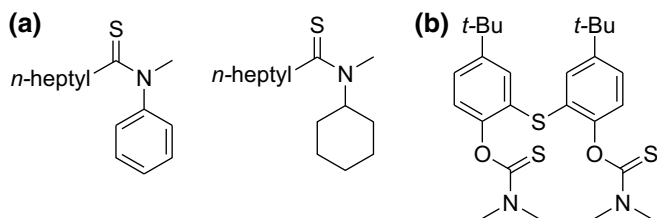
As described earlier, TA exhibits high coordination ability toward transition metals. Therefore, its coordination ability was also evaluated analytically as a sorbent and

S-side  $\alpha$ -C(sp<sup>3</sup>)-H bond activation and functionalizationS-side  $\beta$ -C(sp<sup>3</sup>)-H bond activation and functionalization**Scheme 7.32** S-side C(sp<sup>3</sup>)-H bond functionalization of TAs

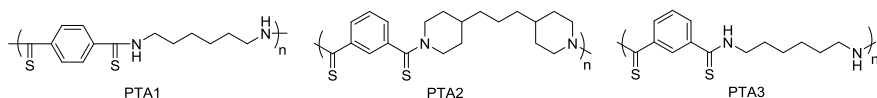
extractant for precious metals [122]. Alternatively, the recovery and recycling of precious metals from chemical, electronics, and plating industry wastes has gained importance from the viewpoint of the effective utilization of resources. Thus, TA compounds have recently been applied for solvent extraction for the recovery of precious metals.

Several recent studies focused on the selective separation and recovery of Pd(II). Paiva et al. investigated two TA derivatives as extractants for Pd(II) from chloride media (Scheme 7.33a) [123]; the toluene solutions of these compounds efficiently extracted Pd(II) from concentrated hydrochloric acid solutions. The extractants showed good selectivity; the coexistence of other metals such as Pt(IV), Rh(III), and Al(III), except for Fe(III), did not practically disturb Pd(II) extraction. Besides, the use of thiourea as a stripping agent enabled successive and cyclic extraction-stripping of Pd(II). A similar concept using TA modified 2,2'-thiobis(4-tert-butylphenol) was reported by Yamada et al. (Scheme 7.33b) [124]; the selective extraction of Pd(II) from leach liquors of automotive catalysts containing ions of Rh, Pd, Pt, Zr, Ce, Ba, Al, La, and Y in chloride media was also demonstrated.

Sorption using polymer sorbents is one of the most practical techniques for the recovery of metals from solutions. Polymeric TAs (PTAs, Scheme 7.34) prepared by the Willgerodt–Kindler reaction were examined as sorbents [125]. The PTAs exhibited excellent sorption behavior for Pd(II) not under only acidic conditions but also under basic conditions, whereas Au(III) and Pt(IV) were hardly sorbed on PTAs under basic conditions [126, 127]. PTA1 (Scheme 7.34) also has the ability to sorb Pd(II) in various organic solutions, which enables the effective separation of Pd(II) from methanolic solutions containing a large amount of Pt(IV). Highly selective

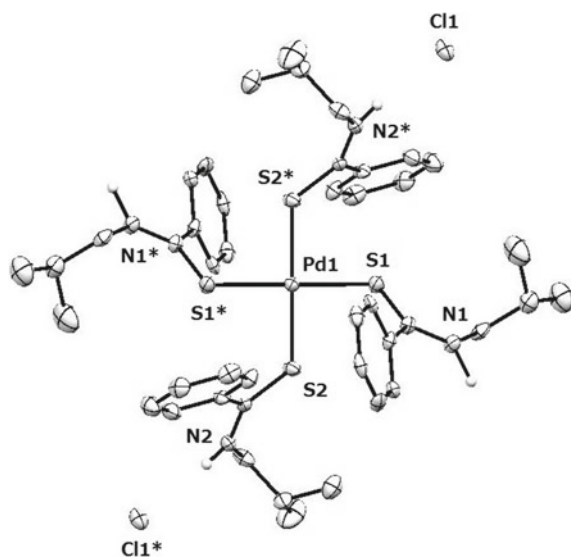


**Scheme 7.33** Structures of TA sorbents



**Scheme 7.34** Structures of polythioamide sorbents

**Fig. 7.2** Molecular structure of  $[\text{Pd}(\text{C}_{11}\text{H}_{15}\text{NS})_4]\text{Cl}_2$



and effective separation techniques for organic liquid waste generally have limited success because of the interference of coexisting organic and inorganic constituents; in this context, the sorption characteristic of PTA1 can contribute to the separation and recovery of Pd(II) in various chemical processes. In one study, a model complex ( $[\text{Pd}(\text{C}_{11}\text{H}_{15}\text{NS})_4]\text{Cl}_2$ ) was also prepared and its molecular structure was determined (Fig. 7.2) [127]. The ORTEP drawing indicates that the presence of a S donor plays an important role in the sorption of Pd(II) by PTA. Chemical modification of lignin with thiourea yields a resin-bearing TA group, which can quantitatively recover Pt(IV) from acidic and neutral aqueous media [128]. Copolymers consisting of amides and

TA were also investigated as sorbents for the treatment of wastewater containing heavy metals such as Cu(II), Cd(II), and Zn(II) [129].

The potential and feasibility of PTAs as Hg(II) sorbents were also evaluated [130]. Because Hg(II) forms a stable complex with the TA ligand [6, 131], PTAs function as excellent sorbents for the removal of Hg(II) from solutions containing large amounts of heavy metals such as Mn(II), Fe(III), Cu(II), Zn(II), and Pb(II) under acidic conditions. Their large capacity (0.70–0.85 g-Hg g<sup>-1</sup>) and the good selectivity of PTA2 and PTA3 were also demonstrated under actual field conditions for the removal of Hg(II) from wastewater.

## 7.5 Conclusion and Outlook

Continuous and considerable progress has been made in the TA-based transition metal complexes. At the early stage of this chemistry, researchers' interests were in whether TAs could afford targeting transition metal complexes or not. However, it has gradually come to understand the strong coordination ability to late transition metals and the usage of thiol/thione tautomeric equilibrium of *sec*-TA; compared to common phosphine ligand, the feature of TA ligands could be expressed as “versatility” which is associated with charge versatility, bridging ligation, or unprecedented ligand design. The second stage of TA-based transition metal complexes thereby involves utilization of TA-based metal complex catalysts for cross-coupling and application in photoluminescent materials. Alternatively, in this decade, the development of C–H functionalization is the most attractive topic in not only for organic synthesis but also organometallic chemistry. In this context, TA motifs assisted a part of the C–H functionalization as directing groups. Noteworthy, the number of reports about medical usage of TA-based transition metal is getting increased. Future research effort on TA-based transition metal complexes would contribute to the development of further tunable photoluminescent complexes, controlled multinuclear molecular assemblies, and catalysts for various applications in the field of materials and organic chemistry.

## References

1. H.-J. Lee, Y.-S. Choi, K.-B. Lee, J. Park, C.-J. Yoon, *J. Phys. Chem. A* **106**, 7010–7017 (2002)
2. G.F. Bordwell, *Acc. Chem. Res.* **21**, 456–463 (1988)
3. F.G. Bordwell, G.-Z. Ji, *J. Am. Chem. Soc.* **113**, 8398–8401 (1991)
4. Z. Mirjafary, L. Ahmadi, M. Moradi, H. Saeidian, *RSC Adv.* **5**, 78038–78046 (2015)
5. A. Ranskiy, N. Didenko, O. Gordienko, *Chem. Chem. Technol.* **11**, 11–18 (2017)
6. M.H. Habibi, S. Tangestaninejad, A. Fallah-shojaie, I. Mohammadpoor-baltork, S.F. Tayyari, G. Emtiazi, R. Hamidimotlagh, *J. Coord. Chem.* **58**, 955–962 (2005)
7. D. Moran, K. Sukcharoenphon, R. Puchta, H.F. Schaefer III, P.V.R. Schleyer, C.D. Hoff, *J. Org. Chem.* **67**, 9061–9069 (2002)
8. G. Dyson, A. Hamilton, B. Mitchell, G.R. Owen, *Dalton Trans.*, 6120–6126 (2009)
9. P. Halder, S. Ghorai, S. Banerjee, B. Mondal, A. Rana, *Dalton Trans.* **46**, 13739–13744 (2017)

10. T. Hamaguchi, K. Ujimoto, I. Ando, *Inorg. Chem.* **46**, 10455–10457 (2007)
11. D. Milstein, J.C. Calabrese, I.D. Williams, *J. Am. Chem. Soc.* **108**, 6387–6389 (1986)
12. J.C. Lee, E. Peris, R.H. Crabtree, A.L. Rheingold, R.H. Crabtree, *J. Am. Chem. Soc.* **116**, 11014–11019 (1994)
13. S. Park, R. Ramachandran, A.J. Lough, R.H. Morris, *J. Chem. Soc. Chem. Commun.*, 2201–2202 (1994)
14. S. Park, A.J. Lough, R.H. Morris, *Inorg. Chem.* **35**, 3001–3006 (1996)
15. K.N. Kouroulis, S.K. Hadjikakou, N. Kourkoumelis, M. Kubicki, L. Male, M. Hursthouse, S. Skoulika, A.K. Metsios, V.Y. Tyurin, A.V. Dolganov, E.R. Milaeva, N. Hadjiliadis, *Dalton Trans.*, 10446–10456 (2009)
16. K. Fukumoto, A. Sakai, T. Oya, H. Nakazawa, *Chem. Commun.* **48**, 3809–3811 (2012)
17. K. Fukumoto, A. Sakai, K. Hayasaka, H. Nakazawa, *Organometallics* **32**, 2889–2892 (2013)
18. M.N. Xanthopoulou, S.K. Hadjikakou, N. Hadjiliadis, E.R. Milaeva, J.A. Gracheva, V. Yu, N. Kourkoumelis, K.C. Christoforidis, A.K. Metsios, S. Karkabounas, K. Charalabopoulos, *Eur. J. Med. Chem.* **43**, 327–335 (2008)
19. A.L. Catherall, S. Harris, M.S. Hill, A.L. Johnson, M.F. Mahon, *Cryst. Growth Des.* **17**, 5544–5551 (2017)
20. A. Buffard, B. Nadal, H. Heuclin, G. Patriarche, B. Dubertret, *New J. Chem.* **39**, 90–93 (2015)
21. H. Brunner, T. Zwack, M. Zabel, *Z. Krist. NCS* **217**, 551–553 (2002)
22. C. Alagöz, D.J. Brauer, F. Mohr, *J. Organomet. Chem.* **694**, 1283–1288 (2009)
23. Y. Sekioka, S. Kaizaki, J.M. Mayer, T. Suzuki, *Inorg. Chem.* **44**, 8173–8175 (2005)
24. V. Miranda-Soto, J.J. Pérez-Torrente, L.A. Oro, F.J. Lahoz, M. Luisa Martín, M. Parra-Hake, D.B. Grotjahn, *Organometallics* **25**, 4374–4390 (2006)
25. K. Ogata, A. Toyota, *J. Organomet. Chem.* **692**, 4139–4146 (2007)
26. T. Satoh, M. Miura, *Chem. Lett.* **36**, 200–205 (2007)
27. H. Mizuno, M. Nonoyama, *Polyhedron* **9**, 1287–1292 (1990)
28. M. Nonoyama, *Transit. Met. Chem.* **15**, 366–370 (1990)
29. M. Nonoyama, K. Suzuki, *Synth. React. Inorg. Met. Org. Chem.* **23**, 29–37 (1993)
30. M. Fukazawa, M. Kita, M. Nonoyama, *Polyhedron* **13**, 1609–1617 (1994)
31. S. Takahashi, M. Nonoyama, *Transit. Met. Chem.* **20**, 528–532 (1995)
32. M. Nonoyama, K. Nonoyama, *Synth. React. Inorg. Met. Org. Chem.* **25**, 569–574 (1995)
33. Y. Nojima, M. Nonoyama, *Polyhedron* **15**, 3795–3809 (1996)
34. W.B. Yu, P.F. Cui, W.X. Gao, G.X. Jin, *Coord. Chem. Rev.* **350**, 300–319 (2017)
35. B. Xu, Y. Wang, Z. Yao, G. Jin, *Dalton Trans.* **44**, 1530–1533 (2015)
36. P.-F. Cui, Y.-J. Lin, G.-X. Jin, *Dalton Trans.* **46**, 15535–15540 (2017)
37. Y.P. Wang, L. Zhang, Y.-J. Lin, Z.-H. Li, G.-X. Jin, *Chem. A Eur. J.* **23**, 1814–1819 (2017)
38. S.M. Meier, M. Hanif, Z. Adhireksan, V. Pichler, M. Novak, E. Jirkovsky, M.A. Jackupeć, V.B. Arion, C.A. Davey, B.K. Keppler, C.G. Hartinger, *Chem. Sci.* **4**, 1837–1846 (2013)
39. E. Sindhuja, R. Ramesh, N. Dharmaraj, Y. Liu, *Inorg. Chim. Acta* **416**, 1–12 (2014)
40. K. Lyczko, M. Lyczko, S. Meczynska-Wielgosz, M. Kruszewski, J. Mieczkowski, *J. Organomet. Chem.* **866**, 59–71 (2018)
41. P.-H. Leung, Y. Qin, G. He, K.F. Mok, J.J. Vittal, *J. Chem. Soc., Dalton Trans.*, 309–314 (2001)
42. D. Pandiarajan, R. Ramesh, *J. Organomet. Chem.* **723**, 26–35 (2013)
43. R.R. Kumar, R. Ramesh, J.G. Małeckı, *New J. Chem.* **41**, 9130–9141 (2017)
44. M. Albrecht, G. van Koten, *Angew. Chem. Int. Ed.* **40**, 3750–3781 (2001)
45. G. van Koten, *Top. Organomet. Chem.* **40**, 1–20 (2013)
46. E. Peris, R.H. Crabtree, *Chem. Soc. Rev.* **47**, 1957–1968 (2018)
47. G. van Koten, *J. Organomet. Chem.* **730**, 156–164 (2013)
48. O.S. Wenger, *Chem. Rev.* **113**, 3686–3733 (2013)
49. L.A. van de Kuil, H. Luitjes, S.D.M. Grove, J.W. Zwikker, J.G.M. van der Linden, A.M. Roelofsens, L.W. Jenneskens, W. Drenth, G. van Koten, *Organometallics* **13**, 468–477 (1994)
50. M. Contel, M. Stol, M.A. Casado, Klink G.P.M. Van, D.D. Ellis, A.L. Spek, G. van Koten, *Organometallics* **21**, 4556–4559 (2002)

51. P. Steenwinkel, R.A. Gossage, T. Maunula, D.M. Grove, G. van Koten, *Chem. Eur. J.* **4**, 763–768 (1998)
52. T. Kanbara, K. Okada, T. Yamamoto, H. Ogawa, T. Inoue, *J. Organomet. Chem.* **689**, 1860–1864 (2004)
53. M. Akaiwa, T. Kanbara, H. Fukumoto, T. Yamamoto, *J. Organomet. Chem.* **690**, 4192–4196 (2005)
54. K. Okamoto, T. Kanbara, T. Yamamoto, *Chem. Lett.* **35**, 558–559 (2006)
55. J. Kuwabara, G. Munezawa, K. Okamoto, T. Kanbara, *Dalton Trans.* **39**, 6255–6261 (2010)
56. T. Koizumi, T. Teratani, K. Okamoto, T. Yamamoto, Y. Shimoi, T. Kanbara, *Inorg. Chim. Acta* **363**, 2474–2480 (2010)
57. T. Teratani, T. Koizumi, T. Yamamoto, K. Tanaka, T. Kanbara, *Dalton Trans.* **40**, 8879–8886 (2011)
58. K. Okamoto, J. Kuwabara, T. Kanbara, *J. Organomet. Chem.* **696**, 1305–1309 (2011)
59. Y. Komiyama, J. Kuwabara, T. Kanbara, *Organometallics* **33**, 885–891 (2014)
60. H. Wang, J. Liu, Y. Deng, T. Min, G. Yu, X. Wu, Z. Yang, A. Lei, *Chem. Eur. J.* **15**, 1499–1507 (2009)
61. V.A. Kozlov, D.V. Aleksanyan, Y.V. Nelyubina, K.A. Lyssenko, E.I. Gutsul, L.N. Puntus, A.A. Vasil'ev, P.V. Petrovskii, I.L. Odinets, *Organometallics* **27**, 4062–4070 (2008)
62. D.V. Aleksanyan, V.A. Kozlov, Y.V. Nelyubina, K.A. Lyssenko, L.N. Puntus, E.I. Gutsul, N.E. Shepel, A.A. Vasil'ev, P.V. Petrovskii, I.L. Odinets, *Dalton Trans.* **40**, 1535–1546 (2011)
63. D.V. Aleksanyan, Z.S. Klemenkova, A.A. Vasil'ev, A.Y. Gorenberg, Y.V. Nelyubina, V.A. Kozlov, *Dalton Trans.* **44**, 3216–3226 (2015)
64. J. Kuwabara, T. Kanbara, *J. Photopolym. Sci. Tech.* **21**, 349–353 (2008)
65. K. Okamoto, T. Yamamoto, M. Akita, A. Wada, T. Kanbara, *Organometallics*, 3307–3310 (2009)
66. Y. Ogawa, A. Taketoshi, J. Kuwabara, K. Okamoto, T. Fukuda, T. Kanbara, *Chem. Lett.* **39**, 385–387 (2010)
67. K. Okamoto, T. Yamamoto, T. Kanbara, *J. Nanosci. Nanotechnol.* **9**, 646–649 (2009)
68. J. Kuwabara, Y. Ogawa, A. Taketoshi, T. Kanbara, *J. Organomet. Chem.* **696**, 1289–1293 (2011)
69. Y. Hong, J.W.Y. Lam, B.Z. Tang, *Chem. Soc. Rev.* **40**, 5361–5388 (2011)
70. H. Honda, Y. Ogawa, J. Kuwabara, T. Kanbara, *Eur. J. Inorg. Chem.* 1865–1869 (2014)
71. H. Honda, J. Kuwabara, T. Kanbara, *J. Organomet. Chem.* **772–773**, 139–142 (2014)
72. O.R. Luca, S.J. Konezny, J.D. Blakemore, D.M. Colosi, S. Saha, G.W. Brudvig, V.S. Batista, R.H. Crabtree, *New J. Chem.* **36**, 1149–1152 (2012)
73. P. Kang, T.J. Meyer, M. Brookhart, *Chem. Sci.* **4**, 3497–3502 (2013)
74. K. Umehara, S. Kuwata, T. Ikariya, *J. Am. Chem. Soc.* **135**, 6754–6757 (2013)
75. H. Tanaka, K. Arashiba, S. Kuriyama, A. Sasada, K. Nakajima, K. Yoshizawa, Y. Nishibayashi, *Nat. Commun.* **5**, 3737 (2014)
76. E.A. Bielinski, P.O. Lagaditis, Y. Zhang, B.Q. Mercado, C. Würtele, W.H. Bernskoetter, N. Hazari, S. Schneider, *J. Am. Chem. Soc.* **136**, 10234–10237 (2014)
77. T. Teratani, T. Koizumi, T. Yamamoto, T. Kanbara, *Inorg. Chem. Commun.* **14**, 836–838 (2011)
78. C.-H. Wang, N.N. Ma, X.-X. Sun, S.-L. Sun, Y.-Q. Qiu, P.-J. Liu, *J. Phys. Chem. A* **116**, 10496–10506 (2012)
79. T. Suzuki, Y. Kajita, H. Masuda, *Dalton Trans.* **43**, 9732–9739 (2014)
80. T. Suzuki, J. Matsumoto, Y. Kajita, T. Inomata, T. Ozawa, H. Masuda, *Dalton Trans.* **44**, 1017–1022 (2015)
81. G. Dyson, A. Zech, B.W. Rawe, M.F. Haddow, A. Hamilton, G.R. Owen, *Organometallics* **30**, 5844–5850 (2011)
82. A. Zech, M.F. Haddow, H. Othman, G.R. Owen, *Organometallics* **31**, 6753–6760 (2012)
83. A. Iannetelli, G. Tizzard, S.J. Coles, G.R. Owen, *Organometallics* **37**, 2177–2187 (2018)
84. K. Saha, R. Ramalakshmi, S. Gomosta, K. Pathak, V. Dorcet, T. Roisnel, J.-F. Halet, S. Ghosh, *Chem. A Eur. J.* **23**, 9812–9820 (2017)

85. H. Baba, M. Nakano, *Inorg. Chem. Commun.* **17**, 177–179 (2012)
86. K. Umakoshi, I. Kinoshita, A. Ichimura, S. Ooi, *Inorg. Chem.* **26**, 3551–3556 (1987)
87. K. Umakoshi, I. Kinoshita, S. Ooi, *Inorg. Chem.* **29**, 4005–4010 (1990)
88. M. Kato, A. Omura, A. Toshikawa, S. Kishi, Y. Sugimoto, *Angew. Chem. Int. Ed.* **41**, 3183–3185 (2002)
89. T. Koshiyama, A. Omura, M. Kato, *Chem. Lett.* **33**, 1386–1387 (2004)
90. Z. Wang, L. Jiang, Z.-P. Liu, C.R.R. Gan, Z. Liu, X.-H. Zhang, J. Zhao, T.S.A. Hor, *Dalton Trans.* **41**, 12568–12576 (2012)
91. V. Sicilia, J. Fornie, J.M. Casas, A. Mart, J.A. Lo, C. Larraz, P. Borja, C. Ovejero, D. Tordera, H. Bolink, *Inorg. Chem.* 3427–3435 (2012)
92. V. Sicilia, P. Borja, A. Martín, *Inorganics* **61188**, 508–523 (2014)
93. M.D. Aseman, S.M. Nabavizadeh, H.R. Shahsavari, M. Rashidi, *RSC Adv.* **5**, 22692–22702 (2015)
94. N. Maryam, H.R. Shahsavari, M.G. Haghighi, M.R. Halvagar, H. Samaneh, B. Notash, *RSC Adv* **6**, 76463–76472 (2016)
95. Y. Shu, H. Lei, Y.N. Tan, M. Meng, X.C. Zhang, C.Y. Liu, *Dalton Trans.* **43**, 14756–14765 (2014)
96. C. Jiang, P.J. Young, S. Brown-xu, J.C. Gallucci, M.H. Chisholm, *Inorg. Chem.* **56**, 1433–1445 (2017)
97. T. Chivers, A. Downard, M. Parvez, G. Schatte, *Organometallics* **20**, 727–733 (2001)
98. R. Kapoor, A. Kataria, P. Venugopalan, P. Kapoor, M. Corbella, M. Rodríguez, I. Romero, A. Llobet, *Inorg. Chem.* **43**, 6699–6709 (2004)
99. J. Liu, H. Wang, H. Zhang, X. Wu, H. Zhang, Y. Deng, Z. Yang, A. Lei, *Chem. Eur. J.* **15**, 4437–4445 (2009)
100. L.E. Karagiannidis, P.A. Gale, M.E. Light, M. Massi, M.I. Ogden, *Dalton Trans.* **40**, 12097–12105 (2011)
101. J. Du, Y. Wei, X. Yang, H. Zhu, *Inorg. Chem. Commun.* **93**, 37–41 (2018)
102. Z. Xiong, N. Wang, M. Dai, A. Li, J. Chen, Z. Yang, *Org. Lett.* **6**, 3337–3340 (2004)
103. E. Sindhuja, R. Ramesh, S. Balaji, Y. Liu, *Organometallics* **33**, 4269–4278 (2014)
104. M.U. Raja, R. Ramesh, Y. Liu, *Tetrahedron Lett.* **52**, 5427–5430 (2011)
105. E. Sindhuja, R. Ramesh, Y. Liu, *Dalton Trans.* **41**, 5351–5361 (2012)
106. M.U. Raja, R. Ramesh, *J. Organomet. Chem.* **699**, 5–11 (2012)
107. A. Kanchanadevi, R. Ramesh, D. Semeril, *J. Organomet. Chem.* **808**, 68–77 (2016)
108. T. Satoh, M. Masahiro, *J. Synth. Org. Chem. Jpn.* **64**, 1199–1207 (2006)
109. G. Shi, Y. Zhang, *Adv. Synth. Catal.* **356**, 1419–1442 (2014)
110. R. Das, S. Kumar, M. Kapur, *Eur. J. Org. Chem.*, 5439–5459 (2017)
111. Y. Mutoh, M. Sakigawara, I. Niiyama, S. Saito, Y. Ishii, *Organometallics* **33**, 5414–5422 (2014)
112. K. Inamoto, C. Hasegawa, K. Hiroya, T. Doi, *Org. Lett.* **10**, 5147–5150 (2008)
113. B. Saraiah, V. Gautam, A. Acharya, M.A. Pasha, I. Hiriyakkanavar, *Eur. J. Org. Chem.*, 5679–5688 (2017)
114. Y. Yokoyama, Y. Unoh, R.A. Bohmann, T. Satoh, K. Hirano, C. Bolm, M. Miura, *Chem. Lett.* **44**, 1104–1106 (2015)
115. T. Yamauchi, F. Shibahara, T. Murai, *Org. Lett.* **17**, 5392–5395 (2015)
116. F. Shibahara, Y. Asai, T. Murai, *Asian J. Org. Chem.* **7**, 1323–1326 (2018)
117. K.-X. Tang, C.-M. Wang, T.-H. Gao, C. Pan, L.-P. Sun, *Org. Chem. Front.* **11**, 2167–2169 (2017)
118. J.E. Spangler, Y. Kobayashi, P. Verma, D. Wang, J. Yu, *J. Am. Chem. Soc.* **137**, 11876–11879 (2015)
119. P. Jain, P. Verma, G. Xia, J. Yu, *Nat. Chem.* **9**, 140–144 (2016)
120. H. Bonds, G. Song, Z. Zheng, Y. Wang, X. Yu, *Org. Lett.* **18**, 6002–6005 (2016)
121. P.W. Tan, A.M. Mak, M.B. Sullivan, D.J. Dixon, J. Seayad, *Angew. Chem. Int. Ed.* **56**, 16550–16554 (2017)
122. L. Zhong'e, Z. Runsheng, S. Daqing, *Chem. Res. Chin. Univ.* **7**, 184–187 (1991)



123. O. Ortet, A.P. Paiva, *Hydrometallurgy* **151**, 33–41 (2015)
124. M. Yamada, M.R. Gandhi, D. Sato, Y. Kaneta, N. Kimura, *Ind. Eng. Chem.* **55**, 8914–8921 (2016)
125. T. Kanbara, Y. Kawai, K. Hasegawa, H. Morita, T. Yamamoto, *J. Polym. Sci. Part A Polym. Chem.* **39**, 3739–3750 (2001)
126. S. Kagaya, E. Sato, I. Masore, K. Hasegawa, T. Kanbara, *Chem. Lett.* **32**, 622–623 (2003)
127. S. Kagaya, E. Tanaka, N. Kawai, I. Masore, E. Sato, K. Hasegawa, M. Kishi, T. Kanbara, *J. Inorg. Organomet. Polym.* **19**, 67–73 (2009)
128. N.N. Chopabaeva, E.E. Ergozhin, *Russ. J. Appl. Chem.* **81**, 231–235 (2008)
129. F.Z. Ramdane, G. Tabak, K. Nassima, A. Benaboura, *Polym. Sci. Ser. B* **59**, 443–451 (2017)
130. S. Kagaya, H. Miyazaki, M. Ito, K. Tohda, T. Kanbara, *J. Hazard. Mater.* **175**, 1113–1115 (2010)
131. C.M.V. Stålhandske, C.I. Stålhandske, M. Sandström, I. Persson, *Inorg. Chem.* **36**, 3167–3173 (1997)

# Chapter 8

## Thioamide-Containing Peptides and Proteins



Taylor M. Barrett, Kristen E. Fiore, Chunxiao Liu and E. James Petersson

**Abstract** Thioamidation of the peptide backbone can have both subtle and profound effects on peptide and protein properties. Oxoamide-to-thioamide substitutions can alter hydrogen bonding networks, metal interactions, peptide folding, and photophysical properties. Thioamides are found in a small number of natural products with intriguing antibiotic and anticancer activities. A thioamide residue is also found in a natural protein that is essential to biological methane metabolism. Recent genetic scanning has shed light on the biosynthesis of these molecules and indicated that many other thioamide-containing peptides and proteins exist. Thioamide modifications have been installed synthetically to investigate the biosynthesis and biological activity of these thioamide natural products, as well as to serve as biophysical probes or to enhance the stability and activity of medicinally relevant peptides. The synthesis of these molecules has required the development of methods for the incorporation of thioamides by solid-phase peptide synthesis and through native chemical ligation of protein fragments. The expanding number of known thioamide natural products, the ability to gain detailed insights into protein folding mechanisms, and recent demonstrations of valuable *in vivo* activity for thioamide-modified peptides highlight the impact of thioamides in peptide and protein chemistry.

**Keywords** Thioviridamide · Methyl-coenzyme M reductase · Closthioamide · Native chemical ligation · Thioprotein

---

T. M. Barrett · K. E. Fiore · C. Liu · E. James Petersson (✉)  
Department of Chemistry, University of Pennsylvania, 213 South 34th Street, Philadelphia, PA  
19104, USA  
e-mail: [ejpetersson@sas.upenn.edu](mailto:ejpetersson@sas.upenn.edu)

C. Liu  
Department of Applied Chemistry, China Agricultural University, Yuanmingyuan West Road 2,  
Beijing 100193, China

© Springer Nature Singapore Pte Ltd. 2019  
T. Murai (ed.), *Chemistry of Thioamides*,  
[https://doi.org/10.1007/978-981-13-7828-7\\_8](https://doi.org/10.1007/978-981-13-7828-7_8)

193

## 8.1 Introduction

### 8.1.1 Scope and Nomenclature

The modification of the peptide backbone has long been of interest to biological and medicinal chemists. Numerous methods for backbone modification with peptide bond analogs exist, including esters, thioesters, *N*-methyl amides, thioamides, selenoamides, alkenes, and fluoroalkenes, along with many others [1]. Chalcogen amide modification is of particular interest as they are nearly isosteric with the native oxoamide and retain many key features, including hydrogen bonding donor and acceptor capabilities. However, due to the instability of seleno- and telluroamide modifications, thioamides are by far the most widely studied of these chalcogen backbone modifications.

It should be noted that there is considerable variability in the nomenclature surrounding thioamides. In the literature, thioamides have been referred to as thionoamides, thioxoamides, endothiopeptides, mercaptoamides, thiopeptide units, thiodepsipeptides, and thiocarboxamides. The suggested IUPAC nomenclature is thioxoamide, along with the  $\psi[\text{C}(=\text{S})\text{-NH}]$  symbol [2]. However, our laboratory prefers to refer to them as thioamides, for the sake of brevity and for consistency with the traditional organic chemistry literature. Also, we and others use the superscript S (<sup>S</sup>) rather than  $\psi[\text{C}(=\text{S})\text{-NH}]$  to indicate the position of the thioamide, as this is much less cumbersome, particularly when describing a peptide with multiple thioamide substitutions. In our earlier publications, we used the prime (') symbol to denote the thioamide, but we have since abandoned this nomenclature, since it may lead to confusion when discussing protease substrates, where the prime symbol is used to indicate a residue's location in relation to the scissile bond. Finally, we note that the term thiopeptides has long been used to refer to natural products that contain thiazole and thiazolene functional groups, such as thiostrepton (**66**; Fig. 8.15). Recent discoveries of the similarity of the biosynthetic mechanisms for the installation of thiazoles, thiazolenes, and thioamides, as well as the discovery that "thiopeptides" such as saalfelduracin (**5**; Fig. 8.2) include all three types of modifications, make it difficult to devise a comprehensive nomenclature.

In this review, we will discuss the work that our group and others have done to synthesize and incorporate thioamides into peptides and proteins. We will also describe the recent elucidation of the biosynthetic pathways for the installation of thioamides into naturally occurring peptides and proteins. Finally, we will discuss the usage of thioamides as spectroscopic and proteolysis probes, along with their usage in injectable peptides for therapeutic and diagnostic applications.

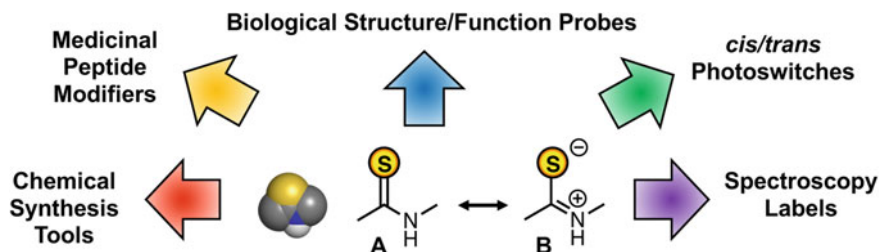


Fig. 8.1 Applications of thioamides

### 8.1.2 Properties of Thioamides

While the thioamide substitution is appealing as an oxoamide isostere, it does have different physicochemical properties, many of which can be understood by considering that the thioamide populates resonance structure **B** in Fig. 8.1 to a greater degree than resonance structure **A**. The increased single bond character in the thiocarbonyl results from a poorer orbital overlap with the carbonyl carbon's  $\pi$  bonding orbitals, making the thiocarbonyl bond slightly longer than the oxocarbonyl bond, with a lower bond dissociation energy [3]. The increased C=N double bond character explains the higher rotational barrier for the thioamides, and the resulting quaternary ammonium character explains the larger dipole moment of the thioamide as well as the lower N–H  $pK_a$  of the thioamide [4, 5]. The decrease in  $pK_a$  correlates with stronger N–H hydrogen bond donation by the thioamide [6, 7]. While one might think that the larger dipole moment of the thioamide would make it a better hydrogen bond acceptor as well, the larger van der Waals radius of sulfur makes the partial negative charge more diffuse and again reduces orbital overlap, significantly weakening the hydrogen bond accepting ability of thioamides [8]. Thioamides exhibit higher reactivity as both nucleophile and electrophile [9, 10]. Thioamides are also known to have greater affinities than oxoamides for soft metals, such as Cu(I), Ag(I), Hg(II), and others [11]. In addition to these effects on covalent and non-covalent interactions, thioamidation red-shifts the  $\pi \rightarrow \pi^*$  absorption and decreases the oxidation potential of an oxoamide [4, 12]. These two properties, respectively, allow thioamides to participate in Förster resonance energy transfer (FRET) and photoinduced electron transfer (PeT) mechanisms when combined with appropriate donor fluorophores [13]. All of these properties are summarized in Table 8.1 and inform our understanding of the roles of thioamides in natural peptides as well as the use of thioamides as synthetic probes.

**Table 8.1** Physical properties of thioamides

Property	Oxoamide	Thioamide
vdW radius (Å) [182]	1.40	1.85
C=X length (Å) [3]	1.23	1.71
Electronegativity [183]	3.44	2.58
C=X...H-N BE (kcal mol <sup>-1</sup> ) [7]	6.1	4.8
N-H pK <sub>a</sub> [4]	17	12
$\pi \rightarrow \pi^*$ absorption (nm) [12]	200	270
$E_{\text{Ox}}$ (V vs. SHE) [4]	3.29	1.21

Abbreviations: vdW radius refers to the van der Waals radius. BE refers to bond energy.  $E_{\text{Ox}}$  is the oxidation potential versus a standard hydrogen electrode (SHE)

## 8.2 Chemical and Biological Synthesis of Thioamides in Peptides and Proteins

### 8.2.1 Thioamides in Natural Peptides and Proteins

Although relatively rare, several thioamide-containing natural products have been isolated and characterized. In 1997, cycasthioamide (**1**), a tripeptide, was isolated from the seeds of the cycad *Cycas revoluta* (Fig. 8.2) [14]. A combination of high-resolution mass spectrometry and NMR studies confirmed the structure of cycasthioamide, which remains the only thioamide-containing natural product isolated from plants. However, no subsequent studies have revealed its biosynthetic pathway or biological activity.

In contrast, the polythioamidated natural product closthioamide (**2a**) has been extensively studied by Hertweck and coworkers (Fig. 8.2). Closthioamide is a secondary metabolite from the anaerobic bacterium *Ruminiclostridium cellulolyticum* (previously known as *Clostridium cellulolyticum*) [15]. At first, isolation was challenging because expression of the closthioamide biosynthetic gene cluster was silenced under normal laboratory conditions. In 2012, an aqueous soil extract was identified that, when added to the culture, induced natural product and secondary metabolite biosynthesis [16]. The main resulting metabolite was closthioamide **2a**, which was found to have promising antibiotic bioactivity against methicillin-resistant *Staphylococcus aureus* (MRSA), as well as vancomycin-resistant enterococci [17]. The potential to strengthen the antibiotic arsenal led Hertweck and coworkers to characterize the biosynthetic mechanism and the structure–activity relationship of closthioamide using synthetic analogs, as described below. Other closthioamides, including compounds **2b–2f**, have been observed in cultures, but their biological activities have not been well characterized [18].

Three types of thioamide-containing ribosomally synthesized and post-translationally modified peptides (RiPPs) have been identified (Fig. 8.2), which

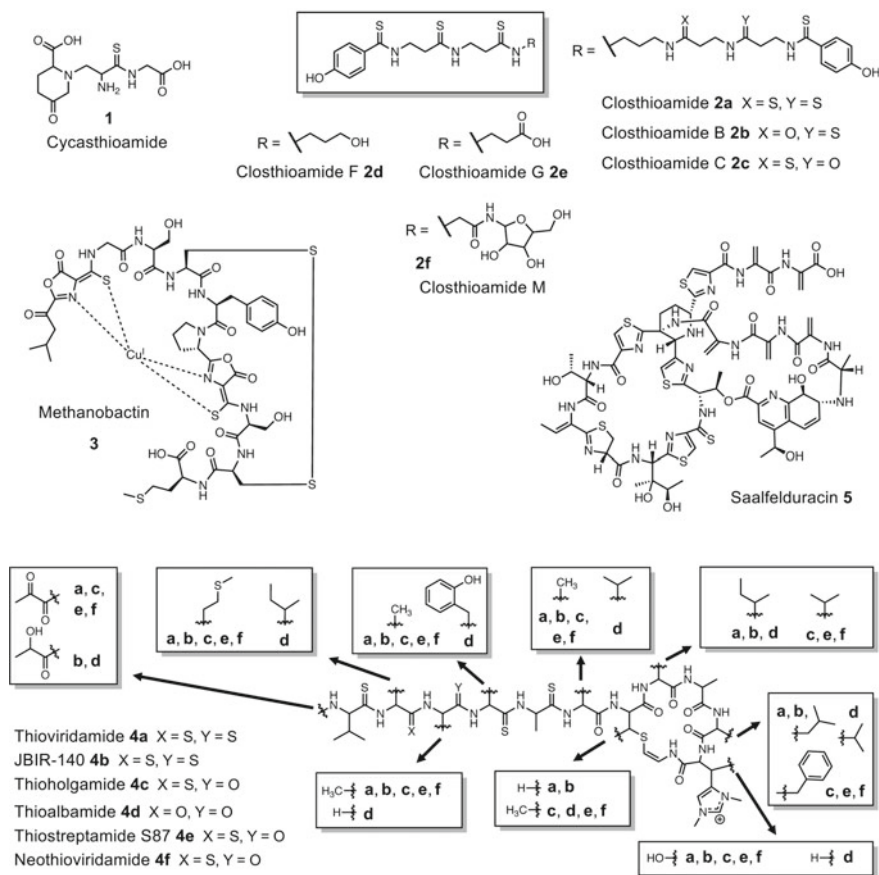


**Fig. 8.2** Structures of peptides with naturally occurring thioamides. Cycstioamide (**1**), clostioamide and clostioamides B, C, F, G, and M (**2a-f**), methanobactin (**3**), thioviridamide (**4a**), JBIR-140 (**4b**), thioholgamide (**4c**), thioalbamide (**4d**), thiostreptamide S87 (**4e**), neothioviridamide (**4f**), and saalfelduracin (**5**)

include methanobactin (**3**), thioviridamide, and related molecules (**4a-f**), as well as saalfelduracin (**5**). RiPPs often contain a diverse assortment of posttranslational modifications (PTMs). RiPPs are classically translated as a precursor peptide which consists of an N-terminal leader sequence and a C-terminal core region. Enzymatic machinery then recognizes and modifies the C-terminal core region to generate the desired PTMs [19]. The RiPP methanobactin (**3**) is produced by methanotrophs. Methanobactin is classified as a RiPP because deletion of the gene encoding its precursor peptide, *mbnA*, results in no production of methanobactin [20]. Methanotrophs metabolize methane using methane monooxygenase (MMO) enzymes. Since particulate methane monooxygenase (pMMO) is copper-dependent, there is a cellular need for copper that is fulfilled by methanobactin, a copper-scavenging peptide. The crys-

tal structure of methanobactin isolated from *Methylosinus trichosporium* was solved in 2004 [21]. This structure revealed two thiocarbonyls coordinated to the Cu(I) ion in a distorted tetrahedral arrangement.

The second identified thioamide-containing RiPP is thioviridamide (**4a**), which selectively induces apoptosis in tumor cells expressing E1A-like oncogenes [22]. This peptide was first isolated by Hayakawa et al. in 2006 from an actinomycete, *Streptomyces olivoviridis*, and NMR analysis confirmed the presence of five thioamide moieties [23]. The biosynthetic gene cluster for thioviridamide was elucidated in 2013, and since then multiple thioviridamide-like structures have been isolated, including JBIR-140 (**4b**) [24], thioholgamide A (**4c**) [25], thioalbamide (**4d**) [26], and thiostreptamide S87 (**4e**) [26]. A recently published structure, neothioviridamide (**4f**) [27], is fairly similar to thioholgamide, but the peptides have differing N termini. This discrepancy has been addressed by the work of Truman and coworkers, who determined that the N terminus reported in the original structure of thioviridamide is an artifact of acetone extraction [26]. They instead suggest that the true structure of thioviridamide has an N-terminal pyruvyl moiety, as shown in Fig. 8.2.

To date, a single protein has been identified that has a thioamide PTM. This protein, methyl-coenzyme M reductase (MCR), catalyzes the reversible oxidation of methyl-coenzyme M (CoM) and coenzyme B (CoB) to release methane (Fig. 8.3) [28]. The enzyme is 300 kDa in size and is organized in an  $\alpha_2\beta_2\gamma_2$  configuration [28]. Tryptic digest of MCRs from various methanogenic archaea (*Methanosarcina barkeri*, *Methanobacterium thermoautotrophicum*, and *Methanopyrus kandleri*) confirmed that all  $\alpha$  subunits contained a thioglycine residue as well as a number of other PTMs [29]. It has been suggested that the thioglycine positioning between the nickel cofactor, CoM, and CoB facilitates the transport of a single electron from a disulfide radical to the nickel [30]. Another possibility is that the thioglycine positions an asparagine residue so that it can hydrogen-bond with the sulfhydryl group of CoB. This decreases the  $pK_a$  of the sulfhydryl group, thereby assisting in deprotonation of CoB [30]. Other data from studies of the  $\alpha$  subunit of MCR from *Methanosarcina acetivorans* (McrA) suggest that the thioglycine increases its thermostability due to its higher *cis/trans* rotational barrier [31]. Since methanogenic archaea can survive in extreme temperature conditions, the stability imparted by the thioglycine modification could have been important in the evolution of the clade.

### 8.2.2 Biosynthesis of Thioamides in Peptides and Proteins

Recently, significant effort has been devoted to discovering the enzymatic machinery that installs thioamides, as well as the biosynthetic gene clusters that encode these enzymes. One class of enzymes that installs the PTMs on RiPPs is the YcaO superfamily. This superfamily utilizes ATP to phosphorylate and activate the carbonyl of the peptide backbone for the generation of PTMs such as azoline heterocycles and azole PTMs [32]. It is also responsible for the thioamidation of McrA and thioamide-containing thiopeptides, as well as thioviridamide and its associated molecules.

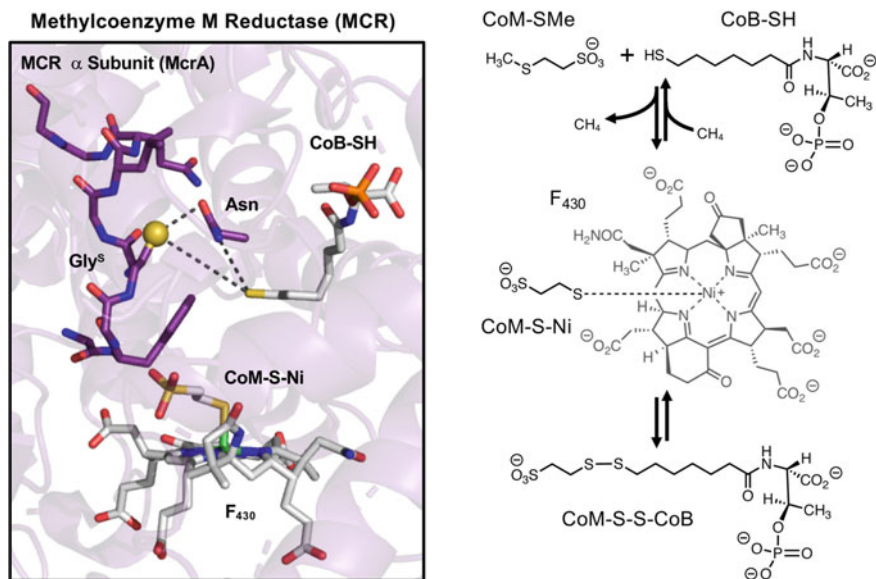


**Fig. 8.3** Methyl-coenzyme M reductase (MCR) structure and function. MCR is the only known protein with a thioamide. (A) This enzyme catalyzes the reversible reduction of methyl-coenzyme M (CoM) and coenzyme B (CoB) to release methane in methanogenic archaea. The reaction is catalyzed by the F<sub>430</sub> cofactor. The thioglycine residue is essential, but its role has not been defined. Left: The active site of the MCR  $\alpha$  subunit (McrA) from the X-ray crystal structure (PDB ID: 1MRO) [28]. Right: A minimal reaction scheme showing the Ni-bound CoM observed in the structure

Discovery of the biosynthetic gene cluster for thioviridamide demonstrated that the *tvaA* gene encodes the precursor peptide and the rest of the cluster consists of ten genes (*tvaC-tvaL*) downstream of a regulatory *tvaB* gene (Fig. 8.4). TvaH, which displays homology to the YcaO superfamily, was hypothesized to control thioamide formation [33]. Adjacent to TvaH in the biosynthetic gene cluster is *tvaI*, which was annotated as TfuA-like. TfuA is involved in the biosynthesis of trifolitoxin, a RiPP antibiotic [34]. Genomic comparison of YcaO domains identified multiple YcaO proteins with TfuA-like partners, defining a class of TfuA-associated YcaOs [35].

Although McrA is not a RiPP, knockout of the *tfaA-ycaO* gene in *M. acetivorans* by Mitchell and Metcalf resulted in no thioglycine generation in McrA (Fig. 8.4) [31]. This association between YcaO-TfuA and thioamidation was further supported when Mitchell showed that purified YcaO and TfuA from *M. acetivorans* could install a thioamide in vitro on a peptide mimicking the native site of thioamidation in McrA [36]. Thioamidation was only possible when both ATP and Na<sub>2</sub>S were supplied to the reaction mixture along with TfuA and YcaO. Biophysical analysis with <sup>31</sup>P NMR supported the proposed mechanism that YcaO phosphorylates and activates the peptide backbone with ATP for thioamidation (Fig. 8.4). The role of TfuA in thioamidation is currently unknown, as well as how the native sulfide



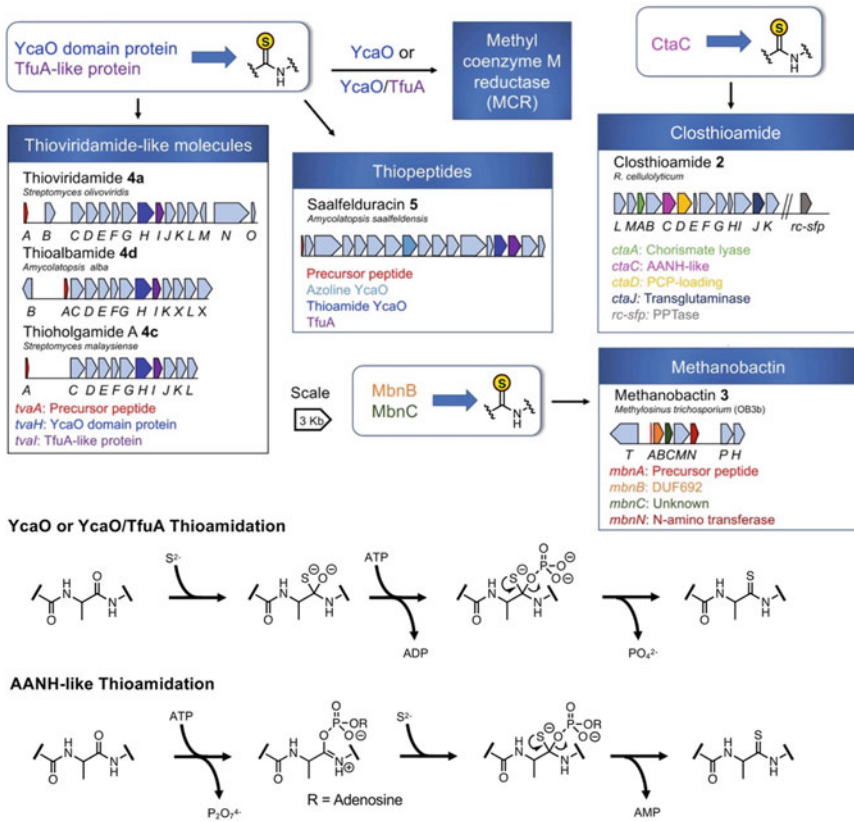


**Fig. 8.4** Thioamide genetics and biosynthesis. Based on the known biosynthetic gene clusters for thioamide-containing peptides and protein, there are three enzymatic routes for thioamidation. YcaO and TfuA generate the thioamide in thioviridamide and related molecules, as well as the thiopeptide, saalfelduracin. The thioglycine in MCR is enzymatically installed by either a YcaO/TfuA pair or a TfuA-independent YcaO [31]. The oxazolone–thioamide pair in methanobactin is generated by MbnB and MbnC [39]. The thioamides in closthioamide are proposed to be installed by an  $\alpha$ -adenine nucleotide hydrolase (AANH)-related enzyme, which is the same enzymatic machinery that generates the thioamide in 6-thioguanidine and thio-tRNA biosynthesis [18]. Bottom: Proposed mechanism for thioamidation by the YcaO superfamily, which utilizes ATP to phosphorylate the peptide backbone and facilitate the generation of the thioamide, as well as other peptide backbone PTMs. Also shown is the potential mechanism for thioamidation by AANH-like CtaC, which differs in that ATP activation is known to precede sulfur attack in AANH-like enzymes [181]

source is delivered. It is hypothesized that TfuA could allosterically activate YcaO for thioamidation.

Interestingly, TfuA is not required for thioamide generation by YcaO; this was demonstrated by the installation of the thioamide on the same McrA peptide mimic with two TfuA-independent YcaOs from *M. kandleri* and *Methanocaldococcus jannaschii*. A structure of the *M. kandleri* YcaO has been published (PDB ID: 6CIB) and shares homology with LynD, an ATP-dependent cyclohydrase for cyanobactin biosynthesis, but has a single Mg<sup>2+</sup> ion rather than two [36]. Due to protein instability, a crystal structure for a TfuA-dependent YcaO is currently lacking, and this has prevented structural comparison between the two enzymes [36].

The extent to which the YcaO-TfuA pair is associated with thioamidation was further tested in another class of RiPPs, thiopeptides. Thiopeptides are macrocyclic peptides characterized by the presence of combinations of thiazoline, thiazole, dehydroalanine, and dehydrobutyrine residues. A [4+2] cycloaddition between two dehydroalanine residues and the amide backbone forms the characteristic pyridine lynchpin of the polymacrocyclic structure. The bioinformatics algorithm Rapid ORF Description and Evaluation Online (RODEO), developed by Mitchell, was used to search for YcaO-TfuA pairs in thiopeptide biosynthetic clusters. This method permitted the discovery of a new thioamide-containing thiopeptide, saalfelduracin (**5**; Fig. 8.2) in *Amycolatopsis saalfeldensis* [37]. The connection between YcaO-TfuA and thioamidation in thiopeptides was further confirmed after observing thioamide incorporation in thiostrepton (**66**; Fig. 8.15) following constitutive expression of a noncognate YcaO-TfuA pair from *Micromonospora arborensis* [37].

Unlike the previously mentioned YcaO-TfuA-facilitated thioamidation, the thioamides in methanobactin are generated by a different enzymatic system. Genome mining of *mbn*-like operons based on the presence of the precursor, *mbnA*, determined that *mbnB* and *mbnC* are also always present (Fig. 8.4) [38]. In vitro, data suggest that MbnB and MbnC form a heterodimer that with the presence of reduced iron and O<sub>2</sub> will install the N-terminal oxazolone and thioamide PTM on the precursor peptide [39]. It remains unknown how the N-terminal leader peptide is cleaved or the mechanism by which the second oxazolone–thioamide pair is generated.

The thioamides in closthioamide (**2a**) are also not generated by a YcaO enzyme. Recently, the CTA gene cluster that is responsible for closthioamide production was identified via genome mining, genome editing, and heterologous expression [18] (Fig. 8.4). Unlike thioviridamide and saalfelduracin, which are RiPPs, closthioamide is a non-ribosomal peptide (NRP). Knockout of a gene encoding for a phosphopantetheinyl transferase (PPTase) in the *R. cellulolyticum* genome resulted in the loss of closthioamide production. This demonstrated that synthesis is “thiotemplated” and therefore proceeds through peptidyl carrier protein (PCP)-mediated elongation, characteristic of the synthesis of an NRP. However, none of the non-ribosomal peptide synthetase (NRPS) gene clusters in the *R. cellulolyticum* genome resembled an assembly that could produce closthioamide. Identification of the biosynthetic gene cluster was achieved following mining for a homolog of the enzyme chorismate lyase, which was hypothesized to produce the aromatic building block of closthioamide, *p*-hydroxybenzoate (PHBA). Knockout of the corresponding gene, *ctaA*, resulted

in no production of closthoamide or associated analogs unless PHBA was supplemented in the culture. The *ctaA* gene was then used to identify the neighboring gene cluster, including *ctaA-ctaM*. The gene *ctaC* is believed to encode the thionating enzyme, as it has homology to alpha-adenine nucleotide hydrolase (AANH). AANH is known to thionate 6-thioguanine and thioamidated tRNA [18], and hence thionation of closthoamide by the CtaC gene product is plausible. Inactivation of the genes *ctaC* and *ctaD* (PCP-loading enzyme) resulted in no production of closthoamide or associated analogs. The *ctaJ* gene product has homology to the transglutaminase protein family, and it is hypothesized that *ctaJ* cross-links the diamino propane linker to the growing precursors. As a result of these findings, Hertweck and coworkers have proposed a mechanism for the biosynthesis of closthoamide (Fig. 8.11, inset). The heterologous production of closthoamide in *Escherichia coli* was attempted, but only thioamide-containing precursors were isolated. Although the full-length product was not produced (for reasons unknown), this was the first occurrence of a thioamide-containing natural product being expressed in *E. coli*.

These advances in genome mining have also allowed for the identification of multiple thioviridamide-like molecules. Since thioviridamide has antiproliferative activity, the discovery of thioviridamide-like molecules is valuable for its potential medicinal purposes. Genome mining for thioviridamide-like molecules has identified 13 homologous biosynthetic gene clusters in actinobacteria (*Streptomyces* spp., *Amycolatopsis alba*, *Micromonospora eburnea*, and *Nocardiosis potens*), as well as another in cyanobacteria (*Mastigocladus laminosus*) [25, 26]. Homologs of the *tvaA* through *tvaI* (except *tvaB*) genes are shared in all 13 biosynthetic gene clusters, and *tvaJ* through *tvaL* are located in all except for one (Fig. 8.4). Although similar, the precursor peptide sequence differs in these organisms, resulting in analogs of thioviridamide. Further characterization and isolation identified thioholgamide, **4c**, from *Streptomyces malaysiense* [25], as well as thioalbamide, **4b**, from *A. alba* (Fig. 8.2) [26]. Similar to thioviridamide, both molecules demonstrated antiproliferative bioactivity against cancerous cell lines. These findings, as well as Mitchell and Metcalf's observation that YcaO-like enzymes occur widely in microorganisms [31], raise the intriguing possibility that natural thioamide-containing peptides and proteins are more widespread than previously appreciated and may harbor interesting thioamide-dependent activity. This expansion of known thioamide-containing natural products prompts renewed interest in methods for incorporating them at specific sites in peptides and proteins.

### 8.2.3 Chemical Synthesis of Thioamides in Peptides

The first reported synthesis of a thioamide was performed in 1815 by Gay-Lussac, where cyanogen and hydrogen sulfide were used to form cyanothioformate and dithiooxoamide [40]. However, the products of this reaction are not very useful for the synthesis of thioamide functionalized molecules. One of the first methods used to create a variety of different thioamides was the Willgerodt–Kindler

reaction, which allowed thioamides to be synthesized from ketones, aldehydes, isothiocyanates, and amides [41]. A key development in the field was the advent of Lawesson's reagent (**6**, 2,4-Bis-(4-methoxyphenyl)-1,3,2,4-dithiadiphosphatane-2,4-dithione) and the use of tetraphosphorous decasulfide ( $P_4S_{10}$ ), which have since served as standard reagents for synthesizing thioamides (Fig. 8.5) [42, 43]. Recently, interest in creating thioamides for uses as biological probes, metal frameworks, and other applications has led researchers to investigate newer, easier methods to synthesize thioamides. These include methods for synthesizing thioamides from methylarenes, aldehydes, ketones, thiols, alkynyl bromides, oximes, and carboxylic acids [44–50]. There has also been an effort to investigate milder conditions to form thioamides, by decreasing the reaction temperature, removing metals, and performing the reactions in different solvents [51–53]. Methods that utilize Lawesson's reagent, elemental sulfur, and  $P_4S_{10}$  produce toxic by-products, so there have been several efforts to create newer, safer thionating reagents (Fig. 8.5). To this end, Bergman and coworkers were able to isolate and use a pyridine- $P_4S_{10}$  complex in acetonitrile to thionate a variety of scaffolds [54]. Interestingly, Yadav and coworkers were able to thionate aldehydes and ketones using *O,O*-diethyl dithiophosphoric acid (**7**) [50]. Similarly, Kaboudin and coworkers reported a method that utilizes ammonium phosphorodithioates (**8**) in the direct conversion of carboxylic acids to thioamides [45]. Due to the difficulty in purifying by-products from reactions with Lawesson's reagent, Ley et al. developed a solid-phase thionating reagent (**9**) that is able to convert secondary and tertiary amides to thioamides [55]. This solid-phase thionating reagent can be removed from the reaction mixture using a simple fritted funnel, which makes purification significantly easier. In an alternative approach, Kaleta and coworkers have created fluorinated derivatives of Lawesson's reagent (**10**) that can be removed from the reaction by extraction [56, 57].

For the incorporation of thioamides into peptides, the use of reagents that are compatible with standard peptide synthesis methods is highly desirable. To our knowledge, the first synthesis of a thiopeptide was completed in 1911 by Johnson and Burnham, where they produced thioimidated glycine derivatives by reactions of nitriles with hydrogen sulfide [58]. However, it was not until 1973 that the first thioamide derivative of a complex peptide was made, when du Vigneaud and coworkers synthesized a thioamide analog of oxytocin (**49**; Fig. 8.12) [59]. They first synthesized thioglycinamide by thionating *N*-benzoyl-glycinamide with  $P_4S_{10}$ . The thioglycinamide was then incorporated into a tripeptide fragment using solution phase peptide synthesis. Finally, this tetrapeptide was coupled to the cyclic core of oxytocin. The incorporation of thioamides into short peptide fragments for later inclusion into a larger peptide paved the way for the rational synthesis of thiopeptides.

Direct thionation of peptides has also been reported as a method for incorporation of thioamides into the backbone of peptides [3, 60]. In these examples, short peptides containing  $\alpha$ -aminoisobutyric acid (Aib) or  $\beta$ -amino acids are directly thionated with **6**. However, in some cases, a mixture of thionated products is observed. Additionally, Heimgartner et al. reported the synthesis of thionated dipeptides containing Aib by the "azirine/thiazolone" method, which incorporates thioamino acids into a peptide through a ring opening reaction [61]. Initially, epimerization of the  $\alpha$ -carbon

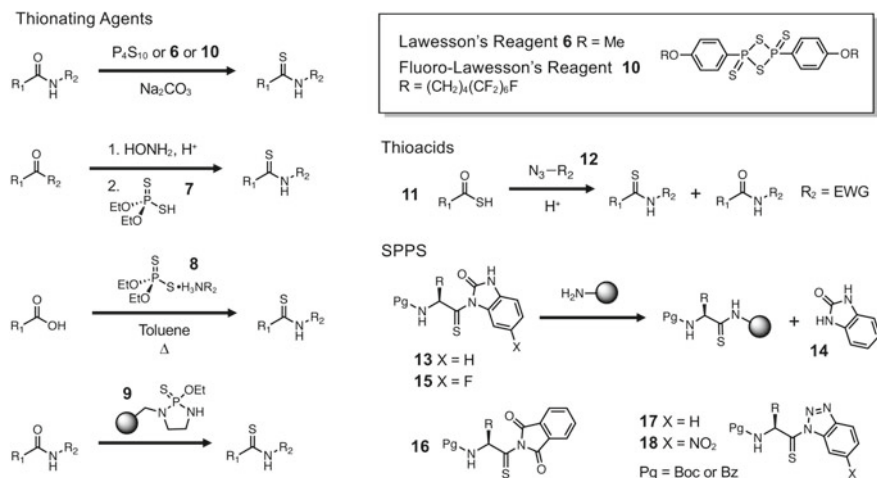


**Fig. 8.5** Previous routes to thioamides. Left: Thionating agents to generate thioamides in small molecules. Right: Thioamide incorporation into peptides using thioacids and azides (EWG: electron-withdrawing group) or activated thiocarbonyl solid-phase peptide synthesis (SPPS) reagents

of the amino acid selected for thionation made this method problematic. Later, it was reported that the use of HCl/ZnCl<sub>2</sub> during the migration of the thioamide from Aib to the *n* + 1 residue abolished epimerization, leading to stereochemically pure thiopeptides [62]. However, the need for including Aib in the peptide sequence still limited the utility of this method.

Thioacids (**11**) have also been used to install thioamides into peptides, both using peptide coupling reagents and reactions with electron-poor azides (**12**). Studies by Williams and coworkers elaborated the mechanistic pathways leading to either oxoamide or thioamide incorporation through reactions with azides [63]. More recently, Hackenberger's group determined that the ratio of oxoamide-to-thioamide peptides could be controlled through optimization of the azide moiety and the pH of the reaction [64]. It was found that electron-poor azides and acidic reaction conditions gave the best conversion to the desired thioamide peptide, but that selectivity was still limited to 11:1 (Fig. 8.5). Thioacids have also been activated for peptide incorporation using benzotriazol-1-yl-oxytripyridinophosphonium hexafluorophosphate (PyBOP) and bis(2-oxo-3-oxazolidinyl)phosphinic chloride coupling reagents [65, 66]. Activation with PyBOP was performed on fluorenylmethoxycarbonyl (Fmoc)-protected amino acids, which enabled easy integration with common solid-phase peptide synthesis (SPPS) procedures, unlike the previous methods. However, it was found that these coupling procedures must be optimized for each amino thioacid, due to the potential for epimerization.

In order to efficiently incorporate thioamides into peptides made by SPPS, Belleau and coworkers established a method using thioacyl-benzimidazolones (**13**) as chemoselective thioacylating agents that were stable and storable (Fig. 8.5) [67].

While this was a valuable first account of a chemoselective thioacylating agent, there were a few drawbacks to this method, including a small loss (2%) of enantiometric purity and a reactive benzimidazole by-product (**14**), reducing the overall yield to 20%. After this report, several others reported similar thioacylating reagents such as fluorobenzimidazolones (**15**), thioacyl-*N*-phthalimides (**16**), benzotriazoles (**17**), and nitrobenzotriazole (**18**) derivatives (Fig. 8.5) [68, 69]. The nitrobenzotriazole thioacylation method reported by Rapoport and coworkers is now by far the most widely used route for high yielding syntheses of thioamide precursors that can be stored and coupled with no observable epimerization [68].

We and others have successfully synthesized Fmoc thioacylbenzotriazole monomers (**22a/22b**) of Ala, Ile, Leu, Phe, Pro, and Val utilizing *N*-Boc-1,2-phenylenediamine (**20a**) and L- and D-Ala, Arg, Asp, Cys, L- and D-Glu, Gly, Ile, Leu, Lys, L- and D-Phe, Pro, Ser, L- and D-Tyr, and Val, as well as D-Trp and L-4-hydroxyproline (Hyp), utilizing 4-nitro-1,2-phenylenediamine (**20b**) as amidating reagents (Fig. 8.6) [70–81]. Fmoc protection of the  $\alpha$ -amine was used due to its compatibility with SPPS methods that do not require HF for sidechain deprotection and resin cleavage. These thioamino acid monomers are stable to storage conditions for several months and can be used without further purification after the ring closing step. Incorporation follows standard Fmoc SPPS procedures, excepting that no additional coupling reagent is required for addition of the thioacylbenzotriazole monomer. Typical yields of thioamide-containing peptides are about 25–50% of the corresponding oxoamide sequence. While this is undesirable, the methods are sufficiently robust that they have been used to synthesize a variety of thiopeptides of up to about 40 amino acids in length, including yeast transcription factor GCN4-p1, villin head piece variant HP35, glucagon-like peptide 1 (GLP-1), gastric inhibitory peptide (GIP), and various  $\beta$ -hairpins [73, 75, 82–84]. To our knowledge, the longest peptide sequence synthesized by SPPS is the B1 fragment of protein (GB1, 56 amino acids) synthesized by the Horne Laboratory, but this was produced in only 1.2% yield [85].

The lower yields of thioamide-containing peptides are caused by side reactions that can arise during SPPS due to the fact that thioamides are more reactive than oxoamides with both nucleophiles and electrophiles. Specifically, in the acidic conditions of resin cleavage, an Edman degradation-like reaction can cause backbone cleavage at the  $n + 1$  position (Fig. 8.7). To avoid this, one must consider shortening cleavage times, which must be balanced with a need to fully deprotect all acid-labile protecting groups. Another side reaction that can occur is a S-to-O exchange when water and base are present (Fig. 8.7). In order to avoid this, our laboratory and others have used anhydrous methylene chloride in the coupling step of the thioamino acid precursor [72]. Finally, epimerization of the  $\alpha$ -carbon of the thioamide residue is a serious issue that can arise during the Fmoc deprotection steps subsequent to incorporation (Fig. 8.7). This epimerization is possible due to the lower  $pK_a$  ( $\sim 13$ ) of the thioamide  $\alpha$ -carbon (see a detailed analysis in the Supporting Information of Szantai-Kis, [85]) [86]. In order to decrease the amount of epimerization, Chatterjee and coworkers decreased the concentration of piperidine used in their Fmoc deprotection solution and shortened the reaction time [79]. While this led to a noticeable decrease in epimerization of the thioamide, they also noted that the yield of their

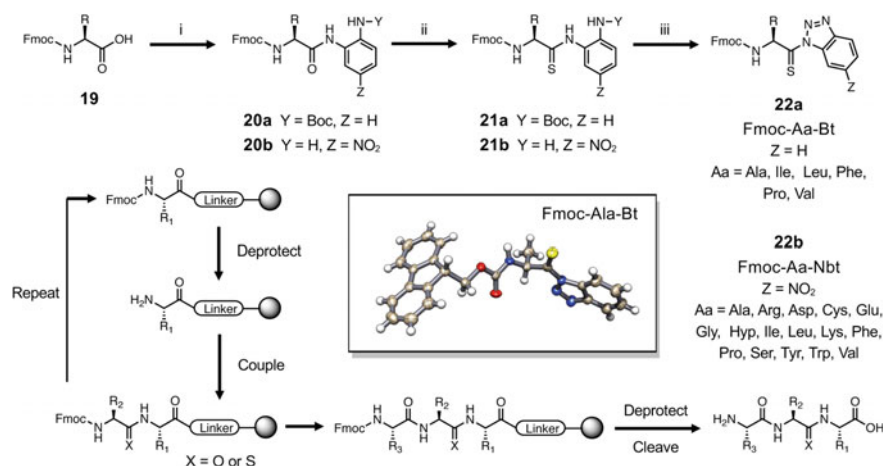


**Fig. 8.6** Thioacylbenzotriazole monomers for solid-phase peptide synthesis (SPPS). Top: Synthesis of benzotriazolide and nitrobenzyltriazolide thioamino acid precursors: (i) 1. *N*-methylmorpholine, isobutyl chloroformate, THF,  $-10\text{ }^{\circ}\text{C}$ , 2. *N*-Boc-1,2-phenylenediamine or 4-nitro-1,2-phenylenediamine; (ii) Na<sub>2</sub>CO<sub>3</sub>, P<sub>4</sub>S<sub>10</sub>, THF; (iii) for benzotriazolide: Trifluoroacetic acid (TFA), then NaNO<sub>2</sub>, 5% H<sub>2</sub>O/AcOH, 0 °C; for nitrobenzyltriazolide: NaNO<sub>2</sub>, 5% H<sub>2</sub>O/AcOH, 0 °C. Bottom: SPPS with thioamides. Deprotect: 20% piperidine is used in deprotections prior to thioamide incorporation, and 2% DBU is used following thioamidation to decrease the amount of epimerization. Couple: For thioamides, Fmoc-Aa-Bt (**22a**) or Fmoc-Aa-Nbt (**22b**); for other amino acids, Fmoc-Aa-OH, (2-(1*H*-benzotriazol-1-yl)-1,1,3,3-tetramethyluronium hexafluorophosphate (HBTU), *N,N*-diisopropylethylamine (DIPEA). Cleave: TFA and other additives, TFA concentrations limited to reduce Edman degradation-like reactions

peptide synthesis decreased significantly due to incomplete Fmoc deprotection. Our laboratory has also investigated methods for decreasing the epimerization of the thioamide. Specifically, we have used a 2% solution of a more hindered base, 1,8-diazabicyclo[5.4.0]undec-7-ene (DBU), in our deprotection solutions for removal of all Fmoc groups subsequent to thioamide incorporation [86]. When treated for a shorter time with the DBU solution, there is a significant decrease in the amount of epimerization of the thioamide.

Due to the difficulty that can come with incorporating thioamides by SPPS, a few groups have studied incorporating thioamides enzymatically. Unverzagt and coworkers utilized chymotrypsin in the enzymatic incorporation of thiodipeptides into growing peptide chains [87]. While this work was only limited to the synthesis of short peptides, it could be applicable to longer sequences upon optimization of the enzyme and protecting groups that are utilized. More recently, Mitchell and coworkers have examined the usage of thiazole/oxazole-modified microcin (TOMM) cyclodehydratases to install thioamides (and other amide modifications) into the backbone of peptides and proteins, a method they call azoline-mediated peptide backbone labeling [88]. Through the use of the Balh cyclodehydratase, Cys, Ser, and Thr residues can be cyclized onto the carbonyl of the *n*-1 residue to form an

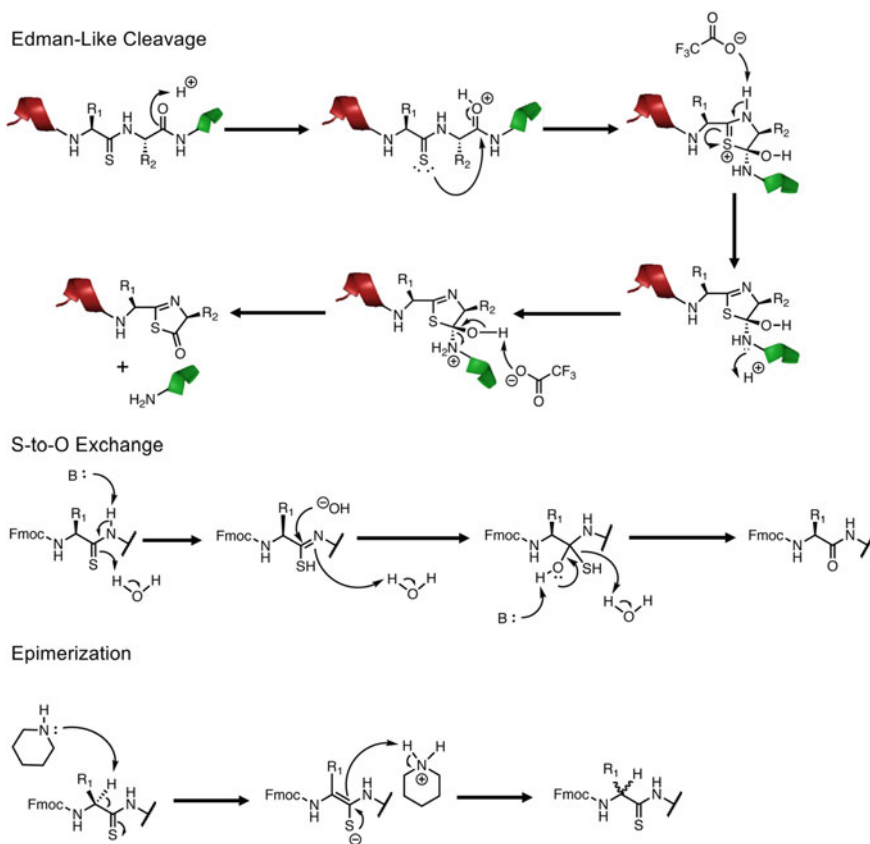


**Fig. 8.7** Side reactions of thioamides. A cleavage reaction similar to Edman degradation occurs through reaction of the thioamide with the  $n + 1$  amide in acidic conditions (i.e., during resin cleavage). S-to-O exchange can occur in basic aqueous conditions due to the lower N-H  $pK_a$  of the thioamide. Epimerization can occur with piperidine during Fmoc deprotection due to the decreased  $C_{\alpha}$ -H  $pK_a$  of the thioamide

azoline. After treatment with KHS, the azoline ring is opened to afford a thioamide N-terminal to the Cys, Ser, or Thr residue. While this reaction is limited in sequence scope, the elucidation of thioamide biosynthesis pathways may lead to more practical enzymatic methods for installing thioamides, for example by use of YcaO enzymes (see above). At this time, SPPS methods remain the most practical way of installing thioamides into peptides of up to about 40 amino acids and coupling of peptide segments must be used to form longer sequences.



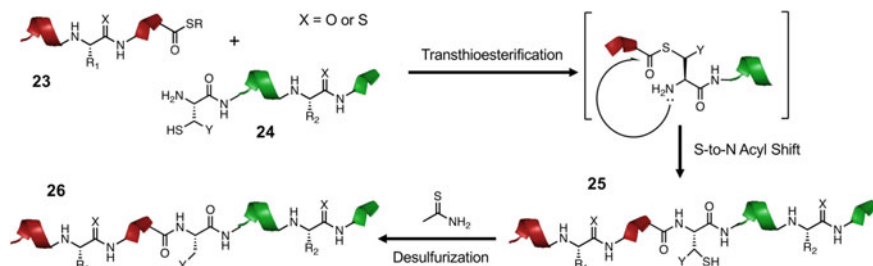


**Fig. 8.8** Native chemical ligation (NCL). NCL generally requires a peptide with a C-terminal thioester (**23**) and a peptide with an N-terminal Cys (**24**) or Cys analog ( $Y =$  amino acid sidechain). Thioamide incorporation is compatible with both the C-terminal thioester portion and the N-terminal Cys portion. In the first step, a transthioesterification reaction between the C-terminal thioester and the N-terminal Cys generates an initial covalent intermediate species. Next, an intramolecular S-to-N acyl shift forms the ligated product (**25**) with a “native” amide bond at the Cys ligation site. Finally, the Cys can be desulfurized to form Ala in the final product protein (**26**). Cys analogs are desulfurized to form the corresponding natural amino acid. In the presence of a thioamide, desulfurization can be performed with the use of organic radical initiator VA-044 and the use of thioacetamide as a sacrificial additive to prevent S-to-O exchange of the thioamide

### 8.2.4 Thioamide Incorporation into Synthetic Proteins

While thioamides can be incorporated into peptides through SPPS, there is currently no way to incorporate backbone thioamides into full-length proteins ribosomally (see Sect. 8.4 for discussion of thioamide dipeptide incorporation by Hecht). Therefore, thioamides must be incorporated into proteins through the use of native chemical ligation (NCL) or expressed protein ligation (EPL) [89]. Briefly, NCL refers to the reaction of a peptide fragment containing a C-terminal thioester (**23**) with a peptide fragment containing an N-terminal Cys or Cys analog (**24**) to yield a peptide product linked by a “native” amide bond. The key step in the reaction is the initial engagement of the two fragments through transthioesterification, as shown in Fig. 8.8. While this step is reversible under the reaction conditions, the subsequent S-to-N acyl shift is not, and the ligated product (**25**) can then be desulfurized to form the final synthetic protein (**26**) if a Cys is not desired at the ligation site. Desulfurization of Cys provides Ala, and a variety of other  $\beta$ - or  $\gamma$ -thiol analogs can be used to produce other amino acids, so that one’s choice of ligation site is not significantly limited when designing a protein retrosynthesis [90]. EPL allows one to produce one of the two fragments by expression and purification from cells to avoid unnecessary synthesis of long stretches of natural amino acids. When we began our study of the applicability of NCL to synthesize thioamide-containing proteins, there were no previous published efforts, and in fact Fischer and coworkers had stated that “the presence of thio-peptide bonds is not compatible with the subsequent synthesis of the thioester which is necessary for the ligation procedure,” presumably referring to HF-based SPPS methods [91]. Thus, much of our early effort was devoted to finding NCL conditions, whereby thioamides would not undergo significant side reactions.

We synthesized short peptides for test ligations where Leu<sup>S</sup> was placed in either the N or the C terminus of fragments with a variety of sequences and lengths [71]. In general, we observed that thioamides were well tolerated in both the C-terminal thioester and the N-terminal Cys containing peptide for NCL, with only a few sequence-specific issues. For example, we found that thioamides are not tolerated at the n-1 position in relation to the C terminus of the fragment due to cyclization caused by the increased electrophilicity of the thioester. Side product formation was observed when Cys disulfides were reduced with *tris*(2-carboxyethyl)phosphine (TCEP), but this was shown to be avoidable upon sparging solvents with argon in order to prevent prior disulfide formation. No side reactions were observed when thiol-reducing agents were used. Thus, we found that one of the most significant barriers to overcome was the need for a robust method for the synthesis of thioamide-containing thioester fragments.

Our initial investigations utilized PyBOP to form the C-terminal thioester (27; Fig. 8.9), which requires that the sidechain-protecting groups remain intact for activation. This can lead to decreased solubility and epimerization of the C-terminal residue at long reaction times, limiting the sequences and sizes of thioester peptides that can be made using this method. To avoid this issue, we investigated using a method developed by Kawakami and MacMillan that would form the thioester through intramolecular cyclization (Fig. 8.9) [92]. In this method, a tripeptide sequence containing Csb-Pro-Gla (28, where Csb is a *t*-butyl thiol-protected cysteine and Gla is glycolic acid) is appended to the C terminus of the peptide of interest through SPPS on Rink amide resin [92, 93]. Upon cleavage of the peptide from resin and subsequent treatment with TCEP, the free Cys residue undergoes an N-to-S acyl shift with the backbone carbonyl of the n-1 residue, yielding a free amine that is able to attack the *O*-ester of the Gla residue to form a diketopiperazine thioester (29). This thioester either can be used directly in a ligation reaction or can undergo transthioesterification with other thiols to yield a different thioester. We utilized this method to create a hexameric peptide containing Leu<sup>S</sup> with the Csb-Pro-Gla sequence that, upon cleavage from the resin, could be used in a one-pot Csb deprotection, cyclization, and ligation reaction with very little side product observed [71].

Our group has also examined the utility of Dawson's *N*-acyl benzimidazolinone (Nbz) method to synthesize a thioamide with a C-terminal Nbz group (31; Fig. 8.9) [70, 94]. 3,4-Diaminobenzyl (Dbz, 30) resin was used to synthesize a Val<sup>S</sup> containing peptide fragment. After peptide synthesis, 4-nitrophenylchloroformate was used to form the *N*-acylurea of the Nbz group. When treated with an N-terminal Cys containing peptide, ligation proceeded with 90% conversion. Despite the high conversion, we were only able to obtain an isolated yield of 15% of the desired peptide. This is likely due to the side reactivity that the Dbz resin can undergo at its secondary amino group. In order to address this issue, many reports suggest that the usage of allyloxycarbonyl (Alloc) protection of this amine can avoid branching and by-products. However, the removal of Alloc groups requires Pd<sup>0</sup>, which desulfurizes thioamides [95, 96]. We investigated a variety of other Fmoc SPPS thioester generation methods, including the use of Botti and Muir's  $\alpha$ -hydroxy Cys analog (Chb), [97, 98] which performed very well in ligations, but was less desirable because the Chb required a

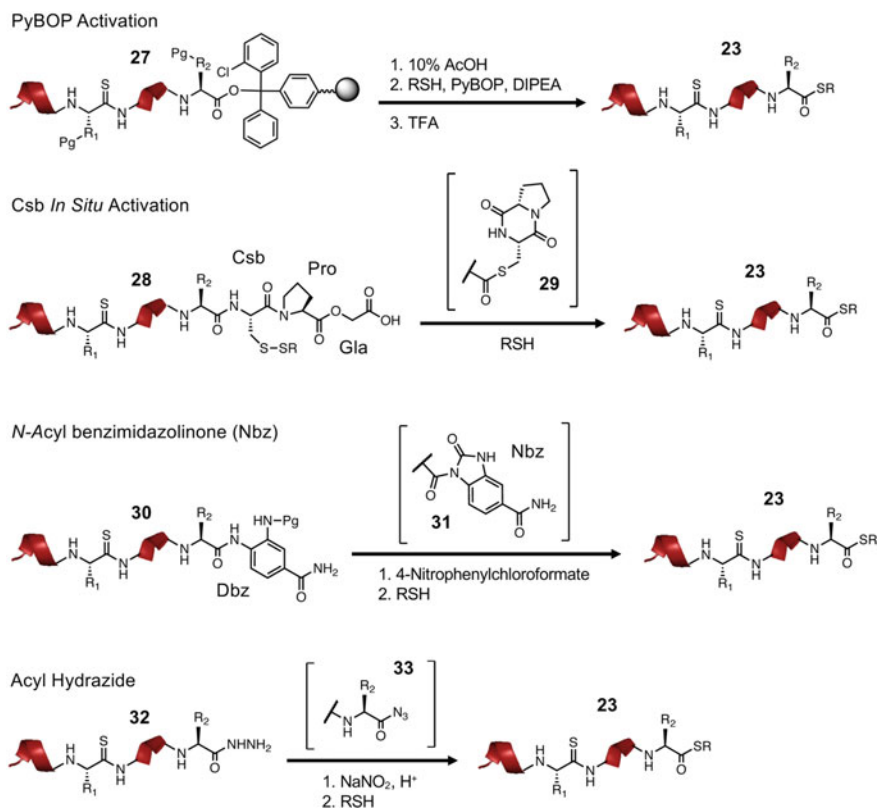


**Fig. 8.9** Thioamide-containing peptide thioester synthesis. PyBOP activation: After cleavage of a peptide (**27**) from 2-chlorotriyl resin with mild acid, leaving sidechain-protecting groups intact, benzotriazol-1-yl-oxytripyrrolidinophosphonium hexafluorophosphate (PyBOP) can be used to activate the carboxy terminus to form the thioester (**23**) for use in ligation. Csb *in situ* activation: Using a Csb-Pro-Gla linker (**28**, where Csb is *t*-butyl thiol-protected cysteine and Gla is glycolic acid), after disulfide reduction, the free Cys is able to attack the Gla ester linkage to form a diketopiperazine thioester (**29**) for use in ligation. The diketopiperazine thioester can be exchanged by treatment with a thiol additive. *N*-Acyl benzimidazolinone (Nbz, **31**): Using resin with a cleavable 3,4-diaminobenzyl (Dbz, **30**) linker, the peptide C terminus can be transformed into an *N*-acyl benzimidazolinone upon treatment with 4-nitrophenylchloroformate. Nbz can be displaced by treatment with a thiol. Acyl hydrazide: After synthesis on hydrazine-loaded 2-chlorotriyl resin and cleavage from the solid phase, the C-terminal acyl hydrazide (**32**) can be reacted with sodium nitrite in acid to form the C-terminal acyl hydrazide (**33**), which can be displaced by treatment with a thiol to form the C-terminal thioester (**23**)

five-step synthesis before resin loading [99]. Therefore, we were intrigued by Liu's 2011 report of the use of C-terminal acyl azides as latent thioesters [100].

We investigated the compatibility of thioamides with C-terminal acyl azides (**33**) in the synthesis of GB1, a 56 amino acid protein that is frequently used as a model system in protein structure investigations. The synthesis of C-terminal acyl azides starts by treating 2-chlorotrityl resin with a 5% hydrazine in DMF solution. This forms a C-terminal hydrazide (**32**) which is stable during the entirety of the peptide synthesis and cleavage. Prior to ligation, the C-terminal hydrazide can be converted to the acyl azide through treatment with  $\text{NaNO}_2$  in acidic buffer. Then, this acyl azide can be converted to the thioester in situ using a thiol (often 4-mercaptophenylacetic acid) in a neutral to a basic buffer solution (Fig. 8.9) [100]. We successfully utilized this method in the ligation of GB1 constructs containing thioamides at positions 5, 6, and 7 [85]. Utilizing the C-terminal acyl azides to access the C-terminal thioester, we were able to synthesize thioamide-containing GB1 constructs with 30–40% yields, after purification.

Our laboratory has also investigated the compatibility of thioamides with methods that are used for multi-part ligations. For a central fragment that will undergo two ligations, the N-terminal Cys needs to be protected so that it will not react with C-terminal thioesters in an intramolecular fashion to cyclize or in an intermolecular fashion to oligomerize. In 2006, Kent and coworkers described a protection method where the Cys could be reversibly masked as a thiazolidine (Thz; Fig. 8.10) [101]. Once the C-terminal thioester has been ligated, the N-terminal Thz can be treated with methoxylamine to reveal an N-terminal Cys that can be used in another NCL reaction. There was some concern that there might be cleavage of the peptide at the thioamide bond due to treatment with a nucleophile like methoxylamine (see Sect. 8.3.5 below). However, we were able to demonstrate that Thz protection was compatible with the three-part ligation of a thioamide-containing peptide with no observable thioamide backbone cleavage [71].

In the pursuit of chemically synthesized proteins, EPL has been an important advance, utilizing the expression of large portions of proteins that can be used in NCL with shorter, synthetic peptides [102]. We have successfully used EPL to incorporate thioamides into  $\alpha$ -synuclein ( $\alpha$ S), calmodulin (CaM), and GB1, with 99% retention of the thioamide [77, 85, 103]. However, we are also interested in double-labeling proteins with thioamide–fluorophore pairs for FRET studies. In order to achieve this, we have used unnatural amino acid mutagenesis to incorporate cyanophenylalanine (Cnf) into  $\alpha$ S<sub>9-140</sub> expressed as in *E. coli*. To obtain an N-terminal Cys, we can express the protein with an N-terminal polyhistidine tag for purification by  $\text{Ni}^{2+}$  affinity chromatography. After this step, the His tag can be removed using the appropriate protease, to reveal an N-terminal Cys for ligation. We have also had success utilizing the endogenous methionine aminopeptidase in *E. coli* to cleave Met from an appended N-terminal Met-Cys sequence. The N-terminal Cys reacts with endogenous aldehydes to form Thz (**34**; Fig. 8.10). Deprotection with  $\text{MeONH}_2 \cdot \text{HCl}$  reveals the N-terminal Cys on the protein for ligation. After purification of the deprotected expressed fragment (**35**), a short peptide containing Phe<sup>S</sup> was ligated for 24 h, resulting in double-labeled protein. However, this method still required the instal-

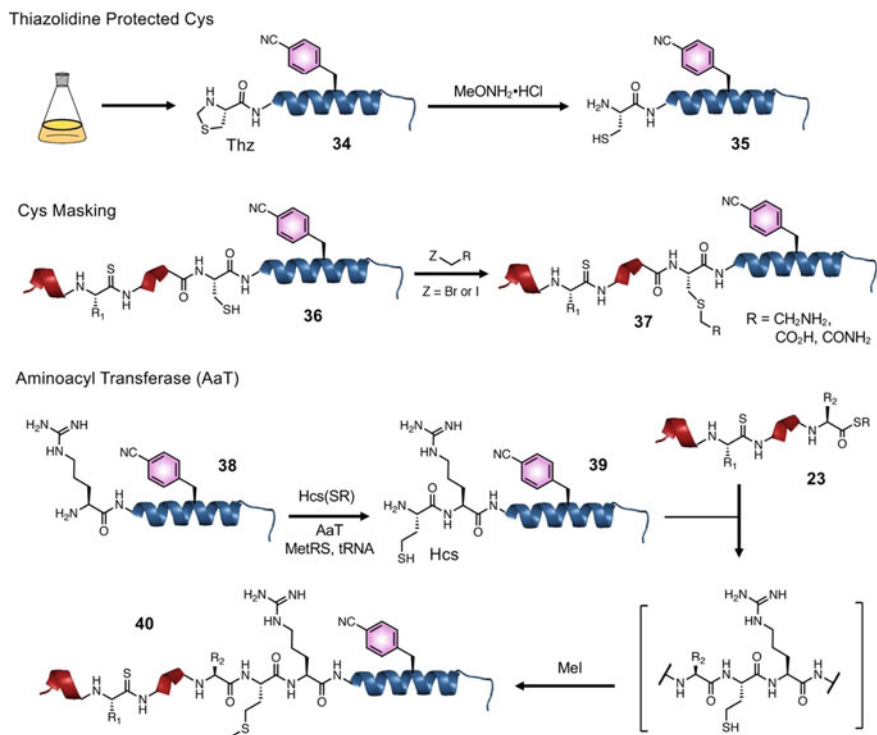


**Fig. 8.10** Thioamide expressed protein ligation (EPL). Thiazolidine protected cys. Proteins expressed with an N-terminal Met-Cys sequence and an unnatural amino acid (**34**) are obtained with the Met residue cleaved by methionine aminopeptidase and the N-terminal Cys converted to a thiazolidine (Thz) by reaction with endogenous aldehydes. Treatment with methoxylamine opens the Thz ring, exposing the Cys residue for ligation (**35**). Cys masking: After ligation (**36**), Cys can be masked as mimics of other amino acids by reaction with alkyl halides (**37**); bromoethylamine yields a Lys mimic, iodoacetic acid, or iodoacetamide yields a Glu or Gln mimic, respectively. Aminoacyl transferase (AaT): AaT and a Met tRNA synthetase (MetRS) can be employed to append an *S*-protected homocysteine (Hcs) to the N terminus of an expressed protein with a terminal Arg (**38**) or Lys (not shown) residue. This segment (**39**) can be used in a ligation reaction with a thioester (**23**) and then masked with methyl iodide to form a Met residue at the ligation site in the product protein (**40**)

lation of a non-native Cys residue in order to perform the chemistry required for ligation. Our group has also shown that C-terminal thioesters can be obtained from expressed proteins by simply incubating an intein-containing protein with MESNa (2-mercaptoethanesulfonate), which will cleave the intein leaving a C-terminal thioester for ligation.

Requirement of a ligation site Cys in order to perform NCL or EPL was a significant initial limitation of the methods which has been largely eliminated through methods for desulfurization of Cys or Cys surrogates after ligation. It has been shown that  $\beta$ - or  $\gamma$ -thiol analogs of many of the natural amino acids can be used in NCL

reactions, with selective desulfurization following, in order to obtain a traceless ligation [104]. The Raney Ni conditions used in early NCL desulfurization reactions were not compatible with thioamides, leading to desulfurization and backbone cleavage [105]. The organic radical initiator VA-044 (2,2'-Azobis[2-(2-imidazolin-2-yl)propane]dihydrochloride) developed by Danishefsky was reported to be selective for desulfurization at Cys, even in the presence of possibly reactive PTMs [106]. Our group was able to demonstrate that thioamides are also compatible with the usage of VA-044 for selective desulfurization, provided that thioacetamide is used as a sacrificial scavenger (Fig. 8.8) [105]. This was then successfully applied to the synthesis of a thioamide-containing analog of GB1.

In addition to desulfurization, reactions which convert Cys to mimics of other amino acids are also valuable ways of masking the ligation site Cys. Previously, it has been reported that Cys can be reacted with bromoethylamine in order to yield a Lys mimic [107, 108]. In this reaction, the protein is dissolved in pH 8.6 Tris buffer and reacted with bromoethylamine in order to obtain the alkylated Lys mimic (37, R=CH<sub>2</sub>NH<sub>2</sub>; Fig. 8.10). In our hands, this reaction has proven to be compatible with thioamides in the semi-synthesis of GB1 constructs. Cys can also be masked to produce Gln/Glu mimics at the site of ligation. In our synthesis of thioamide-containing CaM constructs, a Gln was mutated to a Cys to allow for ligation to occur. After ligation, this free Cys containing CaM was treated with iodoacetamide in order to yield the Gln mimic [85]. Similarly, iodoacetic acid can be used in order to create a Glu mimic at the ligation site [109]. Our group has observed that these masking techniques are compatible with thioamide inclusion provided that Cys alkylation times are limited. These findings allow for a larger sequence space of thioproteins to be synthesized using ligation techniques.

Finally, we have shown that some Cys analogs can be enzymatically transferred to the N terminus of proteins, used in ligation, and then converted to other amino acids (Fig. 8.10). Homocysteine (Hcs) can be used in this manner, as treatment with CH<sub>3</sub>I upon completion of protein synthesis converts it to Met [110]. In order to also expand the scope of possible EPL reactions, our group developed a method to enzymatically incorporate Hcs into proteins [111]. Utilizing the *E. coli* enzyme leucyl/phenylalanyl amino acyl transferase (AaT), a protein with N-terminal Lys or Arg (38) can be functionalized with *S*-(thiomethyl)homocysteine (Hcm) [112–114]. After transfer, the Hcm can be converted to Hcs through TCEP deprotection (39), which allows for subsequent reaction with a C-terminal thioester (23). Hcs can then be converted to Met with CH<sub>3</sub>I (40). We have shown that this can be used with unnatural mutagenesis in the expressed protein fragment to generate Cnf-labeled  $\alpha$ S containing an Asp<sup>S</sup> using Met<sub>5</sub> as the ligation site. AaT can also be used to transfer selenocysteine (Sec) to proteins with N-terminal Lys or Arg. [105] Sec can be used in NCL reactions and selectively deselenized to Ala using TCEP without desulfurizing Cys residues in the ligated protein. Sec can also be converted to Ser [115]. These experiments demonstrate the value of being able to functionalize protein N termini with traceless ligation handles. Our laboratory has investigated mutation of AaT to remove the limitation of specificity for N-terminal Lys or Arg (Unpublished Results), and recently Rozovsky and Wang have developed a tRNA synthetase for

Sec incorporation, which provides a more general method for Sec insertion at ligation sites [116].

Taken together, these developments have enabled the synthesis of large proteins containing thioamides in combination with other unnatural amino acid modifications. We are interested in using these methods to synthesize a variety of thioamide-containing proteins in order to get structural data, such as 2D NMR spectra or a crystal structure, to determine the effect of this substitution on the global structure of the system within which it is placed. Our laboratory is also interested in determining ways to incorporate sidechain thioamides into peptides and proteins as a way to utilize thioamides as biophysical probes with less potential for disrupting the secondary structure of the protein. This method is particularly interesting as there is the possibility that sidechain thioamides can be incorporated ribosomally into the protein of interest [117].

## 8.3 Applications of Synthetic Thioamides

### 8.3.1 Introduction to Applications

The ability to chemically synthesize thioamides enables their site-specific installation to study natural systems and to be used as probes in artificial peptides and proteins. Thioamides have been used to investigate the biosynthesis and the structure/function relationships of natural thioamide-containing peptides. They have also been incorporated to alter the chemical properties of antibiotic peptides in order to better understand their bioactivity, to optimize potency, and to serve as synthetic intermediates for other transformations. Their subtle, yet significant, differences from the native amide bond have been used to probe protease mechanisms and to stabilize peptides for in vivo applications by preventing proteolysis and restricting peptide conformations.

### 8.3.2 Using Synthetic Thioamide Probes to Study Natural Systems: Closthioamide

The most extensive work to date in studying a thioamide natural product has been done by Hertweck and coworkers. Striving to complete a more thorough analysis of the secondary metabolites from *R. cellulolyticum*, they cultured a mutant that over-expressed the antiterminator gene, *nusG* [17]. Closthioamide and hydroxybenzoate were isolated, as well as various analogs of closthioamide. To determine if the analogs were produced as biosynthetic side products or by degradation of closthioamide, deuterium-labeled closamide (the all oxoamide analogs of closthioamide) and fluorinated closthioamide (**46**) were supplemented in the cultured *R. cellulolyticum*

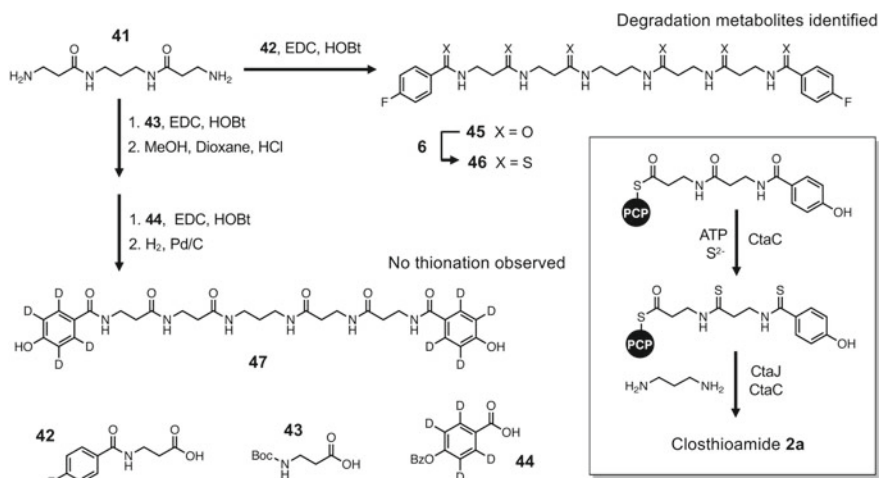


**Fig. 8.11** Thioamide studies of clostioamide. Prior to the identification of the CTA cluster (Fig. 8.4), these clostioamide analogs were used to analyze the biosynthetic pathway [119]. The presence of certain fluorinated fragments after addition of **46** confirmed which of the observed were degradation fragments of clostioamide. Slow S-to-O exchange of **46** to form **45** was also observed. The absence of thionation of deuterated analog **47** demonstrated that biosynthesis of clostioamide did not occur by production of the full oxoamide compound, followed by thioamidation. These data agree with the proposed mechanism of the identified CTA biosynthetic gene cluster, in which CtaC acts on a phosphopantetheinyl-linked tripeptide intermediate on a peptidyl carrier protein (PCP). The union of two tripeptides with a diaminopropane linker occurs concurrently with another thioamidation step to form the final clostioamide (**2a**) product

(Fig. 8.11) [17]. The fluorinated analog was generated by the coupling of a *p*-fluorobenzamide/ $\beta$ -alanine unit (**42**) to a central bis-amide structure (**41**), consisting of two  $\beta$ -alanine units connected by a diaminopropane linker. Treatment of **45** with Lawesson's reagent (**6**) in pyridine was used to generate the final fluorinated clostioamide analog (**46**). The closamide core was made by coupling Boc-protected  $\beta$ -alanine (**43**) to the central bis-amide structure (**41**). Following deprotection, amide coupling was used to introduce a benzyl-protected [D<sub>4</sub>]-*p*-hydroxybenzoyl (**44**). The final deuterium-labeled closamide (**47**) was achieved following ultrasound-mediated hydrolysis. It was determined that some of the previously observed analogs were indeed degradation fragments because fluorine-labeled versions of these analogs were detected after addition of **46**. Since no thionation of **47** occurred, Behnken et al. concluded that thionation occurred during biosynthesis [17]. Considering these results, it was hypothesized that clostioamide is synthesized by the joining of hydroxybenzoate with one, two, or three  $\beta$ -alanine units, while thionation occurs alongside elongation. Two of these units are then linked together by diaminopropane to form the clostioamide product [17]. This hypothesis was further supported when knockout studies revealed the NRPS-type biosynthetic genes responsible for clostioamide production (Fig. 8.11, inset) [18].



Synthetic closthioamide derivatives with single thio-to-oxoamide substitutions did not display the same bioactivity as closthioamide, confirming that the thioamides are vital for antibiotic activity [16]. Although closthioamide has been shown to chelate copper in an elegant fashion, this is not believed to be relevant to its bioactivity [118]. In order to determine which chemical features are crucial for the antibacterial and antiproliferative activity of closthioamide, various analogs were synthesized and assayed for bioactivity [119]. It was found that (1) the six-membered aromatic ring was not essential, but did contribute to antibiotic activity; (2) any analog with a small electron-withdrawing *p*-substituent on the PHBA portion displayed bioactivity; (3) the length of the diamine linker is vital; and (4) the thio-PHBA and two  $\beta$ -thioalanine units are sufficient for bioactivity, and therefore the symmetric structure of closthioamide is not crucial. Later, they used a combination of synthetic and genetic studies to identify the target of closthioamide. In Chiriac et al., they reported that closthioamide impaired DNA replication and inhibited DNA gyrase activity, in particular the ATPase function of gyrase and topoisomerase IV [120].

### 8.3.3 Incorporation of Thioamides to Optimize Bioactivity

In addition to studying their roles in natural peptides, thioamides have been ectopically introduced into peptide natural products as part of structure–activity relationship studies. As noted above, the first example of this type of study was performed by Vincent du Vigneaud in his 1973 analysis of the hormone, oxytocin (**48**; Fig. 8.12). At that time, it was understood that the C-terminal amide of the terminal glycine residue was important for oxytocin bioactivity. The decreased bioactivity of [1-deamino,9-thioglycine]oxytocin (**49**) implicated the importance of hydrogen bond accepting ability over hydrogen bond donation at this position [59].

Similar research has been completed with peptide antibiotics. Lantibiotics are a class of RiPPs classified by cyclic motifs with thioether linkages, but are not known to include natural thioamides. Nisin is a well-studied lantibiotic which is active against MRSA and *Listeria monocytogene*. Nisin binds to the pyrophosphate on lipid II of bacterial cell walls through a series of hydrogen bonds, including one with the N-H of dehydroalanine (Dha) on the A ring fragment (**50**; Fig. 8.12). To increase the hydrogen bonding propensity and further study this binding interaction, the nisin A ring was synthesized with a thioamide in this location (**51**) [121]. The method for solid-phase peptide synthesis of this fragment has been determined, but NMR studies of the structural impact of thioamide incorporation are yet to be published.

Thioamide scanning was performed on the helical lipopeptaibiotic [Leu<sup>11</sup>-OMe] trichogin GA IV at locations terminal and internal to the peptide helix, with the goal of studying the structural implications of thioamide incorporation into various peptide antibiotics that target membranes (**52**; Fig. 8.12) [122]. All thioamide-containing peptides formed right-handed, mixed  $3_{10}/\alpha$ -helices. The membrane permeability of the thiopeptides was 30–50% lower than that of the corresponding oxopeptides. The antibacterial activities were similarly limited, and the analogs were active against

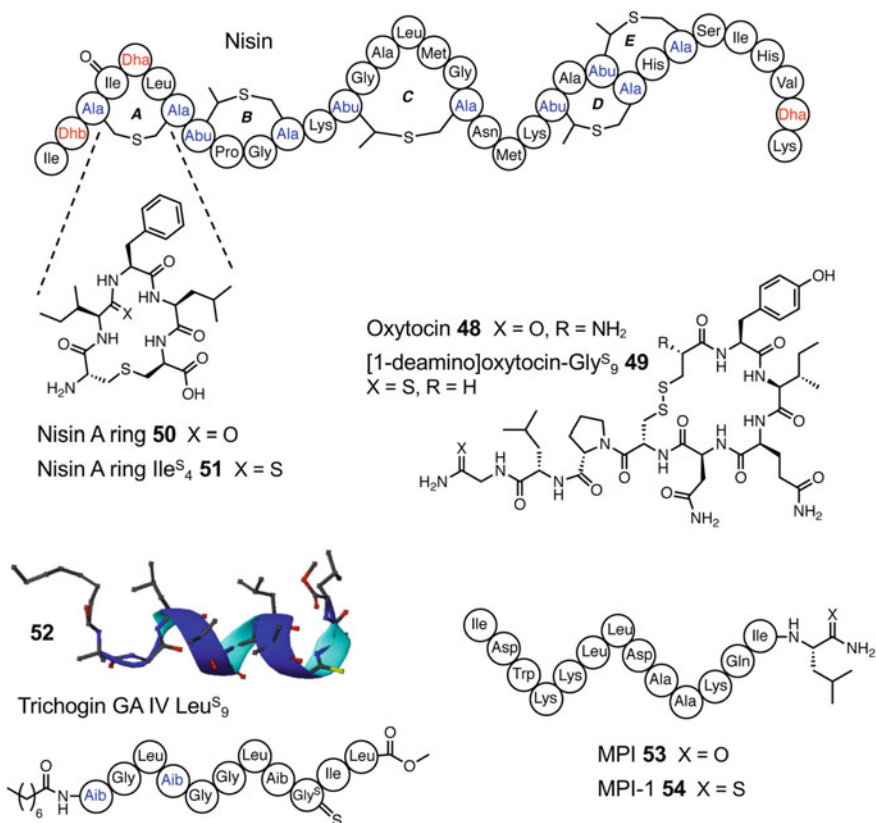


**Fig. 8.12** Thioamides enhancing medicinal peptides. The following are peptide antibiotics of which thioamide-containing derivatives have been synthesized to attempt and increase bioactivity. Nisin: The A ring fragment of nisin (**50**), a lantibiotic food preservative, is essential for bioactivity. At physiological pH, the Dha<sub>5</sub> residue is prone to hydrolysis. To better study the effect of Dha<sub>5</sub> on the structure of the A ring, various analogs were synthesized, including one with a thioamide (**51**). Oxytocin: Vigneaud and coworkers synthesized oxytocin (**48**) with a thioamide at the C-terminal glycine (**49**), which is important for bioactivity. The derivative was less bioactive, but this demonstrated the importance of the Gly amide as a hydrogen bond acceptor. Trichogin GA IV: For helical lipopeptaibiotic [Leu<sup>11</sup>-OMe] trichogin GA IV, thioamide-containing analogs such as trichogin GA IV Leu<sup>S</sup><sub>9</sub> (**52**) exhibited decreased membrane permeability and antibacterial activity [122]. MPI: A peptide antibiotic active against cancerous cell lines, polybia-MPI (**53**), was synthesized with a C-terminal thioamide (**54**) to decrease enzymatic hydrolysis [124]. The derivative was more hydrophobic, which increased its cell lysis potency, but decreased its toxic side effects *in vivo*. Trichogin GA IV structure reproduced with permission from Zotti et al. [122] licensed under CC BY 2.0—published by Beilstein-Institut

fewer bacterial species. Therefore, the introduction of the thioamide did not perturb the helical structure, but it slightly reduced bioactivity.

Another peptide with potential therapeutic value is polybia-MPI (MPI; **53**; Fig. 8.12), a short cationic  $\alpha$ -helical amphipathic peptide isolated from the venom of social wasp *Polybia paulista*. This peptide exhibited promising in vitro activity against cancer cell lines [123]. In order to study its activity in vivo, the C-terminal amide was replaced with a thioamide (MPI-1, **54**) to prevent enzymatic hydrolysis [124]. This resulted in a minimal change to the helical structure, but greatly increased the hydrophobicity. Treatment of cancerous cells with MPI and the more hydrophobic MPI-1 both resulted in the swelling and bursting of the cells. This was further evidenced that these peptides associate within the lipid bilayer and destabilize the membrane. The in vitro anticancer and hemolytic activity of MPI-1 exceeded that of MPI, whereas in vivo studies revealed that MPI-1 was less toxic than MPI. The increased hydrophobicity was hypothesized to result in MPI-1 binding to serum proteins, such as albumin, thereby reducing toxicity. Not only did the introduction of a thioamide develop a new anticancer therapeutic, but it also demonstrated that backbone modification can reduce the general cellular toxicity of antimicrobial peptides.

Recently, Chatterjee and coworkers demonstrated that a thioamide-modified superactive antagonist of pro-angiogenic  $\alpha\beta3$ ,  $\alpha\beta5$ , and  $\alpha5\beta1$  integrins—which are responsible for cancer cell proliferation and survival—showed better efficacy in inhibiting the pro-angiogenic integrins than the drug candidate cilengitide, and suggested the promise of thioamides in markedly improving the affinity, efficacy, and pharmacology of peptide macrocycles (Fig. 8.13) [81, 125]. Verma et al. showed with several NMR experiments that the introduction of a thioamide into a peptide macrocycle restricted conformational flexibility. They used this effect to stabilize active conformations of derivatives of cilengitide (**55**), an *N*-methylated cyclic peptide that failed in Phase III clinical trials against glioblastoma [126]. Intriguingly, thioamide derivatives **57** and **59**, which differ in stereochemistry at residue 4, both were potent against MDA-MB-231 cancer cells. However, the L-Phe<sup>S</sup><sub>4</sub> containing macrocycle **59** was also active against U-87 MG cells, while the D-Phe<sup>S</sup><sub>4</sub> macrocycle **57** was not, in spite of greater similarity to cilengitide. The corresponding oxopeptides **56** and **58** have no significant activity against either cell line. Computational docking of the solution NMR structures of **57** and **59** aligned well to a bound cilengitide molecule in an integrin receptor co-crystal structure [127]. These docking studies allowed them to identify the basis for increased affinity in the optimal thioamide RGD macrocycle as arising from stabilization of this ring conformation. The potential for broader application of this strategy is very exciting as macrocyclic peptides are the subject of much recent attention in the pharmaceutical industry [128].

### 8.3.4 Thioamides in Peptidomimetic Systems

There has been a limited exploration of potential applications of thioamides in structures related to peptides and proteins that are made using similar synthetic methods,

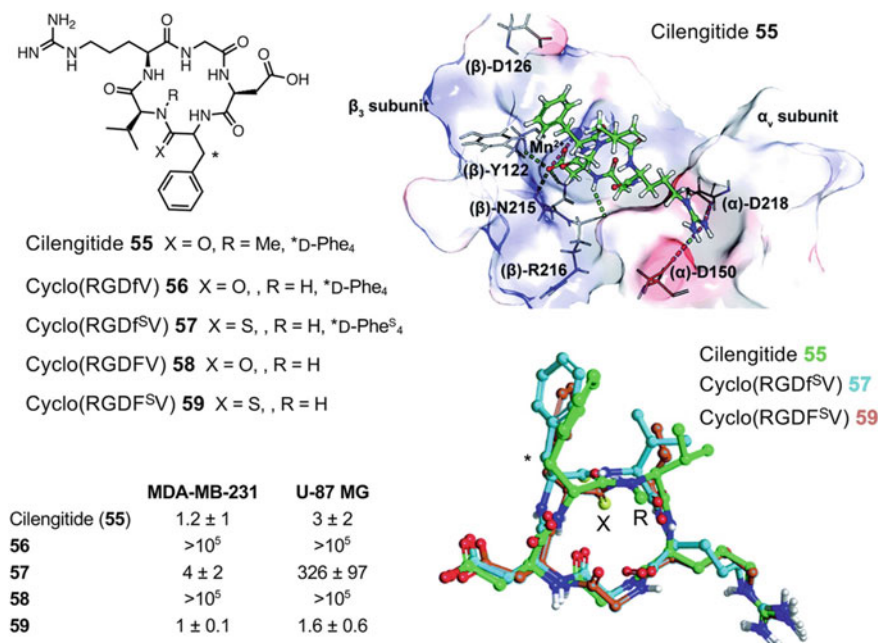


**Fig. 8.13** Thioamide analogs of cilengitide. Top left: Chemical structures of cilengitide (**55**), macrocyclic thioamide analogs **57** and **59**, and the respective oxoamide analogs **56** and **58**. Top right: Structure of cilengitide bound to  $\alpha\beta_3$  integrin from X-ray crystal structure (PDBID: 1L5G). Bottom right: Overlay of integrin bound cilengitide (green) structure docked with NMR structures of **57** and **59**. Bottom left: Cell viability data (IC<sub>50</sub> in nM) demonstrating thioamide-dependent cytotoxicity of **57** against MDA-MB-231 and cytotoxicity of **59** against both MDA-MB-231 and U-87 cancer cells [81]. Figures reproduced with permission from Verma et al. [81] licensed under CC BY 3.0—published by the Royal Society of Chemistry

such as  $\beta$ -peptides and peptoids. Seebach and coworkers studied the effect of incorporating one, two, or three thioamides into the  $\beta$ -peptide H- $\beta^3$ -HVal- $\beta^3$ -HAla- $\beta^3$ -HLeu- $\beta^3$ -HVal- $\beta^3$ -HAla- $\beta^3$ -HLeu-OH ( $\beta^3$ -HXxx refers to the homoligated  $\beta^3$ -amino acid of the corresponding  $\alpha$ -amino acid Xxx) which has a known left-handed, (*M*)- $3_{14}$ -helix (Fig. 8.14) [3]. Thioamides were incorporated into the  $\beta$ -peptides using thioamide dipeptide building blocks prepared using Lawesson's reagent, and there were no reported complications that were new to  $\beta$ -thiopeptides. Incorporation of N-terminal  $\beta$ -thioamides did not change the overall  $3_{14}$ -helix of the peptide. Sifferlen et al. were able to show that  $\beta$ -thiopeptides can switch conformations, like their  $\alpha$ -thioamide counterparts, upon photoirradiation. Olsen and coworkers showed that thioamide incorporation into peptoids (Fig. 8.14) led to thioamide–aromatic interactions that stabilized some of the  $\beta$ -thiopeptoids in the *cis* conformation, likely due to C<sub>sp</sub><sup>2</sup>–H...S<sub>amide</sub> “hydrogen bonds [129].” This was surprising to them as they anticipated seeing  $n \rightarrow \pi^*$  interactions of the backbone carbonyls based on previous work by Raines with thioamides in polyproline II helices and model systems [130,

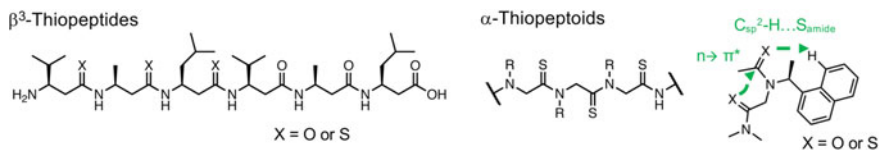


**Fig. 8.14** Thioamide peptidomimetics.  $\beta^3$ -Thiopeptides: Seebach and coworkers synthesized and characterized thioamide analogs of  $\beta^3$ -peptides, showing that properties (including photoswitching) observed in thioamide  $\alpha$ -amino acid peptides were also observed in  $\beta^3$ -peptide.  $\alpha$ -Thiopeptoids: Olsen and Gorske have shown thioamides to be compatible with  $\alpha$ -peptoids as well as  $\beta$ -peptoids. Crystal structure analysis of  $\alpha$ -dipeptoids was used to investigate the role of  $n \rightarrow \pi^*$  carbonyl and aromatic interactions by Olsen

[131]. However, crystal structure analysis revealed that there were no substantial differences with oxoamides in the backbone interactions, but rather in the aromatic interactions. Inspired by this work in  $\beta$ -peptoids, Gorske and coworkers examined the effect of thioamide incorporation on  $\alpha$ -peptoids [132]. They discovered that this  $n \rightarrow \pi^*_{AR}$  interaction can indeed stabilize the *cis* conformation in  $\alpha$ -peptoids as well and is enhanced when an electron-poor aromatic sidechain is present. In all of these works, the authors utilized Lawesson's reagent to selectively thionate the amide bond over the ester bonds present. These studies highlight the potential value of thioamide effects outside of strictly  $\alpha$ -amino acid peptides.

### 8.3.5 Thioamides as Synthetic Intermediates

Thioamides have also been used as synthetic intermediates in the generation of other amide analogs for the study of natural products. This is exemplified in Boger's study of vancomycin (**60**; Fig. 8.15), a glycopeptide antibiotic for bacterial infections [133–136]. Originally discovered in 1954 by Eli Lilly and Co., vancomycin is often considered the “antibiotic of last resort,” used in hospitals to treat MRSA infections. The emergence of vancomycin-resistant strains has prompted interest in the rational design of vancomycin derivatives. Vancomycin binds to the *N*-acyl-D-Ala-D-Ala (**64**) terminus of peptidoglycan cell wall precursors (D-Ala is D-alanine). Resistant strains utilize *N*-acyl-D-Ala-D-Lac instead (**65**, where Lac is lactate). It is believed that the repulsive lone pair interaction between the carbonyl ( $Y=O$  in **60**) of vancomycin and the ester oxygen of *N*-acyl-D-Ala-D-Lac disrupts the binding affinity. The challenge for the rational design came with synthesizing a derivative that could bind both the D-Ala and D-Lac containing substrates.

The  $[\Psi[\text{CH}_2\text{NH}]\text{Tpg}^4]$ vancomycin aglycon derivative (**63**), in which the carbonyl was synthesized as a methylene group ( $Y=\text{H}_2$ ), had a 40-fold increased binding affinity for D-Ala-D-Lac, along with a 35-fold decreased affinity for D-Ala-D-Ala [134]. In order to increase affinity for D-Ala-D-Ala, an amidine derivative (**62**,  $Y=\text{NH}$ ) was synthesized in order to remove the repulsive lone pair interaction, as well as

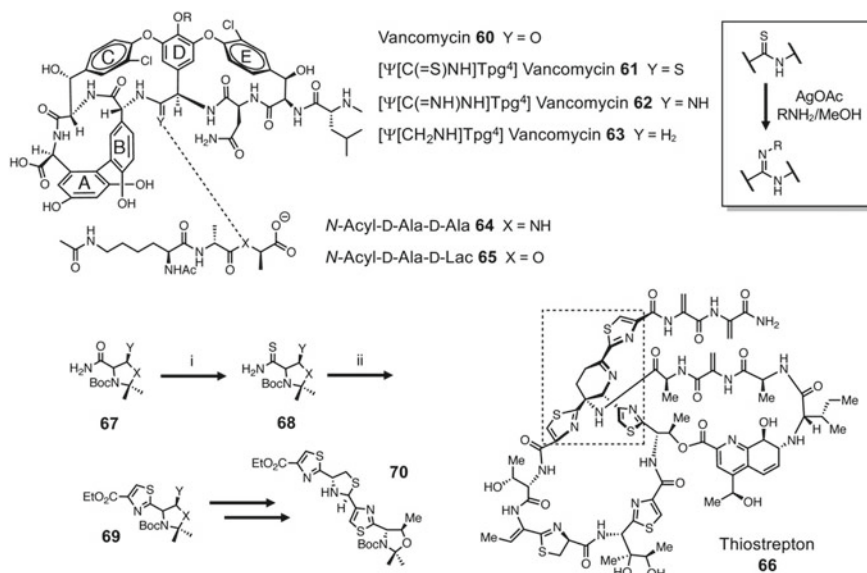


**Fig. 8.15** Thioamides as synthetic intermediates. Top: Vancomycin (**60**, Y=O) binds to the *N*-acyl-D-Ala-D-Ala (**64**) peptidoglycan cell wall precursor, thereby inhibiting bacterial growth. Resistant strains utilize *N*-acyl-D-Ala-D-Lac (**65**), to which vancomycin cannot bind. Synthesized derivatives such as  $[\Psi[CH_2NH]Tpg^4]$ vancomycin aglycon (**63**, Y=H<sub>2</sub>) exhibited increased binding to *N*-acyl-D-Ala-D-Lac **65**, but decreased binding to *N*-acyl-D-Ala-D-Ala **64**. An amidine derivative (**61**, Y=NH) bound well to both **64** and **65** due to its ability to function as both hydrogen bond donor and hydrogen bond acceptor. In order to synthesize this amidine derivative, Okano et al. used a thioamide-containing (**62**, Y=S) intermediate which could be converted to other carbonyl derivatives in the final stages of the synthesis through highly selective, silver-catalyzed reactions [133]. The thioamide derivative exhibited decreased binding to both substrates. Bottom: In the total synthesis of thiostrepton (**66**), Nicolaou and coworkers utilized thioamide precursors (**68**) to synthesize the thiazole rings (**69**) of the central dehydropiperidine core (**70**) [138]. The thioamide precursors were generated by treatment of the L-cysteine (Y=H, X=S)/L-threonine (Y=Me, X=O) derivatives (**67**) using Lawesson's reagent (**6**) as follows: (i) **6**, Na<sub>2</sub>CO<sub>3</sub>, toluene, reflux; (ii) BrCH<sub>2</sub>COCO<sub>2</sub>Et, KHCO<sub>3</sub>/NaHCO<sub>3</sub>, trifluoroacetic anhydride

potentially introduce a hydrogen bond donor to the Lac ester oxygen [136]. This derivative had 600-fold increased binding to D-Ala-D-Lac in comparison with vancomycin aglycon and displayed only twofold decreased binding to D-Ala-D-Ala. The derivative was 1000-fold more active than vancomycin against resistant bacteria in comparison with vancomycin aglycon and vancomycin [137].

In order to synthesize **62**, the authors developed a total synthesis for a thioamide-containing vancomycin derivative (**61**, Y=S) that could then be converted to the amidine in a single step with AgOAc and ammonia in methanol [136]. Lawesson's reagent (**6**) was used to generate the thioamide in an intermediate containing the B, C, and D rings in which all of the alcohols were protected as either methyl or *t*-butyldimethylsilyl (TBS) ethers. Attempts to thionate B/C/D ring intermediates

also containing the A ring or the entire A/B ring macrocycle resulted in much lower yields. The thioamide-containing derivative was also tested for binding affinity and bioactivity, but did not display any potent antibacterial abilities. It was hypothesized that the larger van der Waals radius and the longer C=S bond length prevented binding of the thioamide derivative to the D-Ala-D-Ala substrate. Further research in the Boger group has utilized the thioamide as an intermediate to prepare various vancomycin analogs with Ag(I)-prompted reactions [133, 135, 137].

Thiopeptides are peptide antibiotics that generally inhibit protein biosynthesis in bacteria. The total synthesis of a thiopeptide, thiostrepton (**66**), was completed by Nicolau and coworkers [138]. Taking inspiration from its biosynthesis, Nicolau et al. decided to synthesize the dehydropiperidine core using a Diels–Alder dimerization. Generation of the precursor thiazolidine was achieved by utilizing thioamide-containing precursors (**68**) to generate the surrounding thiazole rings (Fig. 8.15). On L-cysteine and L-threonine derivative **67**, Lawesson's reagent (**6**) was used to establish the thioamide, following which, treatment with ethyl bromopyruvate in basic conditions with  $\text{KHCO}_3$ , followed by trifluoroacetic acid-assisted dehydration with pyridine, yielded the desired thiazole (**69**). These two fragments were condensed in EtOH with  $\text{KHCO}_3$  to produce the desired thiazolidine ring (**70**, 1:1 diastereomers). The thiazolidine fragment was converted to the azadiene with  $\text{Ag}_2\text{CO}_3$  and DBU in pyridine at  $-12^\circ\text{C}$ , following which the Diels–Alder dimerization occurred to produce the desired dehydropiperidine core. Addition of benzylamine to the reaction mixture reduced production of an aza-Mannich rearrangement by-product. This once again demonstrated the value of thioamides for a variety of carbonyl transformations in the presence of many other functional groups.

### 8.3.6 Applications of Thioamides as Spectroscopic Probes

Due to the changes in physical properties upon sulfur substitution, thioamides can be used in a number of applications as spectroscopic probes. Specifically, we will discuss the usage of thioamides as circular dichroism (CD) and fluorescence probes, as well as their applications as photoswitches. More detailed discussion of these applications is available in Walters et al. [139] as well as Petersson et al. [13].

Thioamides can serve as site-specific CD probes due to the redshift in their  $n \rightarrow \pi^*$  and  $\pi \rightarrow \pi^*$  electronic transitions relative to oxoamides. The thioamide  $n \rightarrow \pi^*$  signature is shifted by 120–140 nm, placing it at about 350 nm [140]. This makes thioamides usable as CD probes where their absorbance can be distinguished from normal amide resonances at 200–220 nm and even from Trp or Tyr bands at 270–280 nm (Fig. 8.16). In studies by Hollosi and coworkers, the utility of thioamides as CD probes was extensively characterized in different conformational contexts. It was observed that thioamides are compatible with  $\gamma$ -turn conformations, as well as type II  $\beta$ -turn conformations. Overall, they determined that the  $n \rightarrow \pi^*$  and  $\pi \rightarrow \pi^*$  signatures that are seen reflect the local conformation of the amino acid residue that precedes the thioamide [140]. In order to determine the compatibility of thioamides

with other secondary structures, Miwa and coworkers incorporated a thioamide into the turn of a  $\beta$ -hairpin peptide that had been designed by Stanger and Gellman [83]. Utilizing CD and NMR, it was observed that the peptide had characteristics of a  $\beta$ -sheet, specifically a strongly negative  $\pi \rightarrow \pi^*$  thioamide band, indicating that the thioamide was participating in a  $\beta$ -hairpin structure. More recently, thioamides were used by Raines and coworkers to examine the backbone of collagen. In this work, thioamides were incorporated into either the Yaa-Gly or the Gly-Xaa motif of the collagen triple helix repeat (Xaa-Yaa-Gly) in order to examine the  $n \rightarrow \pi^*$  interactions of the collagen backbone [131]. Environmental effects on thioamide absorption were observed, as both the Gly<sup>S</sup>-Xaa and the Yaa<sup>S</sup>-Gly peptides had minima at 265 nm, while the Gly<sup>S</sup>-Xaa peptide also had a maximum at 287 nm. This work was the first example of a backbone modification that did not negatively impact the thermal stability of the collagen triple helix and showed the utility of thioamides as probes for polyproline type II structures. Lastly, our own group has used CD to examine the stability of proteins containing thioamides in the context of  $\alpha$ -helices,  $\beta$ -sheets, and polyproline II helices. Through CD and thermal denaturation, Walters et al. were able to show that thioamides can be tolerated in some portions of  $\alpha$ -helices and polyproline II helices, along with being moderately perturbing to  $\beta$ -sheet structures [85].

Thioamides also have utility as photoswitches due to their red-shifted  $\pi \rightarrow \pi^*$  absorption band, which allows them to be selectively excited to cause *cis/trans* isomerization through rotation about the C–N bond (Fig. 8.16). Oxoamides can also undergo photoisomerization, but this requires irradiation at 190 nm, which degrades peptides [91]. In studies by Frank and coworkers, the photo-controlled *cis/trans* isomerization of thioamide-containing endomorphins was characterized, with eventual application in studying isomer-specific interactions with the opioid  $\mu$ -receptor [141]. In this report, it was shown that the thiopeptides remained intact after multiple rounds of excitation, illustrating that this application can be performed without degrading the peptide sample. Similarly, Zhao and coworkers showed that secondary thiopeptide bonds can undergo *cis/trans* isomerization in both directions (*trans* to *cis* and vice versa) with a re-equilibration rate that is much slower than the thermal re-equilibration rate of oxopeptides [142]. In one of the first reported applications of thiopeptide *cis/trans* isomerization, Fischer and Kiefhaber modified RNase S with a thioamide in order to monitor the change in enzyme activity upon isomerization [91]. A thionated Ala residue was incorporated into the S peptide of RNase S, far from the active site, which allowed the enzyme to retain activity in the ground state. Photoisomerization of the thioamide led to a drastic decrease in the enzyme efficiency, which increased again upon thermal re-equilibration of the system. In another interesting application of thioamide photoswitches, Huang and coworkers used thioamides to examine the cockroach hindgut myotropic activity of both the *cis* and the *trans* conformations of the insect kinin peptide core. Previously, insect kinin analogs with a significant 1-4 *cis*-Pro type VI  $\beta$ -turn population had been shown to be very active, with the *cis* population believed to be the contributing factor. Due to the long re-equilibration half-life of the thioamide derivative of the insect kinin active core, Huang and coworkers were able to turn on myotropic activity upon irradiation to



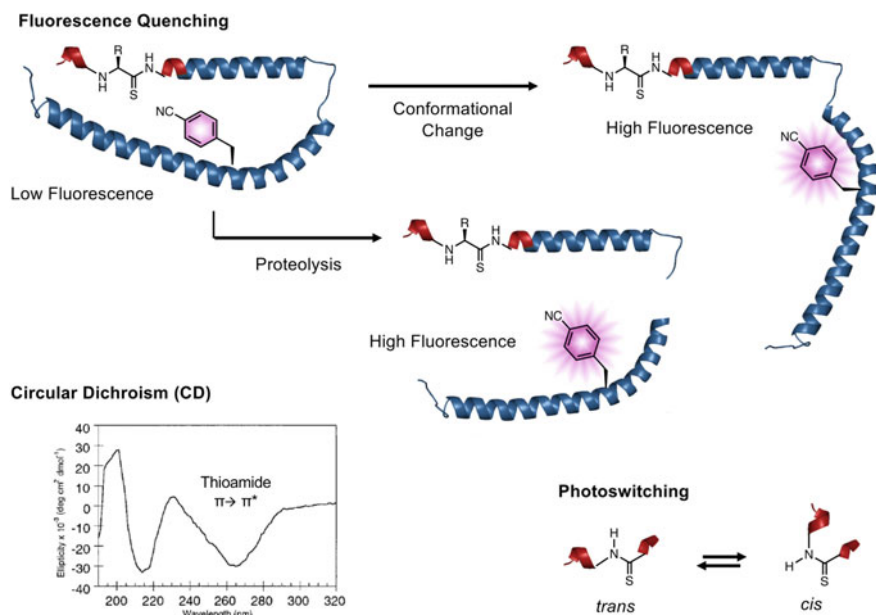


**Fig. 8.16** Thioamides as probes of biological structure/function. Fluorescence quenching: The Petersson laboratory has used thioamides as fluorescent probes, both to study conformational changes in proteins and to monitor proteolysis of a variety of substrates. In a compact conformation, the thioamide quenches the fluorescence of the fluorescent amino acid. Upon refolding or proteolysis, the thioamide and fluorophore move apart, allowing for a turn-on in fluorescence of the fluorophore. Circular dichroism (CD): Thioamides have successfully been employed as circular dichroism probes to examine how they affect the global structure of small, structured systems. In this example from Miwa and coworkers, the thioamide serves as a probe for the environment of a turn in a  $\beta$ -sheet structure [83]. Photoswitching: Thioamides can be irradiated to convert to the *cis* conformation and thus used as a photoswitch to trigger larger conformational changes in proteins. CD figure reprinted (adapted) with permission from Miwa et al. [83], Copyright (2001) American Chemical Society

demonstrate that the *cis* conformer is much more active than the *trans* conformation of the peptide [143]. This work is an elegant example where thioamides were used to interrogate how specific conformations of peptides affect their activity.

Thioamides can be utilized as fluorescent probes due to their red-shifted  $\pi \rightarrow \pi^*$  absorption, which gives them spectral overlap with a number of fluorophores. The first characterization of a thioamide in a FRET pair was reported by Wiczek and coworkers, which described a thioamide–Trp pair in a 4mer peptide [144]. This FRET pair was determined to have a Förster radius ( $R_0$ , a characteristic distance of half-maximal energy transfer) of 16.9 Å in propylene glycol (the  $R_0$  for Trp in water is much shorter) [76]. Our laboratory has had significant success in using thioamides in different FRET and PeT applications. In 2010, we examined the utility of a Cnf–thioamide FRET pair. It was determined that this FRET pair has a theoretical  $R_0$  of ~15.6 Å, which correlated very well with the observed changes in

fluorescence using rigid polyproline spacers to vary the distance between the two fluorophores [73]. The temperature-dependent unfolding of Villin HP35 with a Leu<sup>S</sup> and Cnf FRET pair was also observed, with fluorescence changes correlating well with measurements of unfolding by CD (Fig. 8.16). Our group has shown that the thioamide/Tyr and thioamide/Cnf FRET pairs can be used to characterize the binding of CaM to a known peptide binding partner, pOCNC [76, 77]. Moreover, we have been able to use this pair to characterize the aggregation kinetics of  $\alpha$ S, an intrinsically disordered protein that has been associated with Parkinson's disease [71]. This fluorescence quenching is complementary to the thioflavin T assay, which is typically used to characterize the kinetics of aggregation, and can give insight into oligomerization pathways that are not detected through ThT fluorescence. Similarly, our group has used the thioamide/Cnf FRET pair to characterize the compaction of  $\alpha$ S in the presence of trimethylamine oxide (TMAO), an osmolyte that is typically used to compact proteins. Through these experiments, we were able to see the N terminus of  $\alpha$ S compact with higher concentrations of TMAO, which is consistent with what others have seen with other methods [77, 78]. Our group has also characterized the interaction of thioamides with various fluorophores through a photoinduced electron transfer (PeT) mechanism. We have shown that thioamides can quench 7-azatryptophan, 7-methoxycoumarin-4-yl-alanine (Mcm), 5-carboxyfluorescein, and acridon-2-yl-alanine through a PeT mechanism [72, 75]. Specifically, our group has used this quenching to study the unfolding of Villin HP35, the cleavage of a variety of protease substrates, and the compaction of  $\alpha$ S in the presence of TMAO [72, 75]. Recently, our group has become interested in the implications of utilizing two thioamides in a FRET or PeT pair. Huang, et al. showed that increasing the number of thioamides increases the fluorescence quenching effect that they have in a FRET or PeT pair [145]. In 2018, our group has also demonstrated that the increased fluorescence quenching of dithioamide incorporation can be utilized to study CaM binding to a W-pOCNC peptide [103]. Notably, multiple thionations can also improve the thermal stability of these native, functional protein folds while increasing the quenching efficiency in order to better characterize protein interactions.

The use of thioamides as fluorescence quenching probes has been exploited by our group to make sensors for over 15 different proteases (including Unpublished Results) [74, 84, 145]. The basic design relies on placing a selectively excitable fluorophore on one side of the scissile bond and a thioamide quencher on the other side (Fig. 8.16). Thus, proteolysis will separate the thioamide from the fluorophore, leading to a turn-on of fluorescence that can be used to monitor proteolytic activity. We showed that these substrates were cleaved at rates identical to the corresponding oxoamide peptide provided that the thioamide was placed 3 or more amino acids from the scissile bond. Sensors of this design could even be used to monitor cleavage at one of two adjacent proteolytic sites based on the placement of the thioamide. These studies led us to systematically investigate the positional effects of thioamides on proteolysis rates. Such studies have informed the design of sensors by identifying non-perturbing sites for thioamide labeling. The identification of perturbing sites in these studies has the potential for even greater impact, where highly perturbing sites

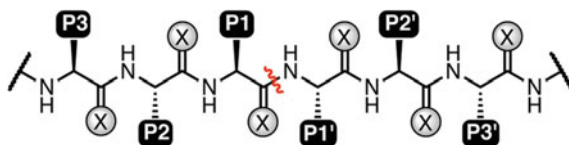


**Fig. 8.17** Thioamide proteolysis scheme. Proteolysis occurs at the position of the red slash. Amino acids surrounding the scissile bond are denoted P3, P2, P1, P1', P2', or P3' as shown. Thioamide substitutions at these sites can be used to probe effects on proteolysis. X=O or S

can be used as the basis for the design of protease inhibitors or for stabilizing peptides for in vivo applications.

### 8.3.7 Thioamide Substitution Effects on Proteolysis

Proteases play an important role in drug development since they are involved in many biological signaling pathways, and underlie a variety of diseases [146]. Inhibitors of well-established protease targets such as angiotensin-converting enzyme and HIV protease have shown significant therapeutic success [147]. Thioamides introduced at the scissile bond of protease substrates or inhibitors have been applied to study catalytic mechanisms of proteolysis with the potential to develop improved protease inhibitors or to stabilize injectable peptides. Throughout our discussion, we will refer to the thioamide position in terms of the common protease nomenclature where P1 is the amino acid at the position of cleavage, or scissile bond, and the other neighboring amino acids in the substrate are designated P3, P2, P1, P1', P2', P3', from the N terminus to the C terminus (Fig. 8.17). Typically, only these 3-4 flanking amino acids are relevant to protease recognition of substrates.

### 8.3.8 Thioamide Probes of Protease Mechanism

Numerous proteases have been investigated through thioamide modifications, including representatives of the major protease classes—Ser, Cys, metallo-, and Asp proteases—which are categorized based on their catalytic mechanism. The zinc metallo-protease carboxypeptidase A (CPA) is one of the most well-studied proteases to date, in terms of thioamide effects [148–151]. A peptide substrate containing a thioamide linkage at the scissile bond (P1) was found to be less efficiently cleaved by CPA [151]. In addition, thioamide incorporation near the scissile bond of substrates yielded peptides with a similar  $K_M$ , but a greater than tenfold decrease in  $k_{cat}$  compared to the corresponding oxoamide substrates. These results suggested a mechanism involving a rate-determining step requiring C–N bond rotation, wherein the higher rotational barrier of the thioamide would slow reaction [148, 149]. In a subsequent study,

**Table 8.2** Protease inhibition by thioamides at the scissile bond (P1)

Thioamide substrate	Enzyme	Thio/Oxo $k_{\text{cat}}/K_{\text{M}}^{\text{a}}$
Bz-Gly-Gly <sup>S</sup> -Phe	Zn(II) CPA	$6.00 \times 10^{-4}$
Z-Gly <sup>S</sup> -Phe		0.18
Z-Gly-Ala <sup>S</sup> -Phe		$3.67 \times 10^{-3}$
Z-Phe <sup>S</sup> -Phe		$1.82 \times 10^{-3}$
Z-Gly-Ala <sup>S</sup> -Phe	Cd(II) CPA	0.03
Z-Phe <sup>S</sup> -Phe		0.05
Z-Gly-Ala <sup>S</sup> -Phe	Mn(II) CPA	$9.44 \times 10^{-4}$
Z-Phe <sup>S</sup> -Phe		$3.44 \times 10^{-4}$
Z-Lys <sup>S</sup> -AIE	Papain	0.18
Z-Phe-Arg <sup>S</sup> -AIE		0.21

<sup>a</sup> $k_{\text{cat}}/K_{\text{M}}$  value of thioamide substrate versus corresponding oxoamide substrate

Bz: benzoyl; Z: *N*-carbobenzyloxy; Gly<sup>S</sup>: thioglycine; Ala<sup>S</sup>: thioalanine; Phe<sup>S</sup>: thiophenylalanine; Lys<sup>S</sup>: thiolysine; Arg<sup>S</sup>: thioarginine; CPA: carboxypeptidase A; AIE: isophthalic acid dimethyl ester

CPA data from Bond et al. [150]; Papain data from Cho [152]

other metal ions, including Cd(II), Mn(II), Co(II), and Ni(II), were substituted for the native zinc to study their effects on the cleavage of oxoamide and P1 thioamide substrates [150]. It was found that thioamidation led to a large increase in the rate of Cd(II) CPA cleavage relative to the oxoamide substrate, but a large decrease in relative activity was observed with Mn(II) CPA. This was explained in that sulfur and oxygen functional groups are classified as soft and hard ligands, respectively, and similarly Cd(II) and Mn(II) are classified as soft and hard metals. Empirically, hard metals tend to form stable complexes with hard ligands, and soft metals act similarly with soft ligands. Thus, the favorable soft/soft thioamide/Cd(II) combination had a 100-fold increase in  $k_{\text{cat}}/K_{\text{M}}$  in comparison with Mn(II) CPA (Table 8.2). These results reflect the mechanism for peptide bond hydrolysis in which the metal atom interacts with the substrate C=X group at the scissile bond during catalysis.

Cho studied the ability of papain and trypsin to catalyze the hydrolysis of thioamide and corresponding oxoamide substrates using dipeptides [152]. They found that both the oxo- and thioamide substrates were cleaved by papain, while a thioamide at P1 significantly suppressed the proteolysis rates of trypsin as compared to the oxopeptides. According to Roberts et al., the classical “oxyanion hole” might be destabilized in the case of the tetrahedral intermediate formed during thioamide cleavage due to the longer C=S bond and poorer hydrogen bond accepting ability of the thioamide [153]. Thus, Cho. et al. concluded that the stabilization of the oxyanion plays an important role for trypsin, but not papain, which may reflect broader rules for P1 thioamide peptide cleavage by serine versus cysteine proteases [152]. However, Foje and Hanzlik reported that papain cleavage of Phe-Gly-NH-R dipeptides with a thioamide at P1 depended on the identity of the R group, demonstrating that the active site interactions are more subtle [154].

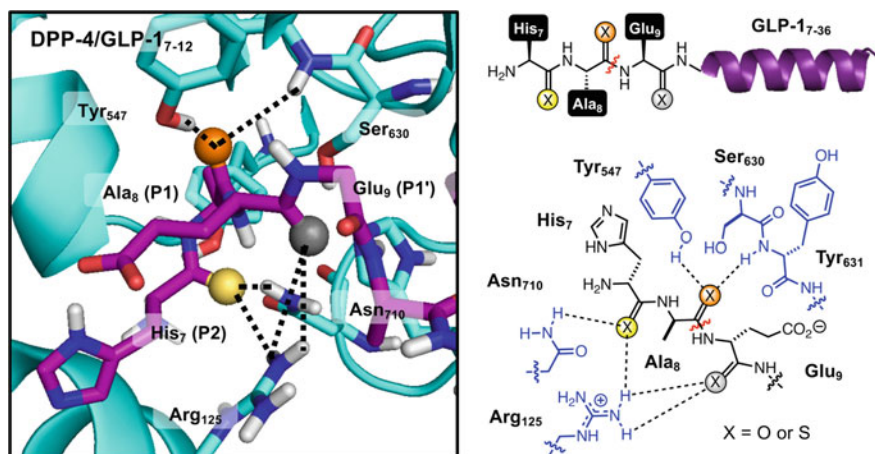


**Fig. 8.18** Structural analysis of the impact of thioamide substitution on DPP-4 substrate recognition. Left: An image of the DPP-4 (cyan) active site with a GLP-1 N-terminal fragment (purple) bound, modeled based on the neuropeptide Y bound DPP-4 structure in PDB entry 1R9N [156]. The P2, P1, and P1' carbonyl oxygens are highlighted as yellow, orange, and gray spheres, respectively. Key interactions with DPP-4 are shown as dashed lines. Right: A schematic representation of the P2, P1, and P1' binding sites. The DPP-4 cleavage site is shown as a red slash

In another example, Fischer and coworkers investigated dipeptidyl peptidase-4 (DPP-4) using Ala<sup>S</sup>-Pro-pNA as substrate, where the enzyme hydrolyzes the bond between Pro and *para*-nitroaniline (pNA) [155]. They found a 1,100-fold decrease of  $k_{\text{cat}}/K_{\text{m}}$  compared to the oxoamide, which they attributed to the decrease of  $k_{\text{cat}}$ , caused by the increased rotational barrier of the thioamide. Recently, our laboratory built on this observation in studying GLP-1 and GIP [84], natural substrates of DPP-4. A thioamide substitution at either of the two terminal positions increased the peptide half-life in an *in vitro* proteolysis assay from 2 min to greater than 12 h. Competition experiments with an alternate DPP-4 substrate revealed that thioamide GLP-1 was not a competitive inhibitor, seemingly in conflict with Fischer's finding of a primary  $k_{\text{cat}}$  effect. This may be due to the fact that the 36 residue GLP-1 peptide cannot be repositioned in the active site to accommodate the thioamide, whereas the Ala<sup>S</sup>-Pro-pNA can, but in a way that is not optimal for catalysis. Examination of the crystal structure of DPP-4 with a peptide substrate reveals bifurcated hydrogen bonds with the carbonyls of the two N-terminal amino acids (Fig. 8.18) [156]. Thioamidation would disrupt these interactions, preventing productive binding of substrates (although the rotational barrier may still play a role). Our laboratory is currently evaluating thioamide effects on other proteases by scanning thioamide incorporation around the scissile bond, and this systematic approach, coupled with the increased availability of protease crystal structures, should provide additional mechanistic insight.

**Table 8.3** Positional effects of thioamides on the inhibition of HIV-1 protease

Thioamide position	IC <sub>50</sub> (μM)
P3	160
P2	51
P1	18
P1'	>200
P2'	4.5

Data from Yao et al. [163]

### 8.3.9 Thioamide Inhibitors of Protease Activity

Given the observed resistance to proteolysis for certain thioamide positions, there have been attempts to introduce them into protease substrates or other peptides to create inhibitors of proteases such as papain, a variety of proline-specific peptidases, leucine aminopeptidase (LAP), and HIV-1 protease [157–161]. Most of the thioamide inhibitors were found to be competitive inhibitors with weak binding affinities. Thioamide-modified inhibitors were studied for the first time by Lowe and Yuhavong in 1971 [157]. A papain substrate was modified by introducing a thioglycine at the scissile bond, and weak competitive inhibition was observed, with a  $K_I$  100-fold greater than the  $K_M$  of the corresponding oxoamide substrate. Moreover, Stöckel-Maschek characterized amino acid thiazolidides (dipeptides with thiazolidine units) as DP II protease inhibitors and found that a thioamide modification could improve its inhibitory effect [162]. Interestingly, in the thioamide positional scanning from P3 to P2' of an HIV-1 protease substrate by Chimeleski and coworkers, the thioamide at the P2' position rather than P1 position produced the most significant inhibition effect (Table 8.3) [163]. Moreover, in the study of the positional effect of thioamide on prolyl oligopeptidase by Schutkowski et al., two series of tetrapeptide-*p*-nitroanilides, Ala-Gly-Pro-Phe-pNa and Ala-Ala-Pro-Phe-pNa, along with all possible thioamide derivatives were examined [164]. They found that a thioamide introduced at the P2 position enhanced  $k_{cat}/K_M$  fivefold in the Gly series substrates, while it resulted in a 1.7-fold decrease in the Ala series substrates. Studies such as this highlight the need for a greater mechanistic understanding of thioamide effects to be able to use them rationally in inhibitor design.

### 8.3.10 Thioamide Modifications to Improve Injectable Peptides

The resistance of thioamide substrates to proteolysis also lends itself to the improvement of peptide therapeutics due to the potential for selective perturbation of proteolysis without altering interactions with a target receptor. There are more than 60 FDA (US Food and Drug Administration) approved peptide drugs on the market

currently. In the USA, over 140 peptide therapeutic candidates are in clinical trials and more than 500 peptide compounds in preclinical development [165, 166]. The global sales of peptide therapeutics increased each year from 2009 to 2011, and the top 25 US-approved products had global sales of US\$14.7 billion in 2011. Peptide therapeutics have obvious advantages compared to traditional small molecule drugs or large protein drugs, such as target specificity deriving from the native peptide and lower production complexity than protein drugs [167]. However, there are problems with utilizing native peptides as therapeutic agents, due to their short duration of in vivo activity coming from low stability against proteolysis as well as other factors such as kidney clearance. To overcome stability problems, a variety of strategies have been developed, such as: (1) polyethylene glycol conjugation, which can protect against proteases and solubilize hydrophobic molecules [122, 168–170]; (2) stabilizing secondary structure by “stapling,” macrocyclization, or the use of structure inducing modifications [171–174]; (3) unnatural amino acid substitutions or peptide bond mimics, including  $\alpha,\alpha$ -disubstitution, *N*-methylation, and D-amino acids [175]; and (4) peptidomimetics such as peptoids [176], urea peptidomimetics [177], and peptide-sulfonamides [178].

Thioamides have significant advantages over these other stabilizing modifications. Since they are a minor modification, they are less likely to disrupt interaction with the target protein or other peptide properties than PEG modification or cyclization. The use of these modifications often involves trial and error testing to find the right place for modification. While the other amino acid modifications discussed are also small, most of them remove one or more of the hydrogen bonding interactions of the peptide bond or introduce significant steric differences around the peptide bond. If the same region of the peptide is necessary for protease recognition and target receptor recognition, use of a D-amino acid may not be a viable option. Thus, thioamides provide a balance of being sufficiently different to suppress proteolysis while not dramatically altering the other peptide properties.

To our knowledge, the idea of using thioamides to stabilize peptides toward proteolysis was first tested by introducing a thioamide at the scissile bond of a CPA substrate, leading to at least 1,000-fold slower turnover compared to its corresponding oxoamide substrate [148, 149, 151]. Substrates of numerous proteases, such as LAP, papain, mammalian membrane dipeptidase, and aminopeptidase P, were stabilized later by introducing a thioamide at the scissile bond [148, 153, 158, 160, 161]. The first tests that included evaluations of biological activity involved the immunostimulant IMREG-1 (Tyr-Gly-Gly) [68]. The half-lives of thionated IMREG derivatives with sequences Tyr<sup>S</sup>-Gly-Gly and Tyr-Gly<sup>S</sup>-Gly were determined as 45 min and over 180 min, respectively, compared to the half-life of natural IMREG-1 at only 1 min. Moreover, Tyr<sup>S</sup>-Gly-Gly was found to display some biological activity as evidenced by mild stimulation of cytotoxic T-lymphocytes and appeared to be well tolerated and devoid of any apparent toxicity. In a study noted above, Zhang et al. introduced a thioamide to the C-terminal residue of MPI (54; Fig. 8.12). In addition to changes in membrane binding and activity, they observed a significant enhancement of stability against proteolysis in mouse serum [124]. After 3 h, almost all of the natural MPI was gone, while only 21% of the thio-MPI was degraded. Similarly, the

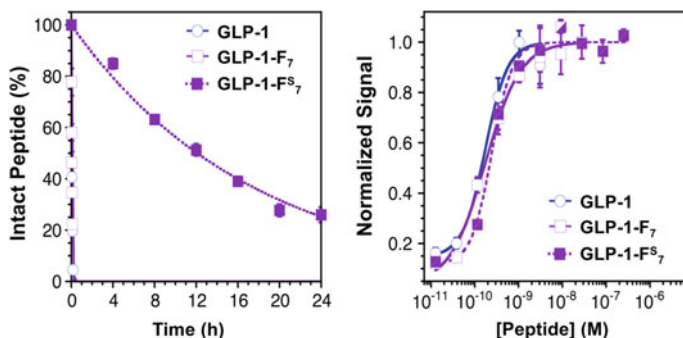


**Fig. 8.19** Thioamide substitution stabilizes GLP-1 analogs without disrupting activity. Left: In vitro proteolysis data demonstrating that thioamide GLP-1-F<sup>S</sup><sub>7</sub> is cleaved by DPP-4 more slowly than the corresponding oxopeptide (GLP-1-F<sub>7</sub>, a Phe mutant to GLP-1) or native GLP-1. Half-lives: GLP-1, 2 min; GLP-1-F<sub>7</sub>, 3 min; GLP-1-F<sup>S</sup><sub>7</sub>, 12 h. Right: Dose–response curves for cAMP stimulation by GLP-1, GLP-1-F<sub>7</sub>, and GLP-1-F<sup>S</sup><sub>7</sub> demonstrating that the thioamide does not affect potency. EC<sub>50</sub>s: GLP-1, 207 pM; GLP-1-F<sub>7</sub>, 171 pM; GLP-1-F<sup>S</sup><sub>7</sub>, 244 pM. Bars represent standard error

thioamide RGD macrocycles studied by Chatterjee and coworkers (Fig. 8.13) were all found to be more stable than cilengitide in ex vivo metabolic stability assays in human serum over 72 h [81]. This was independent of the position of the thioamide, suggesting that it was not due to specific hydrogen bonding interactions, but may be related to the overall conformational rigidity of the macrocycles.

Our laboratory is interested in studying positional effects of thioamides to stabilize peptides, as well as to develop protease sensors and protease inhibitors. GLP-1 and GIP, two therapeutically relevant peptides introduced above, were modified by introducing thioamides [84]. In spite of the large perturbation to interactions with proteases noted above, target receptor activation was largely unperturbed, with increases in receptor EC<sub>50</sub> of threefold or less (Fig. 8.19). Moreover, thioamide-modified GLP-1 was found to improve glycemic control in rats relative to the native GLP-1. We anticipate that thioamides will be highly useful for the stabilization of newly discovered signaling peptides toward key proteolytic events for early in vivo investigations of their signaling activity. In addition, since thioamides increase proteolytic stability without altering physical properties for trafficking or renal clearance, thioamide-stabilized peptides should be excellent for imaging applications, where one wishes for the peptide to be either intact and bound to the target cells (e.g., tumors) or cleared from the bloodstream to eliminate background signal. These types of applications require an understanding of the effects of thioamides on cleavage by various proteases in order to design their placement. Currently, we are using a series of peptide substrates with a thioamide at the P3, P2, P1, P1', P2', or P3' position to study the positional effects on the activity of various proteases. We will use this information to guide the application of thioamides to stabilizing peptides for therapeutic and imaging applications as well as for the development of potential inhibitors.



## 8.4 Outlook

Recent developments in biological, biophysical, and medicinal chemistry have generated much interest in the study of thioamide-containing natural products and synthetic thioamide modifications of peptides and proteins. Discovery of the biosynthetic gene clusters for thioamide installation has vastly increased the number of putative thioamide-containing RiPPs and may indicate that MCR is not the only thioamidated protein. Thioviridamide and closthioamide have been shown to have promising anti-cancer and antibiotic activities, respectively. Making thioamidated analogs of natural products or biosynthetic intermediates has enabled the understanding of biosynthetic pathways and the determination of the role of the thioamides in bioactivity. Stabilization of GLP-1, GIP, cilengitide-like macrocycles, and other peptides has provided promise for directed thioamide substitution for *in vivo* applications. Thioamides can also be used as biophysical probes to study conformational changes in proteins using fluorescence quenching or photoisomerization. Our laboratory has used fluorescence quenching by thioamides in peptides to study the positional effects of the thioamides on cleavage by a wide variety of Ser and Cys proteases. This has informed our design of thioamide modifications of peptides to stabilize them toward proteolysis for *in vivo* therapeutic and imaging applications. These thioamides can also have useful effects on peptide conformation and binding affinity, leading to alterations in selectivity. We anticipate that the seeds planted by these studies will lead to a dramatic increase in the number of laboratories studying peptidyl thioamides in the coming years.

One of the most significant unanswered questions in the study of thioamide effects in proteins is of the structural basis for thioamide effects on protein stability and protein interactions. To achieve a predictive understanding of thioamide effects will require the ability to easily install thioamides in a variety of protein sequences and to prepare sufficient quantities of proteins for structural and biophysical studies. Although current methods allow one to insert thioamides at specific sites with great generality, the synthesis of proteins through NCL is inherently labor-intensive. Biosynthetic insertion of thioamides by YcaO-type enzymes is unlikely to provide a solution since it will probably not be sufficiently general in sequence to enable the exploration of sequence effects. Thus, one of the outstanding areas of need in the field is for an easily scalable, facile method for genetic thioamide insertion. Hecht and coworkers have published a method for *in vitro* protein translation using tRNAs acylated with thioamide-containing dipeptides (**73**) which comes close to filling this need, but is limited by the relatively low yields of thioamide-containing protein (**74**) available from *in vitro* translation and the need to prepare the tRNA acylating precursors (**71**, **72**) as dipeptides (Fig. 8.20) [179]. In spite of some previous reports [180], our own unpublished investigations with chemically thionoacylated tRNAs (**75**) have indicated that S-to-O exchange of the thiocarbonyl (**76**) is a significant concern, providing a challenge to circumventing the use of dipeptide acylated tRNAs for thioamide insertion (Fig. 8.20). If this chemical challenge can be met, the ability to genetically encode thioamides will vastly increase the scope of biological exploration that can be undertaken, from mapping thioamide effects on protein stability

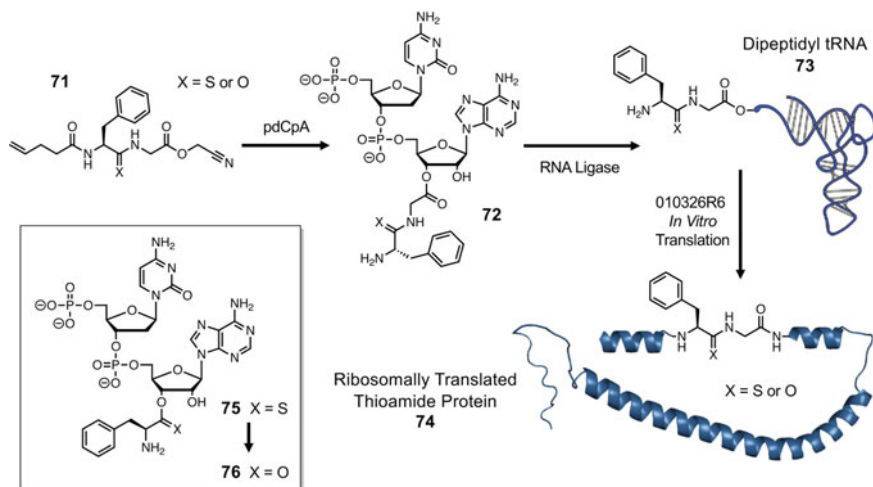


**Fig. 8.20** Prospects for ribosomal translation of thioamides. Acylation of the pdCpA dinucleotide with an *N*-protected dipeptidyl cyanomethyl ester (**71**) to give **72**, followed by ligation to a truncated tRNA with RNA ligase and deprotection, gives a dipeptidyl tRNA (**73**). Hecht and coworkers have shown that this can be used in translation with *E. Coli* extracts containing a mutant 23S ribosome (010326R6) to afford proteins with a backbone thioamide (**74**, X=S) [179]. Inset: Unpublished investigations from the Petersson laboratory using thioacyl pdCpA (**75**) show significant S-to-O exchange in aqueous buffer to generate the acyl pdCpA (**76**)

and binding interactions, to scanning peptide sequences for stabilization effects, and even determining the role of the thioamide in MCR and other natural thioproteins yet to be discovered.

## References

1. A. Choudhary, R.T. Raines, *ChemBioChem* **12**, 1801 (2011)
2. Nomenclature and symbolism for amino acids and peptides. *Eur. J. Biochem.* **138**, 9 (1984)
3. T. Sifferlen, M. Rueping, K. Gademann, B. Jaun, D. Seebach, *Helv. Chim. Acta* **82**, 2067 (1999)
4. F.G. Bordwell, D.J. Algrim, J.A. Harrelson, *J. Am. Chem. Soc.* **110**, 5903 (1988)
5. K.B. Wiberg, D.J. Rush, *J. Am. Chem. Soc.* **123**, 2038 (2001)
6. M. Hollósi, Z. Majer, M. Zewdu, F. Ruff, M. Kajtár, K.E. Kövér, *Tetrahedron* **44**, 195 (1988)
7. E.P. Dudek, G.O. Dudek, *J. Org. Chem.* **32**, 823 (1967)
8. H.-J. Lee, Y.-S. Choi, K.-B. Lee, J. Park, C.-J. Yoon, *J. Phys. Chem. A* **106**, 7010 (2002)
9. T.S. Jagodzinski, *Chem. Rev.* **103**, 197 (2003)
10. T.F.M. La Cour, H.a.S. Hansen, K.I.M. Clausen, S.O. Lawesson, *Int. J. Pept. Protein Sci.* **22**, 509 (1983)
11. S.K. Misra, U.C. Tewari, *Transition Met. Chem.* **27**, 120 (2002)
12. J. Helbing et al., *J. Am. Chem. Soc.* **126**, 8823 (2004)
13. E.J. Petersson, J.M. Goldberg, R.F. Wissner, *Phys. Chem. Chem. Phys.* **16**, 6827 (2014)
14. M. Pan, T.J. Mabry, J.M. Beale, B.M. Mamiyat, *Phytochemistry* **45**, 517 (1997)

15. N. Yutin, M.Y. Galperin, *Environ. Microbiol.* **15**, 2631 (2013)
16. T. Lincke, S. Behnken, K. Ishida, M. Roth, C. Hertweck, *Angew. Chem. Int. Ed.* **49**, 2011 (2010)
17. S. Behnken, T. Lincke, F. Kloss, K. Ishida, C. Hertweck, *Angew. Chem. Int. Ed.* **51**, 2425 (2012)
18. K.L. Dunbar, H. Büttner, E.M. Molloy, M. Dell, J. Kumpfmüller, C. Hertweck, *Angew. Chem. Int. Ed.* **57**, 14080 (2018)
19. P.G. Arnison et al., *Nat. Prod. Rep.* **30**, 108 (2013)
20. J.D. Semrau et al., *Environ. Microbiol.* **15**, 3077 (2013)
21. H.J. Kim et al., *Science* **305**, 1612 (2004)
22. Y. Hayakawa, K. Sasaki, H. Adachi, K. Furihata, K. Shin-Ya, K. Nagai, *J. Antibiot.* **59**, 1 (2006)
23. Y. Hayakawa, K. Sasaki, K. Nagai, K. Shin-Ya, K. Furihata, *J. Antibiot.* **59**, 6 (2006)
24. M. Izumikawa et al., *J. Antibiot.* **68**, 533 (2015)
25. L. Kjaerulff, A. Sikandar, N. Zaburanyi, S. Adam, J. Herrmann, J. Koehnke, R. Müller, *ACS Chem. Biol.* **12**, 2837 (2017)
26. L. Frattaruolo, R. Lacret, A.R. Cappello, A.W. Truman, *ACS Chem. Biol.* **12**, 2815 (2017)
27. T. Kawahara et al., *J. Nat. Prod.* **81**, 264 (2018)
28. U. Ermiler, W. Grabarse, S. Shima, M. Goubeaud, R.K. Thauer, *Science* **278**, 1457 (1997)
29. J. Kahnt, B. Buchenau, F. Mahlert, M. Krüger, S. Shima, R.K. Thauer, *FEBS J.* **274**, 4913 (2007)
30. W. Grabarse, F. Mahlert, S. Shima, R.K. Thauer, U. Ermiler, *J. Mol. Biol.* **303**, 329 (2000)
31. D.D. Nayak, N. Mahanta, D.A. Mitchell, W.W. Metcalf, *eLIFE* (2017)
32. B.J. Burkhart, C.J. Schwalen, G. Mann, J.H. Naismith, D.A. Mitchell, *Chem. Rev.* **117**, 5389 (2017)
33. M. Izawa, T. Kawasaki, Y. Hayakawa, *Appl. Environ. Microbiol.* **79**, 7110 (2013)
34. B.T. Breil, J. Borneman, E.W. Triplett, *J. Bacteriol.* **178**, 4150 (1996)
35. K.L. Dunbar, J.R. Chekan, C.L. Cox, B.J. Burkhart, S.K. Nair, D.A. Mitchell, *Nat. Chem. Biol.* **10**, 823 (2014)
36. N. Mahanta, A. Liu, S. Dong, S.K. Nair, D.A. Mitchell, *Proc. Natl. Acad. Sci. USA* **115**, 3030 (2018)
37. C.J. Schwalen, G.A. Hudson, B. Kille, D.A. Mitchell, *J. Am. Chem. Soc.* **140**, 9494 (2018)
38. G.E. Kenney, A.C. Rosenzweig, *BMC Biol.* **11** (2013)
39. G.E. Kenney et al., *Science* **359**, 1411 (2018)
40. V.V. Richter, in *Chemistry of the Carbon Compounds* (P. Blakiston, son & co., Philadelphia, 1886)
41. R.N. Hurd, G. Delamater, *Chem. Rev.* **61**, 45 (1961)
42. J.W. Scheeren, P.H.J. Ooms, R.J.F. Nivard, *Synthesis* **149** (1973)
43. S. Scheibye, B.S. Pedersen, S.O. Lawesson, *B. Soc. Chim. Belg.* **87**, 229 (1978)
44. T. Guntreddi, R. Vanjari, K.N. Singh, *Tetrahedron* **70**, 3887 (2014)
45. B. Kaboudin, V. Yarahmadi, J. Kato, T. Yokomatsu, *RSC Adv.* **3**, 6435 (2013)
46. M. Muhlberg, K.D. Siebertz, B. Schlegel, P. Schmieder, C.P.R. Hackenberger, *Chem. Commun.* **50**, 4603 (2014)
47. A. Pourvali, J.R. Cochrane, C.A. Hutton, *Chem. Commun.* **50**, 15963 (2014)
48. Y.D. Sun, H.F. Jiang, W.Q. Wu, W. Zeng, J.X. Li, *Org. Biomol. Chem.* **12**, 700 (2014)
49. X. Wang, M. Ji, S. Lim, H.Y. Jang, *J. Org. Chem.* **79**, 7256 (2014)
50. A.K. Yadav, V.P. Srivastava, L.D.S. Yadav, *Tetrahedron Lett.* **53**, 7113 (2012)
51. U. Pathak, S. Bhattacharyya, S. Mathur, *RSC Adv.* **5**, 4484 (2015)
52. B.V. Varun, A. Sood, K.R. Prabhu, *RSC Adv.* **4**, 60798 (2014)
53. H.L. Xu, H. Deng, Z.K. Li, H.F. Xiang, X.G. Zhou, *Eur. J. Biochem.* **2013**, 7054 (2013)
54. J. Bergman, B. Pettersson, V. Hasimbegovic, P.H. Svensson, *J. Org. Chem.* **76**, 1546 (2011)
55. S.V. Ley, A.G. Leach, R.I. Storer, *J. Chem. Soc. Perkin* **1**, 358 (2001)
56. Z. Kaleta, B.T. Makowski, T. Soos, R. Dembinski, *Org. Lett.* **8**, 1625 (2006)
57. Z. Kaleta, G. Tarkanyi, A. Gomory, F. Kalman, T. Nagy, T. Soos, *Org. Lett.* **8**, 1093 (2006)

58. E.S. Gatewood, T.P. Johnson, *J. Am. Chem. Soc.* **48**, 2900 (1926)
59. W.C. Jones, J.J. Nestor, V. Du Vigneaud, *J. Am. Chem. Soc.* **95**, 5677 (1973)
60. O.E. Jensen, S.O. Lawesson, R. Bardi, A.M. Piazzesi, C. Toniolo, *Tetrahedron* **41**, 5595 (1985)
61. J. Lehmann, A. Linden, H. Heimgartner, *Tetrahedron* **54**, 8721 (1998)
62. J. Lehmann, A. Linden, H. Heimgartner, *Tetrahedron* **55**, 5359 (1999)
63. N. Shangguan, S. Katukojvala, R. Greenberg, L.J. Williams, *J. Am. Chem. Soc.* **125**, 7754 (2003)
64. M. Mühlberg, K.D. Siebertz, B. Schlegel, P. Schmieder, C.P.R. Hackenberger, *Chem. Commun.* **50**, 4603 (2014)
65. T. Hoegjensen, M.H. Jakobsen, C.E. Olsen, A. Holm, *Tetrahedron Lett.* **32**, 7617 (1991)
66. H.T. Le, J.F. Gallard, M. Mayer, E. Guittet, R. Michelot, *Bioorg. Med. Chem.* **4**, 2201 (1996)
67. B. Zacharie, R. Martel, G. Sauve, B. Belleau, *Bioorg. Med. Chem. Lett.* **3**, 619 (1993)
68. B. Zacharie, M. Lagraoui, M. Dimarco, C.L. Penney, L. Gagnon, *J. Med. Chem.* **42**, 2046 (1999)
69. C.T. Brain, A. Hallett, S.Y. Ko, *J. Org. Chem.* **62**, 3808 (1997)
70. S. Batjargal, Y. Huang, Y.J. Wang, E.J. Petersson, *J. Pept. Sci.* **20**, 87 (2014)
71. S. Batjargal, Y.J. Wang, J.M. Goldberg, R.F. Wissner, E.J. Petersson, *J. Am. Chem. Soc.* **134**, 9172 (2012)
72. J.M. Goldberg, S. Batjargal, B.S. Chen, E.J. Petersson, *J. Am. Chem. Soc.* **135**, 18651 (2013)
73. J.M. Goldberg, S. Batjargal, E.J. Petersson, *J. Am. Chem. Soc.* **132**, 14718 (2010)
74. J.M. Goldberg, X. Chen, N. Meinhardt, D.C. Greenbaum, E.J. Petersson, *J. Am. Chem. Soc.* **136**, 2086 (2014)
75. J.M. Goldberg, L.C. Speight, M.W. Fegley, E.J. Petersson, *J. Am. Chem. Soc.* **134**, 6088 (2012)
76. J.M. Goldberg, R.F. Wissner, A.M. Klein, E.J. Petersson, *Chem. Commun.* **48**, 1550 (2012)
77. R.F. Wissner, S. Batjargal, C.M. Fadzen, E.J. Petersson, *J. Am. Chem. Soc.* **135**, 6529 (2013)
78. R.F. Wissner, A.M. Wagner, J.B. Warner, E.J. Petersson, *Synlett* **24**, 2454 (2013)
79. S. Mukherjee, J. Chatterjee, *J. Pept. Sci.* **22**, 664 (2016)
80. S. Mukherjee, H. Verma, J. Chatterjee, *Org. Lett.* **17**, 3150 (2015)
81. H. Verma, B. Khatri, S. Chakraborti, J. Chatterjee, *Chem. Sci.* **9**, 2443 (2018)
82. J.H. Miwa, L. Pallivathucal, S. Gowda, K.E. Lee, *Org. Lett.* **4**, 4655 (2002)
83. J.H. Miwa, A.K. Patel, N. Vivatrat, S.M. Popek, A.M. Meyer, *Org. Lett.* **3**, 3373 (2001)
84. X. Chen et al., *J. Am. Chem. Soc.* **139**, 16688 (2017)
85. C.R. Walters, D.M. Szantai-Kis, Y. Zhang, Z.E. Reinert, W.S. Horne, D.M. Chenoweth, E.J. Petersson, *Chem. Sci.* **8**, 2868 (2017)
86. D.M. Szantai-Kis, C.R. Walters, T.M. Barrett, E.M. Hoang, E.J. Petersson, *Synlett* **28**, 1789 (2017)
87. C. Unverzagt, A. Geyer, H. Kessler, *Angew. Chem. Int. Ed.* **31**, 1229 (1992)
88. K.L. Dunbar, D.A. Mitchell, *J. Am. Chem. Soc.* **135**, 8692 (2013)
89. S. Kent, Y. Sohma, S. Liu, D. Bang, B. Pentelute, K. Mandal, *J. Pept. Sci.* **18**, 428 (2012)
90. C.T.T. Wong, C.L. Tung, X. Li, *Mol. Biosyst.* **9**, 826–833 (2013)
91. D. Wildemann, C. Schiene-Fischer, T. Aumüller, A. Bachmann, T. Kiefhaber, C. Lücke, G. Fischer, *J. Am. Chem. Soc.* **129**, 4910 (2007)
92. J. Kang, D. Macmillan, *Org. Biomol. Chem.* **8**, 1993 (2010)
93. T. Kawakami, S. Shimizu, S. Aimoto, *J. Pept. Sci.* **16**, 50 (2010)
94. J.B. Blanco-Canosa, P.E. Dawson, *Angew. Chem. Int. Ed.* **47**, 6851 (2008)
95. P. Grieco, P.M. Gitu, V.J. Hruby, *J. Pept. Res.* **57**, 250 (2001)
96. S.K. Mahto, C.J. Howard, J.C. Shimko, J.J. Ottesen, *ChemBioChem* **12**, 2488 (2011)
97. P. Botti, M. Villain, S. Manganiello, H. Gaertner, *Org. Lett.* **6**, 4861 (2004)
98. E.A. George, R.P. Novick, T.W. Muir, *J. Am. Chem. Soc.* **130**, 4914 (2008)
99. Y.J. Wang, in *Chemical Modification Methods for Protein Misfolding Studies* (University of Pennsylvania, Pennsylvania, 2015)
100. J.-S. Zheng, S. Tang, Y.-K. Qi, Z.-P. Wang, L. Liu, *Nat. Protoc.* **8**, 2483 (2013)
101. D. Bang, B.L. Pentelute, S.B. Kent, *Angew. Chem. Int. Ed.* **45**, 3985 (2006)

102. V. Muralidharan, T.W. Muir, *Nat. Methods* **3**, 429 (2006)
103. C.R. Walters, J.J. Ferrie, E.J. Petersson, *Chem. Commun.* **54**, 1766 (2018)
104. L.R. Malins, R.J. Payne, *Curr. Opin. Chem. Biol.* **22**, 70 (2014)
105. Y.J. Wang, D.M. Szantai-Kis, E.J. Petersson, *Org. Biomol. Chem.* **14**, 6262 (2016)
106. J. Chen, Q. Wan, Y. Yuan, J. Zhu, S.J. Danishefsky, *Angew. Chem. Int. Ed.* **47**, 8521 (2008)
107. M.A. Raftery, R.D. Cole, *J. Biol. Chem.* **241**, 3457 (1966)
108. S. Marincean, M. Rabago Smith, L. Beltz, B. Borhan, *J. Mol. Model* **18**, 4547 (2012)
109. A. Aitken, M. Learmonth, Carboxymethylation of cysteine using iodoacetamide/iodoacetic acid, in *The Protein Protocols Handbook*, ed. by J.M. Walker (Humana Press, Totowa, NJ, 2002), p. 455. <https://doi.org/10.1385/1-59259-169-8:455>
110. Q.-Q. He, G.-M. Fang, L. Liu, *Chin. Chem. Lett.* **24**, 265 (2013)
111. T. Tanaka, A.M. Wagner, J.B. Warner, Y.J. Wang, E.J. Petersson, *Angew. Chem. Int. Ed.* **52**, 6210 (2013)
112. R.E. Connor, K. Piatkov, A. Varshavsky, D.A. Tirrell, *ChemBioChem* **9**, 366 (2008)
113. E. Graciet, R.G. Hu, K. Piatkov, J.H. Rhee, E.M. Schwarz, A. Varshavsky, *Proc. Natl. Acad. Sci. USA* **103**, 3078 (2006)
114. A. Varshavsky, *Nat. Struct. Mol. Biol.* **15**, 1238 (2008)
115. S. Dery, P.S. Reddy, L. Dery, R. Mousa, R.N. Dardashti, N. Metanis, *Chem. Sci.* **6**, 6207 (2015)
116. J. Liu, F. Zheng, R. Cheng, S. Li, S. Rozovsky, Q. Wang, L. Wang, *J. Am. Chem. Soc.* **140**, 8807 (2018)
117. H. Xiong, N.M. Reynolds, C.G. Fan, M. Englert, D. Hoyer, S.J. Miller, D. Soll, *Angew. Chem. Int. Ed.* **55**, 4083 (2016)
118. F. Kloss, S. Pidot, H. Goerls, T. Friedrich, C. Hertweck, *Angew. Chem. Int. Ed.* **52**, 10745 (2013)
119. F. Kloss, A.I. Chiriac, C. Hertweck, *Chem. Eur. J.* **20**, 15451 (2014)
120. A.I. Chiriac, F. Kloss, J. Krämer, C. Vuong, C. Hertweck, H.-G. Sahl, *J. Antimicrob. Chemother.* **70**, 2576 (2015)
121. K. Manzor, K.Ó. Proinsias, F. Kelleher, *Tetrahedron Lett.* **58**, 2959 (2017)
122. M. De Zotti et al., *Beilstein J. Org. Chem.* **8**, 1161 (2012)
123. K.R. Wang, B.Z. Zhang, W. Zhang, J.X. Yan, J. Li, R. Wang, *Peptides* **29**, 963 (2008)
124. W. Zhang, J. Li, L.W. Liu, K.R. Wang, J.J. Song, J.X. Yan, *Peptides* **31**, 1832 (2010)
125. A. Chevalier, C. Massif, P.Y. Renard, A. Romieu, *Chem. Eur. J.* **19**, 1686 (2013)
126. M.-M. Carlos, R. Florian, A. Horst, *Anti-Cancer Agents Med. Chem.* **10**, 753 (2010)
127. J.-P. Xiong, T. Stehle, R. Zhang, A. Joachimiak, M. Frech, S.L. Goodman, M.A. Arnaut, *Science* **296**, 151 (2002)
128. J.E. Bock, J. Gavenonis, J.A. Kritzer, *ACS Chem. Biol.* **8**, 488 (2013)
129. J.S. Laursen, J. Engel-Andreasen, P. Fristrup, P. Harris, C.A. Olsen, *J. Am. Chem. Soc.* **135**, 2835 (2013)
130. R.W. Newberry, B. Vanveller, I.A. Guzei, R.T. Raines, *J. Am. Chem. Soc.* **135**, 7843 (2013)
131. R.W. Newberry, B. Vanveller, R.T. Raines, *Chem. Commun.* **51**, 9624 (2015)
132. B.C. Gorske, R.C. Nelson, Z.S. Bowden, T.A. Kufe, A.M. Childs, *J. Org. Chem.* **78**, 11172 (2013)
133. A. Okano, R.C. James, J.G. Pierce, J. Xie, D.L. Boger, *J. Am. Chem. Soc.* **134**, 8790 (2012)
134. B.M. Crowley, D.L. Boger, *J. Am. Chem. Soc.* **128**, 2885 (2006)
135. A. Okano, A. Nakayama, A.W. Schammel, D.L. Boger, *J. Am. Chem. Soc.* **136**, 13522 (2014)
136. J. Xie, A. Okano, J.G. Pierce, R.C. James, S. Stamm, C.M. Crane, D.L. Boger, *J. Am. Chem. Soc.* **134**, 1284 (2012)
137. A. Okano, N.A. Isley, D.L. Boger, *Proc. Natl. Acad. Sci. USA* **114**, E5052 (2017)
138. K.C. Nicolaou et al., *J. Am. Chem. Soc.* **127**, 11159 (2005)
139. C.R. Walters, J.J. Ferrie, E.J. Petersson, Thioamide labeling of proteins through a combination of semisynthetic methods, in *Chemical Ligation: Tools for Biomolecule Synthesis and Modification*, ed. by L.D. D'Andrea, A. Romanelli, 2nd edn. (Wiley, Hoboken, 2017), p. 355
140. M. Hollósi, E. Kollár, J. Kajtár, M. Kajtár, G.D. Fasman, *Biopolymers* **30**, 1061 (1990)

141. R. Frank, M. Jakob, F. Thuncke, G. Fischer, M. Schutkowski, *Angew. Chem. Int. Ed.* **39**, 1120 (2000)
142. J. Zhao, J.-C. Micheau, C. Vargas, C. Schiene-Fischer, *Chem. Eur. J.* **10**, 6093 (2004)
143. Y. Huang, Z. Cong, L. Yang, S. Dong, *J. Pept. Sci.* **14**, 1062 (2008)
144. W.M. Wiczak, I. Gryczynski, H. Szmajdzinski, M.L. Johnson, M. Kruszynski, J. Zboinska, *J. Biophys. Chem.* **32**, 43 (1988)
145. Y. Huang, J.J. Ferrie, X. Chen, Y. Zhang, D.M. Szantai-Kis, D.M. Chenoweth, E.J. Petersson, *Chem. Commun.* **52**, 7798 (2016)
146. S.H.L. Verhelst, *FEBS J.* **284**, 1489 (2017)
147. M. Drag, G.S. Salvesen, *Nat. Rev. Drug Discov.* **9**, 690 (2010)
148. P.A. Bartlett, K.L. Spear, N.E. Jacobsen, *Biochemistry* **21**, 1608 (1982)
149. P. Campbell, N.T. Nashed, *J. Am. Chem. Soc.* **104**, 5221 (1982)
150. M.D. Bond, B. Holmquist, B.L. Vallee, *J. Inorg. Biochem.* **28**, 97 (1986)
151. W.L. Mock, J.-T. Chen, J.W. Tsang, *Biochem. Biophys. Res. Commun.* **102**, 389 (1981)
152. K. Cho, *Anal. Biochem.* **164**, 248 (1987)
153. M. Roberts, D. Guthrie, C. Williams, S. Martin, in *The Effects of Several Aminopeptidases Towards Thiono-peptides* (Portland Press Limited, 1994)
154. K.L. Foje, R.P. Hanzlik, *Biochim. Biophys. Acta Gen. Subj.* **1201**, 447 (1994)
155. M. Schutkowski, K. Neubert, G. Fischer, *Eur. J. Biochem.* **221**, 455 (1994)
156. A. Kathleen et al., *Protein Sci.* **13**, 412 (2004)
157. G. Lowe, Y. Yuthavong, *Biochem. J.* **124**, 107 (1971)
158. S.A. Thompson, P.R. Andrews, R.P. Hanzlik, *J. Med. Chem.* **29**, 104 (1986)
159. J.C. Kelly, D. Cuerrier, L.A. Graham, R.L. Campbell, P.L. Davies, *Biochim. Biophys. Acta Proteins Proteomics* **1794**, 1505 (2009)
160. R.E. Beattie, C.H. Williams, D.T. Elmore, in *L-Leucine Thioamide as an Inhibitor of Leucine Aminopeptidase* (Portland Press Limited, 1988)
161. J. Mcelroy, D.J. Guthrie, N.M. Hooper, C.H. Williams, in *40 gly-(csh)-phe Resists Hydrolysis by Membrane Dipeptidase* (Portland Press Limited, 1998)
162. A. Stöckel-Maschek, C. Mrestani-Klaus, B. Stiebitz, H.-U. Demuth, K. Neubert, *Biochim. Biophys. Acta Protein Struct.* **1479**, 15 (2000)
163. S. Yao, R. Zutshi, J. Chmielewski, *Bioorg. Med. Chem. Lett.* **8**, 699 (1998)
164. M. Schutkowski, M. Jakob, G. Landgraf, I. Born, K. Neubert, G. Fischer, *Eur. J. Biochem.* **245**, 381 (1997)
165. A.A. Kaspar, J.M. Reichert, *Drug. Discov. Today* **18**, 807 (2013)
166. K. Fosgerau, T. Hoffmann, *Drug. Discov. Today* **20**, 122 (2015)
167. L. Gentilucci, R. De Marco, L. Cerisoli, *Curr. Pharm. Design* **16**, 3185 (2010)
168. J.H. Weiss, D.W. Choi, *Science* **241**, 973 (1988)
169. G. Pasut, F.M. Veronese, *J. Control. Release* **161**, 461 (2012)
170. J.K. Dozier, M.D. Distefano, *Int. J. Mol. Sci.* **16**, 25831 (2015)
171. B.D. Larsen, in *Pharmacologically Active Peptide Conjugates Having a Reduced Tendency Towards Enzymatic Hydrolysis* (Google Patents, 2008)
172. M.E. Houston, A.P. Campbell, B. Lix, C.M. Kay, B.D. Sykes, R.S. Hodges, *Biochemistry* **35**, 10041 (1996)
173. P. Timmerman et al., *Open Vaccine J.* **2**, 56 (2009)
174. S. Sim, Y. Kim, T. Kim, S. Lim, M. Lee, *J. Am. Chem. Soc.* **134**, 20270 (2012)
175. A.O. Subtelný, M.C. Hartman, J.W. Szostak, *J. Am. Chem. Soc.* **130**, 6131 (2008)
176. J.-K. Bang, Y.-H. Nan, E.-K. Lee, S.-Y. Shin, *Bull. Korean Chem. Soc.* **31**, 2509 (2010)
177. P. Claudon et al., *Angew. Chem. Int. Ed.* **49**, 333 (2010)
178. R.C. Elgersma, T. Meijneke, R. De Jong, A.J. Brouwer, G. Posthuma, D.T. Rijkers, R.M. Liskamp, *Org. Biomol. Chem.* **4**, 3587 (2006)
179. R. Maini, L.M. Dedkova, R. Paul, M.M. Madathil, S.R. Chowdhury, S. Chen, S.M. Hecht, *J. Am. Chem. Soc.* **137**, 11206 (2015)
180. L.S. Victorova, V.V. Kotosov, A.V. Azhaev, A.A. Krayevsky, M.K. Kukhanova, B.P. Gottikh, *FEBS Lett.* **68**, 215 (1976)

181. K.L. Dunbar, D.H. Scharf, A. Litomska, C. Hertweck, *Chem. Rev.* **117**, 5521 (2017)
182. A. Bondi, *J. Phys. Chem.* **68**, 441 (1964)
183. L. Pauling, in *The Nature of the Chemical Bond and the Structure of Molecules and Crystals: An Introduction to Modern Structural Chemistry* (Cornell University Press, Ithaca, 1960)